USE OF FLUX BALANCE ANALYSIS AND METABOLOMICS IN THE ANALYSIS OF THE RESPIRATORY PATHWAY IN *SACCHAROMYCES CEREVISIAE*

by

Duygu Dikicioğlu

B.S. in Ch.E., Boğaziçi University, 2003

Submitted to the Institude for Graduate Studies in
Science and Engineering in partial fulfillment of
the requirements for the degree of
Master of Science

Graduate Program in Chemical Engineering

Boğaziçi University

2005

USE OF FLUX BLANCE ANALYSIS AND METABOLOMICS IN THE ANALYSIS OF THE RESPIRATORY PATHWAY IN *SACCHAROMYCES CEREVISIAE*

APPROVED BY:

Prof. Betül Kırdar (Thesis Supervisor)	……...
Assist. Prof. Ebru Toksoy Oner	……...
Prof. Zeynep İlsen Önsan	……...

DATE OF APPROVAL: 19.08.2005

ACKNOWLEDGEMENTS

I would like to express how grateful and obliged I am to my thesis advisor Prof. Betül Kırdar. Her continuous and enlightening support in my life as well as my academic study has been of an incomprehensible help. It has been and will always be such a great privilege to work with such a unique person as herself.

I would also like to thank Prof. Z. İlsen Önsan, Prof. Kutlu Ülgen and Assist. Prof Ebru Toksoy Öner for their continuous support during my studies.

This work was financially supported by Boğaziçi Research Fund through project 04A503 and DPT-03K120250.

For making life more bearable, I am sincerely grateful to my friends. It is great to have people like Şeyda, Canan, Feyza, Ali and İlker around to share your life with. Another very important bunch of people I would like to mention is the former and present KB440 & KB407 residents: Hilal & Emrah, you are dearest, even when you are far away. Burcu, Beste, Saliha, Özde, Deniz, I consider myself very lucky to have you as friends. Tunahan, Yalçın, my computer genies, thank you for not going mad with my everlasting questions. I still wonder how you have a solution to every problem! And there is a very dear friend, whom I would also like to mention here. Pınar, thank you for always being there whenever I needed.

Last, but certainly not the least, I would like to thank the two most important people in my life; my mother and my father. Without their continuous support, it would be impossible for me to achieve anything in my life.

ABSTRACT

USE OF FLUX BALANCE ANALYSIS AND METABOLOMICS IN THE ANALYSIS OF THE RESPIRATORY PATHWAY IN *SACCHAROMYCES CEREVISIAE*

BY4743 parent strain and seven deletion mutants ΔHO, ΔQDR3, ΔMIG1, ΔHAP4, ΔQCR7, ΔRIP1 and ΔCYT1 of *S. cerevisiae* are investigated to improve present knowledge on the regulatory mechanism of respiratory chain and provide a rational design for the construction of a high ethanol production strain. Cells were grown in rich medium in batch and continuous cultivations and the wild type was also cultivated under nutritional stress and relaxed conditions. In batch cultivations, ΔQDR3 had overgrown the wild type and highest ethanol producing strain was ΔQCR7. In continuous cultivation, highest amount of biomass was produced by parental strain whereas the lowest levels of biomass by ΔRIP1, followed by ΔHAP4 and ΔCYT1. ΔRIP1 was has lowest glucose consumption and highest ethanol production. This strain was followed by ΔHAP4 both in steady state ethanol concentrations and yields. These results were used in the metabolic modeling of the yeast cells by using central carbon metabolism and the complete metabolism of the yeast as two models to determine the flux distributions. When the objective function was ethanol excretion optimization the ethanol production of the fully and partially respiratory deficient strains are in agreement with the experimentally obtained values while when oxygen uptake optimized as the objective function the ethanol production of the respiratory sufficient strains are similar to their experimental correspondences. Analysis of minimization of metabolic adjustment indicated that ΔHO and ΔQDR3 were metabolically more adjusted to the wild type. Principle component analysis revealed that the deletion strains resulting in similar deficiencies were found to be clustered together. Gene expression analysis was carried out for HAP4 gene in nutritional limitation experiments performed on the parental strain. In the carbon limitation culture, the expression levels of HAP4 declined rapidly as a response of glucose repression. In nitrogen limitation cultivations, the increase in its expression levels might be due to its regulatory function on the ammonia metabolism in nitrogen catabolite repression in yeast.

ÖZET

SACCHAROMYCES CEREVISIAE'DA SOLUNUM YOLİZİ KONTROLÜNÜN AKI-DENGE VE METABOLOM ANALİZİ İLE İNCELENMESİ

S. cerevisiae'nın solunum yolizinin kontrol mekanizmasını açıklığa kavuşturmak ve ve yüksek etanol üreten bir suşun akılcı tasarımının yapılabilmesi amacı ile BY4743 ve bu suştan her birinde tek bir gen delesyonu yaratılarak üretilen ΔHO, ΔQDR3, ΔMIG1, ΔHAP4, ΔQCR7, ΔRIP1 ve ΔCYT1 çalışma kapsamı içinde incelenmiştir. Bu amaçla, hücreler kesikli ve sürekli üretim ile zengin besi ortamında büyütülmüş, ana suş ayrıca besin stresi yaşanan ve stresin gevşetildiği ortamlarda da büyütülerek incelenmiştir. Kesikli üretimde ΔQDR3'ün ana suştan daha yüksek miktarlarda hücre ürettiği, ΔQCR7'nin ise en yüksek etanol üretim miktarına ulaştığı gözlemlenmiştir. Sürekli üretimde, en fazla biyomas üreten suşun ana suş olduğu, onu sırasıyla ΔRIP1, ΔHAP4 ve ΔCYT1'in takip ettiği saptanmıştır. ΔRIP1 en az glikoz kulanan ve en yüksek miktarda etanol üreten suş olarak bulunmuştur. ΔHAP4, toplam etanol üretimi ve verimi bağlamında bu suşu izlemektedir. Elde edilen sonuçlar, maya hücrelerinin metabolik modellenmesinde kullanılmıştır. Hücre içi akı dağılımlarının belirlenmesi amacıyla merkezi karbon metabolizması ve hücrenin genel metabolizması model olarak kullanılmıştır. Ethanol üretiminin optimizasyonu temel amaç olarak alındığında, tam ya da kısmi solunum eksikliği olan suşlar deneysel sonuçlarla uyum gösterirken, hücre içi oksijen alımının optimizasyonu hedef fonksiyon olarak seçildiğinde solunum yapabilen suşların etanol üretiminin deneysel sonuçlarla uyumluluk gösterdiği belirlenmiştir. Metabolik uyumun minimizasyonu metodu ile ΔHO ve ΔQDR3 suşlarının metabolik açıdan ana suşa en yakın mutantlar olduğu saptanmıştır. Ana bileşenler analizi, benzer eksikliklere yol açan genleri silinmiş suşların bir araya gruplandığını göstermiştir. HAP4 gen ekspresyonu, RT-rtqPCR yöntemi ile incelenmiştir. Karbon kısıtlı üretimde, ortamdaki glikoz miktarı azaldıkça HAP4 geninin ekspresyonunda artış gözlenmiştir. Ortama glikoz eklendiğinde, bir dakikalık bir zaman süresinde genin ekspresyonunda hızlı bir düşüş belirlenmiştir. Genin ekspresyonunda gözüken artış ortama giren azot miktarı ile paralel bulunmuştur ve HAP4 proteininin azot katabolit baskılama mekanizmasında işlevi olduğunu sezindirmiştir.

TABLE OF CONTENTS

ACKNOWLEDGEMENT ……. iii
ABSTRACT ……. iv
ÖZET ……... v
LIST OF FIGURES ……. ix
LIST OF TABLES ……. xvi
LIST OF SYMBOLS/ABBREVIATIONS ……. xx
1. INTRODUCTION ……... 1
1.1. Improvement of Ethanol Production Using Nuclear Petite Yeast Mutants… 3
1.2. Regulation of Respiration……... 12
1.3. YDL227c and YBR043c…… 14
1.4. Stoichometric Models of *S. cerevisiae*……... 16
1.5. Flux Balance Analysis…… 17
1.6. Reverse Transcription Quantitative Real Time Polymerase Chain Reaction. 19
1.7. The Aim of This Thesis…….. 23
2. MATERIALS AND METHODS……. 25
2.1. Materials……. 25
2.1.1. Microorganisms ...…….. 25
2.1.2. Maintenance……... ……..... 25
2.1.3. Chemicals and Disposable Materials…… 26
2.1.3.1. Culture Media……..…..….... 26
2.1.3.2. Kits…….……..……...…..…….... 27
2.1.3.3. Buffers and Chemicals Required for Polymerase Chain Reaction Applications……..... 27
2.1.3.4. Miscellaneous……...…..…….. 28
2.1.4. Laboratory Equipment …….……. 28
2.2. Methods.……. 30
2.2.1. Experimental Methods...……..…….…….. 30
2.2.1.1. Sterilization…...…….…….. 30
2.2.1.2. Growth on Non-Fermentable Carbon Sources……..... 30

2.2.1.3. Cultivation Conditions……..……...…..…….. 31
2.2.1.4. Sample Preparation and Storage……...…..…….. 32
2.2.1.5. Determination of the Cell Dry Weight ……...…..…….. 33
2.2.1.6. Enzymatic Analyses for Determination of Metabolite Concentrations…..…..……..... 33
2.2.1.7. DNA Extraction……..……..……...…..…….. 41
2.2.1.8. PCR Protocols and Gel Electrophoresis……...…..…….. 42
2.2.1.9. RNA Extraction……..……..……...…..…….. 44
2.2.1.10. Reverse Transcription Real Time Quantification Polymerase Chain Reaction (RT-rtqPCR).……..……..... 46
2.2.2. Computational Methods…….…….……..…….. 48
2.2.2.1. Determination of Maximum Growth Rate and Substrate Utilization Constants……..……..……..…….…….... 48
2.2.2.2. Determination of Yield Coefficients……..……...…..……. 49
2.2.2.3. Flux Balance Analysis……..……..……...…..……. 49
2.2.2.4. Minimization of Metabolic Adjustment…… 54
2.2.2.5. Principle Component Analysis…….……..……...…..……. 55
2.2.2.6. Relative Quantification of Gene Expression – Pfaffl Method…… 56
3. RESULTS……. ……..…….. 57
3.1. Verification of the Deletions in the Strains of *S. cerevisiae*……... 58
3.2. Respiratory Deficiency Check for ΔQDR3 Mutant Strain……. 60
3.3. Growth Characteristics of Deletion Mutants in Batch Cultures……. 61
3.4. Growth Characteristics in Continuous Cultures …… 66
3.4.1. Growth Characteristics of Deletion Strains ……. 66
3.4.2. Flux Balance Analysis…… ……. 75
3.4.2.1. Small Scale Model……. 75
3.4.2.2. Genome Scale Model…… 77
3.4.3. Minimization of Metabolic Adjustment……... 79
3.4.4. Principle Component Analysis……. 80
3.5. Investigation of Metabolic and Transcriptional Response of *S. cerevisiae* to Nutritional Limitations in Batch Cultivations with Pulse Injections…….. 82
3.5.1. Metabolic Response of BY4743 to Carbon and Nitrogen Starvations

Followed by Recovery To No-Limitation Conditions…… 82
3.5.2. Optimization of RNA Extraction……..…… 88
3.5.3. The Selection of Control Genes..……..…… 89
3.5.4. Optimization of Annealing Temperature for Reverse Transcription Quantitative Real Time Polymerase Chain Reaction Applications.…… 92
3.5.5. Response of HAP4 Gene to Nutritional Limitations and Pulse Nutrient Injections.…… 94
4. DISCUSSION……..…….……... 97
4.1. Batch Cultivations……..… 97
4.2. Comparison of the Strains of Reference in Chemostat Cultures ……... 101
4.3. Chemostat Cultivations..……. 101
4.4. Batch Cultivations with Nutritional Stress……. 106
5. CONCLUSIONS AND RECOMMENDATIONS ……... 110
5.1. Conclusions ..……. 110
5.2. Recommendations…….…….. 112
APPENDIX……... 114
A.1. Dry Weight / Optical Density Conversions…….…….. 114
A.2. Growth and Metabolite Profiles of Batch and Chemostat Cultivations……. 114
A.3. DNA / RNA Concentration and Contamination Determinations …….. 135
A.4. Flux Balance Analysis – Small Scale Model……. 136
A.5. Flux Balance Analysis – Genome Scale Model and MOMA ……... 146
A.6. Principle Component Analysis……..……..... 207
REFERENCES ……. 210

LIST OF FIGURES

Figure 1.1.	The inverse metabolic engineering approach (Gill, 2003)……	2
Figure 1.2.	Anabolic and catabolic processes in yeast (Feldmann, 2003)……..	3
Figure 1.3.	Central metabolism of *S. cerevisiae* (Walker, 1998)……	4
Figure 1.4.	Summary of aerobic respiration and anaerobic fermentation……..	5
Figure 1.5.	General picture of the respiratory chain. The numbers in boxes are the EC numbers of the proteins involved in complexes (KEGG Encyclopaedia, 2002)……	8
Figure 1.6.	Hypothetical representation of the respiratory chain complex III...……	9
Figure 1.7.	Hypothetical representation of the interactions of QCR7…...……..	10
Figure 1.8.	Hypothetical representation of interactions of RIP1……	11
Figure 1.9.	Hypothetical representation of HAP complex interactions in glucose uptake mechanism……	13
Figure 1.10.	Hypothetical representation of HAP4 interactions in respiratory regulation……..	14
Figure 1.11.	Hypothetical representation of interactions and complex formation of MIG1……	14

Figure 1.12.	Interactions of QDR3……	15
Figure 3.1.	Analysis of deletions in mutants by using A / D primer pairs…….	59
Figure 3.2.	Analysis of deletions in mutants by using uptag / downag primer pairs……..	60
Figure 3.3.	The growth of ΔQDR3 on ethanol containing plates as the sole carbon source……	61
Figure 3.4.	The growth of ΔQDR3 on glycerol containing plates as the sole carbon source……	61
Figure 3.5.	Growth characteristics (a) and Pyruvate concentration profile (b) of WT strain, BY4743 in batch cultures……...	62
Figure 3.6.	Growth characteristics (a) and Pyruvate concentration profile (b) of recombinant strain, ΔQDR3 in batch cultures……..	64
Figure 3.7.	Growth characteristics (a) and Pyruvate concentration profile (b) of recombinant strain, ΔQCR7 in batch cultures…….	65
Figure 3.8.	Growth characteristics (a) and Pyruvate and succinate concentration profiles (b) of WT strain, BY4743 in continuous cultures.....	67
Figure 3.9.	Growth characteristics (a) and Pyruvate and succinate concentration profiles (b) of mutant strain, ΔHO in continuous cultures…….....	68
Figure 3.10.	Growth characteristics (a) and Pyruvate and succinate concentration profiles (b) of mutant strain, ΔQDR3 in continuous cultures……..	69

Figure 3.11. Growth characteristics (a) and Pyruvate and succinate concentration profiles (b) of mutant strain, ΔMIG1 in continuous cultures…….. 70

Figure 3.12. Growth characteristics (a) and Pyruvate and succinate concentration profiles (b) of mutant strain, ΔHAP4 in continuous cultures……..... 71

Figure 3.13. Growth characteristics (a) and Pyruvate and succinate concentration profiles (b) of mutant strain, ΔQCR7 in continuous cultures…….. 73

Figure 3.14. Growth characteristics (a) and Pyruvate and succinate concentration profiles (b) of mutant strain, ΔRIP1 in continuous cultures…….. 74

Figure 3.15. Growth characteristics (a) and Pyruvate and succinate concentration profiles (b) of mutant strain, ΔCYT1 in continuous cultures……. 75

Figure 3.16. Plot of the latent vector……. 80

Figure 3.17. Plot of score 2 against score 1…….. 81

Figure 3.18. Plot of loading 2 against loading 1…… 82

Figure 3.19. Growth characteristics (a) and Metabolic profiles (b) of BY4743 under no limitation conditions in batch cultures……... 83

Figure 3.20. Growth characteristics (a) and Metabolite profiles (b) of BY4743 under carbon limitation conditions in batch cultures with pulse injections……... 85

Figure 3.21. Growth characteristics (a) and Metabolite profiles (b) of BY4743 under nitrogen limitation conditions in batch cultures with pulse injections……... 87

Figure 3.22. Analysis of the integrity and concentration of extracted RNA samples by gel electrophoresis…….. 88

Figure 3.23. Fold change with respect to different conditions for different selections of control and housekeeping choices…… 91

Figure 3.24. Fold change for specific gene expression ratios with respect to various control and housekeeping genes under different conditions..... 92

Figure 3.25. PCR amplification cycle florescence (CF) of DNA fragments at an annealing temperature of 55.3^{o}C in relative florescence units (RFU)…… 93

Figure 3.26. PCR amplification cycle florescence (CF) of DNA fragments at an annealing temperature of 52.2^{o}C in relative florescence units (RFU)…… 93

Figure 3.27. Melt curve graph of the amplified DNA fragments at an annealing temperature of 52.2^{o}C……... 94

Figure 3.28. Expression profile of HAP4 gene under carbon limitation in batch cultures with pulse injections…… 95

Figure 3.29. Expression profile of HAP4 under nitrogen limitation in batch cultures with pulse injections…… 96

Figure 4.1. Comparison of maximum growth rates in batch cultivation……. 98

Figure 4.2. Comparison of saturation constants in batch cultivation..... 99

Figure 4.3. Intracellular glucose concentrations in batch cultivation……..... 100

Figure 4.4. Intracellular pyruvate concentrations in batch cultivation…….. 100

Figure 4.5. Comparison of intracellular glucose concentration in chemostat cultivation……. 103

Figure 4.6. Comparison of intracellular pyruvate concentration in chemostat cultivation……..... 104

Figure 4.7. Comparison of maximum specific growth rates in batch cultivations with nutritional stresses…… 107

Figure 4.8. Comparison of saturation constants in batch cultivations with nutritional stresses…… 108

Figure A.1. ln (x_v) vs. time graph to determine the steady state of the batch cultivation of BY4743……... 115

Figure A.2. Determination of μ_{max} of the batch cultivation of BY4743……... 115

Figure A.3. Determination of K_s of the batch cultivation of BY4743…….. 116

Figure A.4. ln (x_v) vs. time graph to determine the steady state of the batch cultivation of ΔQDR3……... 117

Figure A.5. Determination of μ_{max} of the batch cultivation of ΔQDR3…… 117

Figure A.6. Determination of K_s of the batch cultivation of ΔQDR3……. 117

Figure A.7. ln (x_v) vs. time graph to determine the steady state of the batch cultivation of ΔQCR7…… 118

Figure A.8. Determination of μ_{max} of the batch cultivation of ΔQCR7…… 119

Figure A.9. Determination of K_s of the batch cultivation of ΔQCR7…….. 119

Figure A.10. Exponential phase of BY4743 in continuous cultivation…….. 120

Figure A.11. Exponential phase of ΔHO in continuous cultivation……... 121

Figure A.12. Exponential phase of ΔQDR3 in continuous cultivation…….. 122

Figure A.13. Exponential phase of ΔMIG1 in continuous cultivation……... 122

Figure A.14. Exponential phase of ΔHAP4 in continuous cultivation……... 123

Figure A.15. Exponential phase of ΔQCR7 in continuous cultivation……... 124

Figure A.16. Exponential phase of ΔRIP1 in continuous cultivation……. 125

Figure A.17. Exponential phase of ΔCYT1 in continuous cultivation……... 125

Figure A.18. ln (x_v) vs. time graph to determine the steady state of BY4743 in nutritional limitation cultivations –no limitation……. 127

Figure A.19. Determination of μ_{max} of BY4743 in nutritional limitation cultivations –no limitation……. 127

Figure A.20. Determination of K_s of BY4743 in nutritional limitation cultivations –no limitation……. 127

Figure A.21. ln (x_v) vs. time graph to determine the steady state of BY4743 in nutritional limitation cultivations –C limitation…… 129

Figure A.22. Determination of μ_{max} of BY4743 in nutritional limitation cultivations – C limitation……..... 130

Figure A.23. Determination of K_s of BY4743 in nutritional limitation cultivations – C limitation……. 130

Figure A.24. ln (x_v) vs. time graph to determine the steady state of BY4743 in nutritional limitation cultivations – N limitation……... 132

Figure A.25. Determination of μ_{max} of BY4743 in nutritional limitation cultivations – N limitation……..... 133

Figure A.26. Determination of K_s of BY4743 in nutritional limitation cultivations – N limitation……. 133

LIST OF TABLES

Table 2.1.	Optimum Reaction Mixtures for Specific Mutants……....	43
Table 2.2.	Sequences for A / D primers……..	43
Table 2.3.	Sequences for uptag / downtag primers…….	44
Table 2.4.	RT-rtqPCR primer sequences……	47
Table 2.5.	Experimental inputs used in the stoichiometric matrix ……	51
Table 2.6.	Flux measurements used in the stoichiometric matrix……..…....	52
Table 2.7.	Unitless flux measurements used in the stoichiometric matrix..……...	53
Table 2.8.	The data matrix……..…....	55
Table 3.1.	Comparison of calculated ethanol fluxes by FBA using SSM and experimental…….	76
Table 3.2.	Comparison of experimental and calculated ethanol production using FBA and GSM with an objective function of optimization of O_2 uptake...	78
Table 3.3.	Comparison of experimental and calculated ethanol production using FBA and GSM with an objective function of optimization of ethanol production……	78
Table 3.4.	Comparison of experimental and calculated ethanol production using MOMA……..	79
Table 3.5.	Combinations of sample storage and mechanical disruption techniques..	88

Table 3.6. log_2 expression levels of the genes in quest under different cultivation conditions…….. 89

Table 3.7. log_2 ratios of the genes in quest……. 90

Table 3.8. Squares of ratios…… 91

Table 4.1. Comparison of growth characteristics of *S. cerevisiae* and yields of biomass and ethanol on glucose in batch cultivations……. 98

Table 4.2. Comparison of growth characteristics of reference strains of *S. cerevisiae* and yields of biomass and ethanol on glucose in chemostat cultivations… 101

Table 4.3. Comparison of growth characteristics of *S. cerevisiae* and yields of biomass and ethanol on glucose in chemostat cultivations…….. 102

Table 4.4. Comparison of experimentally obtained and computed ethanol productions (moles / mole glucose)……. 105

Table 4.5. Steady state yields obtained for batch cultivations under nutritional stress 107

Table A.1. Dry weight / optical density conversion equations…….. 114

Table A.2. Growth and metabolite profiles of BY4743 in batch cultivation……. 114

Table A.3. Determination of μ for constant growth region in BY4734 batch cultivation…… 115

Table A.4. Growth and metabolite profiles of ΔQDR3 in batch cultivation……. 116

Table A.5. Determination of μ for constant growth region in ΔQDR3 batch

cultivation…… 116

Table A.6. Growth and metabolite profiles of ΔQCR7 in batch cultivation……. 118

Table A.7. Determination of μ for constant growth region in ΔQCR7 batch cultivation…… 118

Table A.8. Growth and metabolite profiles of BY4743 in continuous cultivation…… 119

Table A.9. Growth and metabolite profiles of ΔHO in continuous cultivation……. 120

Table A.10. Growth and metabolite profiles of ΔQDR3 in continuous cultivation…… 121

Table A.11. Growth and metabolite profiles of ΔMIG1 in continuous cultivation……. 122

Table A.12. Growth and metabolite profiles of ΔHAP4 in continuous cultivation……. 123

Table A.13. Growth and metabolite profiles of ΔQCR7 in continuous cultivation…… 123

Table A.14. Growth and metabolite profiles of ΔRIP1 in continuous cultivation…….. 124

Table A.15. Growth and metabolite profiles of ΔCYT1 in continuous cultivation……. 125

Table A.16. Growth and metabolite profiles of BY4743 in nutritional limitation cultivations –no limitation-1…… 126

Table A.17. Growth and metabolite profiles of BY4743 in nutritional limitation cultivations –no limitation-2…… 126

Table A.18. Determination of μ for constant growth region of BY4743 in nutritional limitation cultivations –no limitation……... 126

Table A.19. Growth and metabolite profiles of BY4743 in nutritional limitation

cultivations –C limitation-1……. 128

Table A.20. Growth and metabolite profiles of BY4743 in nutritional limitation cultivations –C limitation-2……. 128

Table A.21. Determination of μ for constant growth region of BY4743 in nutritional limitation cultivations –C limitation…… 130

Table A.22. Growth and metabolite profiles of BY4743 in nutritional limitation cultivations – N limitation-1…… 131

Table A.23. Growth and metabolite profiles of BY4743 in nutritional limitation cultivations – N limitation-2…… 131

Table A.24. Determination of μ for constant growth region of BY4743 in nutritional limitation cultivations – N limitation……... 133

Table A.25. Gene expression data of BY4743 in C limitation and N limitation with pulse injections…… 134

Table A.26. DNA concentration and contamination results…… 135

Table A.27. RNA concentration and contamination results…… 136

Table A.28. Complete list of metabolites…… 146

Table A.29. Complete list of reactions…… 161

LIST OF SYMBOLS / ABBREVIATIONS

A	absorbance
b	Vector of known metabolites
C_t	Threshold cycle
D	Distance to be minimized
his	Histidine
K columns	Variables
k_s	The saturation constant (kg m^{-3})
L	Linear part of objective function
leu	Leucine
met	Methionine
mRNA	Messenger RNA
N	Cycle number
N rows	Objects
P'	Variable patterns
psig	Per square inch gague
P_i	Inorganic phpsphate
Q	Quadratic part of objective function
rRNA	Ribosomal RNA
r_x	Rate of reaction (grams of S uptake L^{-1} s^{-1})
S	Stoichiometric matrix
S	The limiting substrate concentration (kg m^{-3})
t	Time (s)
T	Object patterns
T_m	Melting temperature
ura	Uracil
v	Vector of fluxes
V	fluxes
v/v	Volume per volume
w/v	Weight per volume

X_i	Metabolite
X	Vector of metabolites, Data matrix
x_v	Viable cells (kg cell m^{-3})
$Y_{s/a}$	Yield of acetic acid on glucose
$Y_{s/e}$	Yield of ethanol on glucose
$Y_{s/g}$	Yield of glycerol on glucose
$Y_{s/x}$	Yield of biomass on glucose
α, β	Constraints imposed on the metabolism
ε	Extinction coefficient
μ	Mean
μ_{max}	Maximum specific growth rate (hr^{-1})
σ	Standard deviation
syn	Abbreviation for synthesis
deg	Abbreviation for degradation
use	Growth and maintenance requirements
trans	Uptake or secretion
AVID	Annotation via integration of data
CF	Cycle fluorescence
DEPC	Diethylpolycarbonate
EDTA	Ethylenediaminetetraacetic acid
EUROSCARF	European *Saccharomyces cerevisiae* Archive for Functional Analysis
FBA	Flux balance analysis
FRET	Fluorescence resonance energy transfer
GSM	Genome scale model
LP	Linear programming
MAT	Mating
MOMA	Minimization of metabolic adjustment
OD	Optical density
ORF	Open reading frames
PC	Principle component

PID controller	Proportional, integral, derivative controller
RFU	Relative fluorescence units
RT-rtqPCR	Reverse transcription real time quantification polymerase chain reaction
SSM	Small scale model
TBE	Tris – Borate - EDTA
TCA cycle	Tricarboxyacidic cycle
YPE	Yeast extract – peptone – ethanol
YPG	Yeast extract – peptone - glycerol
YPD	Yeast extract – peptone - dextrose

1. INTRODUCTION

In metabolic engineering, it is important to be able to link genes and pathways to phenotype. The developments in functional genomics have provided new tools and approaches for understanding, mapping, modeling and manipulating cells and these tools allow the application of a genome-wide approach to map specific mutations (Bro and Nielsen, 2004). Even though the functions of many genes are known on the biochemical level, the function of many of these genes is not known at the phenotypic level in all details, i.e., since many proteins catalyze reactions in several pathways or are involved in regulation of several pathways (Förster *et al.,* 2003).

Analysis of the metabolome might aid inverse metabolic engineering by giving insight into metabolic function of mutated genes in mutants by comparison with a reference strain. The metabolome, consisting of all the intracellular metabolites, is a function of the fluxome, which again is a function of the other 'omes'. Analysis of the fluxome gives information about which pathways are active and to what extent they are active. Flux analysis is easy to perform even on many strains and gives direct information about the fluxes, but as in the case of metabolite profiling, the integrative nature of the information obtained makes it difficult to translate it into specific strategies for metabolic engineering (Bro and Nielsen, 2004).

In inverse metabolic engineering approach, first, evolutionary mechanisms operating in nature or in the laboratory result in the generation of the phenotype of interest. Genetic studies are performed to elucidate the basis of the phenotype, which provides guidance for further metabolic engineering. The genes are either engineered into a strain more suited to the intended application or the natural host is used for industrial production (Gill, 2003) (Figure 1.1).

Yeast metabolism refers to the biochemical assimilation and dissimilation of nutrients by yeast cells. The subject therefore encompasses all enzymatic reactions within

the yeast cell and regulation of these reactions. Assimilatory (anabolic) pathways are energy-consuming, reductive processes which lead to the biosynthesis of new cellular material. Dissimilatory (catabolic) pathways are oxidative processes, which remove electrons from intermediates and use these to generate energy. Such biosynthetic and decomposing pathways, however, do not operate in isolation and should be regarded as components of the integrated processes which are associated with the growth and survival of the yeast cell (Feldmann, 2001) (Figure 1.2).

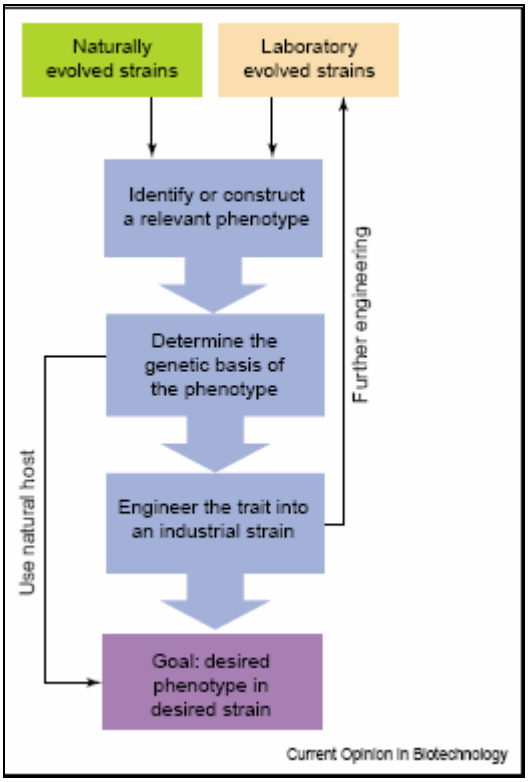

Figure 1.1. The inverse metabolic engineering approach (Gill, 2003)

Most yeasts employ sugars as their preferred carbon and energy sources. The sequence of enzyme-catalyzed reactions that oxidatively convert glucose to pyruvic acid in the yeast cytoplasm is known as glycolysis. Glycolysis provides yeast with energy, together with precursor molecules and reducing power for biosynthetic pathways. The key regulatory enzymes in glycolysis are irreversible phosphofructokinases (PFK) and pruvate kinase (PYC) whose activity is influenced by numerous effectors, including ATP (Figure 1.3).

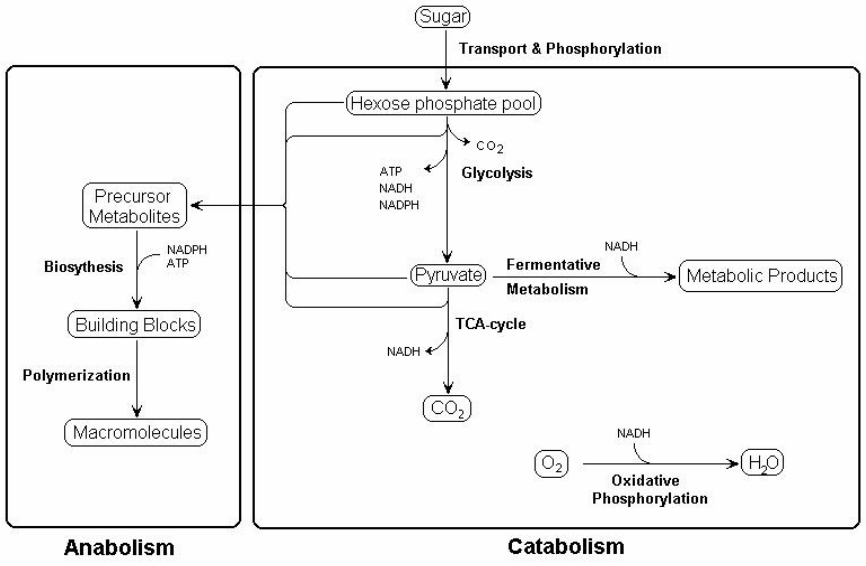

Figure 1.2. Anabolic and catabolic processes in yeast (Feldmann, 2001)

1.1. Improvement of Ethanol Production Using Nuclear Petite Yeast Mutants

The regulation of respiration and fermentation is fundamental to the success of several industrial processes, which exploit yeast metabolism. In *S. cerevisiae*, optimization of respiration is important in the production of yeast biomass (e.g. for food industry), while optimization of fermentation is important in potable and industrial ethanol production (Walker, 1998) (Figure 1.4).

Previous work has highlighted the potential of utilizing the respiratory deficient phenotype of cytoplasmic petite mutants for the production of ethanol. Lacking functional mitochondrial DNA, cytoplasmic petite mutants are incapable of growth by means of respiration and are not subject to the Pasteur effect, i.e. the oxygen suppression of glycolysis. Examination of the effect of exogenous ethanol on strains FY23, FY23Δ*pet191*, FY23*Δcox5a* and FY23p^0 demonstrated that functional mitochondria are essential to maintain the tolerance of yeast to ethanol, the cytoplasmic petite exhibiting the lowest tolerance in the series. The increased productivity exhibited by two nuclear petites was a result of their inability to respire in the "respiro-fermentative" phase of batch growth, and of their retained tolerance to ethanol.

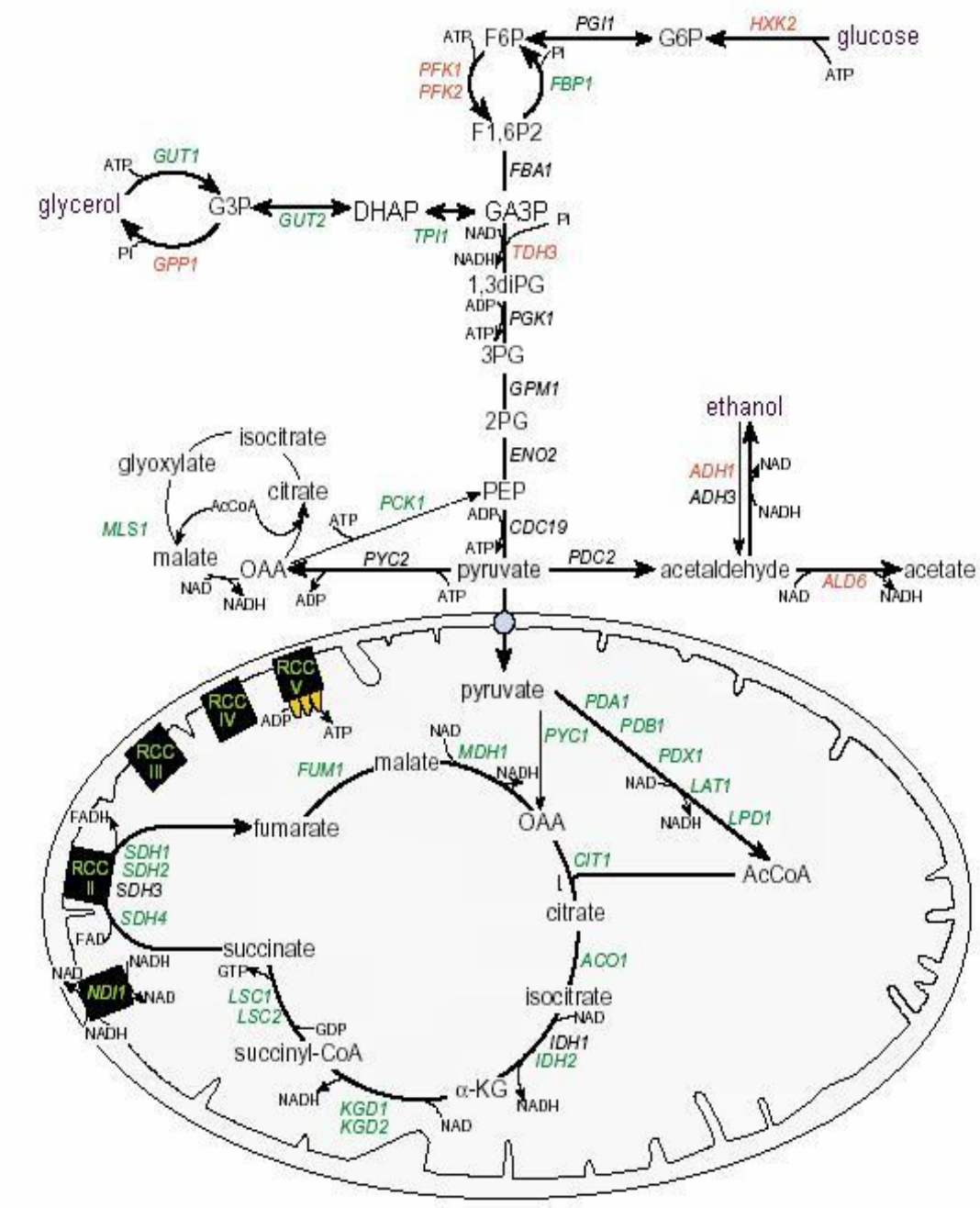

Figure 1.3. Central metabolism of *S. cerevisiae* (Walker, 1998)

It is suggested, therefore, that 100 per cent respiratory deficient nuclear petites will be of use in the commercial production of ethanol in circumstances where the oxygen supply cannot be tightly controlled. Nuclear petites are unable to grow in a diauxic growth phase and so will not metabolize the product of fermentation, ethanol, as their secondary

substrate (Hutter and Oliver, 1998). In another study, batch fermentations were performed in homebrew style for strains K1 and K1Δpet191ab and revealed a 40 per cent higher volumetric ethanol production rate and a 9 per cent higher ethanol ceiling for the mutant. This demonstrates that, because of their respiratory deficiency, nuclear petites are not subject to the Pasteur effect and so exhibit higher rates of fermentation. Furthermore, nuclear petites cannot metabolize the product of fermentation, ethanol, allowing higher ethanol titres to be achieved (Panoutsopolou *et al.,* 2001).

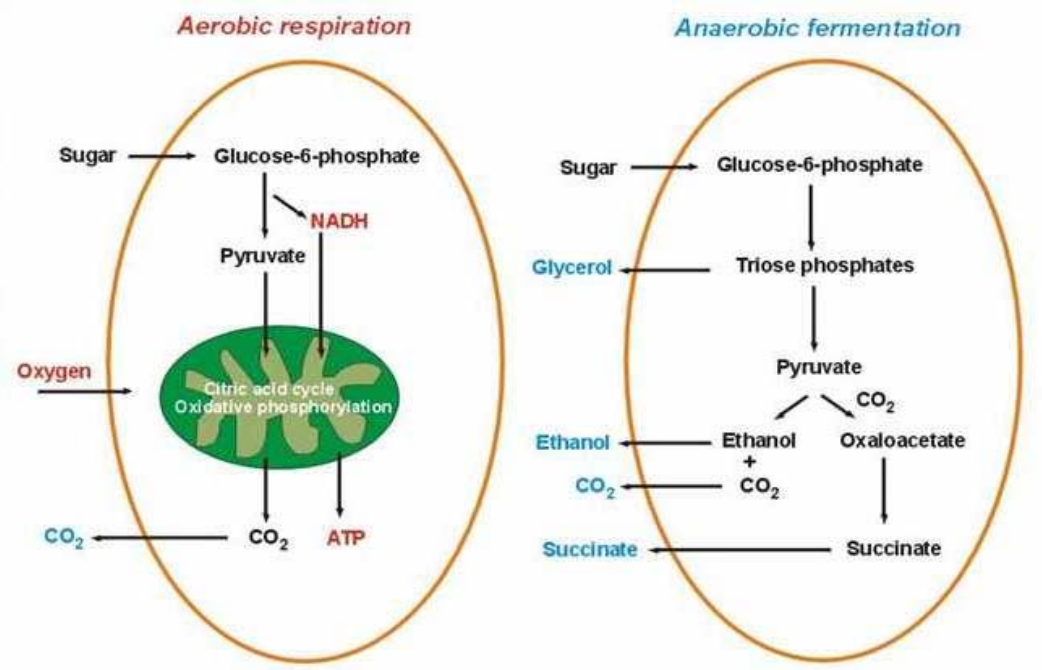

Figure 1.4. Summary of aerobic respiration and anaerobic fermentation

The citric acid cycle accounts for most of the total oxidation of carbon compounds in yeast cells, and its end products are CO_2 and high-energy electrons, which pass via NADH and $FADH_2$ to respiratory chain. None of the reactions leading to NADH or $FADH_2$ production makes direct use of molecular oxygen; only in the final catabolic reactions that take place on the mitochondrial inner membrane, oxygen is directly consumed (Alberts *et al.*, 1994). There are several types of electron carriers and five large membrane bound enzyme complexes in respiratory chain which are embedded in the inner mitochondrial membrane. The cytochromes, iron-sulfur proteins, ubiquinone and flavins are the major electron carriers in respiratory chain. The pathway involves about 40 different proteins in all. The order of the individual electron carriers in the chain has been determined by

sophisticated spectroscopic measurements, and many of the proteins were initially isolated and characterized as individual polypeptides. A major advantage in understanding the respiratory chain, however, was the later realization that most of the proteins are organized into three large enzyme complexes. Each of these complexes acts as an electron-transport-driven H^+ pump (Güldener *et al*., 2005). The mitochondrial respiratory chain consists of multisubunit enzyme complexes that are embedded in the inner mitochondrial membrane. Electron transport through the ubiquinol-cytochrome c reductase and cytochrome oxidase complexes in *S. cerevisiae* is coupled to vectorial H^+ translocation into the intermembrane space, resulting in the establishment of a H+ gradient and subsequent membrane potential. The energy from this gradient is then used as the driving force for ion translocation, protein import into mitochondria, and ATP synthesis, which is catalyzed by ATPases (Malaney *et al*., 1997). These complexes are given as follows with a stronger emphasis on Complex III since the effects of the deletions of QCR7, RIP1 and CYT1 whom all belong to this complex are investigated through experimental and computational work within the framework of this thesis (Figure 1.5).

Complex I: The first complex, NADH-dehydrogenase complex does not exist in *S. cerevisiae*, it is replaced by the enzyme NADH-ubiquinone-6 oxido-reductase (NDI1, 57 kDa). This enzyme catalyzes the oxidation of NADH to NAD^+, ubiquinone is reduced to ubiquinol in the same reaction (Güldener *et al*., 2005).

Complex II: The second complex, succinate dehydrogenase (fumarate reductase) is composed of four proteins in *S. cerevisiae*, which are: a membrane-anchoring protein (encoded by SDH4, precursor weight is 20 kDa), a flavoprotein (SDH1, 70 kDa), an iron-sulfur protein (SDH2, 27 kDa) and a cytochrome b (SDH3, 22 kDa). This complex is responsible for transfering electrons from succinate to ubiquinone, that is, succinate is converted to fumarate and ubiquinone is reduced to ubiquinol. Succinate dehydrogenase is the only TCA cycle enzyme to be bound to mitochondrial inner membrane (Güldener *et al*., 2005).

Complex III: The mitochondrial cytochrome bc1 complex, a multisubunit membrane protein, is one of the fundamental components of the respiratory chain. It catalyzes

electron transfer from ubiquinol to cytochrome c, while the process is coupled to electrogenic translocation of protons across inner mitochondrial membrane.

The proton motive Q cycle is a widely accepted model for the functioning of this protein (Lange *et al.,* 2001). The third complex (or ubiquinol-cytochrome c reductase) complex is composed of 10 subunits. It accepts electrons from Rieske iron-sulfur protein and transfer electrons to cytochrome c. Cytochrome bc1 complex is composed of 10 proteins in *S. cerevisiae*. Only one of them is encoded by mitochondrial DNA: CTYb (44kDa) (Güldener *et al*., 2005). This is the organizing component of the bc1 complex (Zara *et al*., 2004). The other subunits are all encoded by nuclear genes and are translated on cytoplasmic ribosomes as precursors that are proteolytically processed in one or more steps during transport into their designated internal compartment of the mitochondria. CTYb has protein-protein interactions with Qcr9 and suppresses the transcription of QCR2 (Güldener *et al*., 2005). CYT1 (cytochrome c1) accepts electrons from Rieske protein and transfers electrons to cytochrome c in the mitochondrial respiratory chain. Its disruption blocks respiration. It has no stated interactions other than with the members of complex III. Its expression is regulated by the heme-activated, glucose-repressed Hap2/3/4/5 CCAAT-binding complex.

The protein Qcr1 (precursor size is 50 kDa), an essential subunit of bc1 complex, is required to convert apocytochrome b to mature cytochrome b. It may also mediate formation of the complex between cytochromes c and c1. It is regulated by heme although it is not a heme protein. The protein Qcr2 (40.5 kDa) is also regulated by heme although it is not a heme protein. It is a component of the bc1 complex and it also required for assembly (Güldener *et al*., 2005).

The protein encoded by QCR6 (17 kDa), is another component of bc1 complex. It may help bind CYT1 to CYC1 (cytochromes c and c1). It has a protein-protein interaction with Sin4. Product of QCR7 (15 kDa) gene plays a role in formation of complex bc1 (Güldener *et al*., 2005). This gene is essential for respiration. This subunit faces the matrix and is involved in the uptake of protons from the matrix (Malaney *et al*., 1997). It binds to ubiquinone and stabilizes ubisemiquinone radicals.

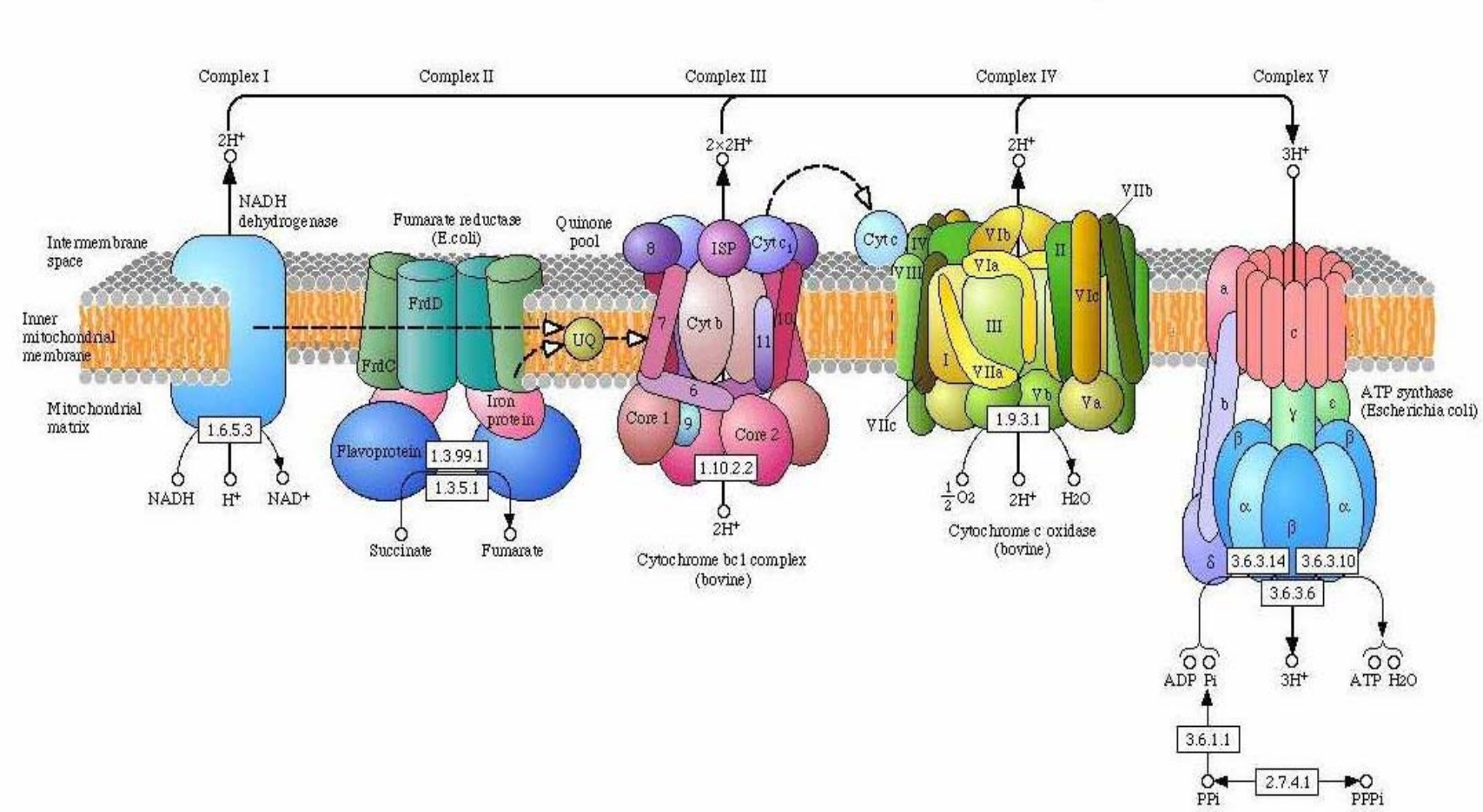

Figure 1.5. General picture of the respiratory chain. The numbers in boxes are the EC numbers of the proteins involved in complexes (KEGG Encyclopaedia, 2002)

QCR7 is the ubiquinol-cytochrome-c reductase subunit 7. It forms the core subcomplex together with QCR8 and cytochrome c. It is an essential component of the complex and its absence causes complete respiratory deficiency. QCR7 forms complex III with QCR6, 8, 9, 10, RIP1, COR1, COR2, CYT1 and COB. It interacts with DUO1 which is a cell cycle protein and BZZ1 which is involved in stress response and chemo-perception. QCR7 also forms a mini-complex with UBC4; which is involved in protein folding, modification and destination together with cellular transport and cell rescue defense and UFD4; which degrades ubiquitin fusion proteins (Figure 1.6 and Figure 1.7).

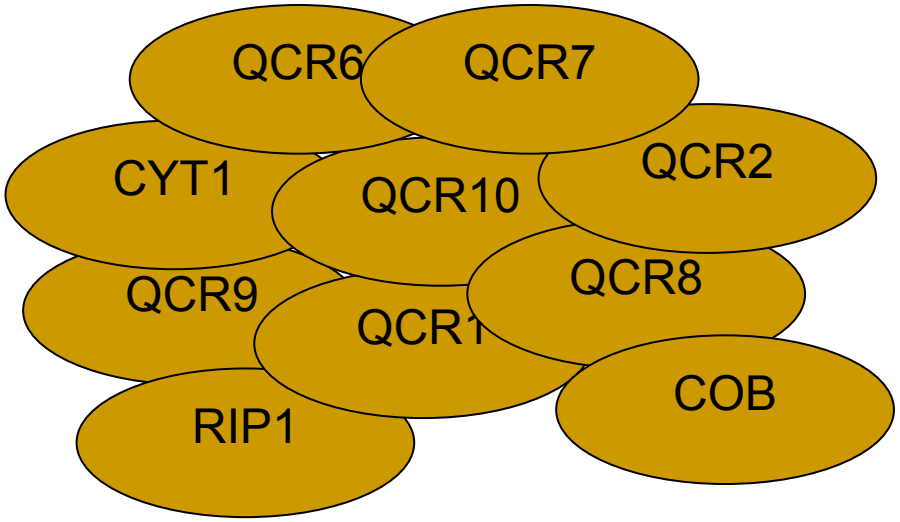

Figure 1.6. Hypothetical representation of the respiratory chain complex III

QCR7 forms an initial core complex with QCR8 that is essential for subsequent assembly of mature complex (Güldener *et al*., 2005). Deletion of the genes encoding either QCR subunits 7 or 8 results in a more severe phenotype than the deletion of the rest of the subunits. Moreover, deletion of either CYTb, QCR7 or QCR8 causes a strong decrease in the concentrations of the other two components. It may also be suggested that these three proteins may form a nucleating subcomplex in the lipid bilayer of the inner mitochondrial membrane, around which the other subunits are assembled (Zara *et al*., 2004). Transcription of QCR8 (11 kDa) needs HAP2/3/4 complex for rapid induction during transition from repressed to derepressed conditions. ABF1 may act in coordination with HAP2/3/4 complex while CPF1 is a negative regulator modulating the induction response. QCR8 also has an upstream binding site for MIG1 (Güldener *et al*., 2005).

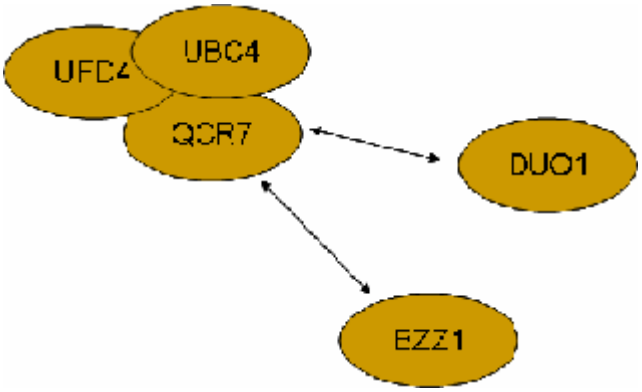

Figure 1.7. Hypothetical representation of the interactions of QCR7

QCR9 (7.5 kDa) is also essential for formation of a fully functional bc1 complex. It interacts with RIP1. It contains an intron that is nearly identical to the intron of COX4 suggesting coordinated regulation of splicing. QCR10 (8.6 kDa) is subunit of bc1 complex, whose presence is probably required for stable association of the Rieske iron-sulfur protein (RIP1).

RIP1 is the ubiquinol--cytochrome-c reductase iron-sulfur protein precursor. It is involved in electron transport and membrane associated energy conservation. Its disruption causes complete respiratory deficiency. It is located in the respiratory chain complex III as QCR7 and it interacts with the RNA export mediators GLE1 and GLE2 other than its role in complex III (Güldener *et al*., 2005) (Figure 1.8).

The last component is the cytochrome c1 (CYT1 or CTC1, 34 kDa). The function of the protein encoded by this gene is accepting electrons from Rieske Fe-S protein and transferring electrons to cytochrome c (Güldener *et al*., 2005). It contains a heme, and it has an upstream binding site for MIG1 as well as being a target gene for the binding factor HAP4 (Schüller, 2003). The expression of CYT1 closely follows the expression of HAP4 in rich medium containing glucose. (Lascaris *et al*., 2004).

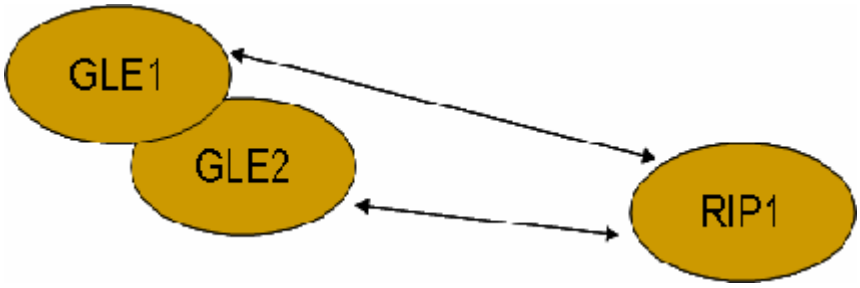

Figure 1.8. Hypothetical representation of interactions of RIP1

The catalytic subunits of bc1 complex are COB, CYT1 and RIP1. These proteins, together with the other non-catalytic subunits (QCR1, QCR2, QCR6, QCR7, QCR8, QCR9, QCR10), assemble to form an enzymatically active complex. The analysis of the steady state levels of these subunits has suggested that the assembly pathway of this complex occurs in a coordinated fashion, involving the formation of specific assembly intermediates. According to this model, cytochrome b initially forms a subcomplex with QCR7 and QCR 8, which subsequently joins with the QCR1 and QCR2 proteins. Cytochrome c1, on the other hand, is proposed to form another subcomplex with QCR6 and QCR9. Formation of each of these subcomplexes ensures stability against proteolytic attack for the individual subunits contained within them. The cytochrome b and cytochrome c1 subcomplexes subsequently unite to form a 'cytochrome bc1 precomplex' prior to the assembly of the Rieske FeS protein and, presumably, the non-essential subunit QCR10. (Stuart, 1999).

Complex IV: The fourth complex, cytochrome c oxidase is composed of 11 subunits and this complex is responsible for transfering electrons from cytochrome c to molecular oxygen. Cytochrome c oxidase may exist either in a monomer or a dimer in the mitochondrial membrane. There is also evidence that it forms a dimer with complex III (Stuart *et al*., 2000, Berden *et al*., 1998).

Complex V: ATP synthase, which catalyses the conversion of ADP + P_i to ATP is the fifth complex. In *S. cerevisiae*, mitochondrial ATPase is of F type. This F0/F1 ATP synthase complex is composed of 18 types of proteins, three of which are encoded by mitochondrial DNA (Güldener *et al*., 2005).

1.2. Regulation of Respiration

The yeast *Saccharomyces cerevisiae* has a predominantly fermentative metabolism. When grown on media containing glucose as carbon source, yeast cells repress their respiratory metabolism up to the point where all glucose has been consumed, leaving only ethanol as carbon source. In order to use ethanol, the cell has to reprogram its metabolism, a phase called "diauxic shift". This reprogramming is under the control of the HAP complex. The HAP complex is a heteromeric transcriptional regulator composed of four proteins. HAP2, HAP3 and HAP5 associate to form the DNA-binding part, while HAP4 contains the activation domain (Buschlen *et al*., 2003).

Expression of HAP4 is repressed to a low level in the presence of glucose and induced when only non-fermentable carbon sources are available, while HAP2 and HAP3 are expressed constitutively. This suggests that HAP4 is necessary for activity of the Hap2/3/4/5 complex (van Maris *et al*., 2001). The HAP complex controls the complete TCA cycle and related pathways. All subunits of the respiratory chain complex III possess the CCAAT binding site required for HAP4 and their expressions are reduced even down to 29 per cent in the absence of this gene (Buschlen *et al*., 2003). The HAP complex is originally identified as up-regulating the expression of cytochrome c and later on of several genes encoding TCA cycle and respiratory chain enzymes. The expressions of several hundred genes are controlled directly or indirectly by the HAP complex (Buschlen *et al*., 2003). Presence of a fermentable substrate like glucose inhibits the expression of HAP4 via the Mig1 pathway, and hereby the activation of respiration is prevented at high glucose concentrations (Raghevendran *et al*., 2005).

The HAP complex is also known to regulate ammonia metabolism and the nitrogen catabolite repression via regulation of the activity of two major enzymes in ammonia metabolism, GDH1 and GDH3 (ter Schure *et al*., 2000).

The HAP complex interacts with STD1; a protein kinase activator, TUP1; a stress response and DNA damage regulator, SSN6; repressor of SUC2 at high glucose levels, LYS14; a lysine pathway transcriptional activator, MTH1; a negative regulator of HXT gene expression, SNF3; the sensor of low external glucose concentrations, RGT1; a

transcriptional activator, RGT2; the sensor of high external glucose concentrations and SUC2; which is involved in molecular hydrolysis. The Figures 1.9 and 1.10 show HAP4 as a part of the glucose uptake regulatory mechanism and the respiratory regulation, respectively.

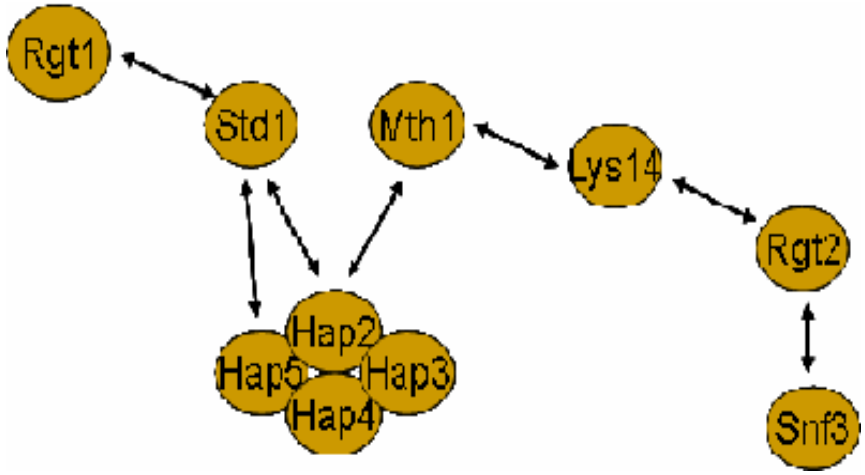

Figure 1.9. Hypothetical representation of HAP complex interactions in glucose uptake mechanism

MIG1 is a transcriptional repressor involved in glucose repression of SUC, GAL and MAL genes together with CAT8. It mediates repression at high glucose concentrations. HAP4 gene is also under MIG1 control hence affecting fermentation and respiration mechanisms utilizing fermentable carbon sources. MIG1 deletion has a greater impact on peripheral functions than on central metabolism. However, a deletion of MIG1 is not able to eliminate glucose repression entirely (Klein *et al*., 1998). This may be due to the fact that MIG1 binding sites can also function as activating elements in the absence of MIG1 (Schüller, 2003). Its systematic deletion has no effect on the expression of HAP4 though HAP4 is a MIG1 repressed regulator. HAP4 and CYT1 possess binding sites for MIG1. It forms a complex with MSS116 which is required for splicing of group II introns of COX1 and COB and with NOP12 which is involved in nucleic acid binding. The complex interacts with MUD2 which is an mRNA splicing factor, TPS1 which is a probable regulator of glucose influx and glucose induced signaling activation, CUS1 which is involved with protein fate and binding and YPL025c whose coding sequence contains DNA dependent SNF3 supressor element (Figure 1.11).

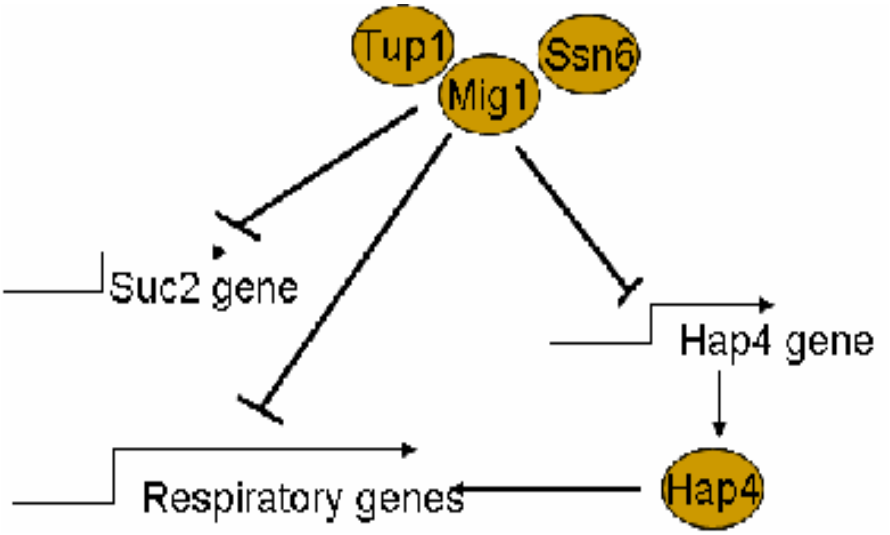

Figure 1.10. Hypothetical representation of HAP4 interactions in respiratory regulation

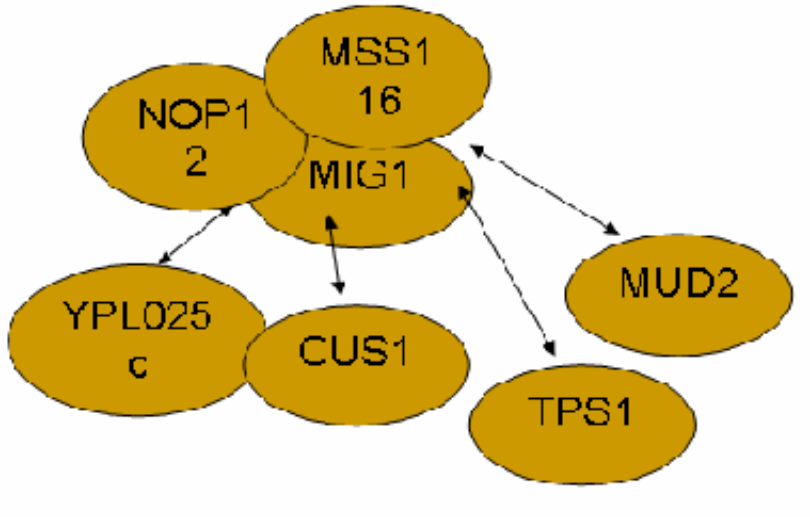

Figure 1.11. Hypothetical representation of interactions and complex formation of MIG1

1.3. YDL227c and YBR043c

HO (YDL227c) encodes the homothallic switching endonuclease enzyme. The enzyme resides under the functional category of cell cycle and DNA processing. It is a site-specific endonuclease that cleaves a site in the MAT locus on chromosome III by making a double-strand cleavage. It belongs to the mating type switching pathway and there is no evidence for it having any distinct interactions or involvement in complex formations. HO is used because it has been demonstrated to be a neutral site for replacement (Baganz *et al*., 1998). HO has no known role, apart from mating-type switching and it has been used as

the site of insertion of heterologous genes in brewing yeasts without any perceptible effect on fermentation characteristics of the organism or the quality of the product. Competition experiments between *HO* deletion mutants and their wild-type parents confirms HO gene being a neutral site for replacement (Baganz *et al*., 1997).

QDR3 is a multidrug transporter, functioning as a quinidine, barban, cisplatin, and bleomycin resistance determinant. It resides under the functional category of cellular transport, transport facilitation and transport routes. It is located in the plasma membrane. It interacts with FBP26 which is an enzyme involved in the phosphate metabolism in glycolysis and SMD1 which is involved in transcription, protein fate and essential for pre-mRNA splicing. The interactions are shown in Figure 1.12.

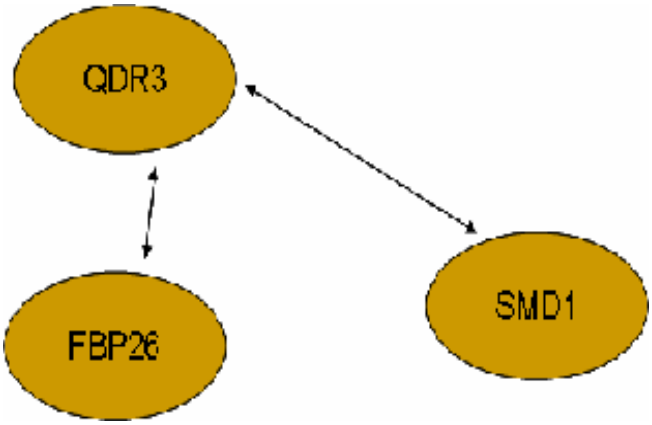

Figure 1.12. Interactions of QDR3

Recent findings indicate that QDR3 expression is required for increased tolerance of *S.cerevisiae* to a broad range of inhibitory compounds, structurally and functionally unrelated, including the quanoline-containing antiarrythmia and antimalarial drug quinidine, and the post-emergence herbicide barban. (Tenreiro *et al*., 2005). However, several studies hint at this protein being involved in other various mechanisms one of them being the ammonia metabolism and the nitrogen catabolite repression. QDR3 is found to possess a common sequence promoter element with one of the nitrogen regulated genes, GLN1 (ter Shure *et al*., 2000). Another recent work presents QDR3 as a plasma membrane associated protein involved in glucose transport and/or galactose metabolism through a computational method called Annotation Via Integration of Data (AVID) (Jiang and Keating, 2005). This gene was found to be not completely unrelated with respiratory

processes through growth on glycerol and ethanol within the framework of the present thesis.

1.4. Stoichometric Models of *S. cerevisiae*

The knowledge of a complete genome sequence holds the potential to reveal the 'blueprints' for cellular life. The genome sequence contains the information to propagate the living system, and this information exists as open reading frames (ORF) and regulatory information (Edwards and Palsson, 2000). Mathematical models of the cellular metabolism have a special interest within biotechnology. Many different kinds of commercially important products are derived from the cell factory, and metabolic engineering can be applied to improve existing production processes, as well as to make new processes available. Both stoichiometric and kinetic models have been used to investigate the metabolism, which has resulted in defining the optimal fermentation conditions, as well as in directing genetic changes to be introduced in order to obtain a good producer strain or cell line. With the increasing availability of genomic information and powerful analytical techniques, mathematical models also serve as a tool for understanding the cellular metabolism and physiology (Gombert and Nielsen, 2000).

The complex composition of a biological system requires the use of computational tools to describe its integrated function. Genome-scale models have focused primarily on metabolism and associated transcriptional regulation, but are aimed at a complete representation of an organism and have already been used to simulate cell behavior under a variety of conditions (Price *et al*., 2004).

Baker's yeast, *Saccharomyces cerevisiae*, was the first eukaryotic genome that was fully sequenced, annotated, and made publicly available. Along with its industrial importance, *S. cerevisiae* serves as a model organism for understanding and engineering eukaryotic cell function (Förster *et al*., 2003). To gain insight into cell synthesis and the metabolic capability through mathematical modeling, a natural first step is to reconstruct the underlying metabolic network, as this is responsible for the synthesis capacity of the cell, and, as well, it allows detailed analysis of the interactions between the individual pathways functioning in the cell. A genome scale reconstruction of a metabolic network is

currently a non-automated and iterative decision making process. Once a metabolic network is reconstructed, mathematical models, such as convex analysis and linear programming, can be applied to analyze structural properties, such as connectivity, etc., and simulation of cellular behavior under different genetic and physiological conditions can be conducted (Förster *et al.*, 2003).

1.5. Flux Balance Analysis

Metabolic engineering is defined as directed improvement of product formation or cellular properties through the modification of specific biochemical reactions or the introduction of new ones with the use of recombinant DNA technology (Olsson and Nielsen, 2000) and thus seen as a rational approach for the development of production strains (Buchholz *et al.*, 2002).

Metabolic pathways are sequences of biochemical reaction steps connecting a specified set of input and output metabolites. The rate at which input metabolites are processed to form output metabolites is named “pathway flux” (Olsson and Nielsen, 2000). A method for the *in silico* analysis of metabolic networks is the constraints-based approach. This approach is based on the fact that the underlying cellular functions of biochemical reaction networks are subject to certain constraints that limit their possible behaviors. In this approach, “hard” physicochemical constraints are used to define a closed solution space within which the steady-state solution to the flux vector must lie. The “best" solution is then found in the solution space using linear optimization. This analysis method has been called flux-balance analysis (FBA). The constraints-based framework, with FBA, has been used successfully to predict time course of growth and by-product secretion, effects of mutation and knock-outs, and gene expression profiles. Further, incorporation of transcriptional regulatory events in FBA is shown to be useful in interpretation and prediction of the effects of transcriptional regulation on cellular metabolism at the systemic level (Palsson, *et al*. 2001).

Previously, FBA found several applications in studying metabolic networks based on genomic, biochemical, and strain specific information. Edwards and Palsson

computationally mapped the metabolic capabilities of *E. coli* using FBA and examined the optimal utilization of the *E. coli* metabolic pathways as a function of environmental variables. They have used an *in silico* analysis to identify seven gene products of central metabolism (glycolysis, pentose phosphate pathway, TCA cycle, electron transport system) essential for aerobic growth of *E. coli* on glucose minimal media, and 15 gene products essential for anaerobic growth on glucose minimal media (Edwards and Palsson, 2000). In another study, the metabolic network in the yeast *Saccharomyces cerevisiae* was reconstructed using currently available genomic, biochemical, and physiological information. The metabolic reactions were compartmentalized between the cytosol and the mitochondria, and transport steps between the compartments and the environment were included (Förster, *et al*. 2003).

An important application of FBA is the prediction of phenotypic effects arising from complete or partial metabolic gene deletions. A complete gene deletion is implemented by constraining the corresponding flux to zero. Linear programming provides then the flux distribution and maximal growth yield for the new genotype. Crucially, this approach assumes that the mutant bacteria display an optimal metabolic state; yet, mutants generated artificially in the laboratory are generally not subjected to the same evolutionary pressure that shaped the wild type. Therefore knockouts probably do not possess a mechanism for immediate regulation of fluxes toward the optimal growth configuration. To better understand the flux states of mutants, a new procedure is introduced; the method of minimization of metabolic adjustment (MOMA) which is based on the same stoichiometric constraints as FBA, but relaxes the assumption of optimal growth flux for gene deletions. A mutant is likely to initially display a suboptimal flux distribution that is somehow intermediate between the wild-type optimum and the mutant optimum. MOMA provides a mathematically tractable approximation for this intermediate suboptimal state, based on the conjecture that the mutant remains initially as close as possible to the wild-type optimum in terms of flux values. In other words, through MOMA, we test the hypothesis that the real knockout steady state is better approximated by the flux minimal response to the perturbation than by the optimal one. Predicting a metabolic phenotype by MOMA involves a different optimization problem than FBA, namely distance minimization in flux space. (Segré *et al.,* 2002).

1.6. Reverse Transcription Quantitative Real Time Polymerase Chain Reaction

Many cellular functions are regulated by changes in gene expression. Thus, quantification of transcription levels of genes plays a central role in the understanding of gene function and of abnormal alteration in regulation that may result in a disease state (Overbergh *et al*., 2003). With the ability to measure the PCR products as they are accumulating, or in "real time", it is possible to measure the amount of PCR product at a point in which reaction is still in the exponential range. It is only during this exponential phase of the PCR reaction that it is possible to extrapolate back to determine the starting amount of the template (Ginziger, 2002). The real-time chemistries allow for the detection of PCR amplification during the early phases of the reaction. The real-time PCR system is based on the detection and quantification of a fluorescent reporter. This signal increases in direct proportion to the amount of PCR product in a reaction. By recording the amount of fluorescence emission at each cycle, it is possible to monitor the PCR reaction during exponential phase. The higher the starting copy number of the nucleic acid target, the sooner a significant increase in fluorescence is observed.

A primer is a synthetic oligonucleotide with a sequence complementary to that of a section of a DNA (or RNA) molecule of interest. Primer anneals to DNA and is extended by a polymerase, resulting in a copy of a selected region. Primers generally should be chosen from a region where sequence error is likely to be low, should be restricted to area close to/within the region of interest, should not self-hybridize or form hairpins and should be site-specific. There are several criteria required for primer design.

The recommended primer length is 18-24 nucleotides. The length of the PCR product (amplicon) should be 100-150 base pairs or 200-250 base pairs. The GC content of the primers should range between 50 per cent and 60 per cent. The 3' ends (where amplification starts) should be free of secondary and repetitive sequences. The sequences should lack complementarity to each other, especially at their 3' ends (so primer-dimer will not form). Repeats of G's or C's longer than 3 bases should be avoided. G's and C's should be placed on ends of the primer.

Most primers should have melting temperatures between 50°C and 65°C where 55°C is considered to be the best. Primers that are used together should have similar T_m values unless there is contamination, mis-priming, primer-dimer artifacts, etc.

Real-time PCR systems rely upon the detection and quantification of a fluorescent reporter. The reporter signal increases in direct proportion to the amount of PCR product in a reaction. There are two main types of reporters; DNA-binding dyes such as SYBR® Green and probes such as TaqMan® and Molecular Beacons.

In the simplest and most economical case, the reporter is the double-strand DNA-specific dye SYBR® Green. The unbound SYBR Green exhibits little fluorescence. SYBR® Green binds double-stranded DNA, and upon excitation emits light. Thus, as a PCR product accumulates, fluorescence increases. It has the advantage of being inexpensive and it is easy to use. However, it binds to any double-stranded DNA in the reaction, including primer-dimers and other non-specific reaction products resulting in an overestimation of the target concentration. Therefore it creates a sensitivity problem. Molecular Beacons are DNA hybridization probes that form a stem-and-loop structure. The loop portion of the molecule is complementary to the target nucleic acid molecule. A fluorescent marker is attached to the end of the one arm and a quencher is attached to the end of the other arm. It is advantageous in the sense that it has good specificity but it is tricky to design the loop-and-stem structure and it is expensive. TaqMan® Probes are hybridization probes relying on fluorescence resonance energy transfer (FRET) for quantification. They are oligonucleotides that contain a fluorescent dye, typically on the 5' base, and a quenching dye, typically located on the 3' base. They are designed to hybridize to an internal region of a PCR product. Their advantage is having high specificity and their high efficiency. The T_m of the probes must be significantly greater (approximately 10°C) than that of the primers, to ensure that they hybridize before the primers. This factor is affected by length and GC content and T_m is computed using many different formulae.

Molecular beacon probe sequence should be so long that, at the annealing temperature of the PCR, it is able to bind to its target and such that it dissociates from its target at temperatures 7-10°C higher than the annealing temperature of the PCR. They are typically 15-30 nucleotides long. A stem that melts 7-10°C higher than the annealing

temperature which is 5-7 base pairs long should be chosen with a very high GC content (75-100 per cent). The target amplicon should be less than 150-basepairs long. Beacon Designer (Premier Biosoft International) is one of the available softwares for design purposes.

TaqMan® probe sequence should not contain a G at their 5' ends, because this arrangement quenches reporter fluorescence, even after cleavage. It should have G/C content of around 50 per cent with about 30 bases of length. The target amplicon should be less than 250-base pairs long. Primer Express is one of the available softwares for design purposes.

The fluorescence of the reporter molecule or the dye increases as products accumulate with each successive round of amplification. The point, at which the fluorescence rises appreciably above the background, has been called the threshold cycle. There is a linear relationship between the log of the starting amount of a template and its threshold cycle during real-time PCR. Given known starting amounts of the target nucleic acid, a standard curve can be constructed by plotting the log of starting amount versus the threshold cycle. This standard curve can then be used to determine the starting amount for each unknown template based on its threshold cycle.

Performance of a real-time PCR application is evaluated by its sensitivity, uniformity and dynamic range of linear response to a variety of input sample concentrations.

Linearity deals with the dilutions of the same sample to determine baseline cycles. The purpose of the baseline cycle calculation is to characterize and correct for drift in the background fluorescence over the course of the experiment. Data are generally improved by extending the baseline cycles to include as many cycles as possible before any of the traces begin to rise above background. Since the amount of fluorescence stays constant until the baseline cycle region, this shows how linear the process is.

For sensitivity measurements, a range of dilution series of the same DNA is followed by RT-PCR. The threshold cycles of each successive replicate group were separated from its predecessor and successor by at least 3 standard deviations. Theoretically, the threshold

cycles of each replicate group should be separated by exactly 1 cycle for 2 fold dilutions and 3.3 cycles for 10 fold dilutions.

The quantification of gene expression is carried out in either of the two ways; absolute quantification which requires a known amount of DNA as the standard curve or relative quantification. The amount of DNA theoretically doubles with every cycle of PCR. After N cycles, there will be 2^N times as much DNA. Since the reaction cannot go on forever, and it eventually tails off and reaches a plateau phase. There is a linear relationship between amount of DNA and cycle number when investigated on a logarithmic scale since PCR amplification is a logarithmic reaction. On a regular scale, the linear part is the very early part of the curve.

The melting temperature of a DNA double helix depends on its base composition (and its length if it is very short). All PCR products for a particular primer pair should have the same melting temperature - unless there is contamination, mis-priming, primer-dimer artifacts, or some other problem. At the melting point, the two strands of DNA will separate and the fluorescence will rapidly decrease. The rate of change of the fluorescence with temperature will be recorded against the temperature and this will result in a peak at the melting temperature (T_m). If the peaks are not similar, this might suggest contamination, mis-priming or primer dimer artifact.

The threshold value of the reaction should be in the linear part of the reaction curve. The threshold should be high enough that you are sure that reactions cross the line due to amplification rather than noise. The same threshold should be used for all the samples in the same experiment on the same plate. The C_t values can be plotted for the dilutions against concentration - the result is a linear graph. It should have an excellent correlation coefficient (more than 0.990) to be used in absolute quantification. Standard curve method and the Pfaffl method are the two methods used in relative quantification with respect to reference genes. Relative quantification requires the presence of control and housekeeping genes to be taken as reference. The housekeeping gene should not be regulated or influenced by the experimental procedure (Radonic *et al*., 2004).

There are a few numbers of applications of RT-rtqPCR cited in literature. Overbergh *et al.,* 2003 determined cytokine gene expression through this method. Cell concentrations of *Bacillus cereus*, *B. subtilis* and *Pseudomonas fluorescens* in liquid culture were monitored by TaqMan®-PCR using the 16S rDNA target sequence of *Escherichia coli* as external standard for quantification (Bach *et. al*, 2002). In the study by Neuvians *et al.,* 2003 real-time RT-PCR using SYBR® Green I detection was employed to determine mRNA expressions of the following factors: ubiquitin (UBQ), insulin-like growth factor I (IGF I), IGF II, IGF-receptor type 1 (IGFR-1), growth hormone receptor (GH-R) and IGF-binding proteins-1–6 (IGFBP-1–6). Pfaffl *et al.,* 2001, have examined the tissue-specific mRNA expression of ERa and ERb in various bovine tissues using real-time RT-PCR. Reist *et al.,* 2003 carried out Quantitative mRNA Analysis of Eight Bovine 5-HT Receptor Subtypes in Brain, Abomasum, and Intestine by Real-Time RT-PCR. A SYBR® Green LightCycler PCR assay using a single primer pair allowed simultaneous detection of *stx1* and/or *stx2* of *Escherichia coli* O157:H7. A distinct sequence of the Shiga-like toxin genes was amplified to yield products of 227 and/or 224 base pairs, respectively. The two products were distinguished by melting point curve analysis (Jothikumar and Griffiths, 2002). Pfaffl *et al.*, 2003, have examined the tissue-specific mRNA expression pattern of androgen receptor (AR), both estrogen receptor (ER) subtypes ERα and ERβ and progestin receptor (PR) in 10 bovine gastrointestinal compartments. To quantify the very low abundant steroid receptor mRNA transcripts sensitive and reliable real-time (kinetic) reverse transcription (RT)-PCR quantification methods were validated on the LightCycler.

1.7. The Aim of This Thesis

This study aims to improve present knowledge on the regulatory mechanism of respiratory chain in *S. cerevisiae* and ultimately to provide a rational design strategy for the construction of a high ethanol production strain.

For this purpose, metabolic profiles and growth behavior of seven deletion mutants ΔHO, ΔQDR3, ΔMIG1, ΔHAP4, ΔQCR7, ΔRIP1 and ΔCYT1 together with the wild type strain BY4743 were investigated in batch and continuous cultivations. Batch experiments involving nutritional limitations and pulse injections were also carried out for the wild type strain and HAP4 gene expression profiles were obtained under different nutritional

stresses. Flux balance analysis on small scale and genomic scale were performed as well as minimization of metabolic adjustment procedure. Principle component analysis was also carried out to reveal information about the functional relations of the genes investigated within this study and the relevancy of the metabolites measured in the study.

The experimental and computational methods pursued as well as the materials are explained in detail in the Materials and Methods section. Results section covers all experimental and computational findings that are obtained in a compact form. The details are left to the Appendix as well as the computational codes and inputs. The comprehensive argument of the obtained results is given in Discussion. The study is summarized with important key points in the Conclusions and Recommendation section. Some new techniques and additional work to improve the study is suggested also in the same section.

2. MATERIALS AND METHODS

2.1. Materials

2.1.1. Microorganisms

The parent strain *Saccharomyces cerevisiae*, BY4743 (MATa/MATα his3Δ1/his3Δ1 leu2Δ0/leu2Δ0 lys2Δ0/+ met15Δ0/+ ura3Δ0/ura3Δ0) seven homozygous deletion mutants of this strain ΔHO, ΔQDR3, ΔMIG1, ΔHAP4, ΔQCR7, ΔRIP1 and ΔCYT1 were used in the experiments.

These strains were kindly provided by Prof. Stephen G. Oliver (Faculty of Life Sciences, University of Manchester). The deletion mutants were generated by European *Saccharomyces cerevisiae* Archive for Functional Analysis (EUROSCARF).

2.1.2. Maintenance

For long term storage of the cultures, approximately 50 ml of complex (YPD) medium was inoculated with a single colony of cells and was incubated overnight at 30^{o}C and 180 rpm agitation. Frozen stocks of 2 ml were prepared by mixing equal volumes of culture with 30 per cent (v / v) glycerol. The stocks were kept at -80^{o}C.

YPD agar plates were inoculated with a frozen stock of 2 ml, the cells were spread evenly onto the plates and they were left to grow at 30^{o}C overnight. The plates were kept at 4^{o}C and were used for the inoculation of the fermenters.

200 µg/ ml of geneticin was added to the media of the deletion mutants in order to ensure presence of geneticin resistant deletion mutants only.

Solid media stocks were renewed monthly while frozen stock renewal was carried out twice a year.

2.1.3. Chemicals and Disposable Materials

2.1.3.1. Culture Media Complex medium (YPD) in solid and liquid forms and F1 medium with limitations on carbon and nitrogen as well as its non-limited form were used as culture media in the experiments. The compositions were as follows in (w/v) for solids and (v/v) for liquids:

YPD

Yeast Extract 1 per cent (Lab M), Bacteriological Peptone 2 per cent (Acumedia), D-Glucose 2 per cent (Merck) – for solid media Agar-Agar 1.8 per cent (Merck).

Glucose was added from previously prepared stocks after sterilization of the remaining of the media.

F1

D-Glucose 2.1 per cent or 0.21 per cent in limited cases (Merck), $(NH_4)_2SO_4$ 0.313 per cent or 0.0313 per cent in limited cases (Merck), KH_2PO_4 0.2 per cent (Merck), $MgSO_4.7H_2O$ 0.055 per cent (Merck), NaCl 0.01 per cent (Merck), $CaCl_2.2H_2O$ 0.009 per cent (Merck), Uracil 0.002 per cent (Fluka), Histidine 0.002 per cent (Lifco), Leucine 0.01 per cent (Merck), Trace Element Solution 1 0.01 per cent, Trace Element Solution 2 0.01 per cent, Vitamin Stock Solution 0.17 per cent.

Trace Element Solution 1

$ZnSO_4.7H_2O$ 0.07 per cent (Merck), $CuSO_4.5H_2O$ 0.01 per cent (Merck), H_3BO_3 0.01 per cent (Merck), KI 0.01 per cent (Merck)

Trace Element Solution 2

$FeCl_3.6H_2O$ 0.05 per cent (BDH)

The filter sterilized vitamin stock solution was added after the sterilization of the rest of the medium, except for glucose 6 hours prior to inoculation. The glucose stock was added half an hour before inoculation in order to prevent undesired phenomena such as Malliard reactions.

Vitamin Stock Solution

Inositol 3.72 per cent (Merck), Thiamine / HCl 0.84 per cent (Sigma), Pyridoxine 0.24 per cent (Fluka), Ca-panthothenate 2.4 per cent (Fluka), Biotin 0.018 per cent (Merck)

2.1.3.2. Kits Enzymatic kits for acetaldehyde, acetic acid, D-glucose, ethanol, glycerol and succinic acid concentration determination were purchased from BOEHRINGER MANNHEIM – Roche and kits for pyruvate concentration determination was purchased from Sigma.

DNeasy Tissue Kit (50) for DNA extraction, RNeasy MiniKit (250) for RNA extraction and QuantiTect SYBR Green RT-PCR Kit for reverse transcription real time quantification polymerase chain reaction (one step procedure) were purchased from Quiagen.

2.1.3.3. Buffers and Chemicals Required for Polymerase Chain Reaction Applications All primers were provided from Integrated DNA Technologies, Inc. Hind III, Buffer E, Taq Polymerase, $MgCl_2$ and Mg Free PCR Buffer were provided from Promega. λDNA was purchased from New England Biolabs and dNTP mix was supplied by Biorad.

5X TBE (Tris Borate) Buffer which was required for agarose gel electrophoresis was as follows:

Tris Base 5.4 per cent (Merck), Boric Acid 2.75 per cent (Merck), EDTA 0.01 M (Fluka)

1 per cent Agarose Gel was prepared as follows:

Agarose 1 per cent (BDH), 0.5X TBE Buffer, Ethidium Bromide 0.008 per cent (AppliChem)

Bromophenol Blue (Merck) was used in loading the gel with samples.

2.1.3.4. Miscellaneous Other chemicals used in various processes and applications were as follows:

Lyticase (Sigma), Geneticin (Sigma), β-mercaptoethanol (Merck), Absolute Ethanol (Sigma), DEPC (Sigma), RNase Away (Invitrogen), Perchloric Acid (Merck), Glycerol (Merck), Nitric Acid (Merck), Methanol (Merck), Hepes (Sigma), RNAlater – RNA Stabilization Reagent (Quiagen), Tris .Cl (Merck), D-Sorbitol (Fluka).

Disposable plasticware as well as the PCR tubes were supplied by USA Scientific Inc. iCycler 96 well PCR Plates and Optical Tapes were purchased from BIORAD. Millex Sterile filter units (0.22 μm) were provided from Millipore.

2.1.4. Laboratory Equipment

Autoclave	Eyela Model MAC-601(Japan)
Balance	Precisa 80A-200M (Switzerland)
Centrifuges	SORVALL RC-5B Refrigerated Superspeed Centrifuge, DuPont (USA) Eppendorf 5415 C (Germany)
Deep freezers	-80^{o}C, Hetofrig CL410, HETO (Denmark) -20^{o}C, BOSCH (Germany)
Dismembrator	Biolab Micro-Dismembrator S (New England, USA)
Electrophoresis Equipment	Horizon 58, Model 200, Horizontal Gel Electrophoresis Apparatus, BRL (USA)
Fermenter	Bioflo III Batch/Continuous Fermenter, New Brunswick (England)

Heating Magnetic Stirrers	MR 3001, Heidolph (Germany) Scientifca ARE, VELP (Italy)
Incubators	NÜVE EN500 (Turkey)
Laminar Flow Cabinet	HBB 2460 LaminAir, Holten (Denmark)
Orbital Shakers	GFL 3032, GFL (Germany) INNOVA 4340 Illuminated refrigerated Incubator Shaker, New Brunswick Scientific (USA)
Refrigerators	+4^{o}C Ariston (Italy) +4^{o}C Arçelik (Turkey)
Rotavapor	HETO VR1 (Denmark)
Sonifier	Labsonic 1510, B.Brown (Germany) Model 250/450 Sonifier Branson Ultrasonic Co., USA
Spectrophotometer	DU 640 Beckman (USA)
Thermo-cyclers	Thermal Reactor TR1, HYBAID (UK) GeneAmp PCR System 9600 Perki-Elmer Cetus (USA) BIORAD iCycler (USA)
Transilluminators	Reprostar II, CAMAG (Switzerland) Foto/uv 15, Fptpdyne (USA)
Vortex	Elektromag (Turkey)
Water Baths	HETO, CB 8-30e AT_{110} (Denmark) HETO, CB 8-30e DT_1 (Denmark) HETO DT Hetotherm (Denmark)

Water Purification Systems	Millipore, Milli Ro Plus (USA)
	Millipore, Milli-Q UF Plus (USA)

2.2. Methods

2.2.1. Experimental Methods

2.2.1.1. Sterilization Throughout this study, contamination in any form was prevented by sterilization. Generally, steam sterilization was preferred due to its short cycle time and good penetration properties. The sterilization was performed in an autoclave at 15 psig pressure at 121^{o}C. Prior to the process every source of external contact that may occur after the sterilization was prevented by taking appropriate measures into account, such as sealing the necks of bottles.

The duration of sterilization was varied according to the nature of the material to be sterilized. For culture media and any sort of chemical stock solutions except for glucose, the sterilization time was set to 15 minutes. Glucose was an exception to this because of its highly susceptible nature to caramelization at elevated temperatures. Therefore its sterilization time was limited to 3 minutes. All glassware and plasticware that were to be used were steam sterilized for 20 minutes. The fermenters and their complementary parts which were used in chemostat and batch experiments were also sterilized for 15 minutes.

As an exception to steam sterilization method, another type, filter sterilization was preferred for the sterilization of the vitamin stock solution which was a component of the F1 medium. Vitamins, due to their nature are heat degradable. Therefore steam sterilization was not suitable for the vitamin sock solution. As an alternative, this solution was filter sterilized using 0.22 μm sterile Millipore disposable filter units in the sterile laminar flow cabinet.

2.2.1.2. Growth on Non-Fermentable Carbon Sources YPethanol (YPE) 2 per cent and YPglycerol (YPG) 2 per cent agar plates were prepared. A single colony of cells was diluted in 200 μl of sterile water. 20 μl of this solution was transferred onto 120 μl of sterile water in another Eppendorf tube. A set of 6 dilutions were prepared as such. On

each plate, 2 µl of 6 dilutions were spotted in order of dilution. The plates were left to inoculate for 48 hours at 30^{o}C. The cell growth was expected to yield a qualitative conclusion on the level of respiratory deficiency of the strain.

2.2.1.3. Cultivation Conditions All precultures were prepared as 150 ml of YPD medium corresponding to 10 per cent of the volume of the batch and the chemostat cultures. They were harvested with a single colony of cells from agar plates. The colonies were inoculated via flame sterilized inoculation needles. The precultures were incubated in orbital shakers at 30^{o}C and 180 rpm. The preculture was ready to be used at its late exponential phase when the optical density was measured to be between 0.9 and 1.1.

Batch cultivations were carried out in 3 L Erlenmayer flasks with a cultivation volume of 1.5 L of YPD medium. The experiments were carried out at 30^{o}C and 180 rpm in orbital shakers. 5-10 ml of preculture was used to inoculate the culture. The pH was kept between 5.5 and 6.5. Samples were collected on an hourly basis.

Chemostat cultivations were carried out in BIOFLO3000 fermenters with a working volume of 1.5 L of YPD medium. The temperature was kept constant at 30^{o}C via PID controllers and the agitation was set to 400 rpm. 5-10 ml of preculture was used to inoculate the culture. The dilution rate was set to 0.1 hr^{-1} and the cultivations lasted to circulate three reactor volumes of fresh medium in the fermenter. The pH is kept between 5.5 and 6.5. Supernatant collection was carried out on a regular basis.

Batch cultivation with pulse injection experiments were carried out as batch experiments in BIOFLO3000 fermenters and in the orbital shaker. F1 medium with C limitation, N limitation or without any limitations were used as prescribed before. The batch volume in limited cases was 2.5 L and they were inoculated with 15-20 ml of preculture. For the no limitation case, the batch volume was 1.5 L and it was inoculated with 5-10 ml of preculture. The temperature was maintained at 30^{o}C and the agitation was 400 rpm for the BIOFLO3000 fermenters while it was 180 rpm for the orbital shakers. The pH of the media was maintained between 5.0 and 5.5. Sampling was carried out every 4 hours for the no limitation case until the end of the experiment. For the limitation cases, sampling was on a four hourly basis until the first pulse injections of glucose or

ammonium sulfate to the carbon limited or nitrogen limited cultures, respectively. For both cultures, four samples from each batch were taken for RNA extraction purposes in the first minute after the pulses were given and then for the same purpose samples were taken on 15 minute basis for the first 2.5 hours. Then sampling time was extended to hourly and two hourly basis until steady state was reached where the second pulses were given. The exact procedure was carried out again. Sampling for extracellular metabolites was carried out on hourly and two hourly bases at all times. The pulses which were introduced into the cultures were adjusted such that they aimed to reserve the system to concentrations of no limitation. In order not to alter the inner dynamics of the batch cultivation system, small volumes, namely 30 ml aqueous solutions of glucose and ammonium nitrate were used in every injection.

2.2.1.4. Sample Preparation and Storage Samples for extracellular metabolite analyses were collected in 2 ml Eppendorf tubes. They were centrifuged at 8000 rpm for 6 minutes in the Eppendorf (Germany) centrifuge with rotor 5415C. The supernatant was transferred to a new Eppendorf tube and was stored at -20^{o}C. Prior to enzymatic analyses, they were incubated at 80^{o}C for 3 minutes to cease any possible enzymatic activity that would have remained.

Samples for intracellular enzymatic analyses were collected according to the following procedure:

5 ml of sample was sprayed into 26 ml of cold solution containing 60% methanol and 70mM Hepes pH 7.5. The sample was kept on ice for 3 minutes and then centrifuged at 6800 rpm for 5 minutes at -10^{o}C in Sorvall RC 5B (DuPont, USA) centrifuge with SS-34 rotor. The supernatant was discarded. For extraction of metabolites from the cell pellets, 5 ml of 75 per cent boiling absolute ethanol containing 0.25M Hepes at 7.5 pH was used. The samples were incubated at 80^{o}C for 3 minutes and then cooled down on ice for 3 minutes. Their volume was reduced by evaporation at 45^{o}C and 5 millibars using a rotavapor. The residue was resuspended to a final volume of 1 ml and was centrifuged for 10 minutes at 6800 rpm at 4^{o}C to remove insoluble particles. The supernatant was stored at -20^{o}C until use.

For RNA extraction, samples were shock frozen in equal volume of culture and RNA stabilization solution. They were kept at -80^{o}C until use.

2.2.1.5. Determination of the Cell Dry Weight The optical density was determined by the spectrophotometer at a wave length of 600 nm. Then this value was converted to weight using pre-prepared calibration charts individually created for each strain.

The calibration charts were prepared from batch cultures. A known volume of samples was centrifuged at 5000 rpm in Eppendorf centrifuge with rotor 5415 C for 15 minutes, the supernatant was removed and biomass was resuspended in 1 ml deionized water, it was transferred to a 1.5 ml preweighed Eppendorf tube. The cell and cell debris were precipitated by centrifugation at 14000 rpm for 10 minutes in the Eppendorf (Germany) centrifuge with rotor 5415C and the precipitate was dried at 60^{o}C for a day. The Eppendorf tube was reweighed to determine the dry weight of the cell. Dry weight versus optical density graph was plotted and a line was fitted through the data points using least square analysis. This line provides the correlation between the optical measurements obtained from the spectrophotometer and the dry weight of the cells that are used in the study.

2.2.1.6. Enzymatic Analyses for Determination of Metabolite Concentrations Concentration profiles of extracellular ethanol, glucose and pyruvate were generated for batch cultures and also final intracellular glucose and pyruvate concentrations were determined. For the chemostat cultures, metabolic profiles of extracellular ethanol, glucose, pyruvate and succinic acid as well as steady state intracellular glucose, pyruvate and succinic acid concentrations were determined. For the nutritional limitation batch experiments, extracellular acetaldehyde, acetic acid, ethanol, glucose, glycerol, pyruvate and succinic acid profiles were developed. The necessary dilutions of supernatants were carried out as indicated in the protocols prior to the analyses. The metabolite concentrations were determined by enzymatic analysis kits supplied by Boehringer – Mannheim, Germany and Sigma Aldrich, USA. The kits are used as described by the manufacturers.

Determination of Acetaldehyde Concentration

Acetaldehyde is quantitatively oxidized to acetic acid in the presence of aldehyde dehydrogenase (Al-DH) and nicotinamide- adenine dinucleotide (NAD).

$$Acetaldehyde + NAD^+ + H_2O \xrightarrow{Al-DH} acetic\ acid + NADH + H^+ \qquad (2.1)$$

The test combination contains solution I containing potassium diphosphate buffer at pH 9.0, tablets containing NAD 0.8 mg each and solution III lyophilizate aldehyde dehydrogenase containing 4 U / 0.6 ml in each bottle. Reaction mixture 2 is prepared by dissolving one tablet in 3.0 ml solution I.

In a cuvette, 1.5 ml of reaction mixture II, 0.1 ml sample were pipetted. In another cuvette as blank, 1.5 ml reaction mixture II and 0.1 ml distilled water were pipetted. They were mixed and after approximately three minutes, the absorbences (A_1) were read at 340 nm. Then 0.025 ml of solution III was added and after about 3 to 5 minutes, the reaction ceased and absorbences (A_2) were read.

Absorbance difference of the blank (A_2-A_1) was subtracted from the absorbance difference of the samples (A_2-A_1), thereby obtaining $\Delta A_{acetaldehyde}$. The concentration of the acetaldehyde was calculated by the following equation:

$$c_{Acetaldehyde} = \frac{0.7158}{\varepsilon} \Delta A_{acetaldehyde} (g/L) \qquad (2.2)$$

where ε was the extinction coefficient of NADH at 340 nm = 6.3 [L/(mmol x cm)].

Determination of Acetic Acid Concentration

Acetic acid (acetate) is converted to acetyl-CoA in the presence of the enzyme acetyl-CoA synthetase (ACS), adenosine-5'-triphosphate (ATP) and coenzyme A.

$$\text{Acetate} + \text{ATP} + \text{CoA} \xrightarrow{\text{ACS}} \text{acetyl} - \text{CoA} + \text{AMP} + \text{pyrophosphate} \qquad (2.3)$$

Acetyl-CoA reacts with oxaloacetate to citrate in the presence of citrate synthase (CS)

$$\text{Acetyl} - \text{CoA} + \text{oxaloacetate} + \text{H}_2\text{O} \xrightarrow{\text{CS}} \text{citrate} + \text{CoA} \qquad (2.4)$$

The oxaloacetate required for Reaction 2.4 is formed from L-malate and nicotinamide-adenine dinucleotide (NAD) in the presence of L-malate dehydrogenase (L-MDH).

$$\text{L} - \text{Malate} + \text{NAD} \xleftrightarrow{\text{L-MDH}} \text{oxaloacetate} + \text{NADH} + \text{H}^+ \qquad (2.5)$$

The test combination contains solution I containing triethanolamine buffer, pH 8.4, L-malic acid and magnesium chloride x $6H_2O$, solution II containing lyophilizate consisting of , ATP, CoA, and NAD, Solution III containing L-malate dehydrogenase, citrate synthetase and solution IV containing lyophilizate acetyl-CoA synthetase.

In a cuvette, 0.5 ml of solution I, 0.1 ml solution II, 0.05 ml sample solution, and 0.95 ml redistilled water were pipetted. In another cuvette as blank, 0.5 ml of solution I, 0.1 ml solution II and 1.0 ml redistilled water were pipetted. The absorbances (A_0) were read. The first reaction was initiated by the addition of 0.005 ml of Solution III. After about three minutes absorbences (A_1) were read again. The final reaction was carried out by the addition of 0.01 ml solution IV. After about 10-15 minutes the final absorbences (A_2) were read again.

$\Delta A_{\text{acetaldehyde}}$ was obtained as:

$$\Delta A_{\text{Acetic acid}} = \left[\left(A_2 - A_0\right)_{\text{sample}} - \frac{\left(A_1 - A_0\right)^2_{\text{Sample}}}{\left(A_2 - A_0\right)_{\text{sample}}} \right] - \left[\left(A_2 - A_0\right)_{\text{Blank}} - \frac{\left(A_1 - A_0\right)^2_{\text{Blank}}}{\left(A_2 - A_0\right)_{\text{Blank}}} \right] \qquad (2.6)$$

The concentration of the acetic acid was calculated by the following equation:

$$c_{Acetic\ acid} = \frac{1.940}{\varepsilon} \times \Delta A_{Acetic\ acid}(g/L) \quad (2.7)$$

where ε was the extinction coefficient of NADH at 340 nm = 6.3 [L/(mmol x cm)].

Determination of D-Glucose Concentration

D-Glucose is phosphorylated to D-Glucose-6-phosphate (G6P) in the presence of the enzyme hexokinase (HK) and adenosine-5'-triphosphate (ATP) with the simultaneous formation of adenosine-5'-diphosphate (ADP).

$$D-Glu\cos e + ATP \xrightarrow{HK} G6P + ADP \quad (2.8)$$

In the presence of the enzyme glucose-6-phosphate dehydrogenase (G6P-DH), G6P is oxidized by nicotinamide adenine dinucleotide phosphate (NADP) to D-gluconate-6-phosphate with the formation of reduced nicotinamine adenine dinucleotide phosphate (NADPH).

$$G6P + NADP^{+} \xrightarrow{G6P-DH} D-gluconate-6-phosphate + NADPH + H^{+} \quad (2.9)$$

The test combination contains solution I consisting of triethanolamine buffer, pH 7.6, NADP, ATP, magnesium sulphate and stabilizers, and Solution II consisting of hexokinase and glucose-6-phosphate dehydrogenase.

In a cuvette, 0.5 ml of solution I, 0.05 ml sample solution and 0.95 ml redistilled water were pipetted. In another cuvette as blank, 0.5 ml of solution I and 1.0 ml redistilled water were pipetted. The absorbencies (A_1) were read at 340 nm against air. Then the reaction was initiated by the addition of 0.01 ml of Solution II. After about 10-15 minutes, the absorbences (A_2) were read again.

Absorbance difference of the blank (A_2-A_1) was subtracted from the absorbance difference of the samples (A_2-A_1), thereby obtaining $\Delta A_{D\text{-}glucose}$. The concentration of D-glucose was calculated by the following equation:

$$c_{D-glucose} = \frac{d \times 5.441}{\varepsilon} \times \Delta A_{D-glucose}(g/L) \quad (2.10)$$

where ε was the extinction coefficient of NADH at 340 nm = 6.3 [L/(mmol x cm)] and d is the dilution factor of the sample.

Determination of Ethanol Concentration

Ethanol is oxidized to acetaldehyde in the presence of the enzyme alcohol dehydrogenase (ADH) by nicodinamide-adenine dinucleotide (NAD).

$$\text{Ethanol} + \text{NAD}^+ \xrightarrow{\text{ADH}} \text{acetaldehyde} + \text{NADH} + \text{H}^+ \quad (2.11)$$

Acetaldehyde is oxidized in the presence of aldehyde dehydrogenase (Al-DH) quantitatively to acetic acid.

$$Acetaldehyde + NAD^+ + H_2O \xrightarrow{Al-DH} acetic\ acid + NADH + H^+ \quad (2.12)$$

The test combination contains Mixture I containing potassium diphosphate buffer, pH 9.0, tablets containing NAD, aldehyde dehydrogenase and stabilizers, and Solution II consisting of ADH.

In a cuvette, 1.5 ml of mixture I and 0.05 ml sample were pipetted. In another cuvette as blank, 1.5 ml mixture I and 0.05 ml distilled water were pipetted. The absorbencies (A_1) were read at 340 nm against air. About 10-15 minutes after the addition of 0.025 ml of Solution II the absorbences (A_2) were read again.

Absorbance difference of the blank (A_2-A_1) was subtracted from the absorbance difference of the samples (A_2-A_1), thereby obtaining $\Delta A_{Ethanol}$. The concentration of the ethanol was calculated by the following equation:

$$c_{Ethanol} = \frac{d \times 0.7256}{\varepsilon} \Delta A_{Ethanol}(g/L) \quad (2.13)$$

where ε was the extinction coefficient of NADH at 340 nm = 6.3 [L/(mmol x cm)] and d is the dilution factor of the sample.

Determination of Glycerol Concentration

Glycerol is phosphorylated by adenosine-5'-diphosphate (ATP) to L-glycerol-3-phosphate in the reaction catalysed by glycerokinase (GK).

$$\text{Glycerol} + \text{ATP} \xrightarrow{\text{GK}} \text{L} - \text{glycerol} - 3 - \text{phosphate} + \text{ADP} \qquad (2.14)$$

The adenosine-5'-diphophate (ADP) formed in the above reaction is reconverted by phosphoenolpyruvate (PEP) with the aid of pyruvate kinase (PK) in to ATP with the formation of pyruvate.

$$\text{ADP} + \text{PEP} \xrightarrow{\text{PK}} \text{ATP} + \text{Pyruvate} \qquad (2.15)$$

In the presence of the enzyme L-lactate dehydrogenase (L-LDH), pyruvate is reduced to L-lactate by reduced nicotinamide-adenine dinucleotide (NADH) with the oxidation of NADH to NAD.

$$\text{pyruvate} + \text{NADH} + \text{H}^+ \xrightarrow{\text{L-LDH}} \text{L} - \text{lactate} + \text{NAD}^+ \qquad (2.16)$$

The test combination contains solution I consisting of glycylglycine buffer, pH 7.4, NADH, ATP, magnesium sulfate and stabilizers, solution II consisting pyruvate kinase and L-lactate dehydrogenase and solution III consisting of glycerokinase.

In a cuvette, 0.5 ml of solution I 0.05 ml, sample solution 0.95 ml redistilled water and 0.005 ml solution II were pipetted. In another cuvette as blank, 0.5 ml of solution I , 1.0 ml redistilled water and 0.005 ml solution II were pipetted. The absorbences (A_1) were read at 340 nm against air after 5-7 minutes. By addition of 0.005 ml of solution III the reaction began and after about 5 to 10 minutes absorbences (A_2) were read again at the same conditions both for sample and for the blank.

Absorbance difference of the blank (A_1-A_2) was subtracted from the absorbance difference of the samples (A_1-A_2), thereby obtaining $\Delta A_{Glycerol}$. The concentration of the glycerol was calculated by the following equation:

$$c_{Glycerol} = \frac{2.781}{\varepsilon} \Delta A_{Glycerol} (g/L) \tag{2.17}$$

where ε was the extinction coefficient of NADH at 340 nm = 6.3 [L/(mmol x cm)].

Determination of Pyruvate Concentration

The procedure utilizes the enzyme, lactate dehydrogenase, which catalyzes the following reversible reaction,

$$\text{pyruvate} + \text{NADH} \xleftrightarrow{\text{LD}} \text{Lactate} + \text{NAD} \tag{2.18}$$

The test combination contains Trisma base solution consisting of Trishydroxymethyl aminomethane and sodium azide, NADH solution containing disodium salt of reduced nicotinamide-adenine dinucleotide, and enzyme solution containing lactate dehydrogenase.

Before the analyses the samples needed to be deproteinized. For this process, 0.5 ml of sample was quickly sprayed in to a centrifuge tube containing 1 ml of ice cold 8 per cent perchloric acid. The mixture was vortexed for 30 seconds. And then, the sample was kept in ice for 5 minutes. The protein free supernatant was obtained after 10 min of centrifugation at 14000 rpm. After the deproteinization, 0.5 ml of sample, 0.125 ml Trisma base solution and 0.125 ml NADH solution were pipetted in a cuvette. They were mixed and the absorbences (A_1) were read at 340 nm against water as reference. By addition of 0.05 ml of lactate dehydrogenase after about five to ten minutes absorbencies (A_2) were read again at the same conditions. Absorbance difference of the sample (A_1-A_2) =$\Delta A_{Pyruvate}$ was determined. The concentration of the pyruvate was calculated by the following equation:

$$c_{pyruvate}(mmol/L) = 0.723 \times \Delta A_{pyruvatel}$$
$$c_{pyruvate}(mg/dL) = 6.37 \times \Delta A_{pyruvatel} \quad (2.19)$$

Determination of Succinic Acid Concentration

Succinic acid (succinate) is converted to succinyl-CoA by the enzyme succinyl-CoA synthetase (SCS), is also known as succinate thiokinase, and inosine-5'-triphosphate (ITP) and coenzyme A CoA with the simultaneous formation of the inosine-5'-diphosphate (IDP) and inorganic phosphate (P_i).

$$\text{succinate} + \text{ITP} + \text{CoA} \xrightarrow{\text{SCS}} \text{IDP} + \text{succinyl} - \text{CoA} + \text{P}_\text{i} \quad (2.20)$$

Inosine-5'- diphosphate (IDP) reacts with phosphoenolpyruvate (PEP) in the presence of pyruvate kinase (PK) to pyruvate and ITP.

$$\text{IDP} + \text{PEP} \xrightarrow{\text{PK}} \text{ITP} + \text{Pyruvate} \quad (2.21)$$

Pyruvate is reduced by NADH in the presence of L-lactate dehydrogenase (L-LDH).

$$\text{pyruvate} + \text{NADH} + \text{H}^+ \xrightarrow{\text{L-LDH}} \text{L} - \text{lactate} + \text{NAD}^+ \quad (2.22)$$

The test combination contains reaction mixture consisting of glycylglycine buffer, pH 8.4, NADH, CoA, ITP, PEP-CHA, Solution III consisting pyruvate kinase and L-lactate dehydrogenase and Solution IV consisting of succinyl-CoA synthetase.

In a cuvette, 0.5 ml of reaction mixture, 0.05 ml sample solution 0.025 ml solution III and 0.95 ml redistilled water were pipetted. In another cuvette as blank, 0.5 ml of reaction mixture, 0.025 ml solution III and 1.0 ml redistilled water were pipetted. The mixture was incubated at 37^{o}C for five minutes. The absorbences (A_1) were read at 340 nm against air. Then after addition of 0.01 ml of Solution IV and mixing about 20 minutes of incubation at 37^{o}C absorbences (A_2) were read again.

Absorbance difference of the blank (A_1-A_2) was subtracted from the absorbance difference of the samples (A_1-A_2), thereby obtaining $\Delta A_{Succinate}$. The concentration of the succinate was calculated by the following equation:

$$c_{Succinate} = \frac{3.625}{\varepsilon} \Delta A_{succinate} (g/L) \quad (2.23)$$

where ε was the extinction coefficient of NADH at 340 nm = 6.3 [L/(mmol x cm)].

2.2.1.7. DNA Extraction DNA extraction was carried out by using DNeasy kit as described by the manufacturer (Quiagen, USA) in order to verify the presence of the correct deletions in the mutant strains of the wild type yeast BY4743. For the process Quiagen DNeasy protocol for yeast was used. The kit contents were DNeasy mini spin columns, 2 ml collection tubes, Buffer ATL, Buffer AL, Buffer AW1, Buffer AW2, Buffer AE, Proteinase K.

The cells were first harvested by centrifuging for 10 min at 7500 rpm and the supernatants was discarded. The pellet was resuspended in 600 µl sorbitol buffer containing 1 M sorbitol, 100 mM sodium EDTA and 14 mM β-mercaptoethanol. 200 units of lyticase were added and the sample was left to incubate at 30°C for 3 hours. The spheroplasts were pelleted by centrifuging for 10 min at 1000 rpm and they were resuspended in 180 µl of Buffer ATL. 20 µl of proteinase K was added and it was mixed by vortexing, and later it was incubated at 55°C on a rocking platform until the cell walls were completely lysed. Then the sample was vortexed for 15 s and 200 µl of Buffer AL was added to the sample and was mixed thoroughly by vortexing. It was later incubated at 70°C for 10 min. 200 µl of ethanol (96–100 per cent) was added to the sample, and was mixed thoroughly by vortexing. The mixture was pipetted into the DNeasy Mini spin column placed in a 2 ml collection tube. It was centrifuged at 8000 rpm for 1 min. The flow-through was discarded. 500 µl Buffer AW1was added and the column was centrifuged for 1 min at 8000 rpm. The flow-through was discarded. 500 µl of Buffer AW2 was added and the column was centrifuged for 3 min at 14,000 rpm to dry the DNeasy membrane. The flow-through was discarded together with the collection tube. DNeasy Mini spin column was placed in a clean 1.5 ml or 2 ml microcentrifuge tube. 200 µl of

Buffer AE was pipetted directly onto the DNeasy membrane. It was incubated at room temperature for 1 min, and then centrifuged for 1 min at 8000 rpm to elute. Elution was repeated once more as described. All centrifugations were carried out using the Eppendorf (Germany) centrifuge with rotor 5415C.

DNA yield was determined by measuring the concentration of DNA in the eluate by its absorbance at 260 nm. Absorbance readings at 260 nm should have fallen between 0.1 and 1.0 to be accurate. An A_{260} of 1 (with a 1 cm detection path) corresponded to 50 µg DNA per milliliter water. The ratio of the readings at 260 nm and 280 nm (A_{260} / A_{280}) provided an estimate of the purity of DNA with respect to contaminants that absorb UV, such as protein. However, the A_{260} / A_{280} ratio was influenced considerably by pH. Hence it was recommended to measure absorbance in 10 mM Tris·Cl, pH 7.5, in which pure DNA has an A_{260} / A_{280} ratio of 1.8–2.0.

2.2.1.8. PCR Protocols and Gel Electrophoresis The following PCR protocol was used in verification of the gene deletions in mutant strains:

Cycle 1 (1X)	Step 1:	94°C	3 minutes
Cycle 2 (35X)	Step 1:	94°C	15 seconds
	Step 2:	55°C	15 seconds
	Step 3:	72°C	1 minute
Cycle 3 (1X)	Step 1:	72°C	3 minutes
Cycle 4 (1X)	Step 1:	4°C	∞

The PCR reactions were optimized via $MgCl_2$ titrations for each individual strain. The following optimized conditions were obtained for reaction mixtures totaling a 25 µl of reaction volume (Table 2.1).

The A / D and uptag / downtag primer pairs were used as selected from literature (primer sequences for the specified deletions available at YeastDeletionWebPages, http://www-sequence.stanford.edu/group/yeast_deletion_project/deletions3.html) for the corresponding deletion mutants individually. The sequences were given in Table 2.2 and

Table 2.3 for the A / D and uptag / downtag primer pairs, respectively in 5' to 3' directions.

Table 2.1. Optimum Reaction Mixtures for Specific Mutants

	HO	QDR3	MIG1	HAP4	QCR7	RIP1	CYT1
Mg Free Buffer (10X)	2.5	2.5	2.5	2.5	2.5	2.5	2.5
$MgCl_2$ (25mM)	1	2	2	2	2	1	2
dNTP	0.2	0.2	0.2	0.2	0.2	0.2	0.2
Primers	1.2X2	1.2X2	1.2X2	1.2X2	1.2X2	1.2X2	1.2X2
Taq Polymerase (10 u/µl)	0.1	0.1	0.1	0.1	0.1	0.1	0.1
DNA	1.5	0.5	1.5	1.0	0.5	1.5	0.5
dH_2O	17.3	17.3	16.3	16.8	17.3	17.3	17.3

Table 2.2. Sequences for A / D primers

	A	D
HO	TATTAGGTGTGAAACCACGA	CATGTCTTCTCGTTAAGACT
QDR3	GCTGCCTTTTATCACTTTTA	GGTGAGTTGGAGAAACAAAA
MIG1	GAAGCAACAACAAATTTTT	GAACAATTAATTATCTCTGC
HAP4	TTAATTCCTTCACCTCTCTA	AACGGATATGTGAAAATGCT
QCR7	GTGGTATGATCCTCGTTAAA	GATATATAGACCACTCGATA
RIP1	TATTTCATCCTTTCAACTTC	GAAAAAGAAGATGGTGAGAC
CYT1	AGTAGAGGCCATTCGTTTTC	CAGCAGTATCTCAGTACATG

The length of the cassette replacing the gene which was deleted was specific which could be checked either by a DNA ladder or a specific marker suitably incised by an enzyme. The second case was used in the experiments. Lambda DNA and Hind III (10 u/µl) enzyme were used. An aqueous mixture of 10 per cent λDNA, 5 per cent Buffer E

and 5 per cent Hind III was prepared and let to incubation at 37^{o}C for 2 hours and the marker was ready for use.

Table 2.3. Sequences for uptag / downtag primers

	Uptag	Dowtag
HO	TATCTATACTTTAAAATGGA	ACTAATATACACATTTTACG
QDR3	CAGAAAGCGATAAACATGGA	TATTAACCGATATGATTACG
MIG1	CATACTACCATAGCCATGGA	AAACTTGTCAGCGTATCACG
HAP4	GATAACTGTAGTTCGATGGA	TTTACGCCATCACGCTCACG
QCR7	TCCAGAAAGAACAAAATGGA	TTTTTATTCTTCTTTTCACG
RIP1	GGAGCAATAACAAACATGGA	GGACGAAAAACAAACCTACG
CYT1	ATAACTAATTTGACAATGGA	TCATTTTTTTGTCAACTACG

2.2.1.9. RNA Extraction Due to its highly degradable nature, any work involving RNA was performed in RNAse and DNAse free environments and this was provided by the use of certified RNAse and DNAse free plasticware and the use of DEPC treated water in cleaning of every surface and glassware. DEPC treated water was prepared as follows: 1 µl DEPC (diethylpolycarbonate) was used per 1 ml of water. It was stored overnight at 37^{o}C and autoclaved.

The RNA was extracted from samples using “RNeasy protocol for extracting yeast via mechanical disruption” as described by the manufacturer (Quiagen, USA). Samples were first lysed and homogenized in the presence of a highly denaturing guanidine isothiocyanate (GITC)-containing buffer, which immediately inactivated RNases to ensure isolation of intact RNA. Ethanol was added to provide appropriate binding conditions, and the sample was then applied to an RNeasy mini column where the total RNA bound to the membrane and contaminants were efficiently washed away. High-quality RNA was then eluted in 30 µl, or more, of water. With the RNeasy procedure, all RNA molecules longer than 200 nucleotides were isolated. The procedure provided an enrichment for mRNA since most RNAs <200 nucleotides (such as 5.8S rRNA, 5S rRNA, and tRNAs, which together comprise 15–20 per cent of total RNA) were selectively excluded.

The kit contents were RNeasy mini spin columns, 2 ml and 1.5 ml collection tubes, Buffer RTL, Buffer RPE, Buffer RW1 and RNase free water.

RNeasy protocols for isolation of total RNA from yeast via mechanical disruption used high-speed agitation in a bead mill in the presence of glass beads and lysis buffer to lyse the cells and release the RNA. The mechanical disruption protocol was suitable for time-course experiments where enzymatic incubation steps could not be tolerated. The first step in the protocol was to prepare acid-washed glass beads, 0.45–0.55 mm diameter, by soaking in concentrated nitric acid for 1 hour, washing extensively with deionized water, and drying in a baking oven. After disruption in a bead mill homogenizer, all steps of the RNeasy protocol were performed at room temperature. It was necessary to work quickly during the procedure. After harvesting the cells, all steps were performed at 20–25°C in a standard microcentrifuge.

Approximately 600 µl of acid-washed glass beads were added to an Eppendorf tube. The yeast cells were harvested by centrifuging at 6800 rpm for 5 min at 4°C. The supernatant was decanted and the remaining media was carefully removed by aspiration. 600 µl of Buffer RLT was added to the tube and vortexed to resuspend the cell pellet. The resuspended sample was added to the Eppendorf tube containing the pre prepared glass beads. The sample was vortexed and agitated at 500 rpm for 5 minutes in a bead-mill homogenizer. The sample was removed from the bead mill, and the beads were allowed to settle. The lysate was transferred to a new microcentrifuge tube and was centrifuged for 2 min at 10000 rpm. The supernatant was transferred to a new microcentrifuge tube. 350 µl of 70 per cent ethanol was added to the homogenized lysate, and mixed by pipetting. The sample was applied to an RNeasy mini column placed in a 2 ml collection tube which was centrifuged for 15 s at 10000 rpm and the flowthrough was discarded. 700 µl of Buffer RW1 was added to the RNeasy column and it was centrifuged for 15 s at 14000 rpm to wash the column. The RNeasy column was transferred into a new 2 ml collection tube and 500 µl of Buffer RPE was added onto the RNeasy column and it was again centrifuged for 15 s at 10000 rpm to wash the column. Another 500 µl of Buffer RPE was applied to the RNeasy column and the column was centrifuged at 14000 rpm to dry the RNeasy silica-gel membrane. For elution, the RNeasy column was transferred to a new 1.5 ml collection tube, 30–50 µl of RNase-free water was pipetted directly onto the RNeasy silica-gel

membrane, the tube was gently closed and centrifuged for 1 min at 10000 rpm. All centrifugations were carried out using Eppendorf (Germany) centrifuge with rotor 5415 C and Sorvall RC-5B centrifuge (DuPont, USA) with rotor SS-34.

Purified RNA was stored at –20°C or –70°C in water. The concentration of RNA was determined by measuring the absorbance at 260 nm (A_{260}) in a spectrophotometer. An absorbance of 1 unit at 260 nm corresponded to 40 μg of RNA per ml. This relation was valid only for measurements in water. Therefore, samples were diluted in water. The ratio between the absorbance values at 260 and 280 nm gave an estimate of RNA purity. The ratio of the readings at 260 nm and 280 nm (A_{260} / A_{280}) provided an estimate of the purity of RNA with respect to contaminants that absorb in the UV, such as protein. However, the A_{260} / A_{280} ratio was influenced considerably by pH. Measuring absorbance in 10 mM Tris·Cl, pH 7.5 solved this problem. Pure RNA had an A_{260}/A_{280} ratio of 1.9–2.1 in 10 mM Tris·Cl, pH 7.5.

The integrity and size distribution was also checked by gel electrophoresis and ethidium bromide staining. The respective ribosomal bands of 18S 2.0 kilobases and 26S 3.8 kilobases appeared as sharp bands on the stained gel. 26S ribosomal RNA bands were present with an intensity approximately twice that of the 18S RNA band and lastly a sharp third band which was larger than the ribosomal RNAs were present for confirmation.

2.2.1.10. Reverse Transcription Real Time Quantification Polymerase Chain Reaction (RT-rtqPCR) Primers required to quantitatively amplify the products of HAP4, COX18, HO, HSP12 and EXG2 genes were designed according to the previously stated criteria (Introduction Section). For each individual sample, duplicates of experiments were carried out using these 5 sets of primers. Negative controls containing no sample but a mixture of the primers were also included into the experiments. The forward and reverse primer sets which were used are given in Table 2.4.

For RT-rtqPCR applications within this study, Quiagen QuantiTect® SYBR® Green RT-PCR kit was used for quantitative, real-time, one-step RT-PCR. The kit included QuantiTect SYBR Green RT-PCR Master Mix; containing HotStarTaq® DNA Polymerase, QuantiTect SYBR Green RT-PCR Buffer, dNTP Mix including dUTP, SYBR Green I, ROX (passive reference dye) and 5 mM $MgCl_2$, QuantiTect RT Mix; containing

Omniscript® Reverse Transcriptase and Sensiscript® Reverse Transcriptase and lastly RNase-free water.

Table 2.4. RT-rtqPCR primer sequences

HSP12_F	5-CTGACGCAGGTAGAAAAGGATTCG-3
HSP12_R	5-CGGCATCGTTCAACTTGGACTTG –3
COX18_F	5-GACCCTAACAGAGACACAG –3
COX18_R	5-CGAGTCTCGATACGTTCAG-3
HAP4_F	5-CACCATGACGAGTTAGGTTCAG –3
HAP4_R	5-GGTGGCAGTTGCATCATTGTTG-3
HO_F	5-CCGCGTCATAAATGTCAC–3
HO_R	5-CCTACCATCAAGCGTCTG–3
EXG2_F	5-GGAACTTGGAGCTAAACC–3
EXG2_R	5-CACCATTTAGCCAGGTTG–3

The reaction mixture for 25 µl total volume was as follows:

QuantiTect SYBR Green RT-PCR Master Mix	12.5 µl
Primers	2X1. 25 µl
QuantiTect RT Mix	0.25 µl
RNA sample	0.5 µl
RNase-free water	8.75 µl

The reaction program including the melt curve analysis which was used in the experiments is given as:

Cycle 1 (1X)	Step 1:	50°C 30 minutes
Cycle 2 (1X)	Step 1:	95°C 15 minutes
Cycle 3 (40X)	Step 1:	94°C 15 seconds
	Step 2:	52.2°C 15 seconds
	Step 3:	72°C 30 seconds
Cycle 4 (1X)	Step 1:	95°C 1 minute
Cycle 5 (1X)	Step 1:	50°C 1 minute

Cycle 6 (80X) Step 1: 48°C 10 seconds with ramp: 0.5°C

2.2.2. Computational Methods

2.2.2.1. Determination of Maximum Growth Rate and Substrate Utilization Constants The Michaelis - Menten equation for single limiting substrate enzyme kinetics could be given as:

$$r_x = \frac{\mu_m \times S}{k_s + S} \times x_v \tag{2.24}$$

where r_x : rate of reaction (grams of S uptake L^{-1} s^{-1})

μ_m : maximum specific growth rate (hr^{-1})

S : the limiting substrate concentration (kg m^{-3})

k_s : the saturation constant (kg m^{-3})

x_v: viable cells (kg cell m^{-3})

This equation held true in the absence of substrate and product inhibition.

The kinetic parameters μ_m and k_s could be determined using the following relations:

$$\frac{dx_v}{dt} = r_x = \frac{\mu_m \times S}{k_s + S} \times x_v = \mu \times x_v \tag{2.25}$$

where $\mu = \frac{\mu_m \times S}{k_s + S}$.

Integrating both sides of the equation yielded:

$$ln\, x_v = \mu t \tag{2.26}$$

For batch processes, $\mu = \mu_{max}$ at the exponential phase and this yielded a constant slope. Hence the first kinetic parameter μ_{max} was determined.

For the saturation coefficient, a Lineweaver-Burke plot was used:

$$\frac{1}{\mu} = \frac{k_s}{\mu_m \times S} + \frac{1}{\mu_m} \tag{2.27}$$

when plots of $\frac{1}{\mu}$ vs. $\frac{1}{S}$ was drawn, the slope multiplied by the μ_{max} gave k_s.

2.2.2.2. Determination of Yield Coefficients Yield coefficients are the ratio of the end products to the major substrate which is glucose for the experiments in this study. The steady state amounts of the metabolites were used for chemostat cultures while for the batch cultures, the ultimate concentrations were taken into account. The yields of biomass ($Y_{s/x}$), ethanol ($Y_{s/e}$), acetic acid ($Y_{s/a}$) and glycerol ($Y_{s/g}$) on glucose were calculated in the following manner:

$$Ys/p = \frac{final\ concentration\ of\ product\ p\ in\ the\ cultivation\ broth}{consumed\ amount\ of\ substrate\ s\ in\ the\ cultivation\ broth} \tag{2.28}$$

2.2.2.3. Flux Balance Analysis As an approach used in the analysis of metabolic behavior, flux-balance analysis (FBA) could be used to get an overview of steady state behavior of living cells. The fundamental principle of FBA was the conservation of mass. A mass balance was written for each metabolite in a metabolic network to yield a dynamic mass balance.

$$\frac{dX_i}{dt} = V_{syn} - V_{\deg} - (V_{use} \pm V_{trans}) \tag{2.29}$$

where the subscripts '*syn'* and '*deg'* referred to the metabolic synthesis and degradation of metabolite X_i. The uptake or secretion flux, V_{trans}, was determined experimentally. The growth and maintenance requirements, V_{use}, were accurately estimated from cellular composition. This equation was typically written in matrix form,

$$\frac{d\mathbf{X}}{dt} = \mathbf{S} \bullet \mathbf{v} - \mathbf{b} \tag{2.30}$$

where ***X*** was an *n* dimensional vector of metabolite amounts per cell, **v** was the vector of *m* metabolic fluxes, **S** was the *n* x *m* stoichiometric matrix, and **b** was the vector of known metabolic demands. The element S_{ij} was the stoichiometric coefficient that indicated the amount of the i^{th} compound produced per unit flux of the j^{th} reaction. The time constants characterizing metabolic transients were typically very rapid compared to the time constants of cell growth and process dynamics, and the transient mass balances could be simplified to only consider the steady state behavior. Eliminating the time derivative in equation 3, yielded,

$$\mathbf{S} \bullet \mathbf{v} = \mathbf{b} \tag{2.31}$$

This equation simply stated that over long times, the formation fluxes of a metabolite needed to be balanced by the degradation fluxes. Otherwise, significant amounts of the metabolite would accumulate inside the metabolic network. Typically the number of metabolic fluxes was greater than the number of mass balances (i.e*., m* > *n*) resulting in a plurality of feasible flux distributions to Equation 2.31. This range of solutions was indicative of the flexibility in the flux distributions that could be achieved with a given set of metabolic reactions. The particular uses of the metabolic network were defined as the *metabolic phenotype* that was expressed under those particular conditions. Objectives for metabolic function were chosen to explore the "best" use of the metabolic network within a given metabolic genotype. The solution was formulated as a linear programming (LP) problem in which one found the flux distribution that minimized/maximized a particular objective. **C**onstraints were also placed on the value of the flux through each of the metabolic reactions.

$$\alpha_i \le v_i \le \beta_i \tag{2.32}$$

These constraints were representative of a maximum allowable flux through a given reaction, resulting from a limited amount of an enzyme present. These constraints were

also used to include the knowledge of the minimum flux through a certain metabolic reaction.

In this study, flux balance analysis whose computational details are given above was used to obtain an overview of the distribution of fluxes amongst the cell in chemostat cultivations. Two different models were applied; a small scale model (SSM) comprising of the central carbon metabolism of the yeast and a comprehensive genome scale model (GSM) including the complete set of reactions and metabolites available within the cell.

The measured input values were inserted in the form of fluxes while the experimental measurements were given as concentrations. The necessary conversions that were done are given in Table 2.5, Table 2.6 and Table 2.7. The raw experimental inputs required for analysis are presented in Table 2.5.

Table 2.5. Experimental inputs used in the stoichiometric matrix

Concentrations in g/L				
Strains	remaining glucose	biomass	pyruvate	succinate
BY4743	1.66	2.70	0.04	0.15
ΔHO	0.41	3.03	0.02	0.11
ΔQDR3	1.39	2.22	0.04	0.19
ΔMIG1	0.21	2.04	0.02	0.29
ΔHAP4	0.46	3.01	0.01	0.29
ΔQCR7	2.14	2.49	0.04	0.10
ΔRIP1	3.11	0.60	0.01	0.16
ΔCYT1	0.16	1.34	0.01	0.06

Metabolite concentrations were converted into flux measurements. The consumed amount of glucose was determined and using the dilution rate of the experimental setup, concentration terms were converted into fluxes in units of g / (gDW.hr) and mmole / (gDW.hr) (Table 2.6).

In order to simplify atomic conservation inspections, unitless fluxes are obtained as ratios with respect to moles of glucose and carbon moles of glucose (Table 2.7).

Table 2.6. Flux measurements used in the stoichiometric matrix

Fluxes in g / (gDW.hr)				
Strains	consumed glucose	biomass	pyruvate	succinate
BY4743	0.68	0.10	0.0014	0.005
ΔHO	0.65	0.10	0.0008	0.004
ΔQDR3	0.84	0.10	0.0015	0.007
ΔMIG1	0.97	0.10	0.0009	0.011
ΔHAP4	0.65	0.10	0.0003	0.011
ΔQCR7	0.72	0.10	0.0016	0.004
ΔRIP1	2.81	0.10	0.0002	0.006
ΔCYT1	1.48	0.10	0.0003	0.002
Fluxes in mmole / (gDW.hr)				
Molecular Weight	**180.00**	**26.40**	**88.10**	**118.09**
Strains	glucose	biomass	pyruvate	succinate
BY4743	3.77	3.79	0.016	0.046
ΔHO	3.59	3.79	0.009	0.036
ΔQDR3	4.66	3.79	0.017	0.059
ΔMIG1	5.39	3.79	0.010	0.090
ΔHAP4	3.61	3.79	0.004	0.090
ΔQCR7	3.99	3.79	0.018	0.031
ΔRIP1	15.62	3.79	0.002	0.050
ΔCYT1	8.24	3.79	0.003	0.020

In SSM, 50 metabolites were considered in the stoichiometric matrix together with 70 irreversible reactions (Cakir, *et al*., 2003). The objective function was set to be maximization of ethanol production within the cell.

In GSM, a total of 822 metabolites participating in 1172 irreversible reactions formed the stoichiometric matrix (Förster, *et al*., 2003). Two different objective functions were used, one being the maximization of ethanol production and the other being the maximization of oxygen uptake. The complete list of metabolites and reactions are given in the Appendix.

Table 2.7. Unitless flux measurements used in the stoichiometric matrix

Fluxes in mole/mole glucose				
Strains	glucose	biomass	pyruvate	succinate
BY4743	1.00	1.00	0.0042	0.012
ΔHO	1.00	1.05	0.0025	0.010
ΔQDR3	1.00	0.81	0.0037	0.013
ΔMIG1	1.00	0.70	0.0018	0.017
ΔHAP4	1.00	1.05	0.0010	0.025
ΔQCR7	1.00	0.95	0.0046	0.008
ΔRIP1	1.00	0.24	0.0001	0.003
ΔCYT1	1.00	0.46	0.0004	0.002
Fluxes in Cmole/Cmole glucose				
Strains	glucose	biomass	pyruvate	succinate
BY4743	1.00	0.17	0.0021	0.018
ΔHO	1.00	0.18	0.0013	0.015
ΔQDR3	1.00	0.14	0.0019	0.019
ΔMIG1	1.00	0.12	0.0009	0.025
ΔHAP4	1.00	0.17	0.0005	0.038
ΔQCR7	1.00	0.16	0.0023	0.012
ΔRIP1	1.00	0.04	0.0001	0.005
ΔCYT1	1.00	0.08	0.0002	0.004

Since only a limited number of fluxes were measured experimentally namely biomass, glucose, ethanol, pyruvate and succinic acid, the solution to the problem became a linear programming problem which was solved by MATLAB 7.0 Optimization Toolbox together with LPSolve 5.1 package. For the SSM, the toolbox provided reasonable results

while it was completely unsatisfactory in the case of GSM. For GSM optimizations, LPSolve 5.1 and TOMLAB were run under MATLAB 7.0 to provide satisfactory output results.

2.2.2.4. Minimization of Metabolic Adjustment In Minimization of Metabolic Adjustment (MOMA), a point in a particular space was searched such that it had a minimal distance from a given vector **w**. The goal was to find a vector **x** whose Euclidian distance was minimized. (Segre *et al*., 2002) The particular space was the solution space obtained for the deletion mutants and the given vector belonged to FBA outcome of the wild type strain. The Euclidean distance given by

$$D(w,x) = \sqrt{\sum_{i=1}^{N}(w_i - x_i)^2} \tag{2.33}$$

was to be minimized. This then became a standard quadratic programming problem with an object to minimize:

$$f(x) = L \bullet x + \frac{1}{2}x^T Qx \tag{2.34}$$

where the vector **L** of length N and the $N \times N$ matrix **Q** defined the linear and quadratic part of the objective function, respectively, and $\mathbf{x}^T$ represented the transpose of **x**. By observing that minimizing the function D of Equation 2.33 was equivalent to minimizing its square, and that constant terms could be omitted from the objective function, one could choose Q to be an $N \times N$ unit matrix and set **L**=**-w**, and hence reduce the minimization of D to the minimization of $f(\mathbf{x})$ (Segre *et al*., 2002). In MOMA, the objective function did not explicitly depend on biomass production. Its linear part reflected the vector of fluxes of the wild type, whereas its quadratic part was the square of the Euclidean norm of **x**. The quadratic programming was performed also using TOMLAB running under MATLAB 7.0. For wild type conditions, GSM results of the wild type strain were used.

2.2.2.5. Principle Component Analysis Principal component analysis (PCA) in many ways formed the basis for multivariate data analysis. PCA provided an approximation of a data

table, a data matrix, X, in terms of the product of two small matrices T and P'. These matrices, T and P', captured the essential data patterns of X. Plotting the columns of T gave a picture of the dominant "object patterns" of X and, analogously, plotting the rows of P' showed the complementary "variable patterns" (Wold *et al*., 1987). The starting point in all multivariate data analysis was a data matrix (a data table) denoted by X. The N rows in the table were termed "objects". The K columns were termed "variables" and comprised the measurements made on the objects. In this study, the variables were the measured metabolites and the objects were the strains. The data matrix used in the study is presented in Table 2.8

Table 2.8. The data matrix

	metabolites (g/L)				
strains	glucose	Ethanol	pyruvate	succinic acid	biomass
BY4743	1.66	9.02	0.038	0.15	2.92
ΔHO	0.78	9.23	0.022	0.11	2.89
ΔQDR3	1.39	10.23	0.041	0.19	2.64
ΔMİG1	0.21	10.07	0.023	0.29	2.51
ΔHAP4	0.29	12.46	0.006	0.29	1.37
ΔQCR7	2.14	9.97	0.042	0.07	2.60
ΔRİP1	4.44	12.40	0.005	0.16	0.60
ΔCYT1	2.85	9.82	0.007	0.06	1.34

This matrix was first mean centered ($\mu = 0$) and then scaled such that its standard deviation equaled unity ($\sigma = 1$). The rest was carried out via PLS Toolbox of MATLAB 7.0 in order to obtain, the matrix of the principle components (PCs), the vector of eigenvalues, the matrices of scores and loadings. The number of principle components required statistically was determined by the latent vector, composed of the eigenvalues. The statistically required number of components was selected such that the eigenvalues of those components needed to cover more than 67 per cent of the total number. The loadings and the scores of the PCs were plotted against each other to reveal statistical information about the data.

2.2.2.6. Relative Quantification of Gene Expression – Pfaffl Method The experimental output files of the BioRad software are given as cycle florescence (CF) in relative fluorescence units (RFU) of the amplified regions where SYBR Green intercalated. The relative quantification of gene expression was provided by a simple Microsoft Excel Macro provided by BIORAD. The Macro quantified genes according to the Pfaffl Method which took efficiency of the PCR reaction into account. In this method, the quantification ratio of the PCR amplification was considered to be $(1 + \text{efficiency})^N$ instead of 2^N. Hence the quantifications were determined. Housekeeping genes HO and COX18 and positive control genes HSP12 and EXG2 were taken to be the reference genes in expression calculations performed by the GENEX Macro (BIORAD, USA).

3. RESULTS

In order to investigate the regulation and the mechanisms involved in respiration and its deficiency, deletion mutants of the genes involved in respiration as well as genes involved in the regulation of respiration either directly or indirectly were studied. The results stated here aim to gain further insight on respiration and its regulation in *S. cerevisiae* with an ultimate goal of rational design of a strain with higher levels of ethanol production. BY4743 wild type strain and seven deletion mutants ΔHO, ΔQDR3, ΔMIG1, ΔHAP4, ΔQCR7, ΔRIP1 and ΔCYT1 were used in order to explore the effect of gene deletions in ethanol production by *S. cerevisiae*.

The particular genes that were investigated were chosen according to some particular criteria. ΔHO mutant was preferred as a reference strain since HO gene was known to be a neutral site for gene replacement in the construction of deletion strains of *S. cerevisiae*. The parental strain, BY4743 was also used as control in order to be able to determine whether the presence of any deletion resulted in differences in either growth characteristics or metabolic profiles. ΔQCR7, ΔRIP1 and ΔCYT1 were selected in this study due to their shared characteristics of their deleted genes. QCR7, RIP1 and CYT1 are all essential genes for the functioning of the respiratory chain complex III, namely, the cytochrome bc1 complex. The disruptions of any of these genes yield a respiratory deficient mutant strain. ΔMIG1 and ΔHAP4 were chosen to get an insight of the complex, intertwined regulatory functions of MIG1 and HAP4 genes, both encoding transcriptional factors acting on respiration, glucose and nitrogen metabolisms of *S. cerevisiae*. At the beginning of this study, QDR3 gene was only an open reading frame (YBR043c) with putative functions. However, its deletion mutant showed partial respiratory deficiency and hence the mutant strain was included into this study.

In this study, preliminary batch cultivations were carried out first for the wild type strain BY4743 together with the deletion mutants ΔQDR3 and ΔQCR7. Enzymatic analyses were carried out for intracellular and extracellular glucose and pyruvate concentrations as well as the extracellular ethanol concentrations. Growth characteristics of

the cultures were also determined. Yields of biomass and ethanol on glucose were calculated.

Following the batch cultivations, chemostat cultivations were performed and the growth characteristics of the wild type strain and the seven deletion mutants, namely ΔHO, ΔQDR3, ΔMIG1, ΔHAP4, ΔQCR7, ΔRIP1 and ΔCYT1 were investigated. Extracellular glucose, pyruvate, ethanol and succinic acid concentrations for all cultivations as well as steady state intracellular glucose and pyruvate concentrations of the strains whose batch cultivations are performed were determined. Flux balance analysis was carried out and compared for each strain both considering only the central carbon metabolism, and the whole metabolism of the yeast with an objective of optimizing ethanol production and oxygen uptake optimization. Minimization of metabolic adjustment was performed for the mutant strains in order to determine the state of being that is closest to that of the wild type. Lastly, principle component analysis was performed on the experimental data set as a statistical evaluation of the experiment.

Batch cultivations with pulse injections were performed using the wild type strain. Metabolite profiles for glucose, pyruvate, succinic acid, acetaldehyde, acetic acid, ethanol and glycerol were obtained as well as the growth curves. Expression profiles of HAP4 gene was determined under carbon and nitrogen limitations via reverse transcription real time quantification polymerase chain reaction.

3.1. Verification of the Deletions in the Strains of *S. cerevisiae*

The deletion strains that were selected to be investigated, namely ΔHO, ΔQDR3, ΔMIG1, ΔHAP4, ΔQCR7, ΔRIP1 and ΔCYT1, were first checked for the presence of deletions of the correct genes. DNA was extracted from cultures of mutant strains as previously described and the cassettes were amplified via PCR using the appropriate deletion mutant specific primer pairs. A / D primer pairs and uptag / downtag primer pairs that belonged to the individual cassettes replacing the deleted genes were selected separately for the seven mutation positions available at Yeast Deletion Web Pages (http://www-sequence.stanford.edu/group/yeast_deletion_project/deletions3.html). Each A

/ D pair was used to check for the presence of a deletion mutant while the uptag / downtag pair verified the presence of the correct deletion at the indicated location.

Analysis of deletions in the seven selected mutants using A / D primer pairs on 1 per cent agarose gels is presented in Figure 3.1. The presence of bands indicates that the strain has a deletion as expected. However, this information did not include knowledge about the deletion being on the correct position of the genome. Therefore, uptag / downtag primer pairs were used to verify that the correct cassette for the aimed deletion is placed in the correct place on the genome.

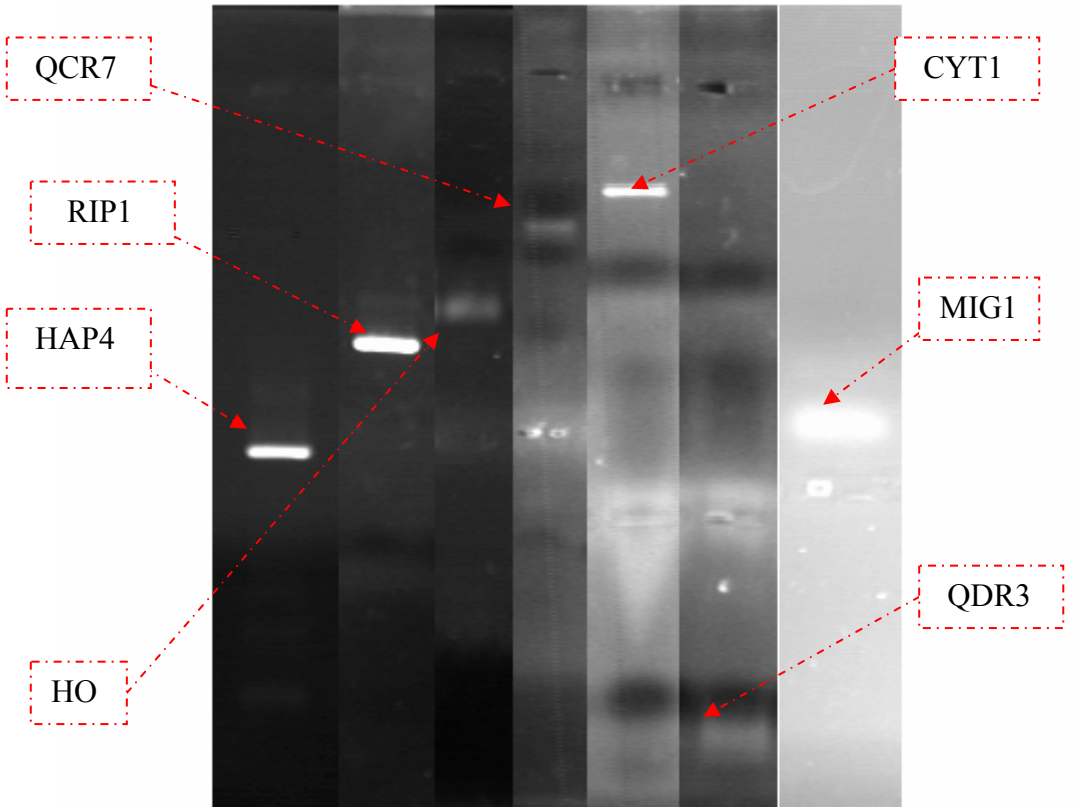

Figure 3.1. Analysis of deletions in mutants by using A / D primer pairs

Analysis of deletions in these seven mutants using uptag / downtag primer pairs on 1 per cent agarose gels resulted in the observation of the bands indicating the presence of a correct deletion in each of these deletion mutants as expected (Figure 3.2).

This preliminary verification aimed to confirm that the mutant strains which were to be used in this study are carriers of the correct deletions of the selected genes. The results

revealed that the seven deletion mutants whose investigation will be presented hence forward were indeed found to possess the correct deletions at the correct locations of their genome.

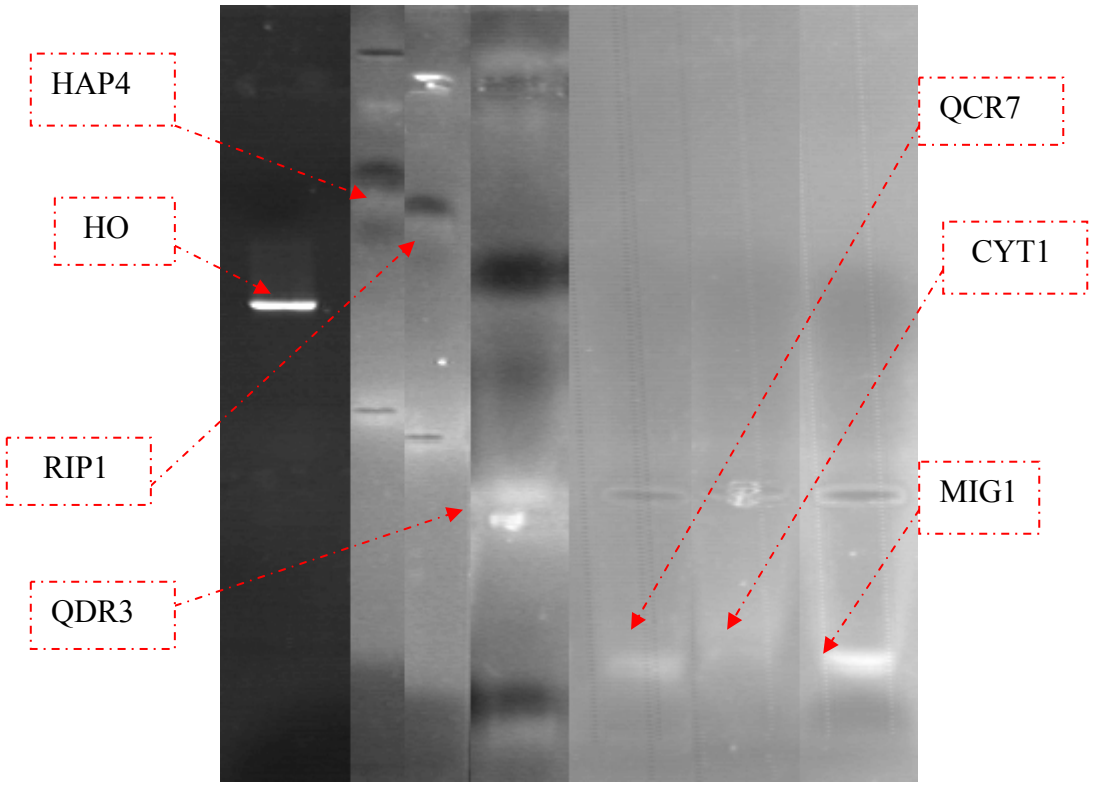

Figure 3.2. Analysis of deletions in mutants by using uptag / downag primer pairs

3.2. Respiratory Deficiency Check for ΔQDR3 Mutant Strain

All genes whose deletion mutants are used in this study were chosen with a prior knowledge of being involved in respiration or in regulation of respiration with the exception of QDR3. At the beginning of this study, as it is stated before, QDR3 gene was only an open reading frame (YBR043c) with putative functions. Therefore any suspicions regarding to this gene being related with respiration needed to be checked. The deletion mutant ΔQDR3 was checked for respiratory deficiency according to its growth characteristics on non-fermentable carbon sources ethanol and glycerol. For this purpose, subsequent dilutions of cell culture were spotted on YPethanol and YPglycerol plates and their growth was observed. The results indicate the presence of partial respiratory deficiency since growth is not maintained at its best condition in none of these non-fermentable carbon sources (Figure 3.3 and Figure 3.4).

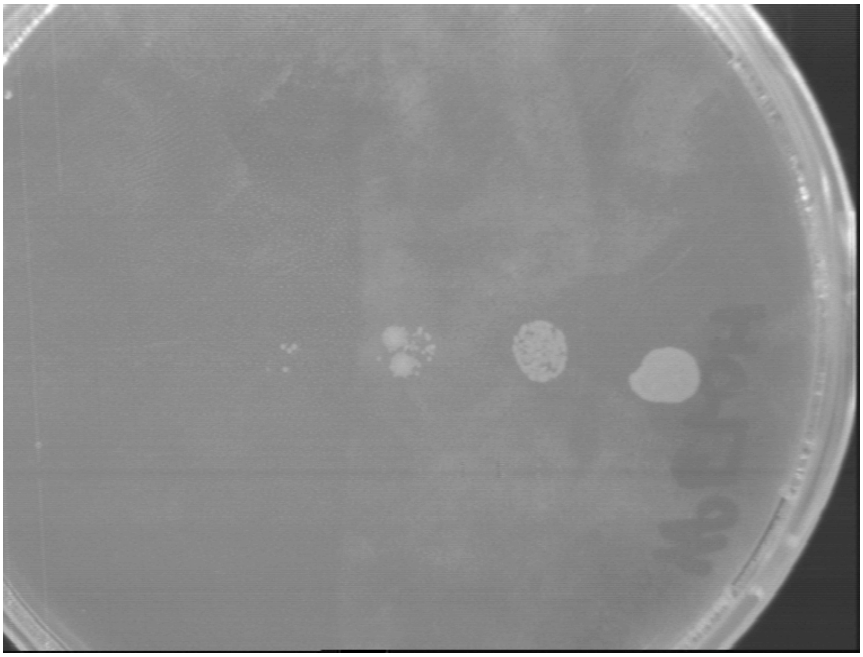

Figure 3.3. The growth of ΔQDR3 on ethanol containing plates as the sole carbon source

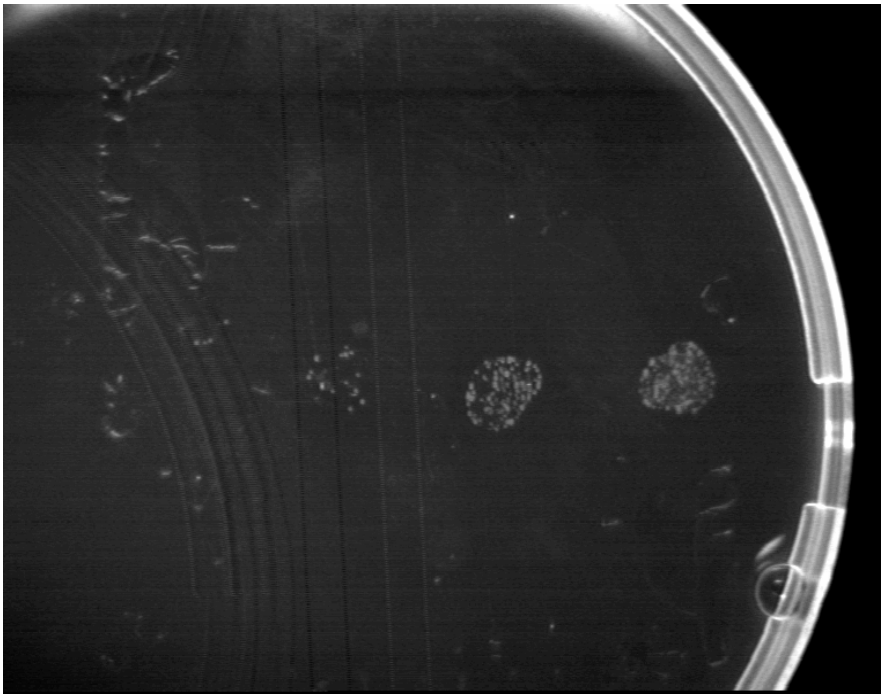

Figure 3.4. The growth of ΔQDR3 on glycerol containing plates as the sole carbon source

3.3. Growth Characteristics of Deletion Mutants in Batch Cultures

The wild type strain BY4743 and two mutants, ΔQDR3 and ΔQCR7 were grown in aerobic batch cultivations. Their growth behavior, glucose consumption, ethanol

production, pyruvate concentration profiles as well as their ultimate intracellular glucose and pyruvate concentrations were determined. The cultures were grown in YPD complex medium at 30^{o}C with pH kept between 5.5 and 6.5. Sampling was done on an hourly basis. The results presented below are the average of the steady state values that were measured.

The metabolic profiles and growth characteristics of BY4743 are shown in Figures 3.5 a and b.

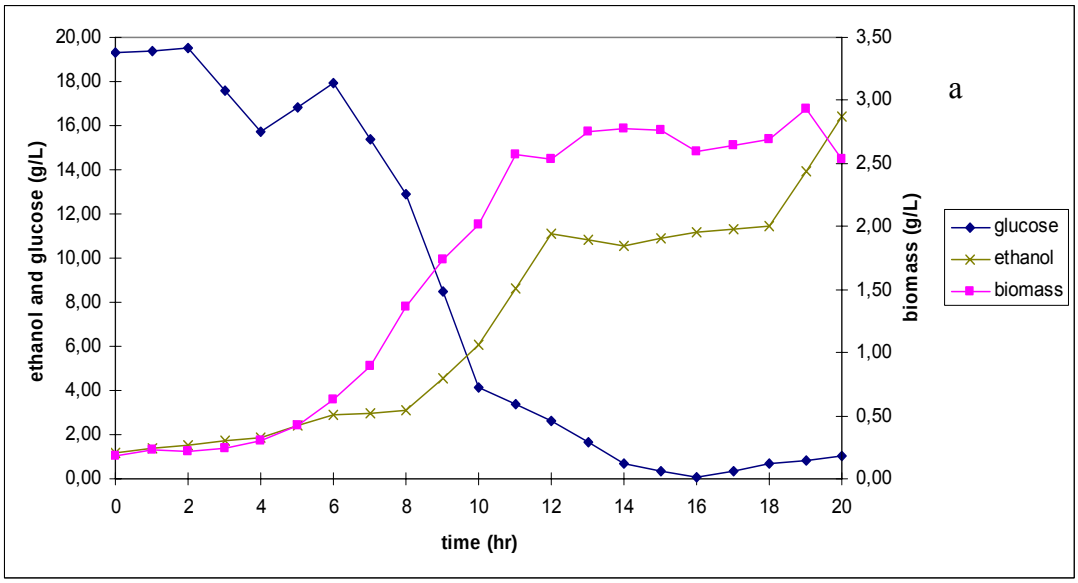

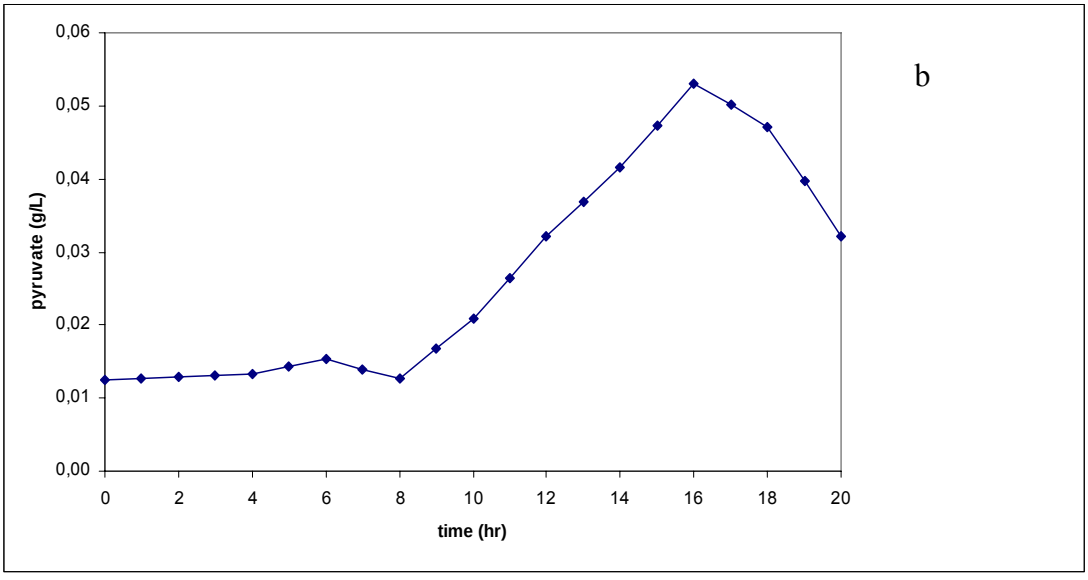

Figure 3.5. Growth characteristics (a) and Pyruvate concentration profile (b) of WT strain, BY4743 in batch cultures

The glucose concentration decreased to a constant average value of 0.61 g/L towards the end of the experiment while ethanol and biomass productions reached 11.08 g/L and 2.69 g/L, respectively. The extracellular pyruvate concentration first increased and then decreased and it reached the maximum value of 0.05 g/L while it had an average value of 0.04 g/L during the time period when the concentration of extracellular metabolites had a constant value. With these results, the yield of biomass on glucose (Y_{sx}) was calculated to be 0.14 g/gDW and the yield of ethanol on glucose (Y_{se}) was found to be 0.57 g/g. The intracellular glucose concentration was obtained as 0.10 g/L while the intracellular pyruvate concentration was measured as 0.010 g/L. For the wild type strain the maximum growth rate, μ_{max} was found as 0.36 hr^{-1} and K_s was found to be 1.29 g/L.

The growth characteristics of the recombinant strain, ΔQDR3 are shown in Figures 3.6.a and b. The glucose concentration decreased to a constant average value of 0.53 g/L towards the end of the experiment while ethanol production reached a concentration of 11.78 g/L and 2.95 g/L of biomass was produced during the same period. The extracellular pyruvate concentration first increased and then decreased and the maximum value it reached was 0.04 g/L while it had an average value of 0.02 g/L during the time period when extracellular metabolic measurements indicated a constant value.

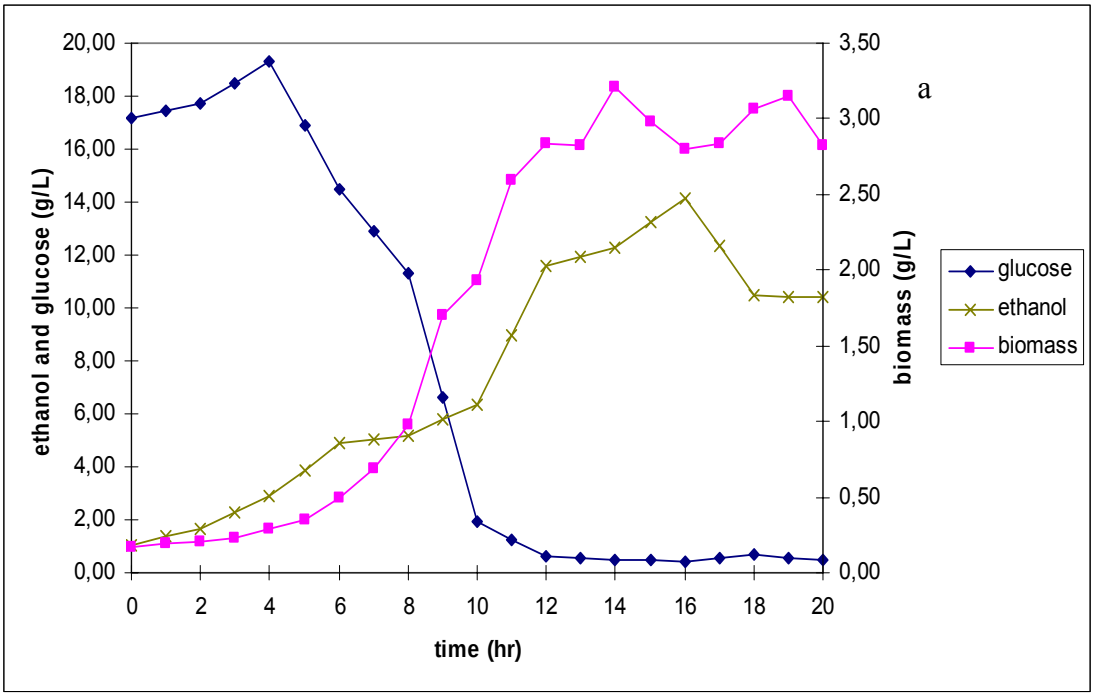

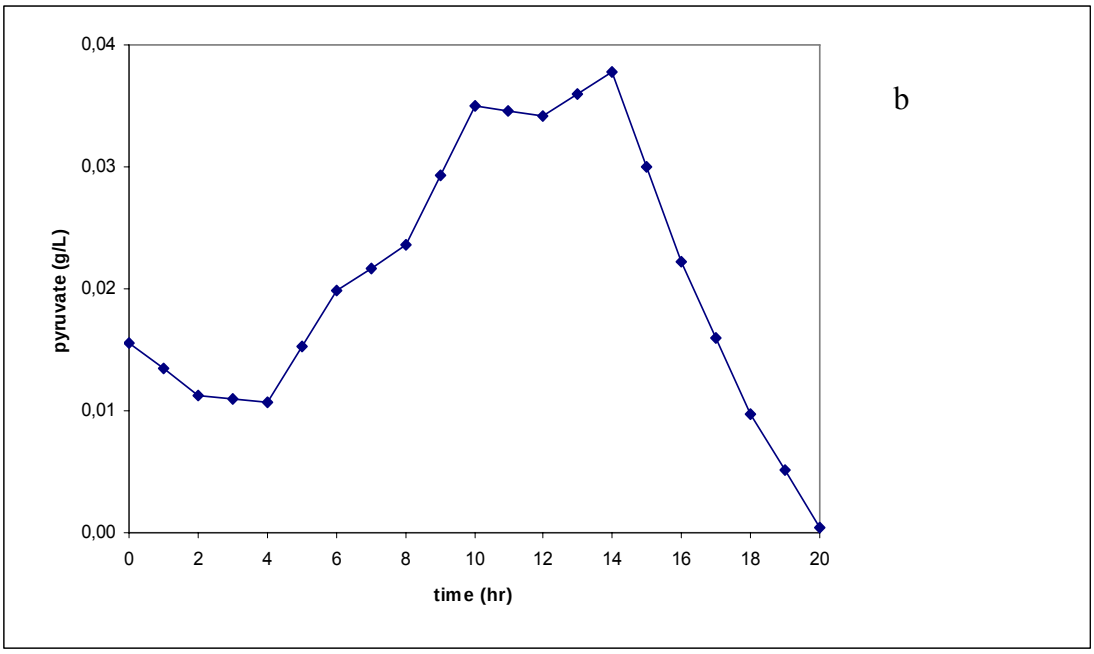

Figure 3.6. Growth characteristics (a) and Pyruvate concentration profile (b) of recombinant strain, ΔQDR3 in batch cultures

With these results, the yield of biomass on glucose (Y_{sx}) was calculated to be 0.15 g/gDW and the yield of ethanol on glucose (Y_{se}) was found to be 0.60 g/g on glucose. The intracellular glucose concentration was obtained as 0.09 g/L while the intracellular pyruvate concentration was measured as 0.01 g/L. For ΔQDR3 mutant strain maximum growth rate, μ_{max} was found as 0.34 hr^{-1} and K_s was found to be 1.11 g/L.

The growth characteristics of ΔQCR7 are shown in Figures 3.7 a and b. The glucose was depleted to a constant average value of 0.50 g/L towards the end of the experiment while ethanol production reached a concentration of 12.80 g/L and 2.49 g/L of biomass was produced during the same period. The extracellular pyruvate concentration first increased up to a certain level and then decreased and the maximum value it reached was 0.04 g/L while it had an average value of 0.03 g/L during the time period when the concentration of extracellular metabolites had a constant value. With these results, the yield of biomass on glucose (Y_{sx}) was calculated to be 0.13 g/gDW and the yield of ethanol on glucose (Y_{se}) was found to be 0.66 g/g. The intracellular glucose concentration was obtained as 0.09 g/L while the intracellular pyruvate concentration was measured as 0.01 g/L. For ΔQCR7 mutant strain maximum growth rate, μ_{max} was found as 0.26 hr^{-1}, which is

the lowest value among batch cultivations and the saturation coefficient, K_s was found to be 2.71 g/L.

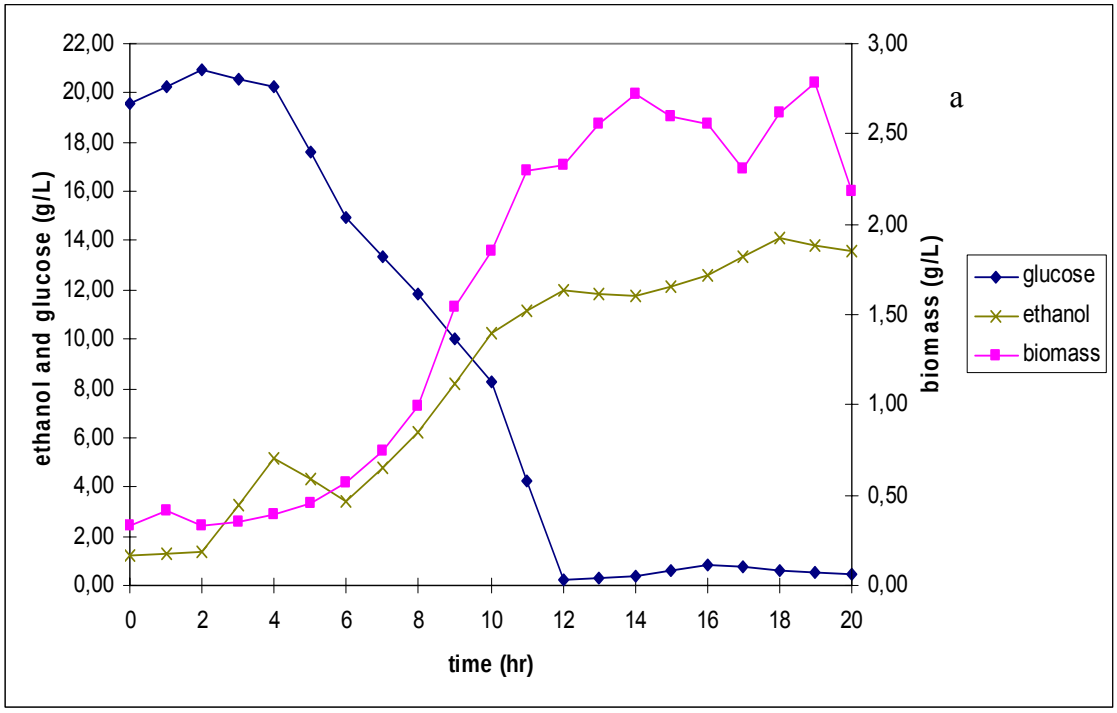

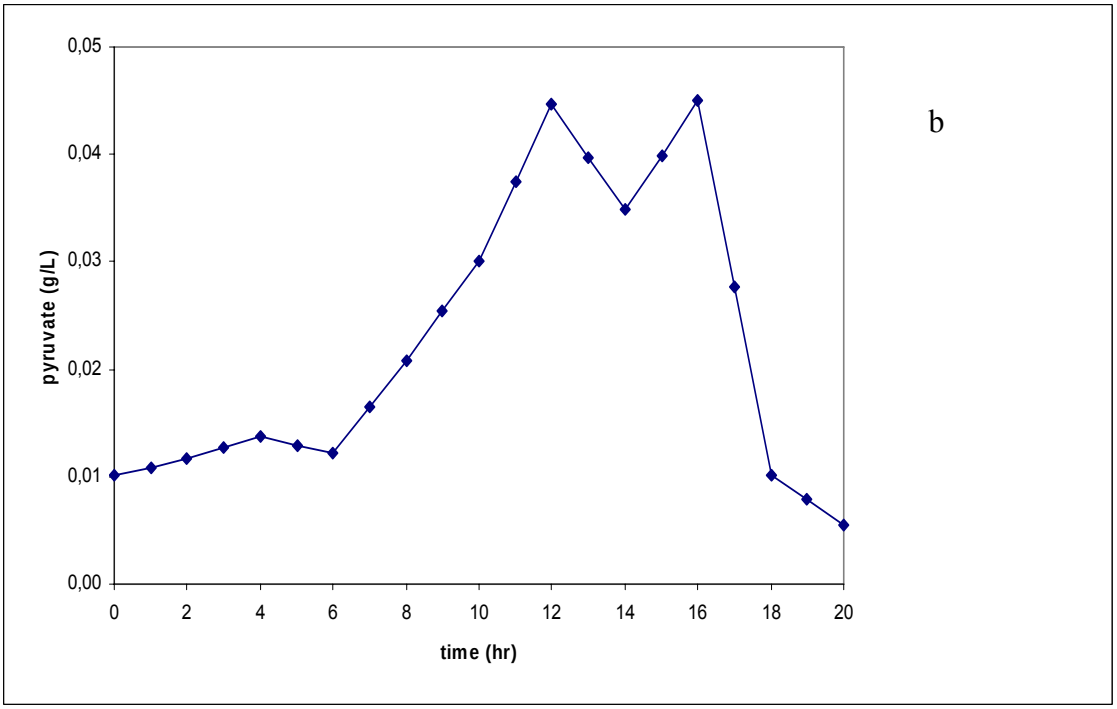

Figure 3.7. Growth characteristics (a) and Pyruvate concentration profile (b) of recombinant strain, ΔQCR7 in batch cultures

3.4. Growth Characteristics in Continuous Cultures

3.4.1. Growth Characteristics of Deletion Strains

Following the batch cultivations, chemostat cultivations were carried out for the wild type BY4743 strain and the seven deletion mutant strains, namely ΔHO, ΔQDR3, ΔMIG1, ΔHAP4, ΔQCR7, ΔRIP1 and ΔCYT1 in complex medium, YPD at 30^{o}C with pH kept between 5.5 and 6.5. The dilution rate was set to 0.1 hr^{-1}.

Regular sampling of the cultivation was carried out. Growth curves, glucose consumption, ethanol production, pyruvate and succinic acid concentration profiles were obtained. Steady state intracellular glucose and pyruvate concentrations were determined for BY4743, ΔQDR3 and ΔQCR7 with the purpose of comparison with their corresponding batch cultivation values.

The yields of ethanol and biomass on glucose were also calculated. All experiments were performed in duplicates and the results presented here are the average of these outcomes. The results presented here are the average of the collection of all available steady state measurements.

Growth curve and the metabolic profiles of BY4743 wild type strain in chemostat culture is shown in Figures 3.8 a and b. The glucose concentration decreased to an average value of 1.66 g/L at steady state while ethanol production reached 9.02 g/L and 2.92 g/L of biomass was produced. The extracellular pyruvate concentration first increased and then decreased and the maximum value it reached was 0.05 g/L while it had an average value of 0.04 g/L at steady state. The succinic acid concentration was determined to be 0.15 g/L at steady state.

With these results, the yield of biomass on glucose (Y_{sx}) was calculated to be 0.16 g/gDW and the yield of ethanol on glucose (Y_{se}) was found to be 0.49 g/g. The intracellular concentrations of glucose, pyruvate and succinic acid were 0.10 g/L, 0.01 g/L and 0.03 g/L, respectively.

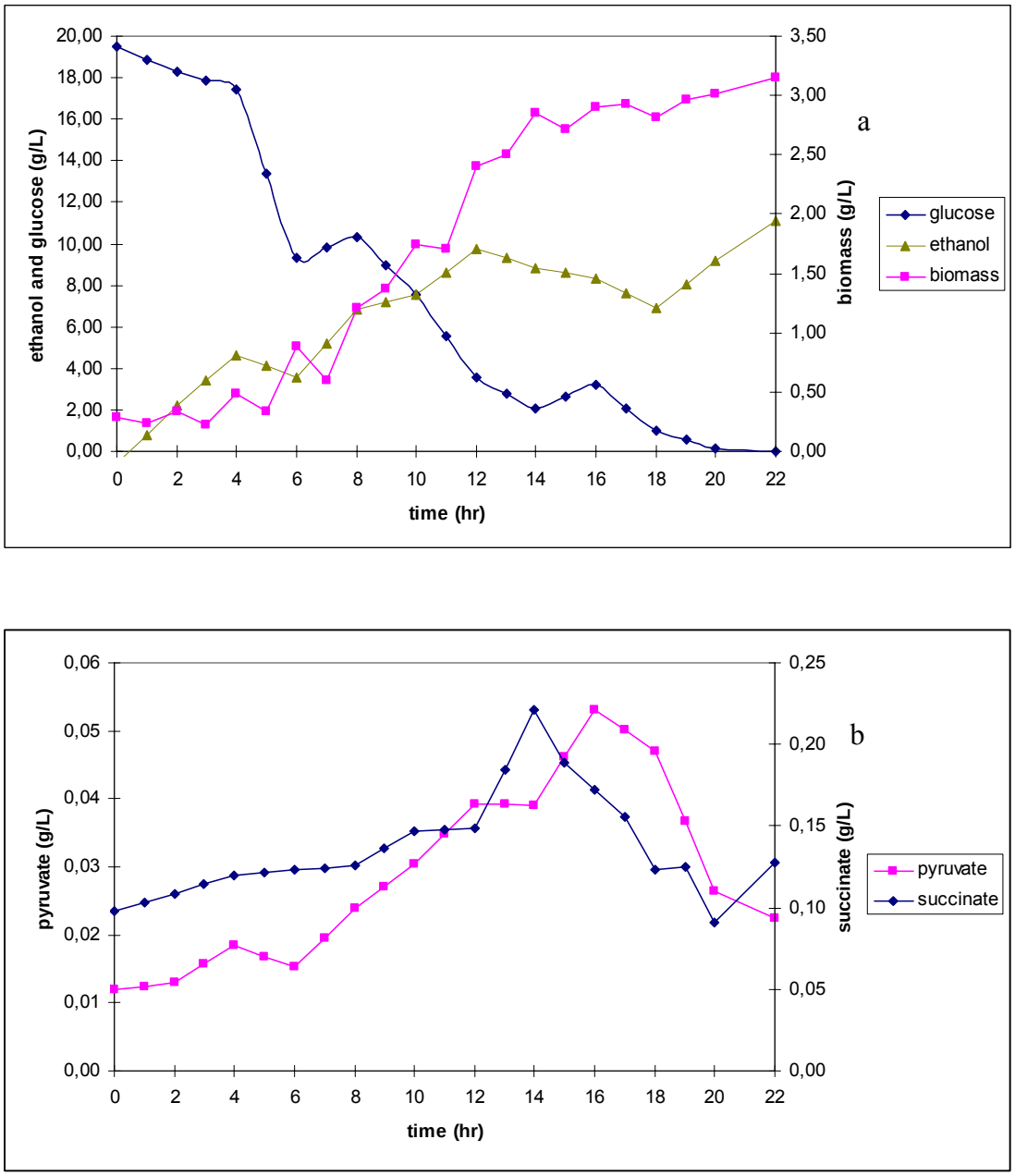

Figure 3.8. Growth characteristics (a) and Pyruvate and succinate concentration profiles (b) of WT strain, BY4743 in continuous cultures

The growth characteristics of ΔHO are depicted in Figures 3.9 a and b. A decrease in glucose concentration was observed to an average value of 0.78 g/L at steady state while ethanol production reached 9.23 g/L and 2.89 g/L of biomass was produced. The extracellular pyruvate concentration first increased and then decreased and the maximum value it reached was 0.03 g/L while it had an average value of 0.02 g/L at steady state. The succinic acid showed an oscillating behavior and its average concentration was determined to be 0.11 g/L at steady state. With these results, the yield of biomass (Y_{sx}) on glucose was

calculated to be 0.15 g/gDW and the yield of ethanol (Y_{se}) on glucose was found to be 048 g/g.

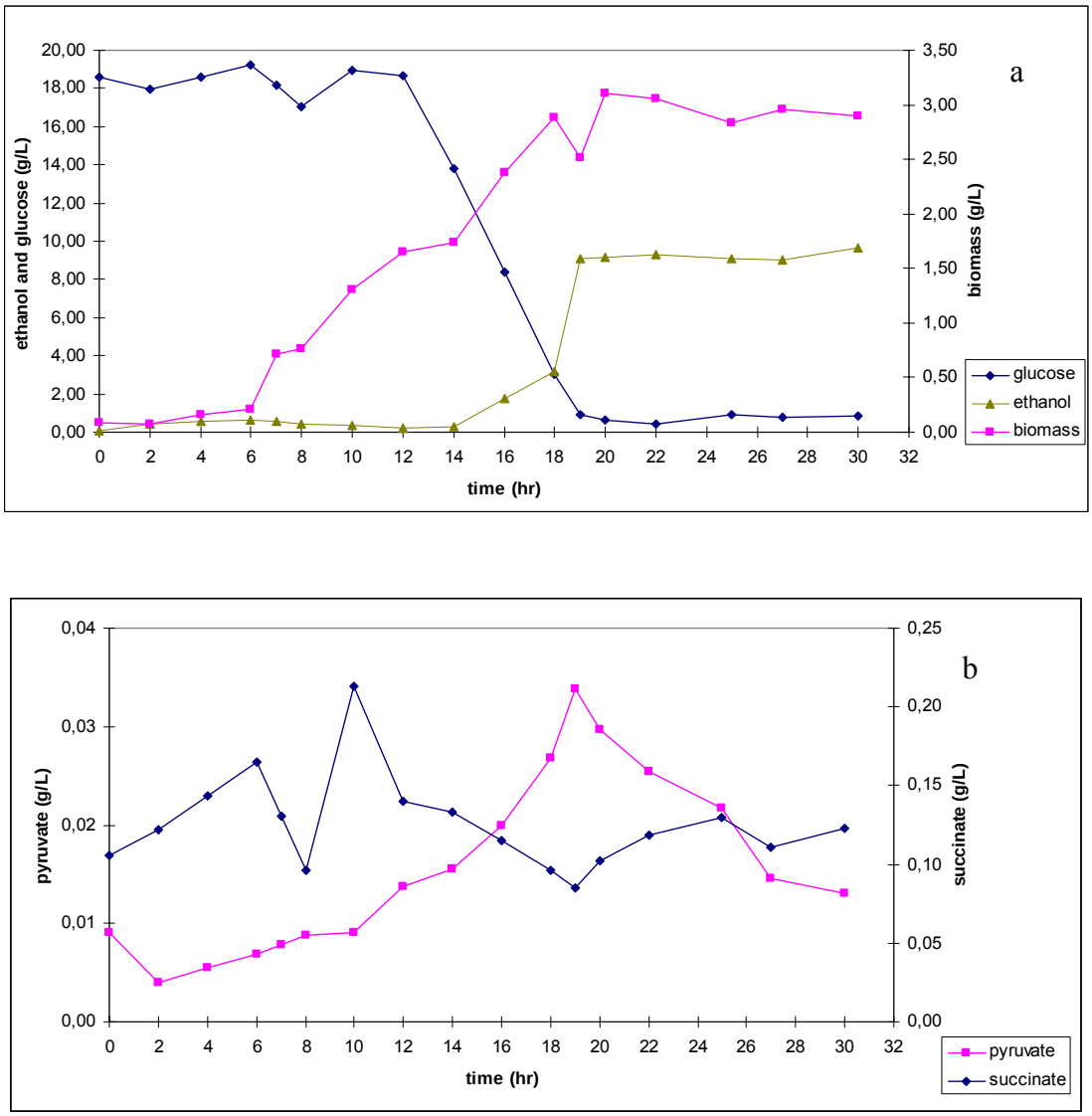

Figure 3.9. Growth characteristics (a) and Pyruvate and succinate concentration profiles (b) of mutant strain, ΔHO in continuous cultures

The growth and metabolic concentration profiles of ΔQDR3 are presented in Figures 3.10 a and b. The glucose concentration decreased to an average value of 1.39 g/L at steady state while ethanol and biomass productions reached 10.23 g/L and 2.64 g/L, respectively. The extracellular pyruvate concentration showed similar trends as with the other produced metabolites that were measured with an average steady state value of 0.04 g/L. The oscillating succinic acid concentration was determined to be 0.19 g/L on average

at steady state. With these results, the yield of biomass (Y_{sx}) on glucose was calculated to be 0.14 g/gDW and the yield of ethanol on glucose (Y_{se}) was found to be 0.55 g/g. The intracellular glucose concentration was obtained as 0.08 g/L while the intracellular pyruvate concentration was measured as 0.11 g/L.

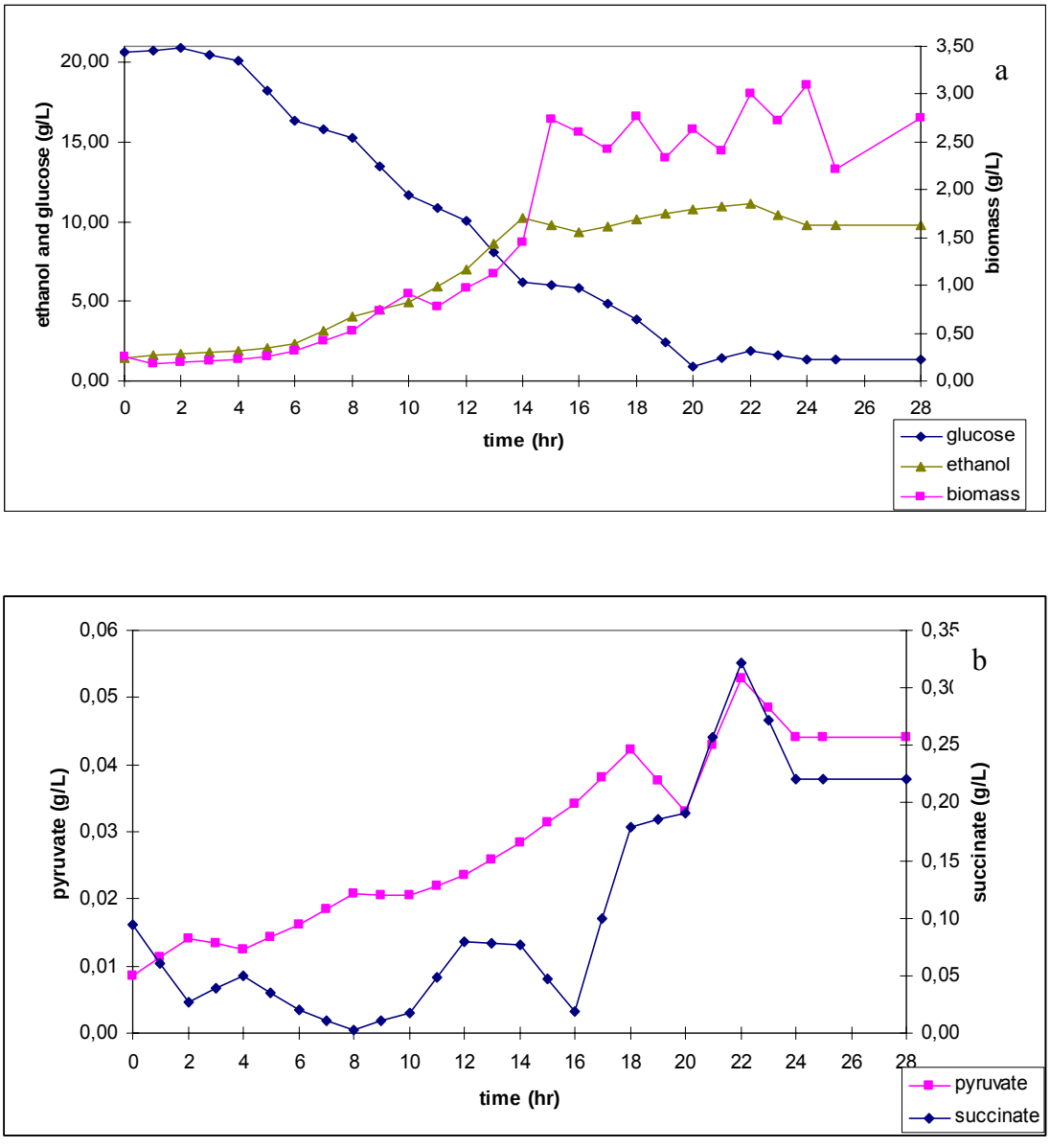

Figure 3.10. Growth characteristics (a) and Pyruvate and succinate concentration profiles (b) of mutant strain, ΔQDR3 in continuous cultures

Growth characteristics of ΔMIG1 are shown in Figures 3.11 a and b. Glucose was consumed until it reached an average value of 0.21 g/L at steady state while 10.07 g/L of ethanol and 2.51 g/L of biomass were produced. The extracellular pyruvate concentration

first increased and then decreased and the maximum value it reached was 0.03 g/L while it had an average value of 0.02 g/L during the time period when extracellular metabolite concentrations had a constant value. The steady state succinic acid concentration was determined to be 0.29 g/L.

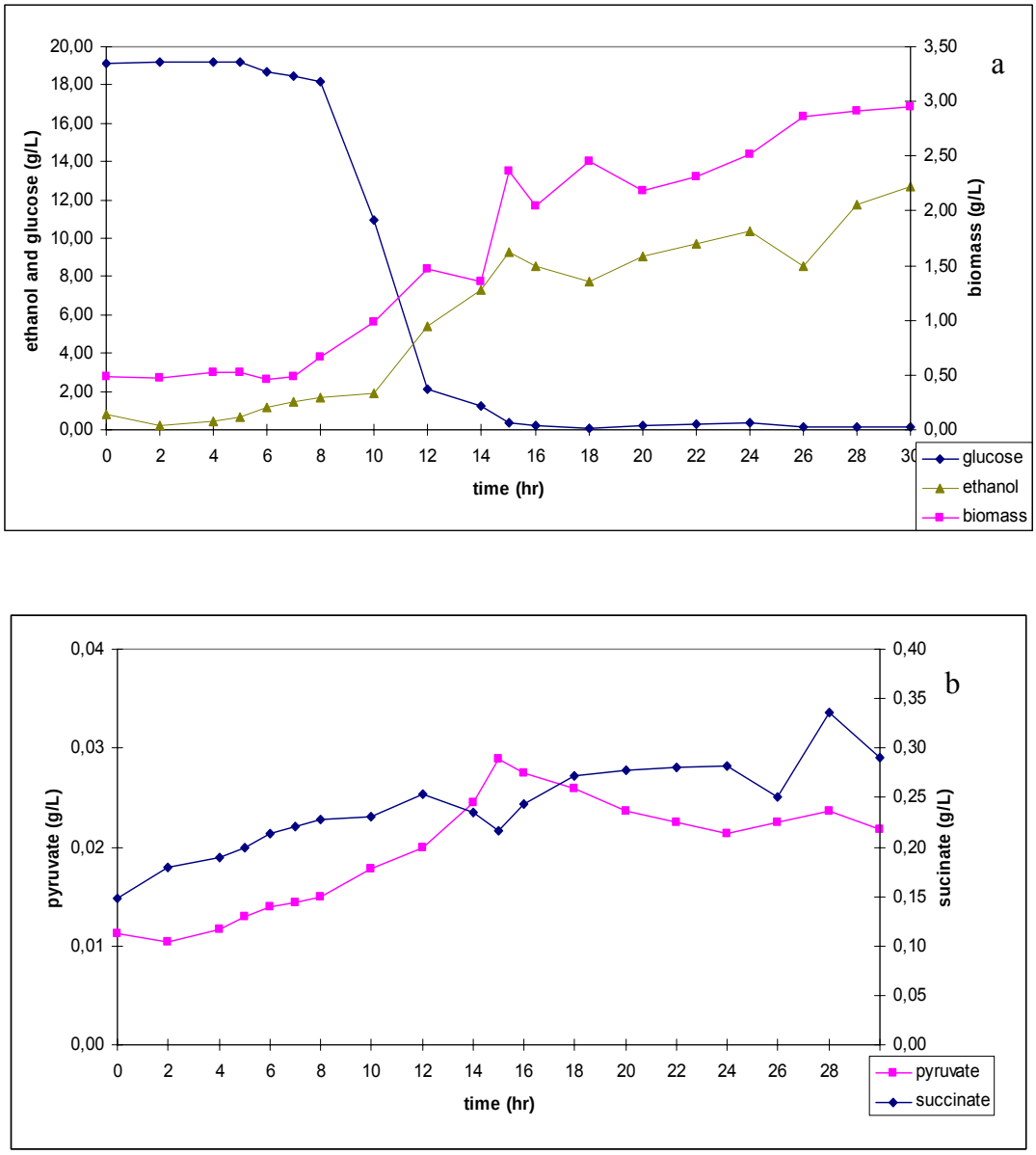

Figure 3.11. Growth characteristics (a) and Pyruvate and succinate concentration profiles (b) of mutant strain, ΔMIG1 in continuous cultures

With these results, the yield of biomass on glucose (Y_{sx}) was calculated to be 0.13 g/gDW and the yield of ethanol on glucose (Y_{se}) was found to be 0.51 g/g on glucose.

Growth and metabolite concentration profiles of ΔHAP4 strain are presented in Figures 3.12 a and b.

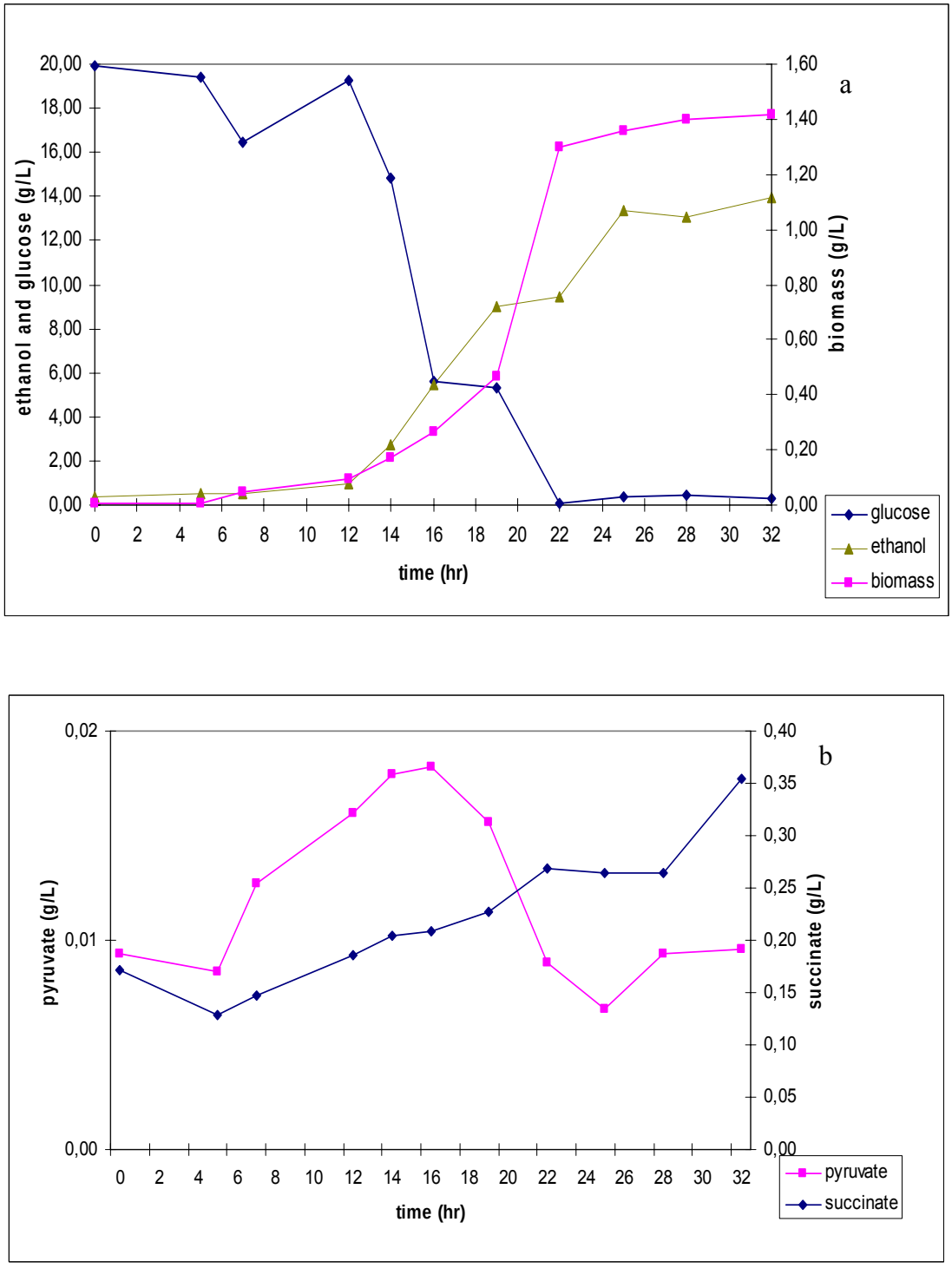

Figure 3.12. Growth characteristics (a) and Pyruvate and succinate concentration profiles (b) of mutant strain, ΔHAP4 in continuous cultures

The remaining glucose of ΔHAP4 cultivation was found to be 0.29 g/L at steady state while ethanol and biomass production reached 12.46 g/L and 1.37 g/L, respectively. The extracellular pyruvate concentration first increased and then decreased and the maximum value it reached was 0.02 g/L while it had an average value of 0.01 g/L at steady state. The succinic acid concentration at steady state was determined to be 0.29 g/L. With these results, the yield of biomass (Y_{sx}) on glucose was calculated to be 0.07 g/gDW and the yield of ethanol (Y_{se}) was found to be 0.63 g/g.

Growth characteristics of the mutant strain ΔQCR7 are displayed in Figures 3.13 a and b. The glucose concentration decreased to an average value of 2.14 g/L at steady state while ethanol production reached 9.97 g/L and 2.60 g/L of biomass was yielded. The extracellular pyruvate concentration showed similar trends as with the other metabolites measured with an average steady state value of 0.04 g/L. The steady state succinic acid concentration was determined to be 0.07 g/L.

With these results, the yield of biomass (Y_{sx}) on glucose was calculated to be 0.15 g/gDW and the yield of ethanol (Y_{se}) on glucose was found to be 0.56 g/g. The intracellular glucose concentration was obtained as 0.09 g/L while the intracellular pyruvate concentration was measured as 0.02 g/L.

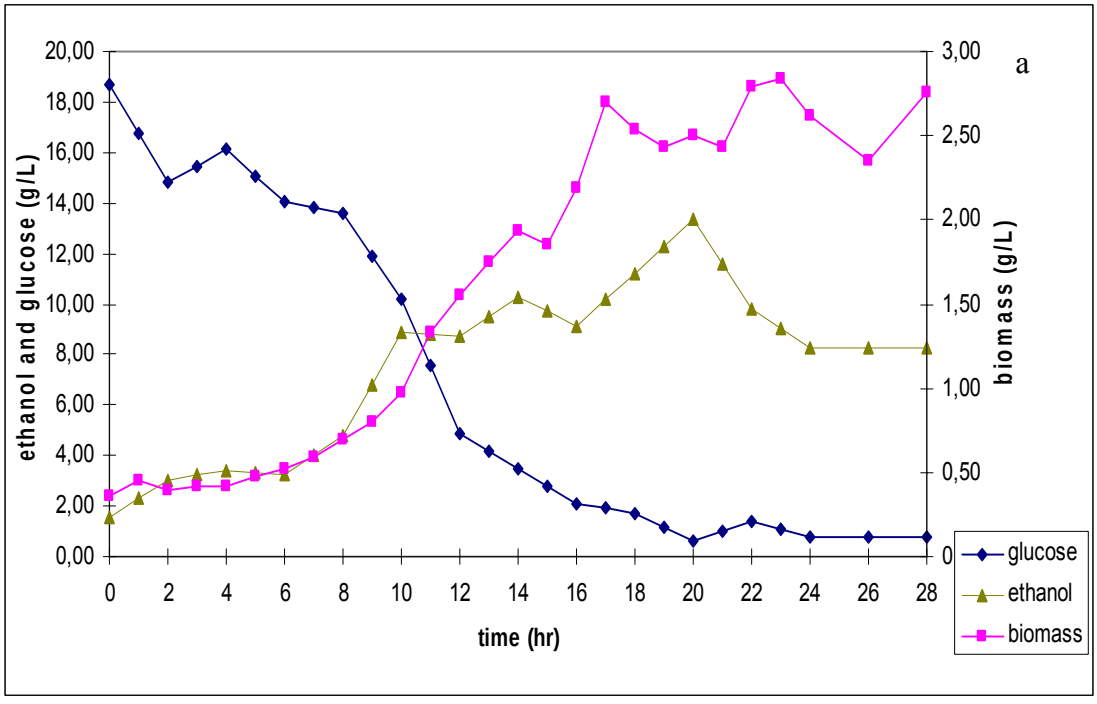

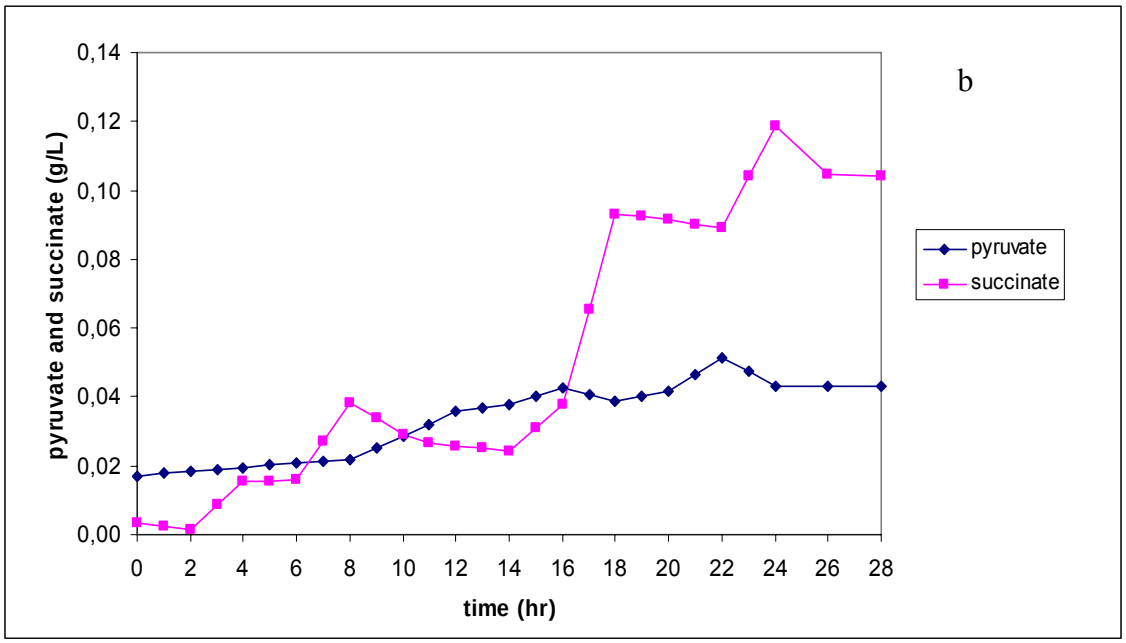

Figure 3.13. Growth characteristics (a) and Pyruvate and succinate concentration profiles (b) of mutant strain, ΔQCR7 in continuous cultures

Growth characteristics of ΔCYT1 are presented in Figures 3.15 a and b. Glucose was consumed until an average value of 2.85 g/L at steady state while ethanol production reached 9.82 g/L and 1.34 g/L of biomass was produced. The extracellular pyruvate concentration reached 0.01 g/L at steady state.

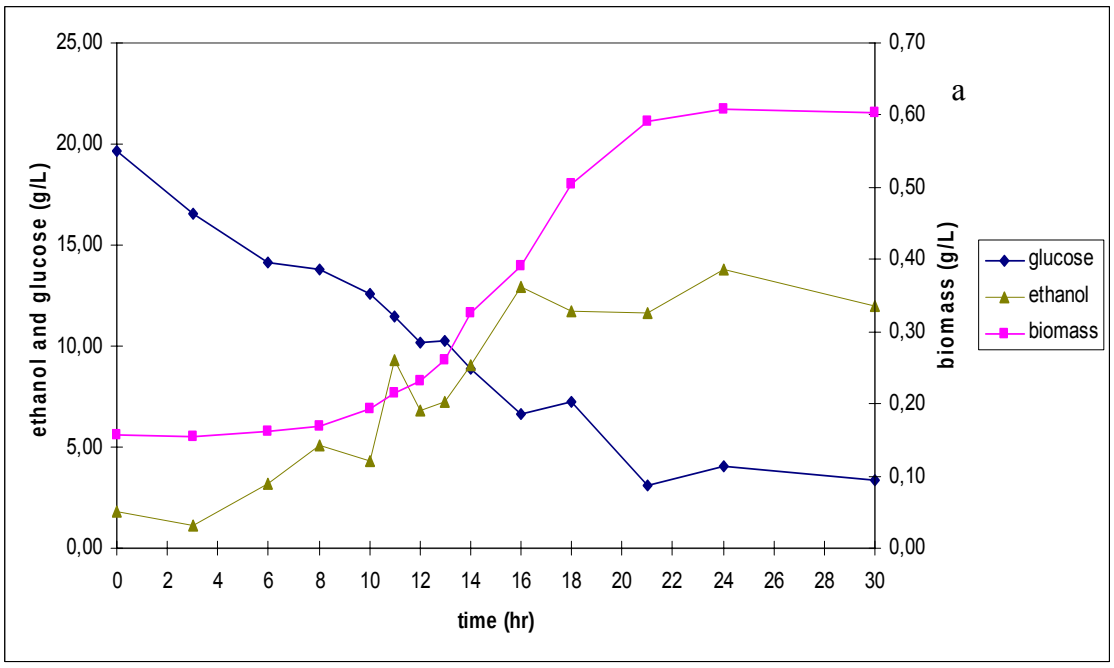

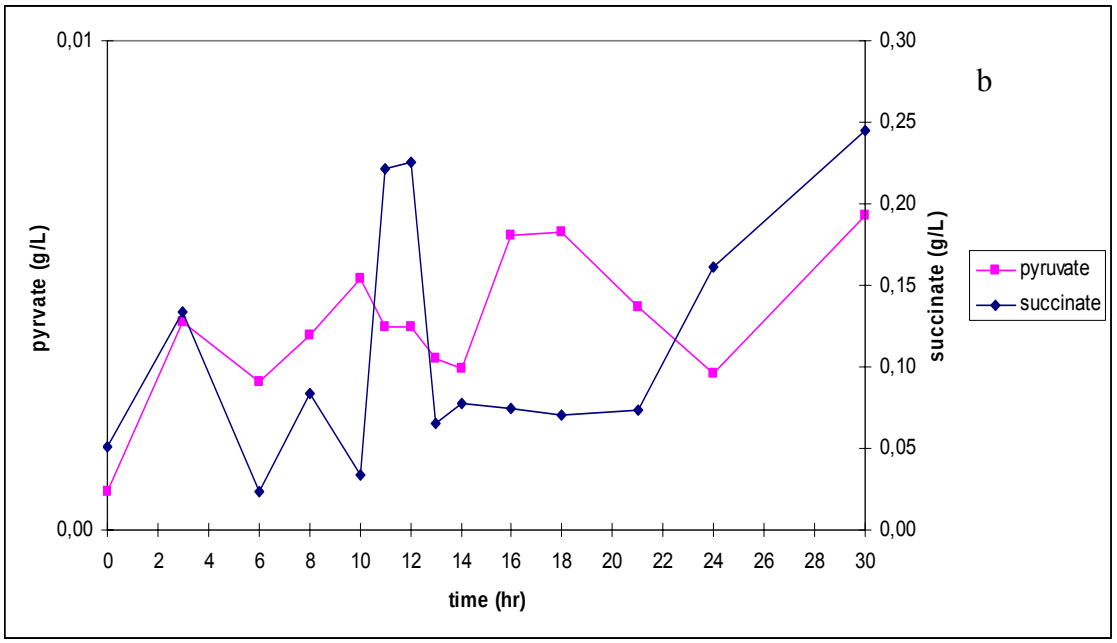

Figure 3.14. Growth characteristics (a) and Pyruvate and succinate concentration profiles (b) of mutant strain, ΔRIP1 in continuous cultures

The average concentration of succinic acid at steady state was determined to be 0.06 g/L. With these results, the yield of biomass on glucose (Y_{sx}) was calculated to be 0.08 g/gDW and the yield of ethanol on glucose (Y_{se}) was found to be 0.57 g/g.

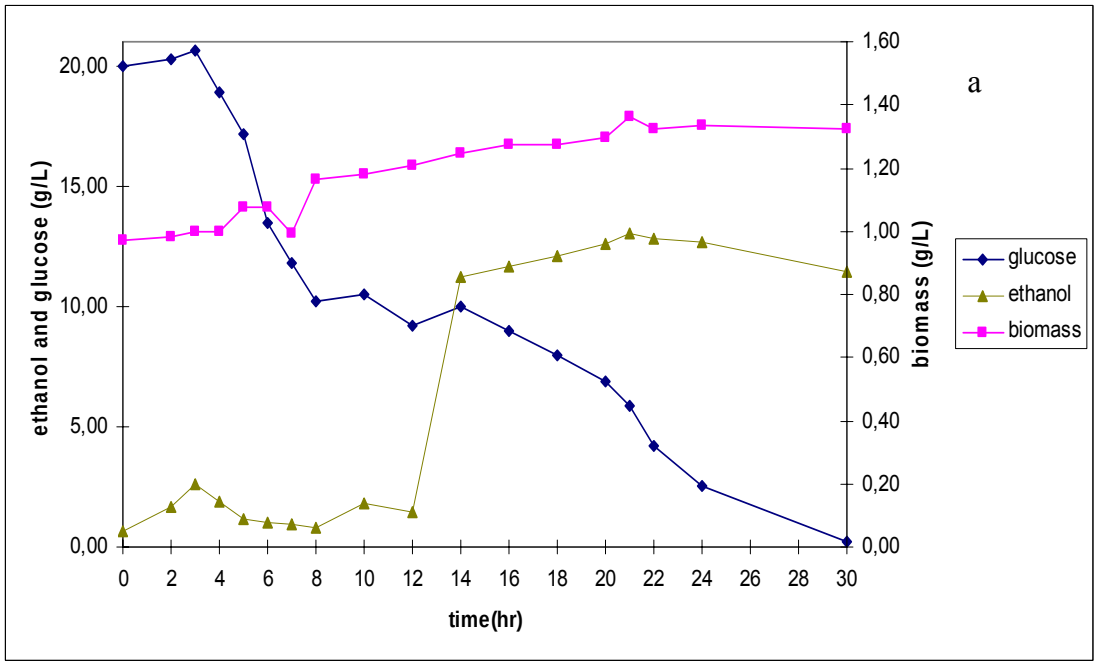

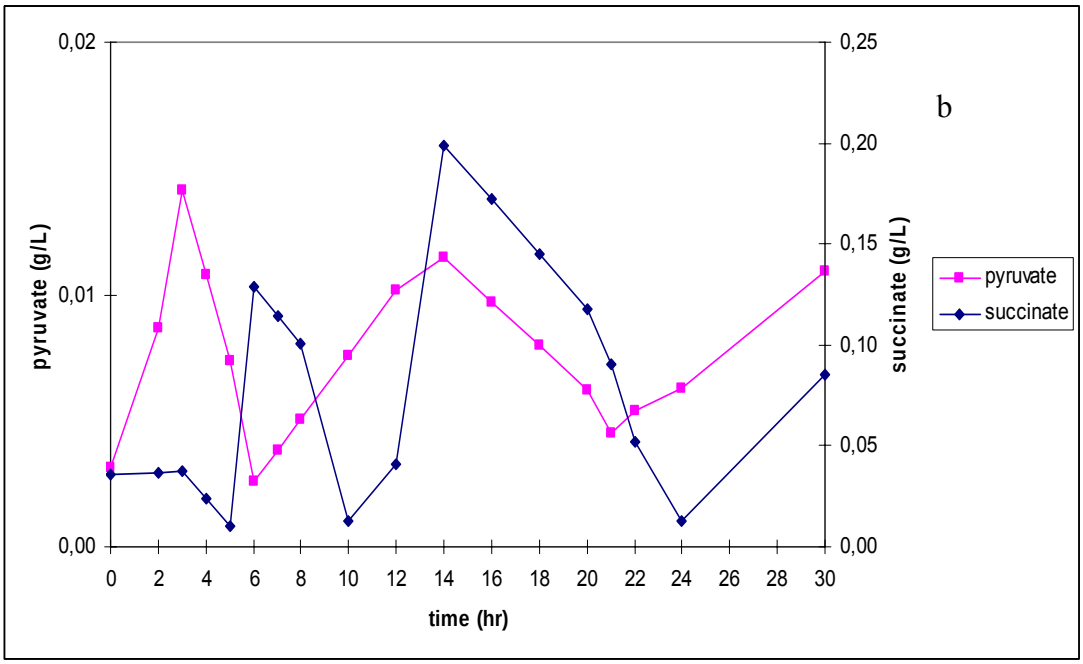

Figure 3.15. Growth characteristics (a) and Pyruvate and succinate concentration profiles (b) of mutant strain, ΔCYT1 in continuous cultures

3.4.2. Flux Balance Analysis

Flux balance analysis (FBA) was performed on the wild type strain and the seven deletion mutant strains in order to be able to check the compatibility of the experimental results with their theoretical correspondences. For this purpose, the central carbon metabolism of the organism was used as the small scale model and the complete metabolic network of the organism was used as the genome scale model (GSM) in flux balance analysis.

3.4.2.1. Small Scale Model The model consisted of 70 irreversible reactions and 50 metabolites constructing the central carbon metabolism of the yeast *S. cerevisiae* (Cakir *et al*., 2003). The measured fluxes of biomass, glucose, succinic acid and pyruvate were set as the equality constraints of the linear programming problem while ethanol was kept unconstrained in order to be able to check with its experimental value. The objective function was set to maximize the ethanol production rate. The calculated ethanol fluxes (mole / mole glucose) using the small scale model (SSM) are presented in comparison to the experimental values in Table 3.1. The strains are listed in order of increasing error as compared to their corresponding experimental values.

Table 3.1. Comparison of calculated ethanol fluxes by FBA using SSM and experimental results

Strain	Experimental Ethanol Production (mole / mole glucose)	Computed Ethanol Production (mole / mole glucose)	difference	per cent error
ΔRIP1	1.91	1.64	0.27	14.10
ΔCYT1	1.93	1.28	0.65	33.81
ΔMIG1	1.53	0.83	0.70	45.83
ΔQDR3	1.77	0.62	1.15	62.57
ΔQCR7	1.80	0.36	1.44	81.40
ΔHO	1.45	0.25	1.20	82.82
BY4743	1.45	0.25	1.20	82.82
ΔHAP4	1. 85	0.17	1.68	93.38

The lowest errors were obtained through fully respiratory deficient strains ΔRIP1 and ΔCYT1 since the objective function was set to be the maximization of ethanol production. The strains BY4743, ΔHAP4 and ΔHO that aimed to optimize their respiratory paths and optimize their biomass production at the same time yielded higher percentage errors with the specified objective function.

Due to the nature of the reactions involved in the central carbon metabolism, optimization of the oxygen uptake could not be utilized as the objective function in the small scale model.

This metabolic model was used to determine the compatibility of experimental and computational outcomes of the system which was studied. The comparison of the production of ethanol revealed that the model had shortcomes in describing the real phenomena that had occurred.

However, it was also clarified that even with the problematic differences in experimental and computational results, the best correlations were obtained for the

respiratory deficient mutants ΔRIP1 and ΔCYT1 due to the nature of the problem that was stated.

3.4.2.2. Genome Scale Model The genome scale model consisted of all the metabolites that the organism utilized and all the reactions that the organism underwent. This corresponded to 822 metabolites and 1172 reactions (Förster *et al*., 2003). The same measured fluxes were used as equality constraints as it was in the case of SSM and ethanol was again kept unconstrained to compare with the experimental findings.

Two separate objective functions were chosen; one being the optimization of oxygen uptake and the other being the optimization of ethanol production. The results of the FBA using the genome scale stoichiometric model with an objective function of maximization of ethanol production or oxygen uptake are depicted in Tables 3.2 and 3.3 respectively, where the strains are again listed in order of increasing error compared with the experimental findings.

The objective function of maximization of oxygen uptake yielded more accurate results for the strains whose respiratory pathways were not blocked as in the case of BY4743 and ΔHO while when the optimization of ethanol production was chosen as the objective function, the fully respiratory deficient strains ΔRIP1 and ΔCYT1 displayed very low errors in comparison to their experimental correspondences. This showed that the genome scale metabolic network modeled the behavior of the organism satisfactorily when the proper objective function was set according to the physiology and metabolic sufficiency of the organism.

Genome scale metabolic model was used with two different objective functions to determine the optimum flux distributions within the organism. The model predicted the real life behavior within acceptable limits for both the optimization of oxygen uptake and the optimization of ethanol production used as objective functions.

Optimization of oxygen uptake best described the state of the wild type BY4743 strain and the reference strain ΔHO as expected. Optimization of ethanol production best

described the behavior of the respiratory deficient strains ΔRIP1, ΔCYT1 and ΔQCR7 together with the partially respiratory deficient ΔQDR3.

Table 3.2. Comparison of experimental and calculated ethanol production using FBA and GSM with an objective function of optimization of O_2 uptake

Strain	Experimental Ethanol Production (mole / mole glucose)	Computed Ethanol Production (mole / mole glucose)	difference	per cent error
ΔHO	1.45	1.56	0.11	7.68
ΔQDR3	1.77	1.62	0.15	8.21
BY4743	1.45	1.58	0.13	8.90
ΔHAP4	1.85	1.68	0.17	9.11
ΔMIG1	1.53	1.72	0.19	12.29
ΔQCR7	1.80	1.52	0.28	15.47
ΔCYT1	1.93	1.51	0.42	21.71
ΔRIP1	1.91	1.25	0.66	34.38

Table 3.3. Comparison of experimental and calculated ethanol production using FBA and GSM with an objective function of optimization of ethanol production

Strain	Experimental Ethanol Production (mole / mole glucose)	Computed Ethanol Production (mole / mole glucose)	difference	per cent error
ΔRIP1	1.91	1.92	0.00	0.22
ΔCYT1	1.93	1.85	0.08	4.46
ΔQDR3	1.77	1.69	0.08	4.46
ΔQCR7	1.80	1.62	0.18	9.95
ΔHAP4	1.85	1.52	0.23	12.09
ΔMIG1	1.53	1.74	0.21	13.92
ΔHO	1.45	1.66	0.21	14.60
BY4743	1.45	1.68	0.23	15.71

3.4.3. Minimization of Metabolic Adjustment

The method of minimization of metabolic adjustment (MOMA) was applied to the mutant strains in order to determine the metabolic flux distribution under which the mutant strain aimed closest to imitate the wild type strain, rather than to optimize its forced metabolic conditions; such as maximizing ethanol production as it was in the case of respiratory deficient mutants (Segre *et al*., 2002).

The ethanol fluxes obtained using MOMA were definitely lower than those obtained via FBA since the method aimed to find the flux distribution which was closest to that of the wild type for the mutant strains. The outcomes of MOMA are presented more comprehensively in Table 3.4.

Table 3.4. Comparison of experimental and calculated ethanol production using MOMA

Strains	Experimental Ethanol Production (mole / mole glucose)	Computed Ethanol Production-GSM (mole / mole glucose)	Computed Ethanol Production-MOMA (mole / mole glucose) - (order of being closest to WT)
ΔHO	1.45	1.66	1.18
ΔQDR3	1.77	1.69	1.18
ΔMIG1	1.53	1.74	1.09
ΔHAP4	1.85	1.52	0.97
ΔQCR7	1.80	1.62	0.87
ΔRIP1	1.91	1.92	0.63
ΔCYT1	1.93	1.85	0.42

As expected, the difference in fluxes was greatest for the strains ΔCYT1 and ΔRIP1 whose sole aims were to maximize their ethanol production and enhance their fermentative pathways.

MOMA was applied to the mutant strains in order to be able to determine their metabolic proximity to the parental strain. ΔHO was found to be the strain with nearest flux distributions as that of the wild type. The respiratory deficient mutants ΔRIP1 and

ΔCYT1 displayed MOMA distributions which indicated that their real flux distributions were far away from that of imitating the wild type behavior as expected.

3.4.4. Principle Component Analysis

Principle component analysis (PCA) was carried out in order to analyze the experimental design as well as the behavior of the eight strains BY4743, ΔHO, ΔQDR3, ΔMIG1, ΔHAP4, ΔQCR7, ΔRIP1 and ΔCYT1 in chemostat cultures in rich medium.

After the new principle components (PCs) were constructed, the latent vector was plotted to decide on the number of PCs that were to be taken into consideration in further analysis of loadings and scores. The latent vector graph is shown in Figure 3.16. It indicated that the first two PCs covered more than 80 per cent of all data of significance and since this value was above the previously determined limit of 67 per cent, it was considered to be sufficient for further analysis.

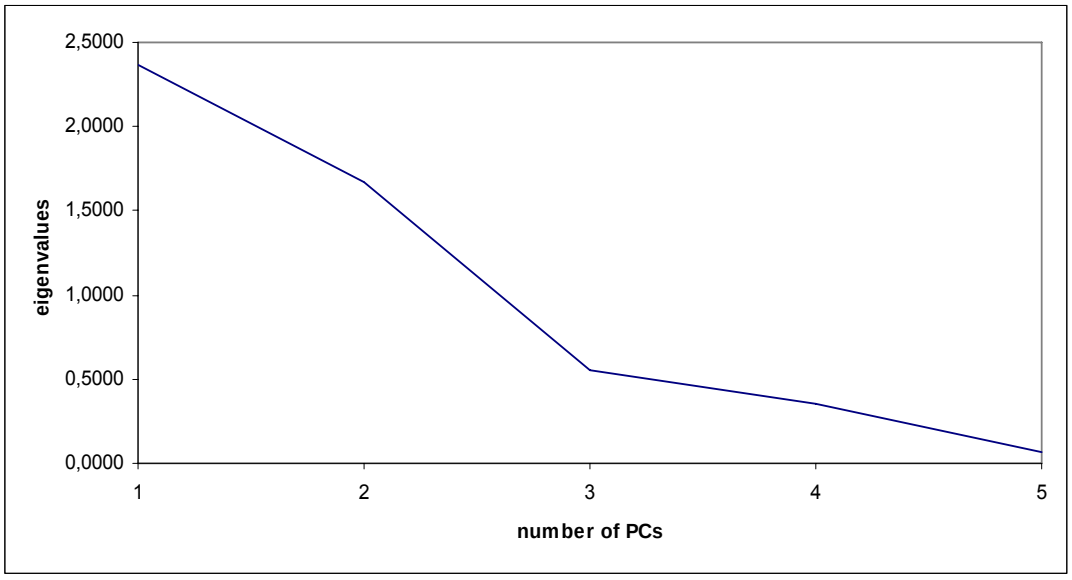

Figure 3.16. Plot of the latent vector

With the number of principle components decided, the first two scores were plotted against each other to cluster the strains according to their physiological characteristics.

The plot of scores is presented in Figure 3.17. ΔRIP1 and ΔCYT1 were clustered together as expected since they were deletion mutants of genes which belonged to the same respiratory chain complex; the cytochrome bc1 complex. The unexpected result was the alienation of ΔQCR7 in the lower left quadrant. Since Qcr7 was again a protein belonging to the same respiratory chain complex with Rip1 and Cyt1, its deletion mutant would have been expected to cluster in the same group as that of ΔRIP1 and ΔCYT1.

Another cluster of strains was formed by BY4743 and ΔHO. This result was expected since ΔHO was selected as the reference gene resembling the wild type behavior for the respiratory pathway analyses.

The mutants of the regulatory genes Mig1 and Hap4 were clustered separately in the upper part of the graph from the other mutants and from each other since they are involved in the regulation of many different pathways and the diversity of their functions disabled any close similarities to any other gene.

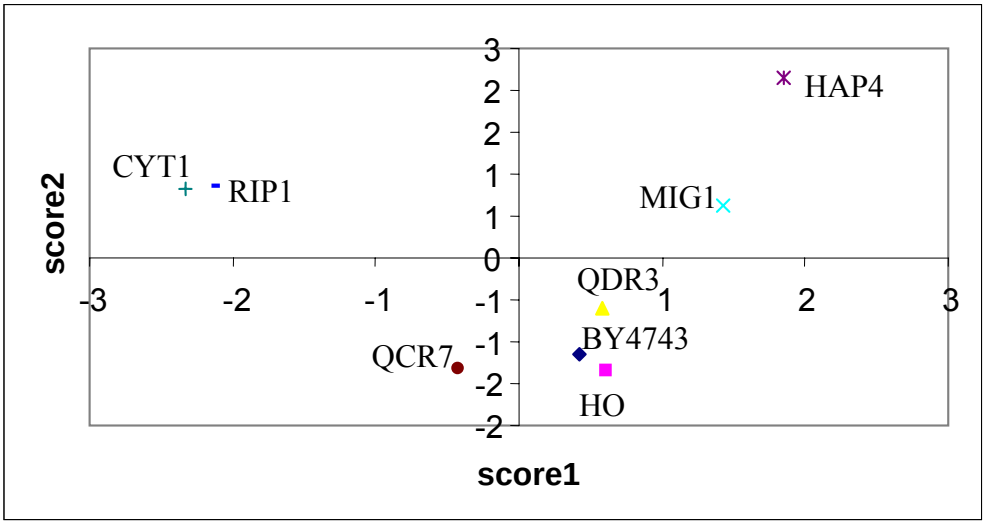

Figure 3.17. Plot of score 2 against score 1

The first two loadings belonging to the first principle components were plotted against each other in order to investigate the relevance and connection of the measured metabolites (Figure 3.18). Clustered metabolites would indicate the irrelevance of one or more of the metabolic measurements. The results did not show any neighboring metabolites and the data is very scattered as expected.

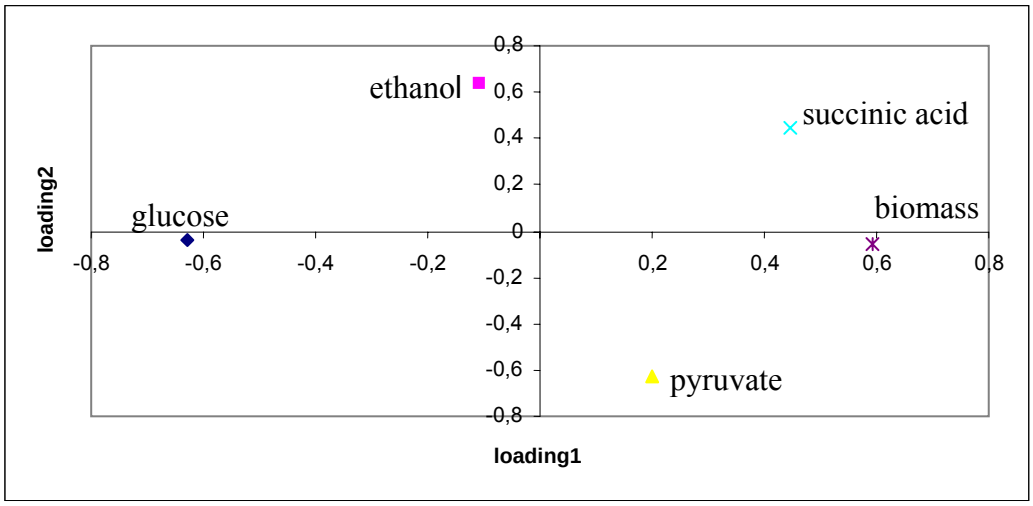

Figure 3.18. Plot of loading 2 against loading 1

3.5. Investigation of Metabolic and Transcriptional Response of *S. cerevisiae* to Nutritional Limitations in Batch Cultivations with Pulse Injections

3.5.1 Metabolic Response of BY4743 to Carbon and Nitrogen Starvations Followed by Recovery To No-Limitation Conditions

In order to investigate the metabolic response of the wild type yeast BY4743 to two major nutritional elements, two simultaneously run fed batch experiments and one batch experiment were conducted. F1 medium was used for its advantageous defined composition. In the batch experiment, F1 medium with no initial limitation was inoculated and via periodic sampling, response of cells to initial abundance of nutrients followed by scarcity towards the end of the cultivation was observed. In the fed batch cultivations, F1 media were prepared such that there was either carbon or nitrogen limitation. Pulse injections were given to the culture so as to recover the media to no limitation conditions as the limited carbon or nitrogen source was completely utilized. A second pulse was given when an intermediary steady state was reached and sampling was carried out until the ultimate steady state conditions were reached. The results presented below belong to the average of the steady state values measured for the biomass and the extracellular metabolites.

The growth characteristics of BY4743 under no limitation conditions are depicted in Figures 3.19 a and b.

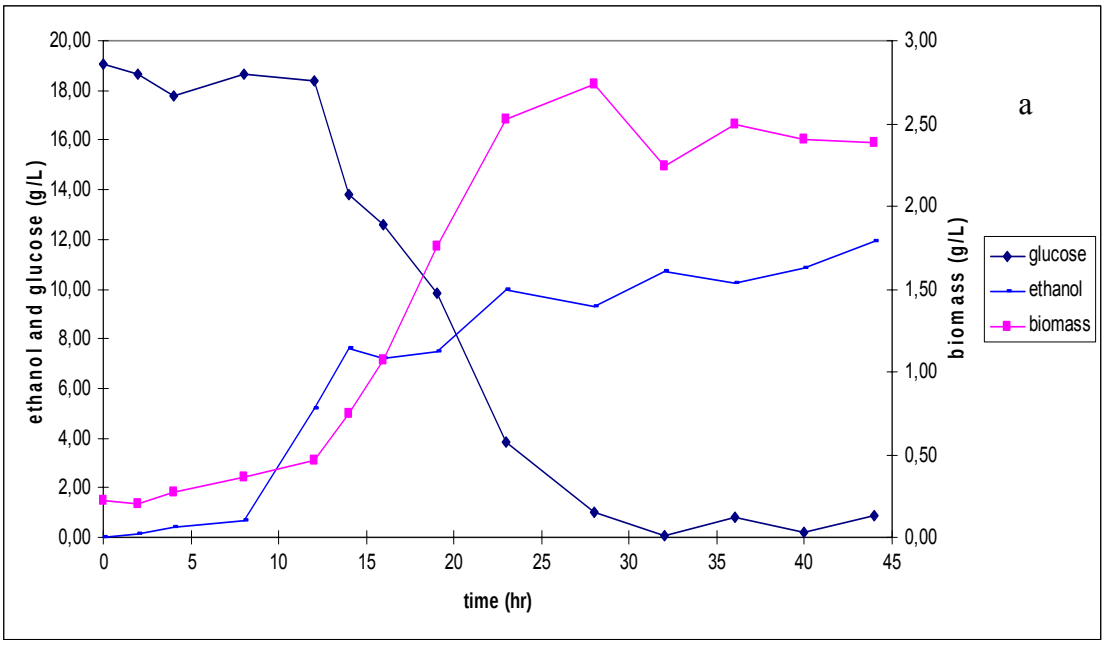

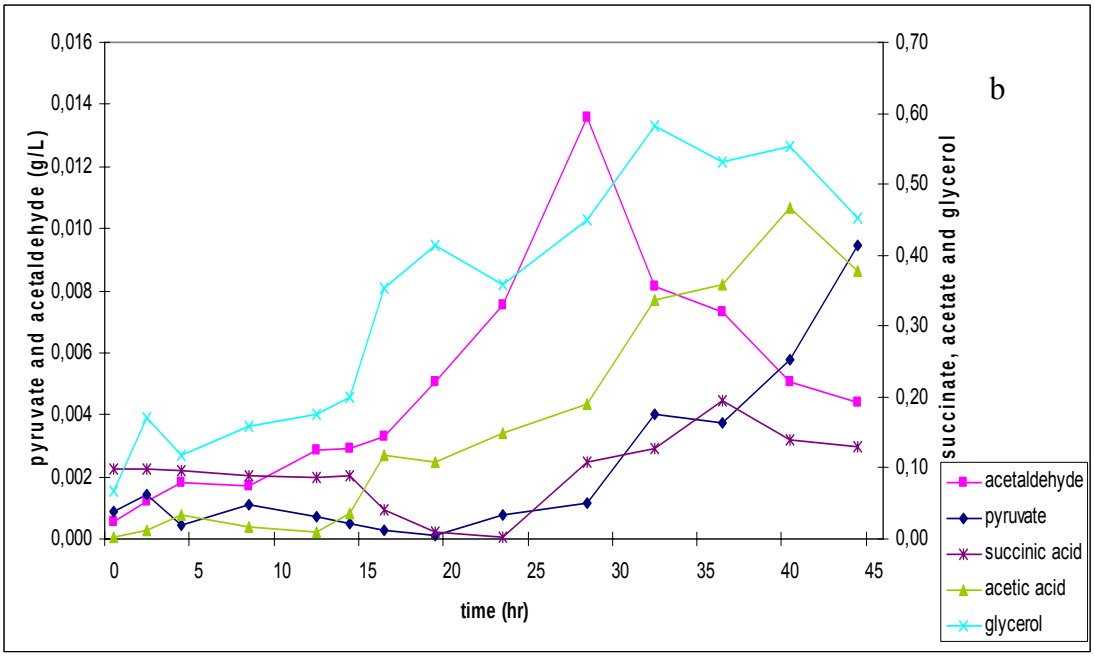

Figure 3.19. Growth characteristics (a) and Metabolic profiles (b) of BY4743 under no limitation conditions in batch cultures

This was a typical batch growth curve with a steady constant value of 2.45 g/L of biomass at the end of the experiment. The maximum growth rate, μ_{max} was found as 0.18

hr^{-1} and K_s was found to be 2.00 g/L. The glucose was consumed up down to an ultimate value of 0.58 g/L. From 30^{th} hour onwards, the extracellular pyruvate concentration climbed up to a value of 0.01 g/L at the end of the experiment. The concentration of extracellular succinic acid remained constant until exponential phase where it showed a steep decline to disappear and then towards the end, it rose to an average value of 0.15 g/L. The fermentative intermediate acetaldehyde showed a peak of 0.01 g/L at the 28.5^{th} hour of cultivation and then decreased. A fermentative product, acetic acid reached a steady state concentration of 0.39 g/L at the end of the cultivation.

The main fermentative product ethanol was produced at a maximum concentration of 10.07 g/L in the culture and the fermentative by-product glycerol is produced at a concentration of 0.51 g/L. The yields of biomass (Y_{sx}), glycerol (Y_{sg}), ethanol (Y_{se}) and acetic acid (Y_{sa}) on glucose were calculated to be 0.13 g/gDW, 0.03 g/g, 0.52 g/g and 0.02 g/g respectively.

The growth characteristics of the carbon limited conditions are given in Figures 3.20 a and b. The pulse injections are indicated with red dashed lines across the figure at the 16.5^{th} and 32.5^{th} hours. The biomass concentration reached 2.28 g/L at the first steady state and 3.06 g/L at the end of the cultivation. The maximum growth rate, μ_{max} for the nutrient limited portion of the experiment was 0.09 hr^{-1} and the substrate utilization constant K_s was calculated as 0.47 g/L. Before the first pulse was given, the initial glucose was almost completely consumed and the remaining glucose concentration was measured as 0.54 g/L. Following the pulse, its concentration increased to 20.50 g/L and then decreased to 4.99 g/L prior to the second pulse. The glucose concentration rose to 17.81 g/L soon after the second pulse and ended at a final concentration of 7.17 g/L. Pyruvate concentration showed no specific trend either a priori or a posteriori to the pulses. However, clear fluctuations were observed around the points at which the pulses were injected. Succinic acid concentration showed a sharp increase as soon as the pulses were given, in the first one reaching 0.22 g/L and in the second one reaching 0.30 g/L. The fermentative intermediate acetaldehyde showed a trend similar to that of succinic acid, giving sharp peaks at injections. The concentrations were 0.02 g/L and 0.02 g/L for the two pulses respectively. A fermentative product, acetic acid was produced in increasing amounts as pulses were introduced. At the beginning, very little production was observed and

considerable amounts of production began with the injection of the first pulse and before the second injection, it reached a final value of 0.28 g/L. After the second pulse, the concentration continued to increase until it reached a steady value at 0.56 g/L.

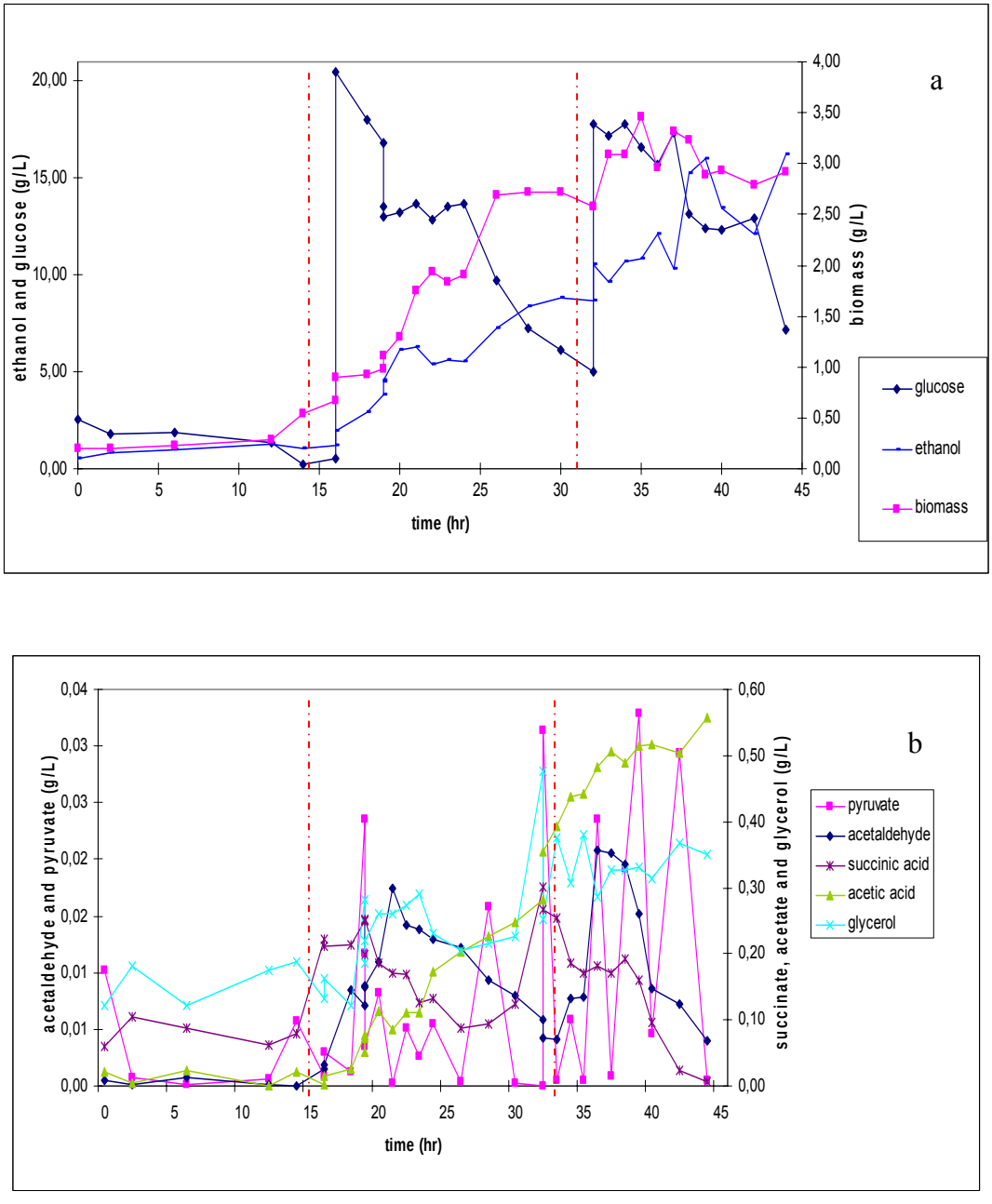

Figure 3.20. Growth characteristics (a) and Metabolite profiles (b) of BY4743 under carbon limitation conditions in batch cultures with pulse injections

The main fermentation product which is ethanol is produced at very low amounts before any pulses were introduced. At the steady state reached following the first pulse, its

concentration rose to 8.14 g/L and it reached 14.61 g/L at the end of cultivation. The fermentative by-product glycerol is measured as 0.25 g/L and 0.34 g/L at the steady states following each pulse injection. The yields of biomass (Y_{sx}), glycerol (Y_{sg}), ethanol (Y_{se}) and acetic acid (Y_{sa}) on glucose were calculated to be 0.15 g/gDW, 0.01 g/g, 0.47 g/g and 0.02 g/g respectively for the first steady state, just reached before the second pulse injection and the ultimate yields were 0.29 g/gDW, 0.01 g/g, 0.48 g/g and 0.05 g/g for biomass, glycerol, ethanol and acetic acid, respectively.

The growth characteristics of the nitrogen limited conditions are presented in Figures 3.21 a and b. The pulse injections are indicated with red dashed lines across the figure at the 14.5^{th} and 30.5^{th} hours. The biomass concentration reached 1.72 g/L at the first steady state and 2.24 g/L at the end of the cultivation. The maximum growth rate, μ_{max} for the nutrient limited portion of the experiment was 0.13 hr^{-1} and the substrate utilization constant K_s was calculated as 0.03 g/L. Before the first pulse was given, the glucose concentration dropped to 7.96 g/L. Following the pulse, the concentration continued to decrease until it was almost completely consumed and it reached 0.33 g/L at the end of the experiment as expected. Pyruvate concentration showed no specific trend either a priori or a posteriori to the pulses as was the case in carbon limitation experiments. However, clear fluctuations were observed around the points at which the pulses were injected. Succinic acid concentration showed a sharp increase as soon as the pulses were given, in the first one reaching a value of 0.23 g/L and in the second one reaching 0.19 g/L. The fermentative intermediate acetaldehyde showed a trend similar to that of succinic acid, giving sharp peaks at injections. The peak concentrations were 0.01 g/L for both pulses. A fermentative product, acetic acid was produced in increasing amounts as pulses were introduced. At the beginning, very little production was observed and considerable amounts of production began with the injection of the first pulse and before the second injection, it reached a final value of 0.17 g/L. After the second pulse, the concentration continued to increase until it reached a steady value at 0.38 g/L. Glycerol was produced in increasing amounts during cultivation while ethanol was produced first and then consumed following a diauxic shift. The concentrations were 9.23 g/L and 0.44 g/L at the first steady state and 2.00 g/L and 0.54 g/L at the second steady state for ethanol and glycerol, respectively.

The yields of biomass (Y_{sx}), glycerol (Y_{sg}), ethanol (Y_{se}) and acetic acid (Y_{sa}) were calculated to be 0.14 g/gDW, 0.04 g/g, 0.77 g/g and 0.01 g/g respectively for the first steady state, reached before the second pulse injection and the ultimate yields were 0.11 g/gDW, 0.03 g/g, 0.10 g/g and 0.02 g/g for biomass, glycerol, ethanol and acetic acid, respectively.

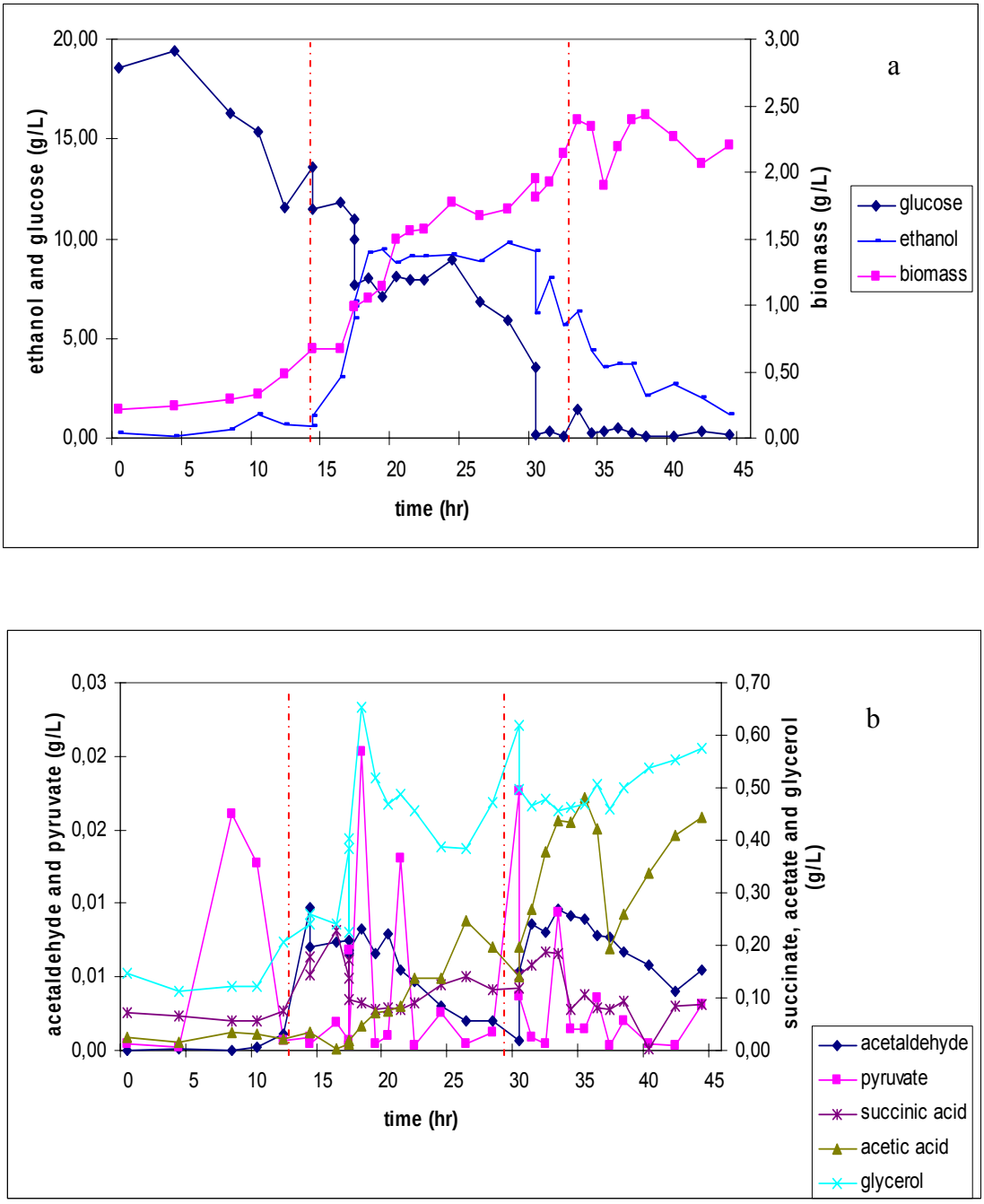

Figure 3.21. Growth characteristics (a) and Metabolite profiles (b) of BY4743 under nitrogen limitation conditions in batch cultures with pulse injections

3.5.2. Optimization of RNA Extraction

Prior to batch cultivations with nutritional limitation, sample storage techniques and protocols for mechanical disruption of cell walls needed to be evaluated to give the optimum performance in order to obtain the maximum amount of high grade and non-degraded RNA from extraction. Sets of samples were either stored in RNA Stabilizing Solution or shock frozen in -80^{o}C. For mechanical disruption, four different speeds; 300 rpm, 500 rpm, 1000 rpm, 1500 rpm, and two different time periods; 3 min, 5 min were tested for disruption performance (Table 3.5) and the extracted samples were checked on gel electrophoresis for integrity and concentration (Figure 3.22).

Table 3.5. Combinations of sample storage and mechanical disruption techniques

Lane 1	Lane 2	Lane 3	Lane 4	Lane 5	Lane 6	Lane 7	Lane 8
5 min., 300 rpm, stabilizing reagent	5 min., 300 rpm, shock freeze	3 min., 1000 rpm, shock freeze	3 min., 1000 rpm, stabilizing reagent	5 min., 500 rpm, shock freeze	5 min., 500 rpm, stabilizing reagent	3 min., 1500 rpm, shock freeze	3 min., 1500 rpm, stabilizing reagent

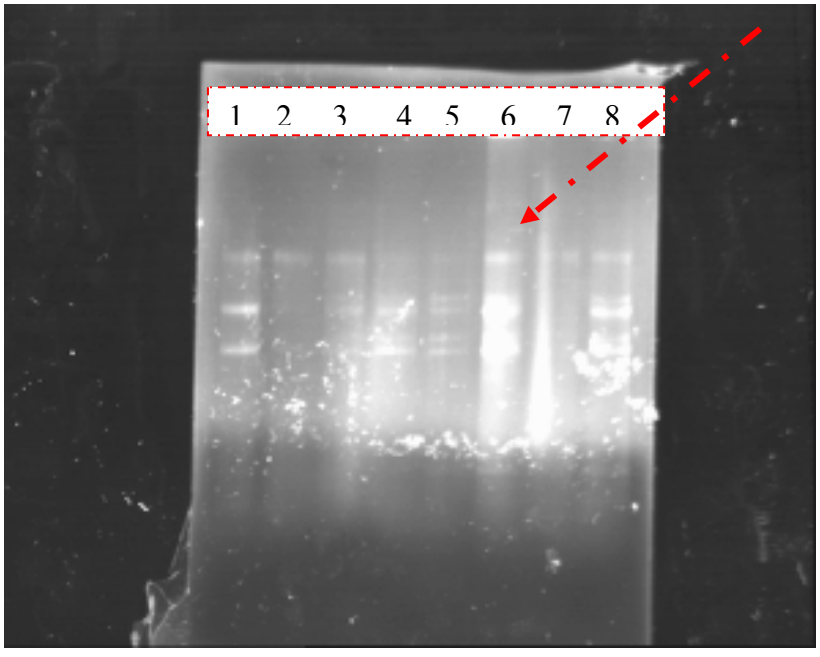

Figure 3.22. Analysis of the integrity and concentration of extracted RNA samples by gel electrophoresis

Analysis of RNA samples prepared under different conditions showed that storage of cell extracts in RNA stabilizing solution and mechanical disruption for 5 minutes at 500 rpm using the dismembrator (Bio-lab, USA) resulted in the purification of high quality RNA which will be suitable for further studies.

3.5.3. The Selection of Control Genes

In order to investigate the expression profile of HAP4 in response to glucose and ammonium sulfate pulses, two housekeeping genes with constant expression regardless of physical conditions for growth and two genes whose expression levels always remain constant with respect to the housekeeping genes were identified as control genes for quantitative real time polymerase chain reaction (rtq PCR) applications.

Microarray databases available on the World Wide Web (yMGV-Yeast Microarray Global Viewer, http://www.transcriptome.ens.fr/ymgv/) were used and COX 18 and HO were selected because these genes were reported to have a constant expression in more than 60 per cent of the array data available.

Since the expression levels of HSP12 and EXG2 are 1.5 fold with respect to that of housekeeping genes in more than 60 per cent of the available array data, these two genes were selected as positive controls. These results were further confirmed using microarray data generated by Pir *et al.* (unpublished data) under 8 different conditions (Table 3.5).

Table 3.6. $\log_2$ expression levels of the genes in quest under different cultivation conditions

Gene Symbol	Case 1	Case 2	Case 3	Case 4	Case 5	Case 6	Case 7	Case 8
COX18	9.58	9.37	9.68	9.28	9.44	9.01	9.85	9.75
HAP4	11.29	11.16	10.31	9.69	5.95	5.99	5.77	6.11
HSP12	12.99	13.12	12.01	11.78	13.125	12.97	12.07	11.20
HO	6.81	7.65	6.91	7.54	7.38	7.72	7.77	7.92
EXG2	8.61	8.71	8.86	8.84	8.67	9.01	8.93	8.81

In this selection procedure, $\log_2$ expression levels of these genes under different conditions (Table 3.5) were used and expression ratios were calculated according to Equation 3.1 (Table 3.6).

$$\log_2 (\text{expression A}) - \log_2 (\text{expression B}) = \log_2 (\text{expression A / expression B}) \quad (3.1)$$

Table 3.7. $\log_2$ ratios of the genes in quest

Expression ratios	Case 1	Case 2	Case 3	Case 4	Case 5	Case 6	Case 7	Case 8
COX18/HAP4	0.85	0.84	0.94	0.96	1.59	1.50	1.71	1.60
COX18/HSP12	0.74	0.71	0.81	0.79	0.72	0.70	0.82	0.87
COX18/HO	1.41	1.22	1.40	1.23	1.28	1.17	1.27	1.23
COX/EXG2	1.11	1.08	1.09	1.05	1.09	1.00	1.10	1.11
HAP4/HSP12	0.87	0.85	0.86	0.82	0.45	0.46	0.48	0.55
HAP4/HO	1.31	1.28	1.16	1.10	0.69	0.66	0.65	0.69
HAP4/EXG2	1.31	1.28	1.16	1.10	0.69	0.66	0.65	0.69
HSP12/HO	1.91	1.71	1.74	1.56	1.78	1.68	1.55	1.41
HSP12/EXG2	1.51	1.51	1.36	1.33	1.51	1.44	1.35	1.27
HO/EXG2	0.79	0.88	0.78	0.85	0.85	0.86	0.87	0.90

The squares of these ratios (Table 3.7) are plotted to determine the ratios that showed least fluctuations (Figure 3.23).

It is preferred to have a few fluctuations in expression ratios of control genes as well as constant expression profiles individually belonging to these selected genes. HO, COX18, EXG2 and HSP12 genes possess this preferred characteristic.

Expression ratios were further investigated to yield similar fold changes under different conditions (Figure 3.24). COX18/HSP12, COX18/EXG2, HO/EXG2 ratios were almost the same under the eight inspected conditions indicating a correct choice of gene set.

Table 3.8. Squares of ratios

	Squares of expression ratios							
Strain ratios	Condit. 1	Condit. 2	Condit. 3	Condit. 4	Condit. 5	Condit. 6	Condit. 7	Condit. 8
COX18/HAP4	0.72	0.70	0.88	0.92	2.52	2.26	2.92	2.55
COX18/HSP12	0.54	0.51	0.65	0.62	0.52	0.48	0.67	0.76
COX18/HO	1.98	1.50	1.96	1.51	1.63	1.36	1.61	1.51
COX/EXG2	1.24	1.16	1.20	1.10	1.19	1.00	1.22	1.22
HAP4/HSP12	0.76	0.72	0.74	0.68	0.21	0.21	0.23	0.30
HAP4/HO	1.72	1.64	1.36	1.20	0.47	0.44	0.42	0.48
HAP4/EXG2	1.72	1.64	1.36	1.20	0.47	0.44	0.42	0.48
HSP12/HO	3.64	2.94	3.03	2.44	3.16	2.82	2.41	2.00
HSP12/EXG2	2.27	2.27	1.84	1.77	2.29	2.07	1.83	1.62
HO/EXG2	0.62	0.77	0.61	0.74	0.73	0.73	0.76	0.81

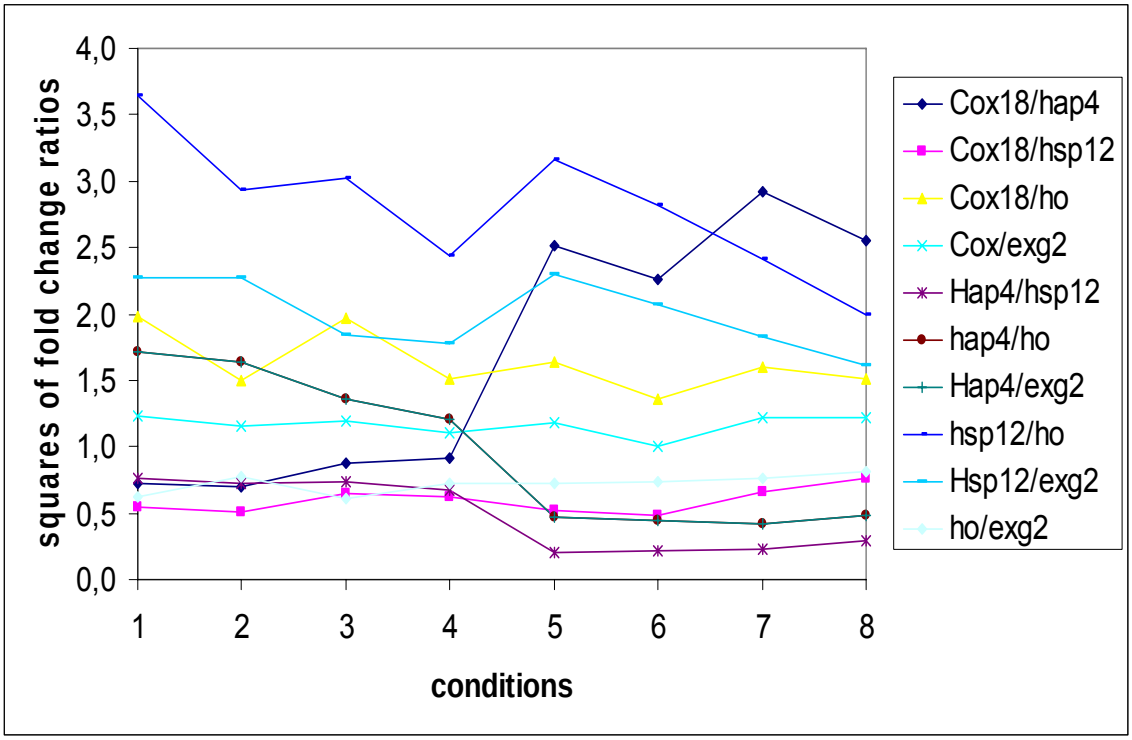

Figure 3.23. Fold change with respect to different conditions for different selections of control and housekeeping choices

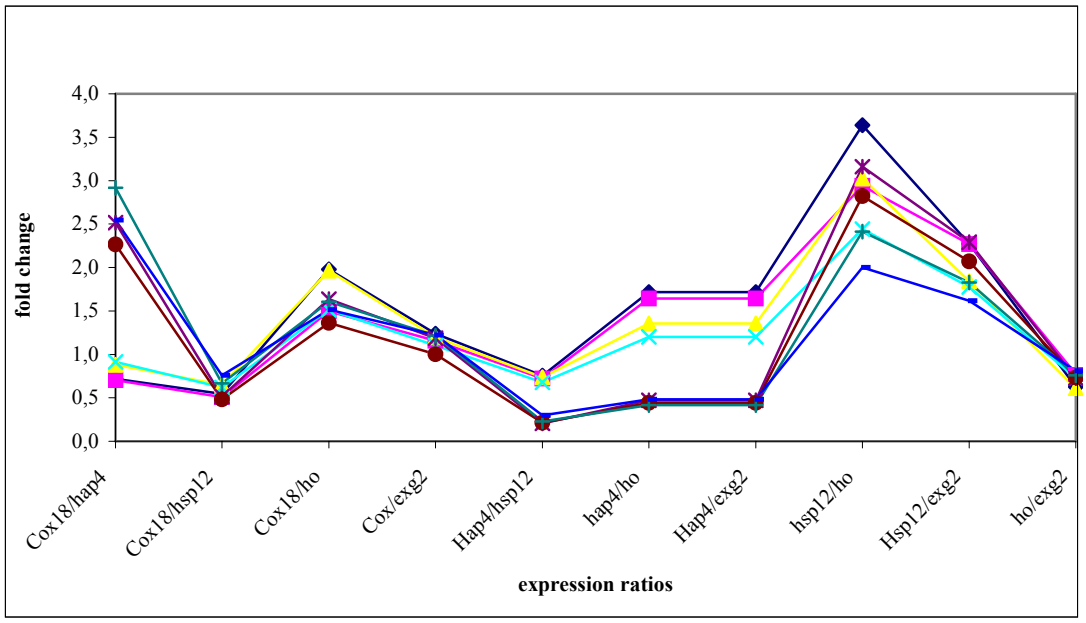

Figure 3.24. Fold change for specific gene expression ratios with respect to various control and housekeeping genes under different conditions

As a result, COX18 and HO were selected as the housekeeping genes while HSP12 and EXG2 were chosen as the positive control genes.

3.5.4. Optimization of Annealing Temperature for Reverse Transcription Quantitative Real Time Polymerase Chain Reaction Applications

Because of the fact that various sets of primers were needed to be used simultaneously due to the nature of rtq PCR applications, the selection of an optimal annealing temperature that was suitable for all primer sets is very important. An optimization procedure was carried out to determine the optimum annealing temperature for the given set of primer pairs. An RNA sample is amplified with the selected set of primers. Ten different runs were conducted where the only difference is in the annealing temperature of the PCR protocol. Annealing temperature was randomly assigned via BIORAD software between 46^{o}C and 56^{o}C, namely 56^{o}C, 55.3^{o}C, 54.1^{o}C, 52.2^{o}C, 49.7^{o}C, 48^{o}C, 46.7^{o}C and 46^{o}C. The PCR florescence results for 55.3^{o}C revealed no significant amplification except for the region amplified by only one set of primer pair among the 5 pairs designed for the regional amplification of HAP4, HO, COX18, EXG2, HSP12 genes (Figure 3.25). The other annealing temperatures gave similar results except for 52.2^{o}C

which showed significant amplification for the regions designed for each primer pair (Figure 3.26).

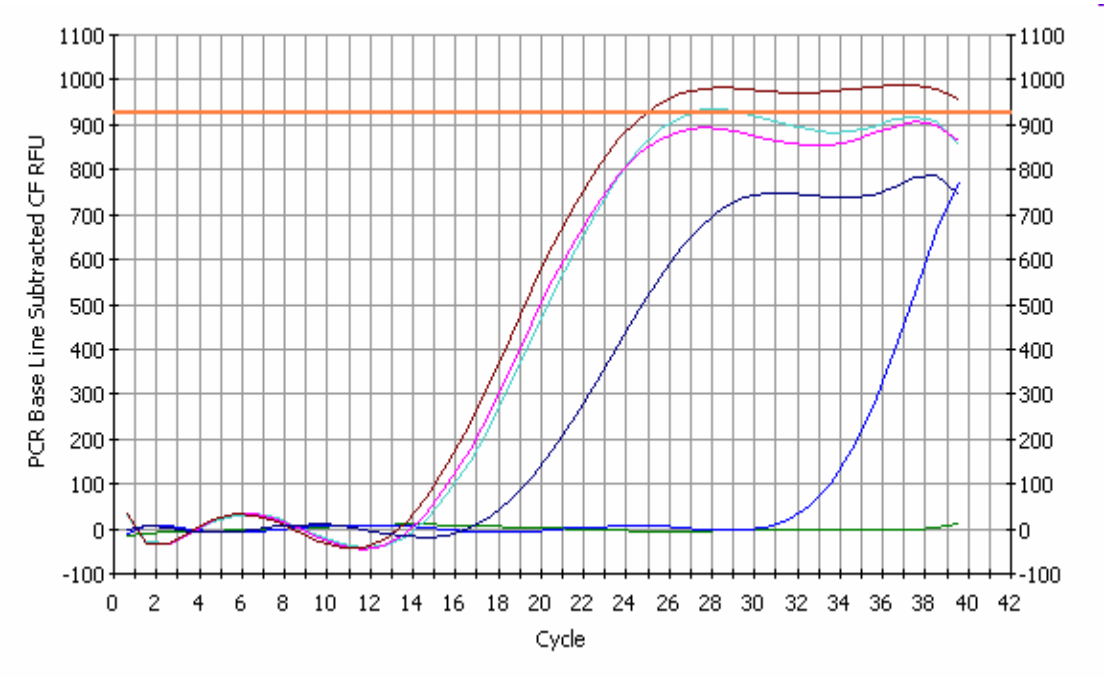

Figure 3.25. PCR amplification cycle florescence (CF) of DNA fragments at an annealing temperature of 55.3^{o}C in relative florescence units (RFU)

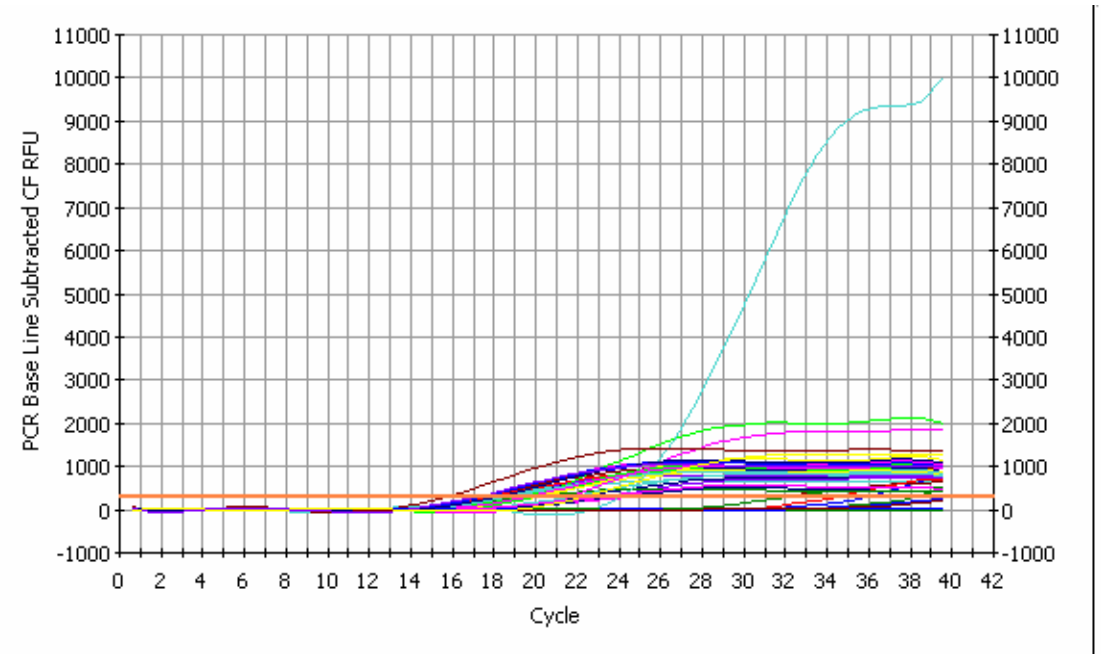

Figure 3.26. PCR amplification cycle florescence (CF) of DNA fragments at an annealing temperature of 52.2^{o}C in relative florescence units (RFU)

The corresponding melt curve analysis is displayed in Figure 3.27. The melt curves provided information about the specificity of the primers producing the amplification product. Sharp, single peaks obtained from the melt curve analysis indicated the specificity of the primers which held true for the primers selected for the amplification of HO, COX18, HAP4, EXG2 and HSP12 genes.

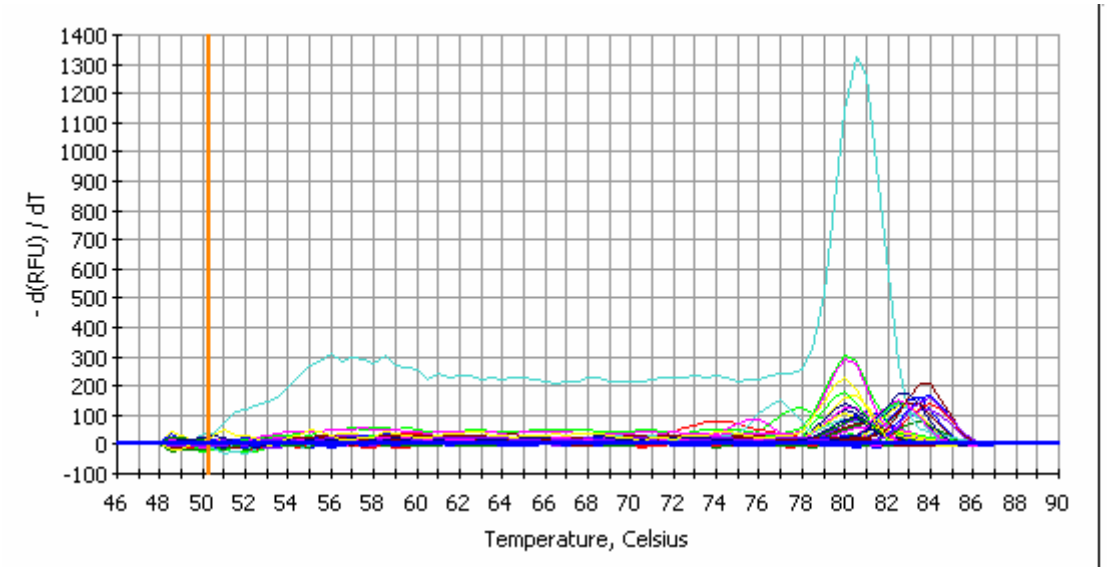

Figure 3.27. Melt curve graph of the amplified DNA fragments at an annealing temperature of 52.2^{o}C

Through analyzing the presence of an amplification and the specificity of the primer pairs, the optimization runs had lead to the conclusion that the optimum annealing temperature that was to be used for amplification protocols was 52.2^{o}C.

3.5.5. Response of HAP4 Gene to Nutritional Limitations and Pulse Nutrient Injections

The wild type strain BY4743 was grown in batch cultures of carbon and nitrogen limited F1 media. Pulse injections of carbon and nitrogen are introduced into the cultures and after a steady state is observed, a second pulse is introduced.

Variations in the expression levels of HAP4 gene is expected to be observed during these periods of starvation and abundance. Samples from nutritionally limited cultures

were collected as previously stated. mRNA was extracted from the samples as described in Materials and Methods section . The extracted mRNA was first reverse transcribed into cDNA and later, amplified at the specified locations. The experimental results were used in relative quantification of the expression of HAP4 gene using Pfaffl method implanted in GENEX macro provided by BIORAD. The expression profile of HAP4 gene for the carbon limited cultivations followed by glucose pulses injected to the system is displayed in Figure 3.28 with pulses indicated by red dashed lines. As soon as the pulse was given, the system responded to abundance of carbon and at the 45th second after each pulse, HAP4 expression reached its maximum value, later declining as time progressed.

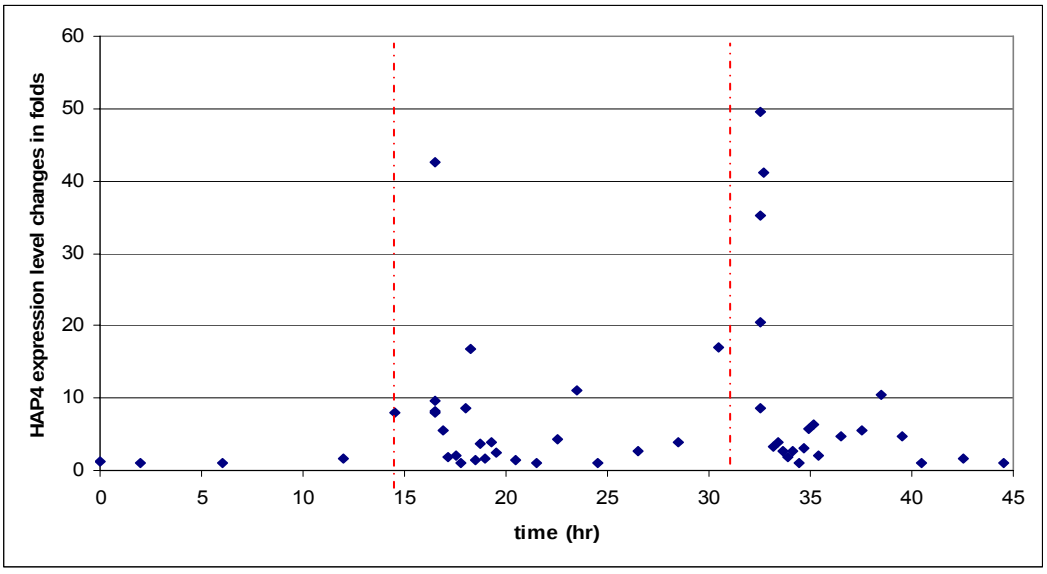

Figure 3.28. Expression profile of HAP4 gene under carbon limitation in batch cultures with pulse injections

The expression profile of HAP4 gene for the nitrogen limited cultivations followed by ammonium sulfate pulses injected to the system is displayed in Figure 3.29 with pulses indicated by red dashed lines. As soon as the pulse was given, the system responded to abundance of nitrogen strongly and within the first 15 seconds of injection after each pulse, HAP4 expression levels started to decline rapidly. The last increase in the expression level of HAP4 after the 40th hour of cultivation in nitrogen limited medium corresponded to exhaustion of ethanol on which the cells grew.

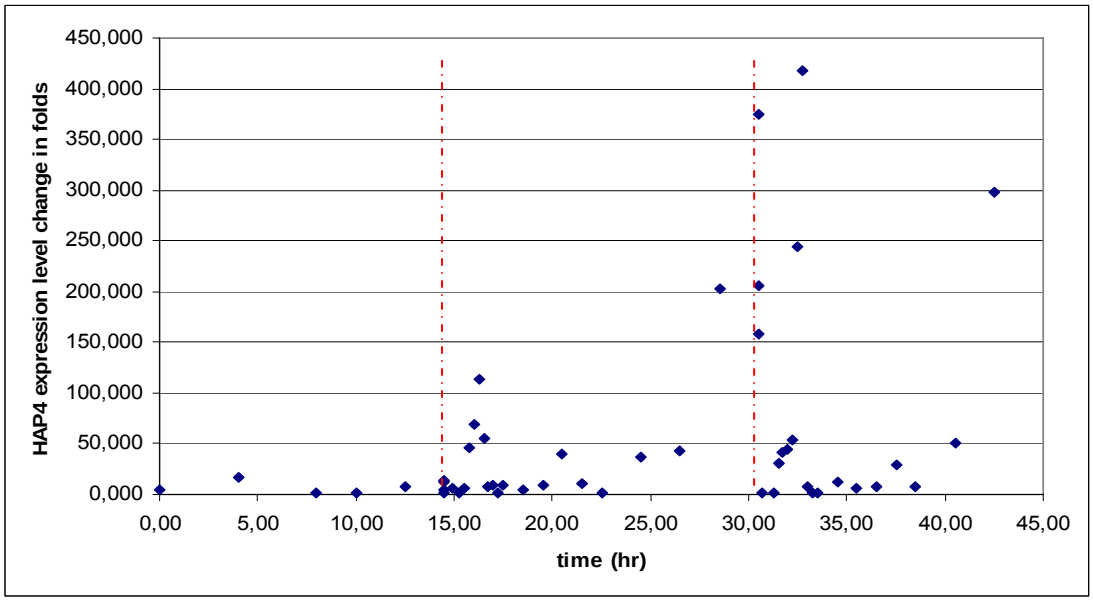

Figure 3.29. Expression profile of HAP4 under nitrogen limitation in batch cultures with pulse injections

4. DISCUSSION

4.1. Batch Cultivations

Preliminary batch cultivations of the strains BY4743, ΔQCR7 and ΔQDR3 in rich medium showed a respiro-fermentative growth. Ethanol was produced during the exponential growth phase on glucose in all cases. The growth patterns observed during the batch cultivation of these recombinant strains were very similar to that of the reference strain. ΔQCR7 strain produced the highest amount of ethanol among these three strains. ΔQDR3 mutant was the one that had reached the highest biomass concentrations. Pyruvate which was a branch point intermediate between respiration and fermentation was excreted in highest amounts in the parent strain cultivation (Table 4.1).

The maximum growth rate of the wild type was higher than that of the deletion mutants as expected. The maximum specific growth rate of wild type in aerobic batch cultures was found to be 0.36 hr^{-1} and this is in accordance with the data obtained from literature. In one study, the specific growth rate of the reference strain was determined as 0.37 hr^{-1} and in another as 0.31 hr^{-1} (Gombert *et al*., 2001 and Westergaard *et al.,* 2005, respectively). The maximum growth rate of the fully respiratory deficient strain ΔQCR7 and ΔQDR3 are 27 per cent and 5 per cent lower from that of the wild type strain, respectively (Figure 4.1). Figure 4.2 depicts the saturation constants for the three studied strains. The constants had similar values for the parent strain and ΔQDR3 mutant while it had a significantly higher value for ΔQCR7, reaching more than twice the value for the wild type.

The biomass yield of the wild type stain which was 0.14 was in accordance with previously stated values (0.11 g/gDW and 0. 10 g/gDW) in literature (Gombert *et al.,* 2001 and Westergaard et al., 2005, respectively). The highest yield of biomass on glucose was obtained with ΔQDR3 (Table 4.1). The biomass produced by ΔQCR7 on glucose was decreased by 7 per cent when compared to that of the wild type while the biomass produced by ΔQDR3 on glucose was increased by 10 per cent. Alcoholic fermentation results in a lower biomass yield per sugar consumed than respiratory dissimilation and is

accompanied by accumulation of metabolites (van Maris *et al*., 2001). The ethanol production of ΔQCR7 on glucose was increased by 16 per cent and the ethanol production of ΔQDR3 was increased by 6 per cent compared with that of the wild type strain. The respiratory deficient phenotype of ΔQCR7 meant that the Pasteur effect was successfully circumvented, allowing higher fermentation rates to be achieved than with the respiratory sufficient wild type. Nuclear petites are unable to grow in a diauxic growth phase and so will not metabolize the product of fermentation, ethanol, as their secondary substrate (Hutter and Oliver, 1998).

Table 4.1. Comparison of growth characteristics of *S. cerevisiae* and yields of biomass and ethanol on glucose in batch cultivations*

	biomass (g/L)	glucose (g/L)	ethanol (g/L)	pyruvate (g/L)	Y_{sx}	Y_{se}
BY4743	2.69 (100)	0.61 (100)	11.08 (100)	0.04 (100)	0.14	0.57
ΔQCR7	2.49 (93)	0.50 (82)	12.80 (116)	0.03 (75)	0.13	0.66
ΔQDR3	2.95 (110)	0.53 (87)	11.78 (106)	0.02 (50)	0.15	0.60

* The results presented in parentheses are the percentages in comparison to the outcomes obtained for the wild type strain.

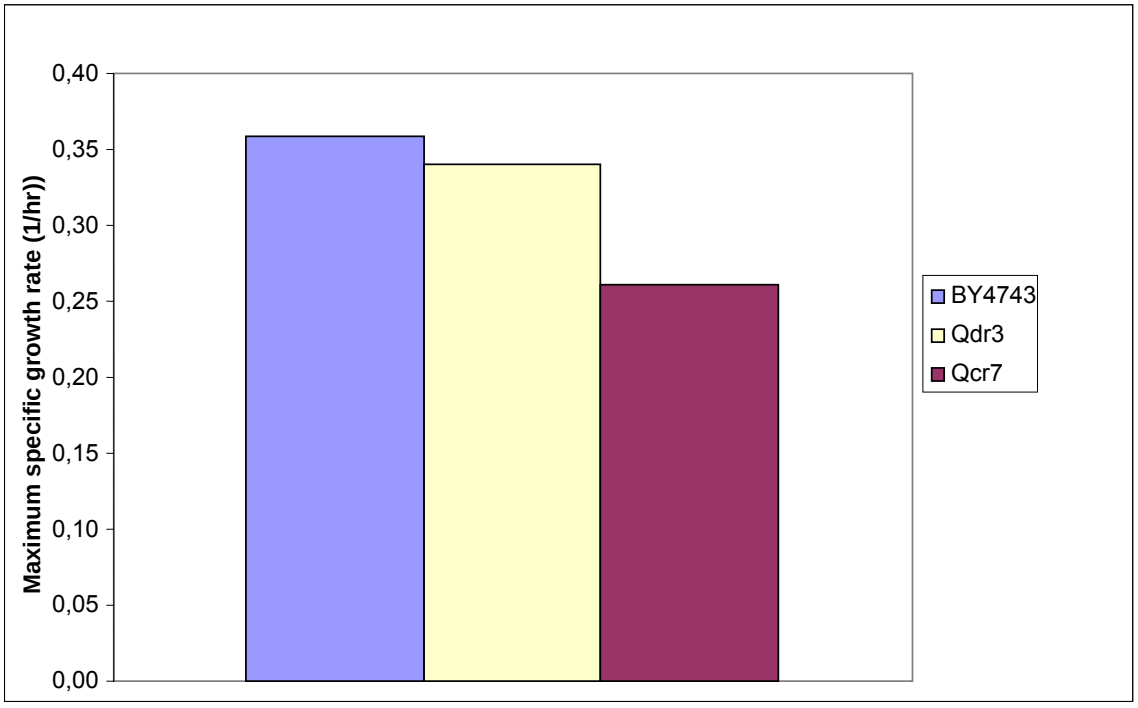

Figure 4.1. Comparison of maximum growth rates in batch cultivation

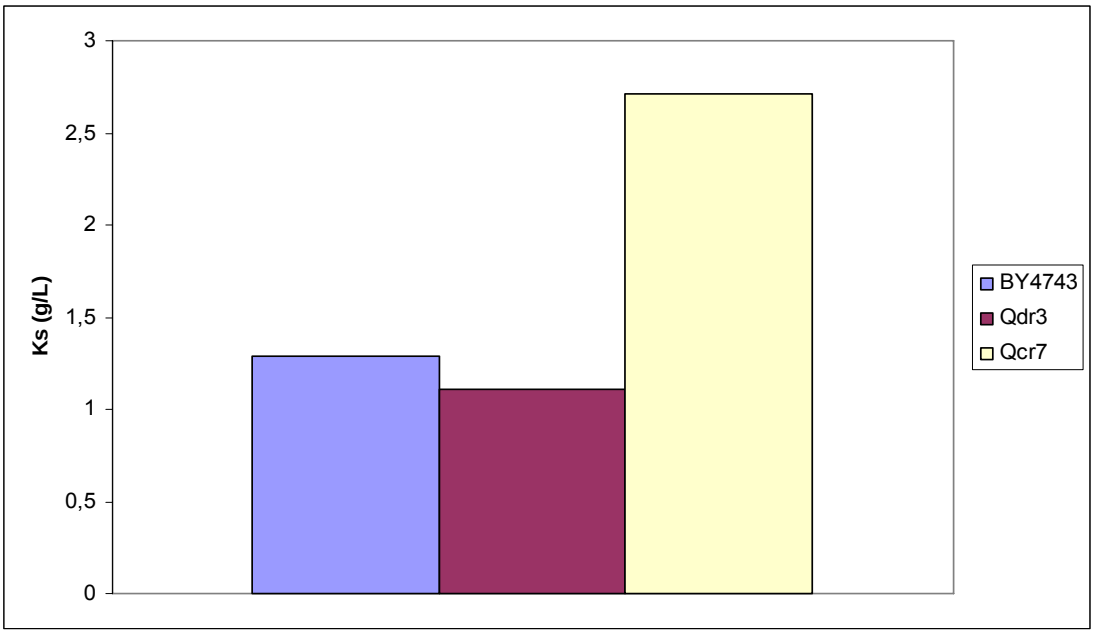

Figure 4.2. Comparison of saturation constants in batch cultivation

The biomass and ethanol yields of ΔQDR3 are both higher, which is contradictory to the behavior expected from the respiratory deficient strains. QDR3 expression is required for increased tolerance of *S. cerevisiae* to a broad range of inhibitory compounds, including quinidine and barban. (Tenreiro *et al*., 2005). However, several studies hint at this protein being involved in other various mechanisms one of them being the ammonia metabolism and the nitrogen catabolite repression (ter Shure *et al*., 2000). Another recent work presents QDR3 as a plasma membrane associated protein involved in glucose transport and/or galactose metabolism (Jiang and Keating, 2005). It may be suggested that the combined effects of the functions of these genes may possibly be the cause of this contradictory phenomenon.

The intracellular glucose concentration of wild type strain was higher than that of the deletion mutants as it was the case with extracellular glucose. The wild type intracellular glucose concentration is 9 per cent higher than both mutants. In contrast, intracellular pyuvate concentration of the wild type was lower than that of the mutant strains. It was 21 per cent lower than ΔQDR3 and 24 per cent lower than ΔQCR7. Intracellular metabolite measurements could be assessed under the light that both of the deletions belong to genes related to the respiratory pathway. These disruptions seem to cause the accumulation of

lower amounts of glucose within the cell while they caused an increased accumulation of pyruvate, when compared to their parent strain (Figure 4.3 and Figure 4.4).

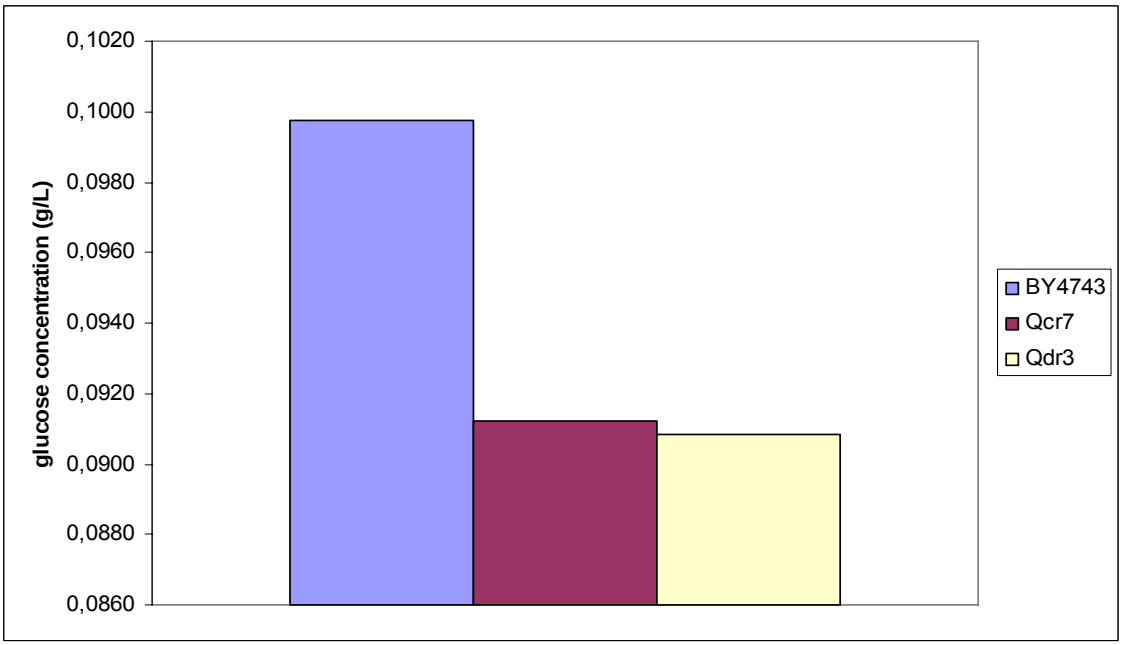

Figure 4.3. Intracellular glucose concentrations in batch cultivation

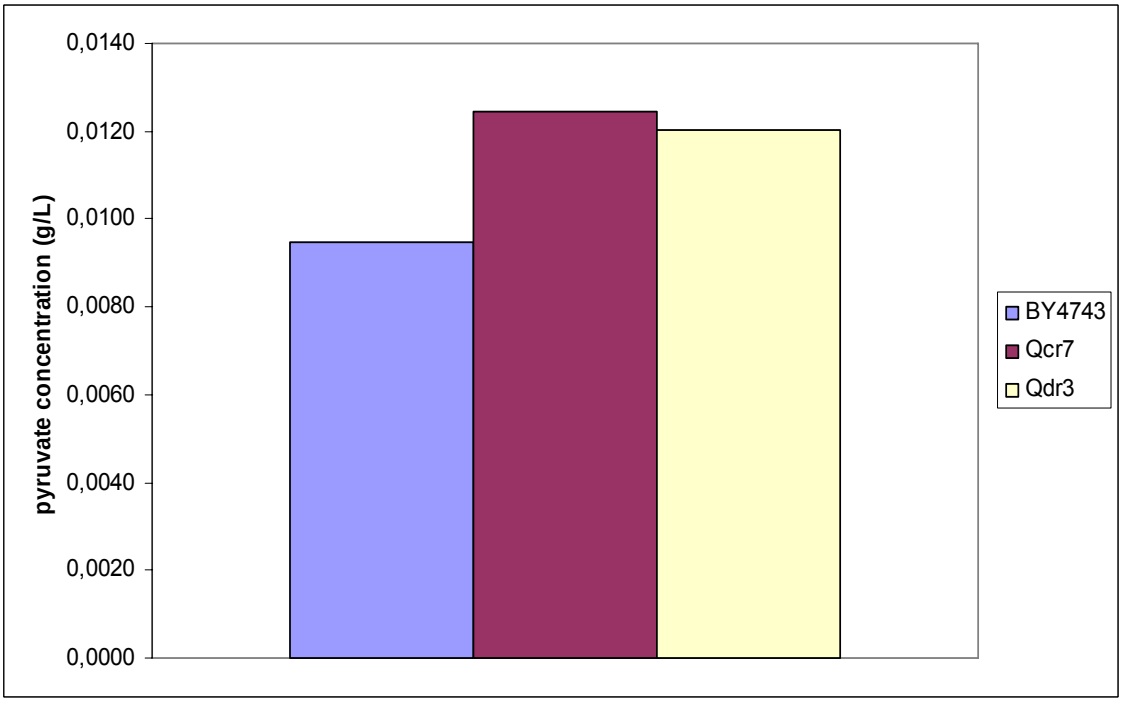

Figure 4.4. Intracellular pyruvate concentrations in batch cultivation

4.2. Comparison of the Strains of Reference in Chemostat Cultures

The parent strain or ΔHO were selected as reference strains in studies related to the investigation of deletion strains of *S. cerevisiae* regarding to the respiratory deficiency. Researches revealed information about ΔHO being indifferent to respiratory metabolism and hence making it a preferential strain as reference (Baganz *et al.,* 1997). The biomass yield of ΔHO is 1 per cent lower than the yield of wild type and its ethanol yield is only 2 per cent lower. This result is in agreement with literature where it is stated that the *ho*::kanMX4 / *ho*::kanMX deletion had a small, but measurable, effect on growth rate of $\leq \pm 4$ per cent under aerobic conditions (Baganz *et al.*, 1997). Therefore, these results indicated that BY4743 and ΔHO could safely be used interchangeably in further studies related to deletion strains in chemostat cultures (Table 4.2).

Table 4.2. Comparison of growth characteristics of reference strains of *S. cerevisiae* and yields of biomass and ethanol on glucose in chemostat cultivations*

strain	biomass (g/L)	glucose (g/L)	pyruvate (g/L)	ethanol (g/L)	succinic acid (g/L)	Y_{sx}	Y_{se}
BY4743	2.92 (100)	1.66 (100)	0.04 (100)	9.02 (100)	0.15 (100)	0.16	0.49
ΔHO	2.89 (99)	0.78 (47)	0.02 (50)	9.23 (102)	0.11 (73)	0.15	0.48

* The results presented in parentheses are the percentages in comparison to the outcomes obtained for the wild type strain.

4.3. Chemostat Cultivations

Chemostat cultivations in rich medium were carried out for the parent strain and its seven deletion mutants of *S. cerevisiae*, namely ΔHO, ΔQDR3, ΔMIG1, ΔHAP4, ΔQCR7, ΔRIP1 and ΔCYT1. Major differences were observed in growth and metabolic measurements. Three strains namely; ΔHAP4, ΔRIP1 and ΔCYT1 were markedly different in growth than the reference strains (Table 4.3). The deletion mutants of these genes belonging to the respiratory chain complex III were the strains that had the most difficulty in utilizing glucose. Maximum ethanol production at steady state was observed for ΔHAP4 and ΔRIP1. The maximum amount of succinic acid was produced by ΔMIG1 and ΔHAP4.

Table 4.3. Comparison of growth characteristics of *S. cerevisiae* and yields of biomass and ethanol on glucose in chemostat cultivations*

strain	biomass (g/L)	glucose (g/L)	pyruvate (g/L)	ethanol (g/L)	succinic acid (g/L)	Y_{sx}	Y_{se}
BY4743	2.92 (100)	1.66 (100)	0.04 (100)	9.02 (100)	0.15 (100)	0.16	0.49
ΔHO	2.89 (99)	0.78 (47)	0.02 (50)	9.23 (102)	0.11 (73)	0.15	0.48
ΔQDR3	2.64 (90)	1.39 (84)	0.04 (100)	10.23 (113)	0.19 (127)	0.14	0.55
ΔMIG1	2.51 (86)	0.21 (13)	0.02 (50)	10.07 (112)	0.29 (193)	0.13	0.51
ΔHAP4	1.37 (47)	0.29 (17)	0.01 (25)	12.46 (138)	0.29 (193)	0.07	0.63
ΔQCR7	2.60 (89)	2.14 (129)	0.04 (100)	9.97 (111)	0.07 (47)	0.15	0.56
ΔRIP1	0.60 (21)	4.44 (267)	0.00 (00)	12.40 (137)	0.16 (107)	0.04	0.80
ΔCYT1	1.34 (46)	2.85 (172)	0.01 (25)	9.82 (109)	0.06 (40)	0.08	0.57

* The results presented in parentheses are the percentages in comparison to the outcomes obtained for the wild type strain.

The lowest biomass yields for ΔRIP1, ΔCYT1 and ΔHAP4 cultivations were 75 per cent, 50 per cent and 69 per cent lower than that of the wild type, respectively (Table 4.3). The lowest growth rates were observed for the recombinant strains ΔRIP1 and ΔCYT1 during exponential growth phase. The rates are only 14 per cent and 5 per cent of that of the wild type for the two strains, respectively. The highest ethanol production was calculated for ΔRIP1 as 63 per cent higher than that of the wild type. Deleted gene was in this case one of the main components of the cytochrome bc1 complex. Ethanol produced by ΔHAP4 on glucose was 29 per cent higher than that of the wild type. In a study conducted by van Maris *et al*., 2001, the ethanol production of the HAP4 overexpressed strain was found to be 17 per cent lower than that of the wild type strain. Raghevendran *et al.* reported an increase of 10 per cent in biomass production when compared to that of the wild type strain in HAP4 overexpressed cells. This is in good agreement with the present findings leading to the statements that HAP4 was proposed to regulate the complete respiratory mechanism in yeast. Deletion strains ΔQCR7 and ΔCYT1, produced 14 per cent and 16 per cent higher ethanol respectively when compared with the ethanol yield of the wild type on glucose. The increased productivity exhibited by these two nuclear petites was a result of their inability to respire in the "respiro-fermentative" phase of batch growth, and of their retained tolerance to ethanol. It is suggested, therefore, that 100 per

cent respiratory deficient nuclear petites will be of use in the commercial production of ethanol in circumstances where the oxygen supply cannot be tightly controlled (Hutter and Oliver, 1998). These deleted genes were also major components of the cytochrome bc1 complex. An interesting result was that ΔQDR3 with ethanol production 12 per cent higher than the wild type strain, closely followed these mutants, suggesting a high respiratory deficiency in the mutant strain. QDR3 is suspected to be a plasma membrane associated protein involved in glucose transport and/or galactose metabolism (Jiang and Keating, 2005). This function may have caused the partial respiratory deficiency and hence the higher yields of ethanol production compared to that of the wild type.

For consistency, intracellular metabolites of the parental strain as well as ΔQCR7 and ΔQDR3 strains were also measured. The differences in intracellular glucose concentration were more distinct when compared to that of batch cultivations (Figure 4.5). The mutant strain ΔQDR3 had the lowest value which is 22 per cent lower than that of the wild type.

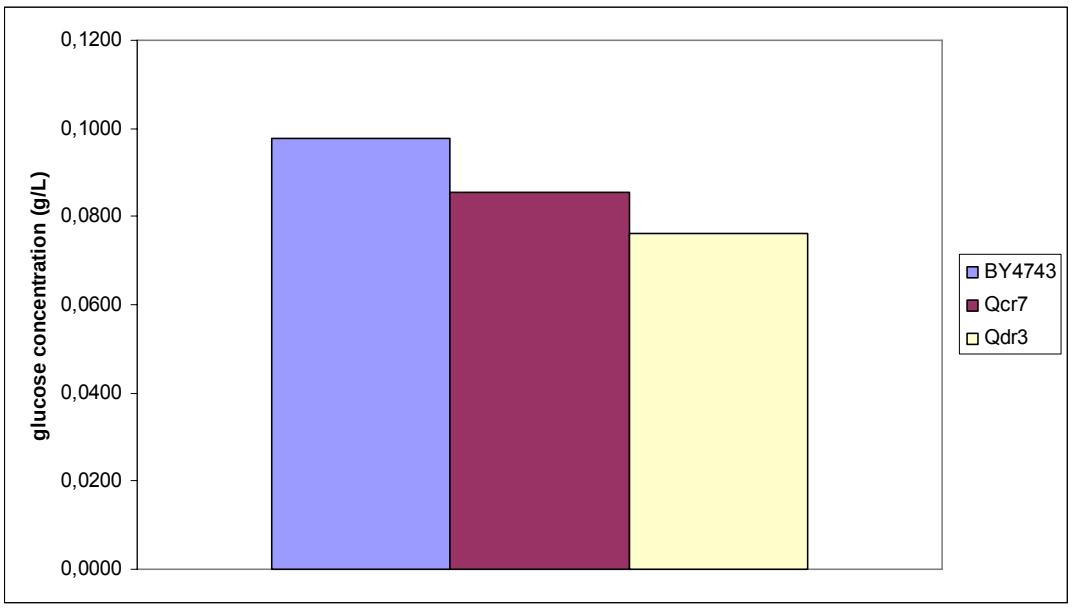

Figure 4.5. Comparison of intracellular glucose concentration in chemostat cultivation

The intracellular pyruvate concentration remained below 0.1 mmol/hr for the wild type strain, as indicated in literature for aerobic chemostat cultures (Cortassa *et al*., 1997) (Figure 4.6). Intracellular pyruvate concentration for ΔQCR7 was 31 per cent higher than

that of the wild type. The intracellular accumulation of this metabolite might be explained by the incompletion of the tricarboxacidic cycle and deficiency in respiration.

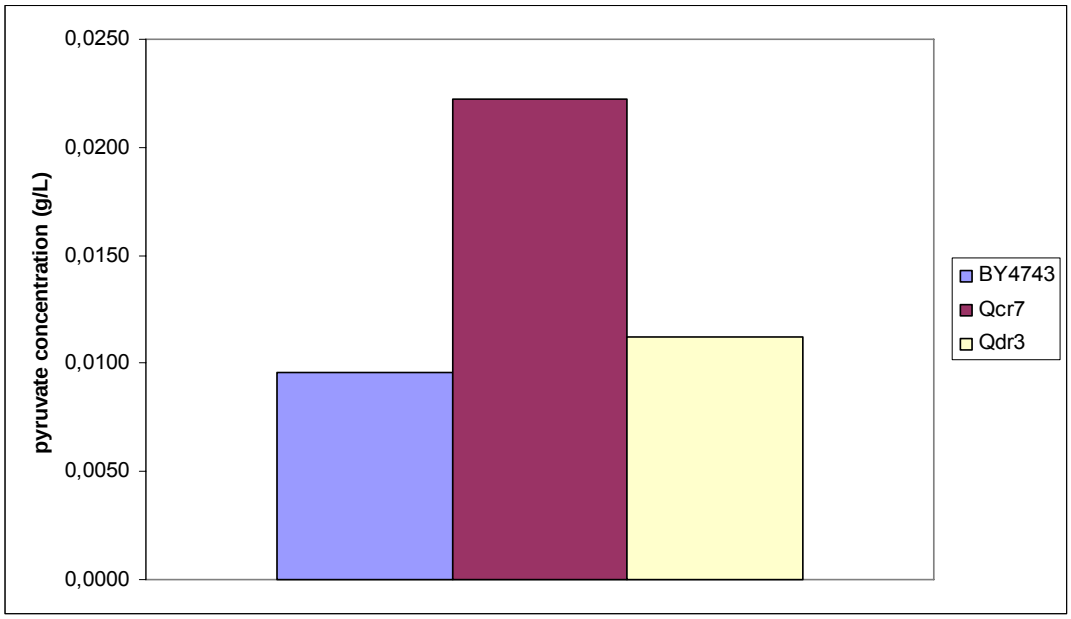

Figure 4.6. Comparison of intracellular pyruvate concentration in chemostat cultivation

Experimental results were also verified through computational methods and as it was explained in previous sections, small scale (SSM) and genome scale (GSM) stoichiometric metabolic models of the yeast were utilized in metabolic flux analysis and the method of minimization of metabolic adjustment (MOMA) was used. Ethanol fluxes in moles / mole glucose, calculated using these computational approaches are compared with the experimental results obtained within the present study are displayed comparatively in Table 4.4 below. The experimental ethanol flux of 1.45 moles /mole glucose for the wild type strain, BY4743 is comparable to the value of 1.59 moles /mole glucose reported by Gombert *et al.*, 2001. Small scale metabolic model comprising only the central carbon metabolism was insufficient to explain the respiratory deficiency phenomena completely. Percentage differences between experimental values and the computed values rose up to 93 per cent for ΔHAP4 and the nearest values were obtained for ΔRIP1 but even so, at the expense of 14 per cent error. Especially when transcriptional factors such as MIG1 or regulatory proteins such as HAP4 need to be included in the model, the flux analysis failed to predict the real phenomena. The way it was used, it could not also explain the behavior of the parental strain and the respiratory sufficient strains since it was run to optimize

ethanol production of the metabolism which was contradictory to the survival program of these strains. For BY4743 and ΔHO, the error percentages rose up to 83 per cent for both strains.

Table 4.4. Comparison of experimentally obtained and computed ethanol productions (moles / mole glucose)

strains	Experimental	GSM-oxygen uptake optimized	GSM- ethanol production optimized	SSM- ethanol production optimized	MOMA
BY4743	1.45	1.58	1.68	0.25	
ΔHO	1.45	1.56	1.66	0.25	1.18
ΔQDR3	1.77	1.62	1.69	0.62	1.18
ΔMIG1	1.53	1.72	1.74	0.83	1.09
ΔHAP4	1.85	1.68	1.52	0.17	0.97
ΔQCR7	1.80	1.52	1.62	0.36	0.87
ΔRIP1	1.91	1.25	1.92	1.64	0.63
ΔCYT1	1.93	1.51	1.85	1.28	0.42

The genome scale model constructed by Förster *et al.,* 2003 took into account the yeast metabolism as a whole. When flux distributions were calculated with oxygen uptake optimization as the objective function, ethanol production could be predicted for the respiratory sufficient strains, BY4743 and ΔHO with differences in experimental and computationally obtained values remaining below 10 per cent. When ethanol excretion optimization was used as the objective function, excellent correlations were obtained for respiratory deficient strains. ΔRIP1 yielded no difference between experimental and computationally obtained values and ΔCYT1 and ΔQDR3 gave only 4 per cent error. ΔQCR7 followed these with 10 per cent error. Deletions involving regulatory proteins or transcriptional factors could not be modeled to obtain results very closely imitating the real phenomena since the model did not include regulation in itself (Table 4.4).

MOMA gave minimal distance results for the reference strain ΔHO as expected since it was the strain among the seven deletion mutants which resembled the parental strain the

most. ΔCYT1 was found to be the strain that was most distant from the wild type configuration (Table 4.4).

Principle component analysis results revealed two distinct types of information through scores and loadings. The scores map related strains, hence functionally related genes closer to each other. The fact that CYT1 and RIP1 proteins were found to be closely mapped indicates that they function together and QCR7 was the closest amongst the others to these pair of proteins. MIG1 and HAP4 remained further apart from the other proteins and from each other though both lied in the same quadrant. The HO and QDR3 genes were mapped close to each other and the wild type strain was also located near them.

The loadings were used to map related metabolites that were measured within this study. Of the metabolites that were closely mapped together, measurement of only one might have been sufficient to reveal information obtained from the scores map. All metabolites measured were clustered far away from each other indicating that there is no redundancy in the selection of measured metabolites.

4.4. Batch Cultivations with Nutritional Stress

Batch cultivations of BY4743 strain were carried out under carbon and nitrogen limited nutritional stress conditions in F1 media. Two steady states were observed following the two pulses that were injected. The ultimate yields of biomass and acetic acid were higher for the carbon limitation case after two subsequent glucose pulses injected into the carbon-starved cultivation (Table 4.5). The very high yield of ethanol at the steady state after the first nitrogen pulse could be explained by the high concentration of glucose remaining unconsumed in the medium.

Growth behavior was also compared for the cultivations of no limitation, carbon limitation and nitrogen limitation, prior to any injections to relieve nutritional stresses (Figure 4.7). The comparison of specific growth rates showed that the maximum specific growth rate obtained for the wild type in batch cultivation in F1 medium under no nutritional limitation was 51 per cent of the maximum specific growth rate obtained for the same strain under the same conditions with the exception of medium, which was the

complex medium, YPD. This drastic difference in maximum specific growth rates was solely due to the difference in media.

Table 4.5. Steady state yields obtained for batch cultivations under nutritional stress

Condition	Y_{sx}	Y_{sa}	Y_{sg}	Y_{se}
no limitation	0.13	0.020	0.029	0.52
carbon limitation 1st steady state	0.15	0.019	0.014	0.47
carbon limitation 2nd steady state	0.29	0.052	0.011	0.48
nitrogen limitation 1st steady state	0.14	0.014	0.039	0.77
nitrogen limitation 2nd steady state	0.11	0.019	0.028	0.10

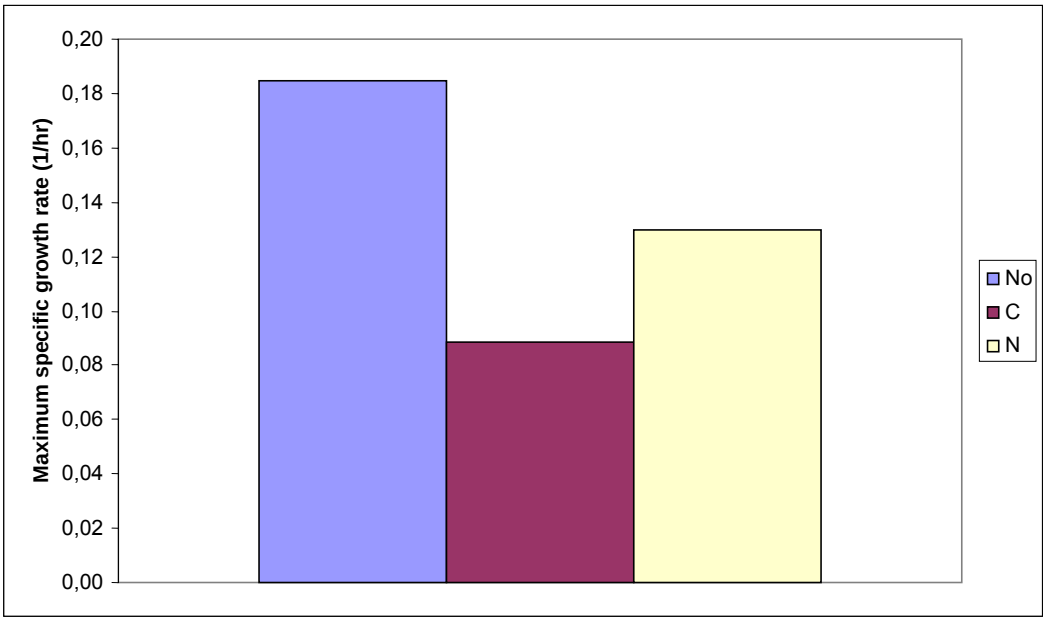

Figure 4.7. Comparison of maximum specific growth rates in batch cultivations with nutritional stresses

The saturation constant obtained from the cultivations in F1 medium is 54 per cent higher than that of cultivations in YPD medium. In the set of nutritional limitation experiments, the lowest maximum specific growth rate was calculated to the carbon limited cultivation indicating the stress imposed by this limitation was essential to the viability of cell cultures. As saturation constants were compared, a lower constant for the nitrogen limitation case may possibly be explained by the fact that the system had a high

affinity for glucose but it could not utilize the carbon source due to insufficient resources of nitrogen (Figure 4.8).

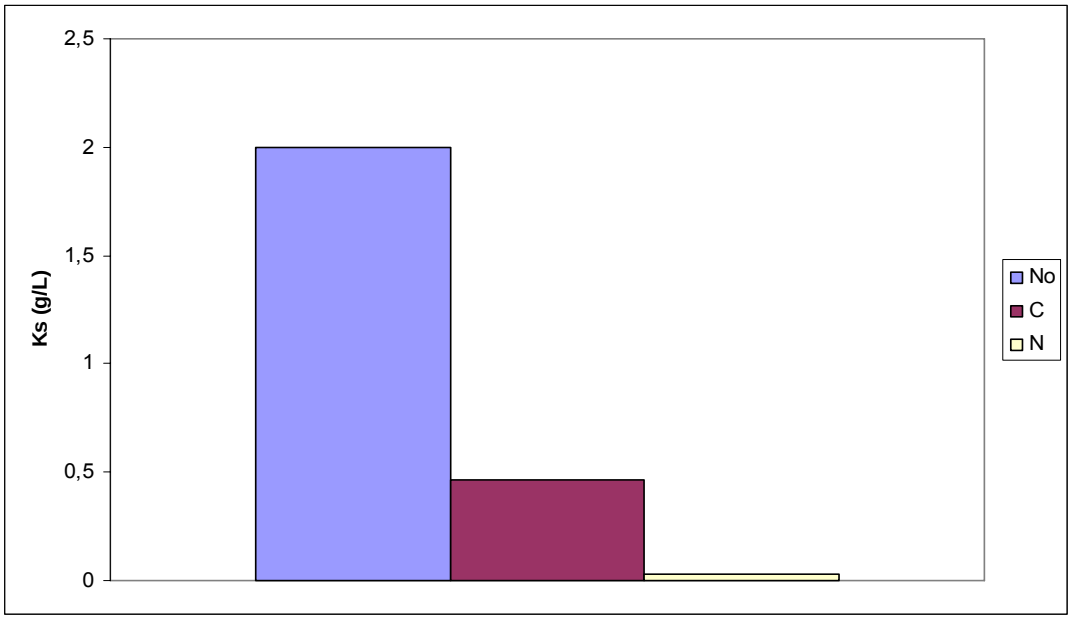

Figure 4.8. Comparison of saturation constants in batch cultivations with nutritional stresses

Although high throughput analysis of the data provides relatively fast and generous amounts of information on systems, it is essential to work with specific regions or paths to get a more comprehensive view of what the real mechanism is. For this reason, the expression levels of HAP4 gene in response to nutrient pulse in either carbon or nitrogen limited nutritional conditions were relatively quantified in this study, using quantitative real time PCR.

In the carbon limitation culture, HAP4 gene is expressed in detectable amounts during the time period when the carbon source glucose was not depleted in the medium. As the concentration of glucose decreases in the medium, the expression level of HAP4 gene starts to increase. The expression of HAP4 is regulated by the carbon source and is upregulated many fold upon glucose exhaustion. Presence of a fermentable substrate like glucose inhibits the expression of HAP4 via the Mig1pathway, and hereby activation of respiration is prevented at high glucose concentrations (Raghavedran, *et al*., manuscript in preparation). As the glucose pulse was injected into the system, it took the yeast cells about

a minute to respond to the abundance of carbon and the expression levels of HAP4 declined rapidly as a response of glucose repression. HAP4 mRNA is transcribed significantly in C-limited cultivations even under anaerobic conditions, where the protein product has no obvious role (Raghavedran, *et al*., manuscript in preparation). The small peaks indicating an increase in expression of HAP4 gene were also observed around 24^{th} and 39^{th} hours. This change in expression was accompanied by sharp increases in consumption of glucose and in production of ethanol and biomass. Hap4 protein was probably experiencing short term glucose derepression conditions prior to the indicated time spans. However, the fast consumption rate of glucose slowed down as time progressed and derepression was relieved. This caused the expression level of HAP4 to decline.

In nitrogen limitation cultivations, response of HAP4 gene was observed when ammonium sulfate pulse injections are introduced into the system. The response of the gene to the first pulse injection might be solely due to its regulatory function on the ammonia metabolism in nitrogen catabolite repression in yeast. The HAP complex regulates the activity of one of the major proteins in the ammonia metabolism, GDH1 (ter Schure *et al*., 2000). This regulatory function reflected in expression ratios of HAP4 gene which is the activation domain of the HAP complex (Buschlen *et al*., 2003). The fold change in the second pulse was dramatically higher than that of the first pulse. This could be explained by the fact that in addition to nitrogen abundance, glucose in the medium is consumed up almost completely during the period corresponding to the pulse injections. Both phenomena induce the expression of HAP4 leading to high fold ratios. The HAP4 gene, encoding a key regulator responded by a combination of effects together and the responses that are obtained cannot be fully held responsible for the behavior of an individual specific phenomenon.

5. CONCLUSIONS AND RECOMMENDATIONS

5.1. Conclusions

In this study, BY4743 parent strain and its seven deletion mutants ΔHO, ΔQDR3, ΔMIG1, ΔHAP4, ΔQCR7, ΔRIP1 and ΔCYT1 of the yeast *Saccharomyces cerevisiae* were investigated to improve present knowledge on the regulatory mechanism of respiratory chain in *S. cerevisiae* and to provide a rational design strategy for the construction of a high ethanol production strain.

For this purpose, cells were grown in rich medium in batch and continuous cultivations and the wild type was also cultivated under nutritional stress and relaxation of this stress, which were imposed on the cell. The obtained results were used in the metabolic modeling of the yeast cells. Central carbon metabolism and the complete metabolism of the yeast were used as two models in order to be able to determine the flux distributions within the cells. Minimization of metabolic adjustment was used to reveal the proximity of the mutant strains to their parent strain. Principle component analysis was used as a statistical evaluation of the study. Gene expression analysis was also carried out for HAP4 gene in nutritional limitation experiments performed on the parental strain.

In continuous cultivation, BY4743 and ΔHO displayed no important differences in their metabolic measurements except for glucose utilization. Since their growth and ethanol production profiles were similar, it was assumed safe to consider either one as the reference strain.

Batch cultivations and continuous cultivations had some differences that need to be pointed out. In batch cultivations, wild type was not the strain with the highest biomass production as it would have been expected. ΔQDR3 had overgrown the wild type. The highest ethanol producing strain was ΔQCR7 as it would be expected since it is the fully respiratory deficient strain among the three strains used.

In continuous cultivation, the parental grande showed the highest growth levels as expected. ΔRIP1 was the least grown strain indicating the importance of the corresponding deleted gene. This strain was followed by ΔHAP4 and ΔCYT1. ΔRIP1 was also the strain that has the largest difficulty in utilizing glucose. On the other hand, it was the highest ethanol producing strain due to its severe deletion on the function of cytochrome bc1 complex. This strain was followed by ΔHAP4 both in steady state ethanol concentrations and yields of ethanol on glucose.

Small scale metabolic model of the yeast which took into account only the central carbon metabolism of the organism was definitely not sufficient since the computationally obtained results remained far away from explaining the experimentally obtained phenomena. On the other hand, when the complete metabolism of the yeast was taken into consideration, satisfactory results were obtained varying the objective function according to the physiological behavior which was expected from the cell. The respiratory deficient strains provided better results when the objective function was ethanol excretion optimization while the respiratory sufficient strains granted better results when oxygen uptake was optimized as the objective function. MOMA results indicated that ΔHO and ΔQDR3 were metabolically more adjusted to the wild type configuration than the other five deletion mutants. However, there was still a considerable amount of difference even between these two strains and the wild type.

PCA results revealed that the strains that had disruptions that resulted in similar deficiencies ended up showing similar metabolic behavior. Clustering results that are obtained confirm the results of the MOMA analysis. One other result of this analysis was the disclosure of the fact that the metabolic measurements which were made were all relevant for the present analysis.

The two nutritional stresses imposed on the cells caused drastic changes in growth indicating the essentiality of the two major nutritional elements carbon and nitrogen. However, of the two stresses, carbon limitation was reflected as a more severe effect on the parental grande.

5.2. Recommendations

Some additional work may be of use to provide a better view of the regulation of respiration in *Saccharomyces cerevisiae*. Some suggestions may be given in computational approaches used and also in gene expression applications.

The weak point of the genome scale model that was used in metabolic flux analysis was the fact that it does not take regulation into account. Therefore, especially the regulatory functions of the transcriptional factors cannot be included and the model is weakest in describing ΔHAP4 and ΔMIG1 mutants with varying objective functions. Transcriptional data obtained from quantitative real time analysis should be imposed into the genome scale metabolic network to better describe regulatory phenomena.

The flux distributions obtained for eight strains should be compared in order to better explain the effects of gene deletions imposed on the organism. Dynamic flux balance analysis may be applied to monitor the transient state response of the strains.

A recent computational approach ROOM maybe used in describing the metabolic fitness of the deletion mutants together with MOMA and this would enable a chance of comparison between the two methods.

Batch experiments with glucose limitation can be carried out without any pulse injections in order to be able to observe the changes in expression levels of the HAP4 gene in response to glucose starvation. Chemostat cultivations with varying dilution rates, carbon and nitrogen sources may be run under real aerobic and non-aerobic conditions.

Several more genes may be investigated for their expression levels in the cultivations under nutritional stress. HXK2 and GLC7, due to their direct control over MIG1 which controls the glucose metabolism of yeast and QDR3, due to its regulatory function in nitrogen metabolism and its computationally unmasked functions on the glucose metabolism may be proper choices to select. Phosphorylation of Mig1 protein is essential in glucose repression patterns in the yeast. Therefore this process may be monitored via

mass spectrometry to reveal information of the transcriptional control of this protein over yeast metabolism.

One last suggestion may be to use TaqMan® probes for detection in RT-rtqPCR applications in order to provide a more specific binding and absolute quantification may be utilized as the ultimate step in quantification of gene expression and this data can further be used in metabolic modeling of the cell as it is previously suggested.

APPENDIX

A.1. Dry Weight / Optical Density Conversions

Dry weight – optical density calibrations were performed as explained in Results. Table A.1 presents the linear conversion equations obtained by least square analysis.

Table A.1. Dry weight / optical density conversion equations

Strain	Linear Relation where x_v (kg cells /m^3)
BY4743	x_v = 1.3155 OD + 0.1553
ΔHO	x_v = 1.2081 OD + 0.0204
ΔQDR3	x_v = 1.2943 OD + 0.1516
ΔMIG1	x_v = 0.9725 OD + 0.4206
ΔHAP4	x_v = 0.5847 OD – 0.0115
ΔQCR7	x_v = 1.0504 OD + 0.2986
ΔRIP1	x_v = 0.2001 OD + 0.1508
ΔCYT1	x_v = 0.1740 OD + 0.9674

A.2. Growth and Metabolite Profiles of Batch and Chemostat Cultivations

The following tables and figures present growth and metabolite profiles, as well as growth characteristics obtained for each strain in all types of cultivation conditions afore mentioned.

Table A.2. Growth and metabolite profiles of BY4743 in batch cultivation

time (hr)	x_v (kg cell/m^3)	Glucose (g/L)	pyruvate (g/L)	ethanol (g/L)
0	0.1783	19.2767	0.0126	1.1517
1	0.2312	19.3803	0.0127	1.3475
2	0.2199	19.4840	0.0129	1.5433
3	0.2432	17.5926	0.0131	1.7161
4	0.3076	15.7012	0.0133	1.8889
5	0.4268	16.8239	0.0143	2.3899
6	0.6318	17.9467	0.0153	2.8909
7	0.8883	15.4075	0.0140	2.9830
8	1.3621	12.8684	0.0127	3.0752
9	1.7415	8.4940	0.0168	4.5839
10	2.0141	4.1196	0.0209	6.0927
11	2.5721	3.3639	0.0265	8.5978
12	2.5374	2.6082	0.0321	11.1028

Table A.2. Growth and metabolite profiles of BY4743 in batch cultivation-continued

13	2.7531	1.6496	0.0368	10.8379
14	2.7805	0.6909	0.0415	10.5730
15	2.7663	0.3757	0.0473	10.8782
16	2.5953	0.0605	0.0531	11.1835
17	2.6421	0.3671	0.0501	11.3274
18	2.6953	0.6736	0.0471	11.4714
19	2.9294	0.8464	0.0397	13.9534
20	2.5385	1.0191	0.0322	16.4354

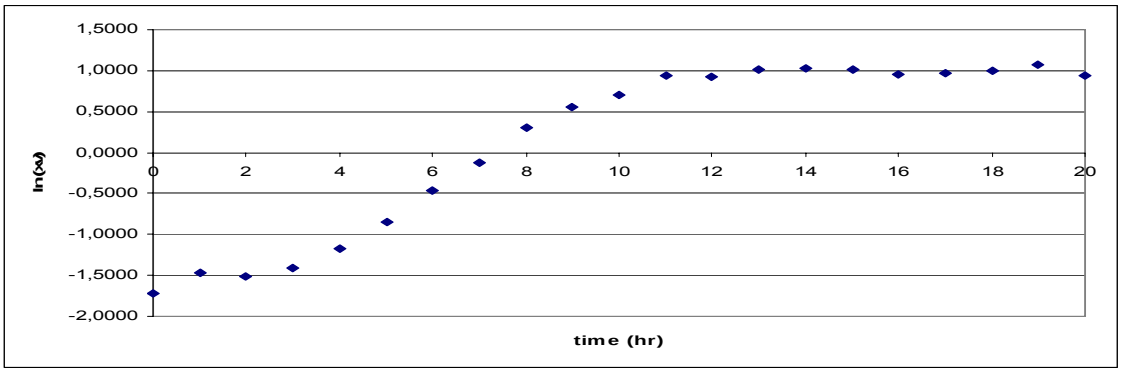

Figure A.1. ln (x_v) vs. time graph to determine the steady state of the batch cultivation of BY4743

Table A.3. Determination of μ for constant growth region in BY4734 batch cultivation

time	x_v (kgcell/m^3)	ln (x_v)	r_x (kgcells/m^3/hr)	μ (1/hr)	1/ μ (hr)
5	0.4268	-0.8514	0.1192	0.2792	3.5812
6	0.6318	-0.4592	0.2050	0.3244	3.0825
7	0.8883	-0.1184	0.2565	0.2888	3.4628
8	1.3621	0.3091	0.4738	0.3479	2.8747
9	1.7415	0.5548	0.3794	0.2178	4.5903

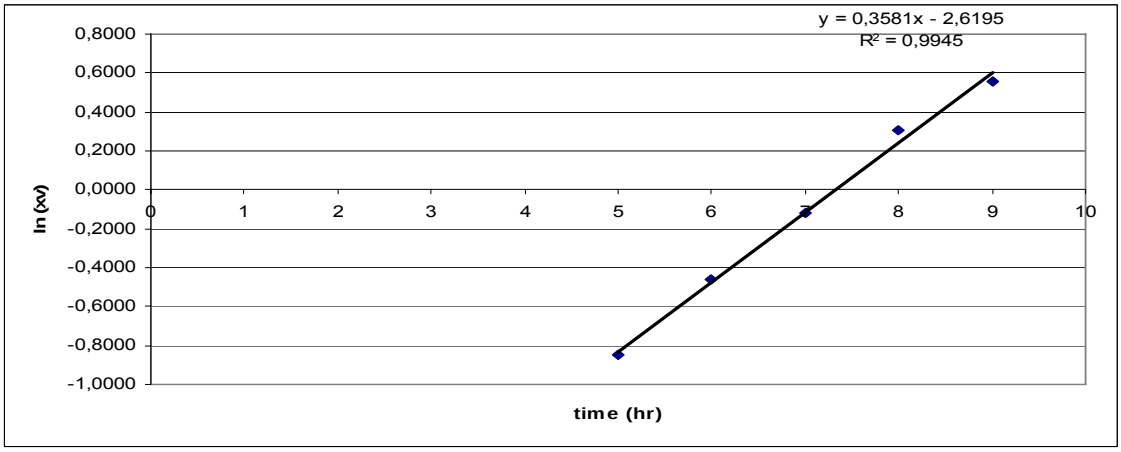

Figure A.2. Determination of μ_{max} of the batch cultivation of BY4743

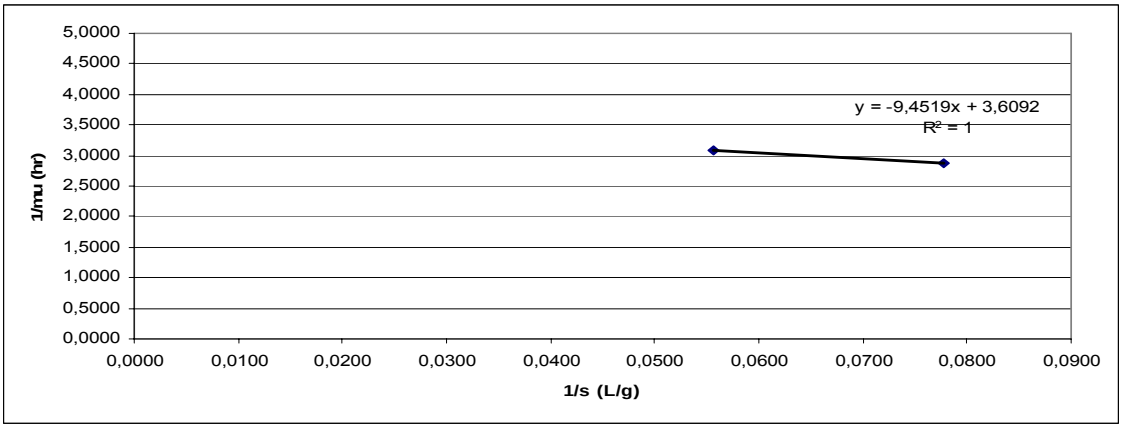

Figure A.3. Determination of K_s of the batch cultivation of BY4743

Table A.4. Growth and metabolite profiles of ΔQDR3 in batch cultivation

time (hr)	x_v (kg cell/m^3)	glucose (g/L)	pyruvate (g/L)	ethanol (g/L)
0	0.1643	17.1780	0.0156	1.0596
1	0.1921	17.4371	0.0134	1.3706
2	0.2007	17.6962	0.0112	1.6815
3	0.2340	18.5124	0.0110	2.2920
4	0.2944	19.3285	0.0107	2.9024
5	0.3495	16.9146	0.0153	3.8929
6	0.5005	14.5007	0.0198	4.8834
7	0.6847	12.9159	0.0217	5.0274
8	0.9784	11.3311	0.0237	5.1713
9	1.7058	6.6328	0.0294	5.7702
10	1.9263	1.9346	0.0351	6.3692
11	2.5921	1.2652	0.0346	8.9779
12	2.8329	0.5959	0.0342	11.5866
13	2.8236	0.5484	0.0360	11.9263
14	3.2061	0.5009	0.0378	12.2661
15	2.9809	0.4707	0.0300	13.2163
16	2.7966	0.4405	0.0222	14.1665
17	2.8417	0.5484	0.0160	12.3179
18	3.0700	0.6564	0.0097	10.4694
19	3.1476	0.5571	0.0051	10.4348
20	2.8251	0.4577	0.0005	10.4003

Table A.5. Determination of μ for constant growth region in ΔQDR3 batch cultivation

time	x_v (kgcell/m^3)	ln (x_v)	r_x (kgcells/m^3/hr)	μ (1/hr)	1/ μ (hr)
5	0.3495	-1.0513	0.0551	0.1578	0.3495
6	0.5005	-0.6921	0.1510	0.3018	0.5005
7	0.6847	-0.3787	0.1842	0.2690	0.6847
8	0.9784	-0.0218	0.2937	0.3002	0.9784

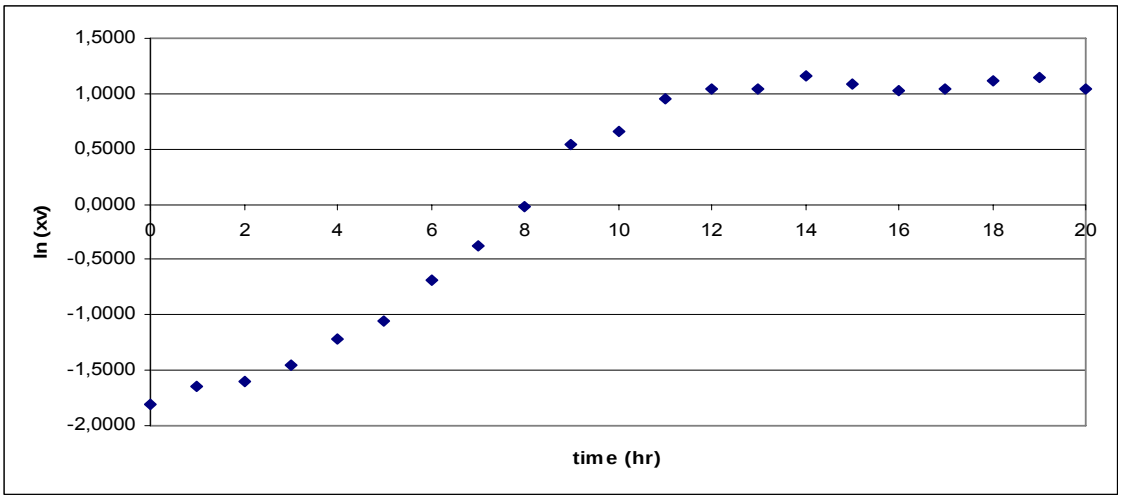

Figure A.4. ln (x_v) vs. time graph to determine the steady state of the batch cultivation of ΔQDR3

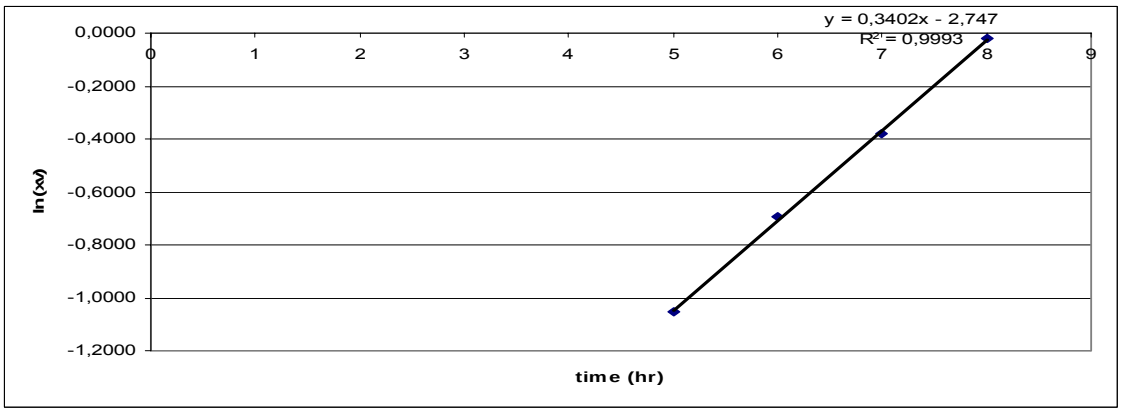

Figure A.5. Determination of μ_{max} of the batch cultivation of ΔQDR3

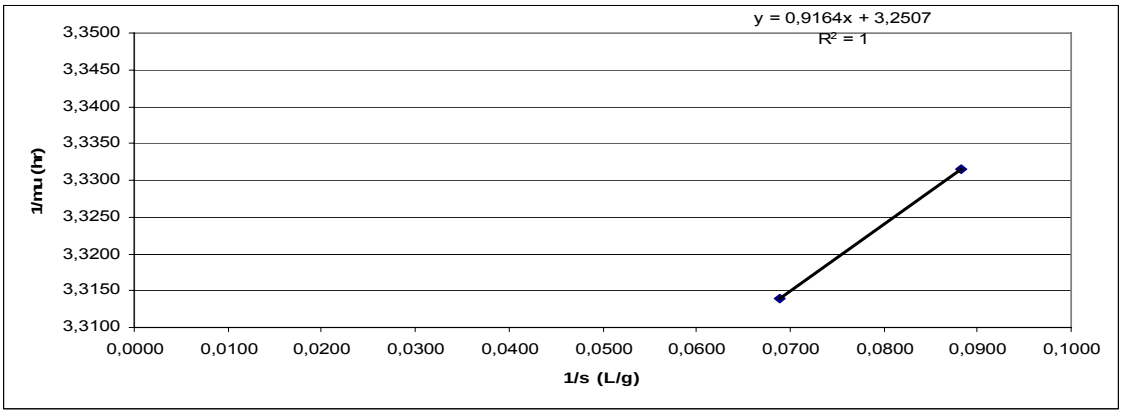

Figure A.6. Determination of K_s of the batch cultivation of ΔQDR3

Table A.6. Growth and metabolite profiles of ΔQCR7 in batch cultivation

time (hr)	x_v (kg cell/m^3)	Glucose (g/L)	pyruvate (g/L)	ethanol (g/L)
0	0.3350	19.5444	0.0101	1.2209
1	0.4156	20.2353	0.0109	1.2900
2	0.3319	20.9263	0.0117	1.3591
3	0.3487	20.5938	0.0127	3.2594
4	0.3929	20.2612	0.0137	5.1598
5	0.4567	17.5926	0.0130	4.2960
6	0.5645	14.9239	0.0122	3.4322
7	0.7406	13.3866	0.0165	4.8143
8	0.9958	11.8493	0.0209	6.1964
9	1.5456	10.0486	0.0255	8.2235
10	1.8475	8.2479	0.0301	10.2505
11	2.2948	4.2276	0.0374	11.1201
12	2.3259	0.2073	0.0447	11.9897
13	2.5515	0.2893	0.0398	11.8687
14	2.7179	0.3714	0.0348	11.7478
15	2.6011	0.6046	0.0399	12.1682
16	2.5515	0.8377	0.0450	12.5886
17	2.3032	0.7211	0.0276	13.3603
18	2.6217	0.6046	0.0102	14.1319
19	2.7780	0.5311	0.0079	13.8440
20	2.1788	0.4577	0.0055	13.5561

Table A.7. Determination of μ for constant growth region in ΔQCR7 batch cultivation

time	x_v (kgcell/m^3)	ln (x_v)	r_x (kgcells/m^3/hr)	μ (1/hr)	1/ μ (hr)
5	0.4567	-0.7838	0.0638	0.1396	7.1626
6	0.5645	-0.5719	0.1078	0.1909	5.2376
7	0.7406	-0.3003	0.1762	0.2378	4.2044
8	0.9958	-0.0043	0.2551	0.2562	3.9027

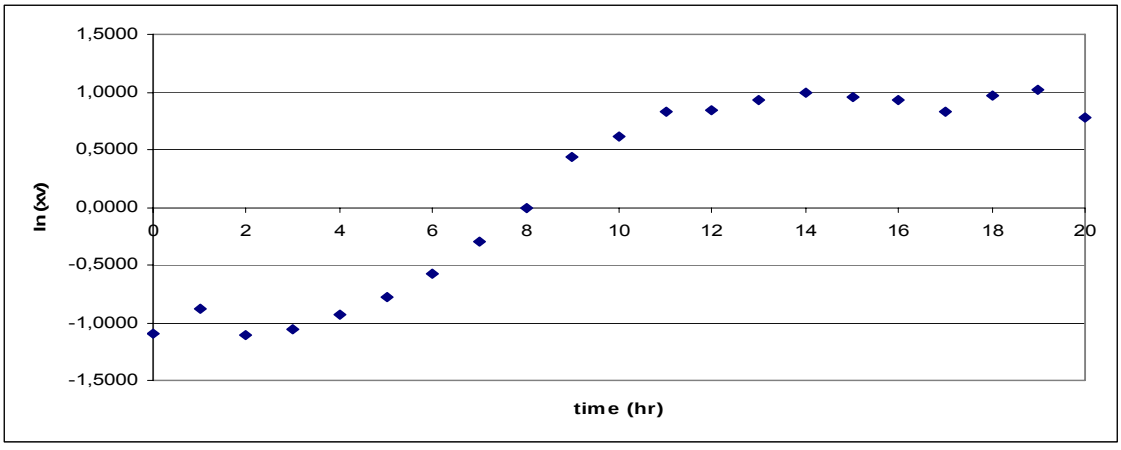

Figure A.7. ln (x_v) vs. time graph to determine the steady state of the batch cultivation of ΔQCR7

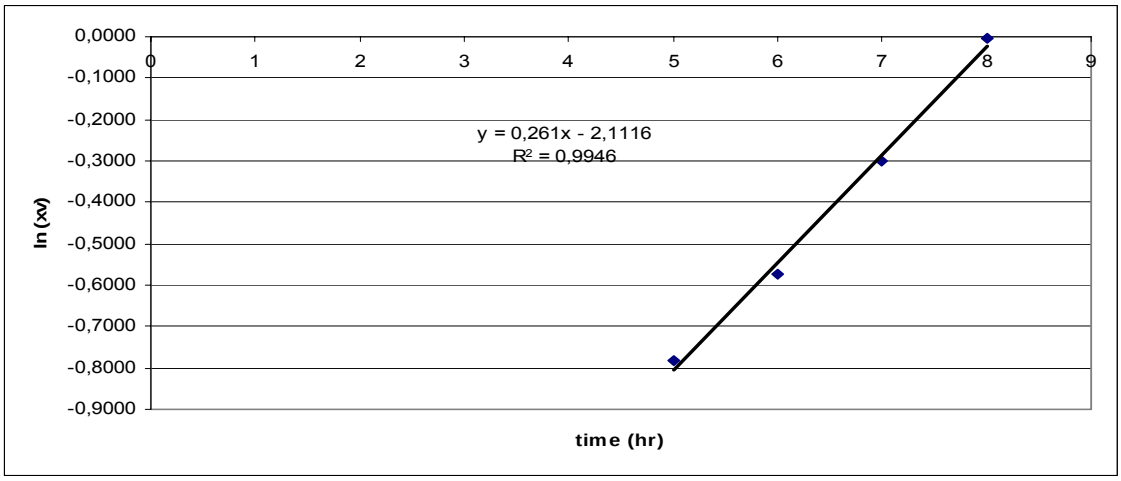

Figure A.8. Determination of μ_{max} of the batch cultivation of ΔQCR7

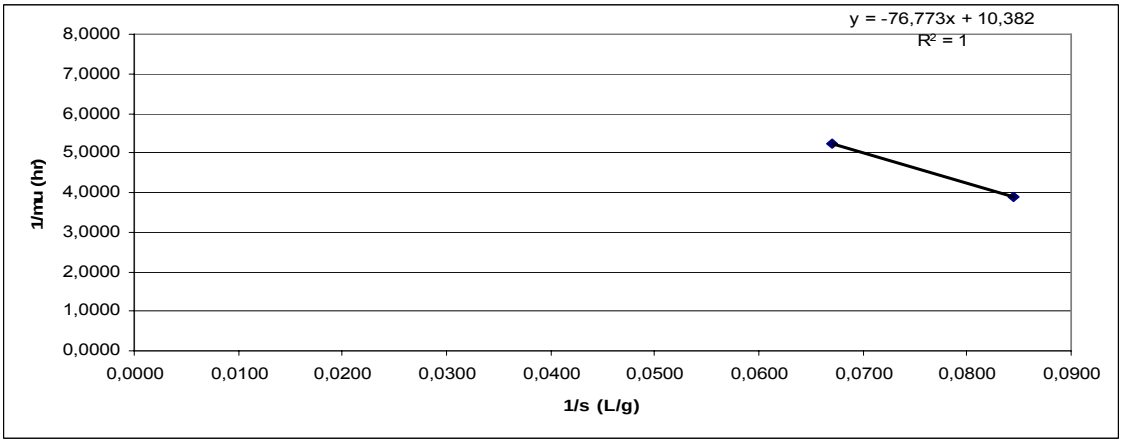

Figure A.9. Determination of K_s of the batch cultivation of ΔQCR7

Table A.8. Growth and metabolite profiles of BY4743 in continuous cultivation

time (hr)	x_v (kg cell/m^3)	glucose (g/L)	pyruvate (g/L)	ethanol (g/L)	succinic acid (g/L)
0	0.2888	19.4753	0.0119	-0.5989	0.0978
1	0.2324	18.8967	0.0124	0.7947	0.1033
2	0.3386	18.3180	0.0129	2.1883	0.1088
3	0.2290	17.8927	0.0157	3.4178	0.1143
4	0.4809	17.4673	0.0185	4.6473	0.1197
5	0.3341	13.3801	0.0169	4.1146	0.1213
6	0.8812	9.2929	0.0153	3.5819	0.1228
7	0.5940	9.8089	0.0196	5.2117	0.1244
8	1.2060	10.3249	0.0239	6.8414	0.1260
9	1.3650	8.9453	0.0271	7.1840	0.1364
10	1.7453	7.5656	0.0304	7.5267	0.1468
11	1.7029	5.5446	0.0348	8.6323	0.1477
12	2.4084	3.5237	0.0393	9.7380	0.1486
13	2.4974	2.8069	0.0392	9.2946	0.1848

Table A.8. Growth and metabolite profiles of BY4743 in continuous cultivation-continued

14	2.8502	2.0900	0.0391	8.8512	0.2210
15	2.7095	2.6428	0.0461	8.6064	0.1884
16	2.9023	3.1955	0.0531	8.3617	0.1722
17	2.9236	2.0944	0.0501	7.6188	0.1559
18	2.8105	0.9932	0.0471	6.8759	0.1233
19	2.9673	0.5722	0.0367	8.0449	0.1254
20	3.0176	0.1511	0.0264	9.2140	0.0907
22	3.1452	0.0345	0.0225	11.0913	0.1274

Table A.9. Growth and metabolite profiles of ΔHO in continuous cultivation

time (hr)	x_v (kg cell/m^3)	glucose (g/L)	pyruvate (g/L)	ethanol (g/L)	succinic acid (g/L)
0.250	0.0863	18.5944	0.0090	0.0691	0.1060
2.125	0.0793	17.9812	0.0040	0.4377	0.1217
4.000	0.1659	18.6160	0.0055	0.5298	0.1434
6.000	0.2038	19.2508	0.0069	0.6219	0.1651
7.000	0.7180	18.1496	0.0079	0.5298	0.1308
8.000	0.7694	17.0485	0.0088	0.4377	0.0964
10.250	1.3090	18.9399	0.0090	0.3340	0.2127
12.250	1.6492	18.6721	0.0137	0.1958	0.1402
14.375	1.7325	13.7839	0.0156	0.3110	0.1335
16.625	2.3739	8.4033	0.0199	1.7391	0.1150
18.000	2.8792	3.0228	0.0268	3.1673	0.0965
19.500	2.5091	0.9068	0.0337	9.0832	0.0850
20.000	3.1054	0.6607	0.0296	9.1811	0.1018
22.500	3.0585	0.4146	0.0255	9.2790	0.1186
25.750	2.8338	0.9414	0.0217	9.1178	0.1293
27.750	2.9556	0.7600	0.0145	9.0026	0.1105
30.500	2.8913	0.8550	0.0131	9.6821	0.1233

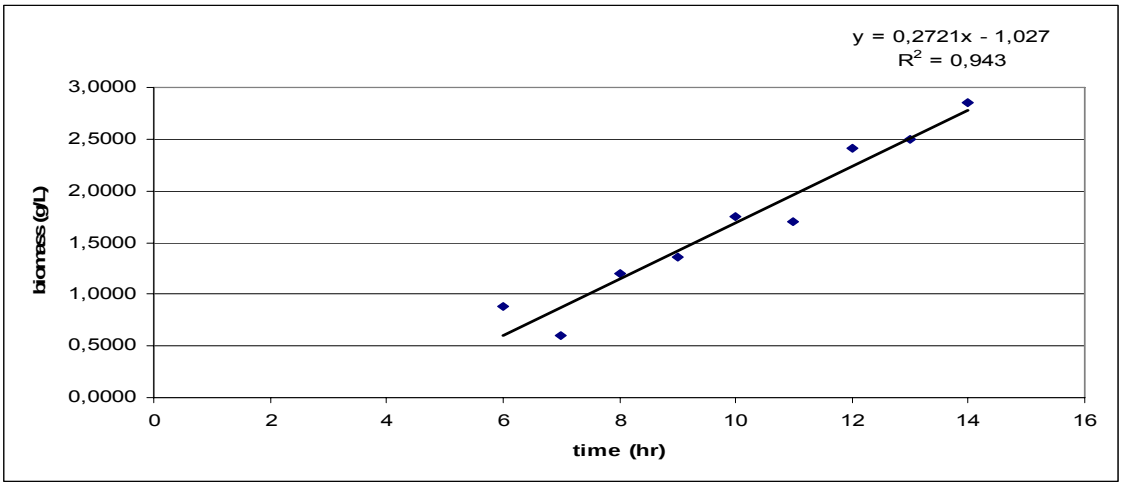

Figure A.10. Exponential phase of BY4743 in continuous cultivation

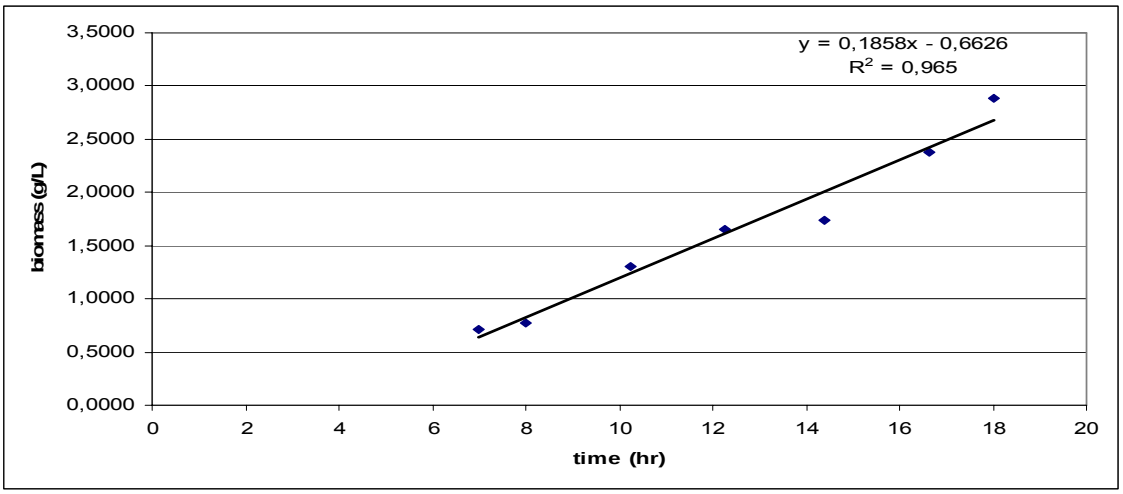

Figure A.11. Exponential phase of ΔHO in continuous cultivation

Table A.10. Growth and metabolite profiles of ΔQDR3 in continuous cultivation

time (hr)	x_v (kg cell/m^3)	glucose (g/L)	pyruvate (g/L)	ethanol (g/L)	succinic acid (g/L)
0	0.2521	20.6499	0.0085	1.4109	0.0940
1	0.1867	20.7600	0.0113	1.5779	0.0606
2	0.1874	20.8701	0.0141	1.7449	0.0272
3	0.2025	20.4685	0.0133	1.8226	0.0388
4	0.2192	20.0669	0.0125	1.9004	0.0503
5	0.2491	18.1928	0.0143	2.1019	0.0351
6	0.3162	16.3187	0.0161	2.3035	0.0198
7	0.4142	15.8091	0.0184	3.1587	0.0114
8	0.5163	15.2996	0.0207	4.0138	0.0030
9	0.7276	13.4622	0.0206	4.4601	0.0104
10	0.9080	11.6247	0.0205	4.9064	0.0178
11	0.7833	10.8194	0.0220	5.9603	0.0483
12	0.9655	10.0140	0.0235	7.0141	0.0788
13	1.1245	8.1010	0.0260	8.6122	0.0779
14	1.4449	6.1881	0.0284	10.2102	0.0769
15	2.7402	6.0283	0.0313	9.7553	0.0478
16	2.6066	5.8685	0.0342	9.3003	0.0186
17	2.4280	4.8688	0.0381	9.7351	0.0992
18	2.7715	3.8692	0.0421	10.1699	0.1797
19	2.3296	2.3815	0.0376	10.4838	0.1857
20	2.6359	0.8939	0.0330	10.7976	0.1918
21	2.4151	1.3970	0.0430	10.9675	0.2569
22	3.0120	1.9000	0.0530	11.1374	0.3220
23	2.7262	1.6323	0.0486	10.4521	0.2714
24	3.0969	1.3646	0.0442	9.7668	0.2207
25	2.2204	1.3646	0.0442	9.7668	0.2207
28	2.7449	1.3646	0.0442	9.7668	0.2207

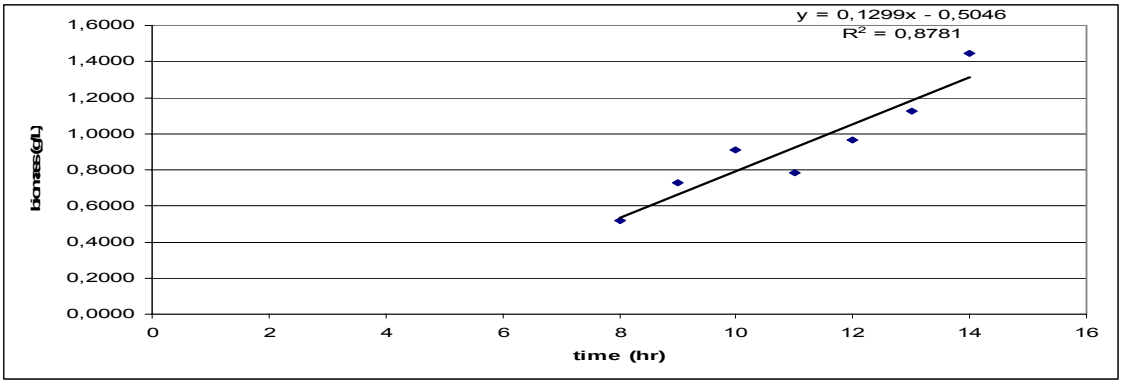

Figure A.12. Exponential phase of ΔQDR3 in continuous cultivation

Table A.11. Growth and metabolite profiles of ΔMIG1 in continuous cultivation

time (hr)	x_v (kg cell/m^3)	glucose (g/L)	pyruvate (g/L)	ethanol (g/L)	succinic acid (g/L)
0.00	0.4793	19.1126	0.0113	0.7717	0.1479
2.13	0.4714	19.1817	0.0104	0.1843	0.1800
4.00	0.5194	19.1903	0.0117	0.4261	0.1895
5.00	0.5252	19.1990	0.0129	0.6680	0.1989
6.00	0.4590	18.6937	0.0139	1.1805	0.2136
7.00	0.4843	18.4411	0.0144	1.4368	0.2210
8.25	0.6657	18.1885	0.0149	1.6931	0.2283
10.50	0.9829	10.9338	0.0178	1.8773	0.2299
12.50	1.4700	2.0814	0.0199	5.3787	0.2531
14.00	1.3550	1.2221	0.0244	7.3309	0.2346
15.83	2.3568	0.3627	0.0289	9.2831	0.2161
16.00	2.0412	0.2159	0.0274	8.5172	0.2441
18.13	2.4537	0.0691	0.0260	7.7513	0.2722
20.00	2.1832	0.2332	0.0236	9.0700	0.2773
22.00	2.3076	0.3152	0.0224	9.7294	0.2798
24.13	2.5191	0.3973	0.0213	10.3887	0.2823
26.00	2.8662	0.1382	0.0225	8.5575	0.2512
28.00	2.9079	0.1641	0.0237	11.7248	0.3364
30.00	2.9557	0.1295	0.0218	12.7153	0.2909

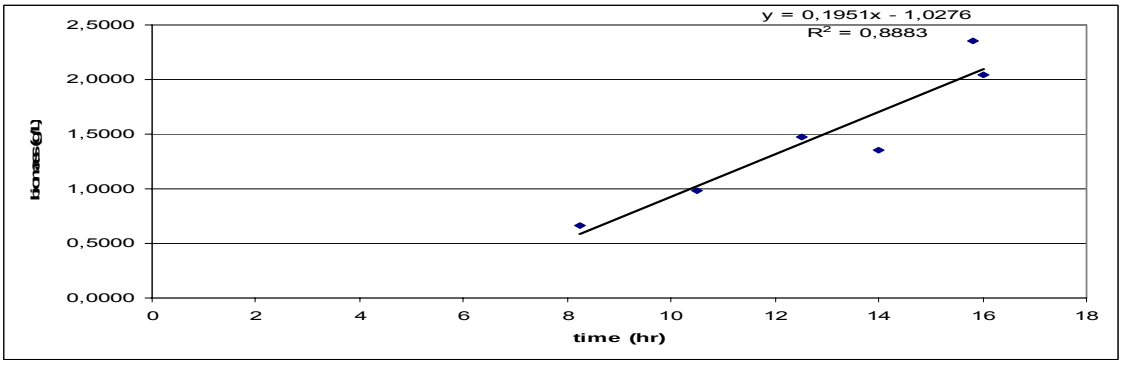

Figure A.13. Exponential phase of ΔMIG1 in continuous cultivation

Table A.12. Growth and metabolite profiles of ΔHAP4 in continuous cultivation

time (hr)	x_v (kg cell/m^3)	glucose (g/L)	pyruvate (g/L)	ethanol (g/L)	succinic acid (g/L)
0.00	0.0041	20.9954	0.0094	0.3570	0.1714
5.25	0.0074	19.3890	0.0085	0.5298	0.1280
7.50	0.0452	16.4871	0.0127	0.5528	0.1470
12.00	0.0946	19.2335	0.0161	0.9444	0.1857
14.00	0.1724	14.8289	0.0179	2.7181	0.2048
16.25	0.2642	5.6310	0.0183	5.4708	0.2088
19.25	0.4657	5.3374	0.0157	8.9721	0.2275
22.75	1.2994	0.0691	0.0089	9.4558	0.2680
25.25	1.3579	0.3627	0.0067	13.3603	0.2649
28.75	1.3986	0.4577	0.0094	13.0723	0.2642
32.00	1.4142	0.2677	0.0095	13.9476	0.3540

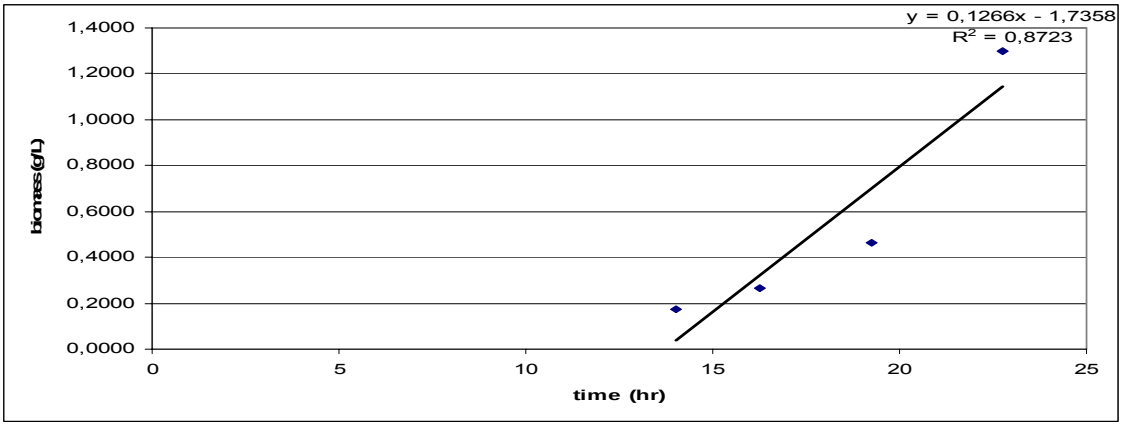

Figure A.14. Exponential phase of ΔHAP4 in continuous cultivation

Table A.13. Growth and metabolite profiles of ΔQCR7 in continuous cultivation

time (hr)	x_v (kg cell/m^3)	glucose (g/L)	pyruvate (g/L)	ethanol (g/L)	succinic acid (g/L)
0	0.3636	18.7024	0.0171	1.5721	0.0036
1	0.4531	16.7656	0.0178	2.3093	0.0026
2	0.3891	14.8289	0.0185	3.0464	0.0017
3	0.4222	15.4658	0.0190	3.2047	0.0085
4	0.4114	16.1028	0.0195	3.3631	0.0153
5	0.4771	15.0750	0.0201	3.3055	0.0157
6	0.5261	14.0473	0.0207	3.2479	0.0161
7	0.5910	13.8314	0.0214	4.0110	0.0272
8	0.6982	13.6155	0.0220	4.7740	0.0384
9	0.8037	11.9227	0.0254	6.8327	0.0338
10	0.9701	10.2299	0.0288	8.8915	0.0292
11	1.3307	7.5591	0.0322	8.8166	0.0268
12	1.5573	4.8883	0.0356	8.7418	0.0256
13	1.7469	4.1693	0.0366	9.5077	0.0250
14	1.9370	3.4503	0.0375	10.2736	0.0245

Table A.13. Growth and metabolite profiles of ΔQCR7 in continuous cultivation-continued

15	1.8566	2.7550	0.0400	9.6977	0.0311
16	2.1922	2.0598	0.0426	9.1218	0.0377
17	2.6931	1.8979	0.0406	10.1786	0.0655
18	2.5418	1.7359	0.0386	11.2353	0.0932
19	2.4284	1.1804	0.0401	12.3150	0.0923
20	2.5047	0.6249	0.0416	13.3948	0.0914
21	2.4355	1.0163	0.0465	11.5981	0.0902
22	2.7948	1.4078	0.0513	9.8014	0.0890
23	2.8435	1.1035	0.0472	9.0326	0.1039
24	2.6141	0.7993	0.0431	8.2638	0.1189
26	2.3490	0.7993	0.0431	8.2638	0.1189
28	2.7532	0.7993	0.0431	8.2638	0.1189

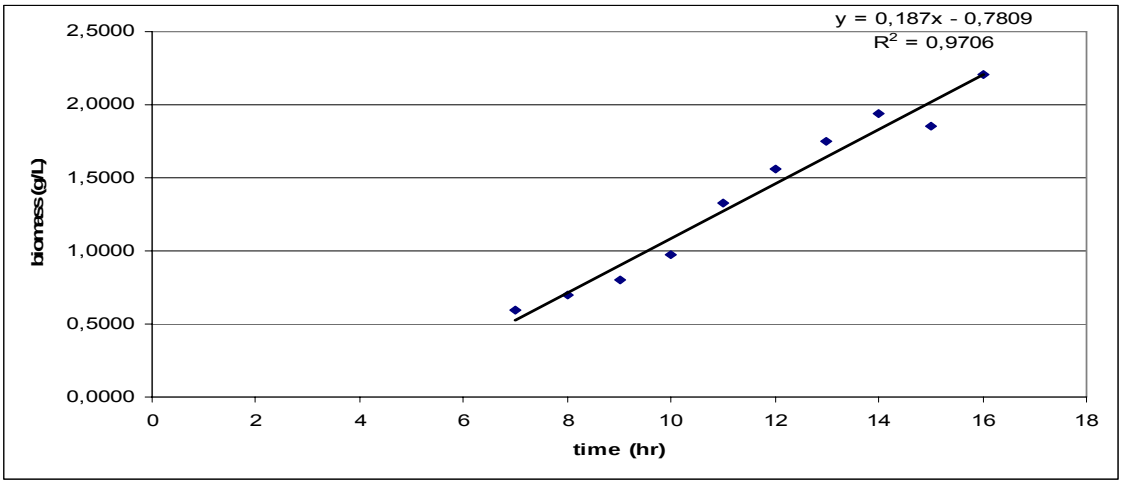

Figure A.15. Exponential phase of ΔQCR7 in continuous cultivation

Table A.14. Growth and metabolite profiles of ΔRIP1 in continuous cultivation

time (hr)	x_v (kg cell/m^3)	glucose (g/L)	pyruvate (g/L)	ethanol (g/L)	succinic acid (g/L)
0	0.1572	19.6531	0.0008	1.8198	0.0509
3	0.1535	16.5790	0.0043	1.1057	0.1332
6	0.1613	14.1095	0.0030	3.1558	0.0237
8	0.1687	13.7641	0.0040	5.0446	0.0836
10	0.1919	12.5638	0.0051	4.3190	0.0338
11	0.2144	11.4672	0.0042	9.2946	0.2210
12	0.2319	10.1978	0.0041	6.8299	0.2252
13	0.2617	10.2928	0.0035	7.2099	0.0648
14	0.3254	8.8508	0.0033	9.0412	0.0776
16	0.3907	6.6143	0.0060	12.8880	0.0745
18	0.5054	7.2533	0.0061	11.6902	0.0705
21	0.5910	3.1086	0.0046	11.6557	0.0734
24	0.6084	4.0670	0.0032	13.7864	0.1612
30	0.6033	3.3417	0.0064	11.9897	0.2449

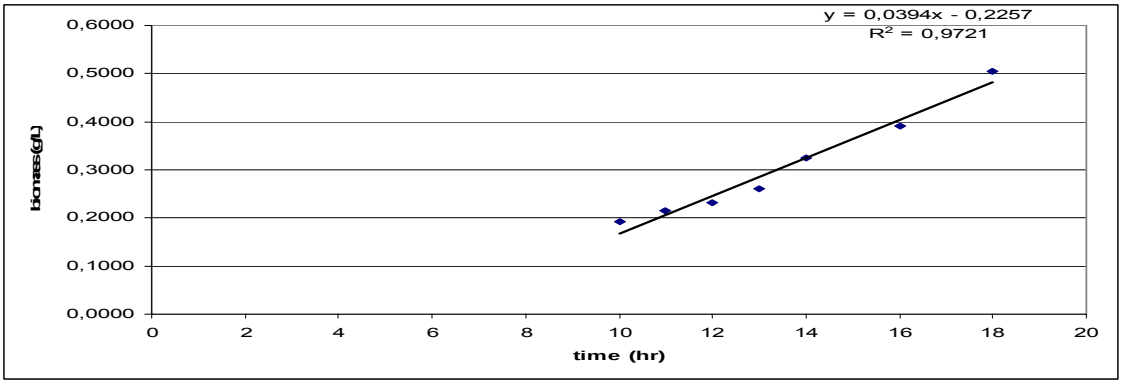

Figure A.16. Exponential phase of ΔRIP1 in continuous cultivation

Table A.15. Growth and metabolite profiles of ΔCYT1 in continuous cultivation

time (hr)	x_v (kg cell/m^3)	glucose (g/L)	pyruvate (g/L)	ethanol (g/L)	succinic acid (g/L)
0	0.9712	19.9503	0.0031	0.6680	0.0355
2	0.9846	20.3044	0.0086	1.6297	0.0367
3	0.9961	20.6585	0.0141	2.5914	0.0378
4	0.9968	18.9010	0.0108	1.8601	0.0240
5	1.0764	17.1435	0.0074	1.1287	0.0102
6	1.0763	13.4384	0.0026	1.0366	0.1286
7	0.9957	11.8363	0.0038	0.9272	0.1147
8	1.1657	10.2343	0.0051	0.8177	0.1008
10	1.1798	10.4674	0.0076	1.7852	0.0130
12	1.2062	9.2324	0.0102	1.4627	0.0413
14	1.2479	10.0270	0.0114	11.2065	0.1992
16	1.2729	8.9863	0.0097	11.6643	0.1720
18	1.2752	7.9456	0.0080	12.1221	0.1449
20	1.2967	6.9049	0.0062	12.5799	0.1177
21	1.3627	5.8642	0.0045	13.0378	0.0905
22	1.3266	4.1973	0.0054	12.8477	0.0517
24	1.3331	2.5305	0.0063	12.6577	0.0128
30	1.3267	0.2073	0.0109	11.4599	0.0857

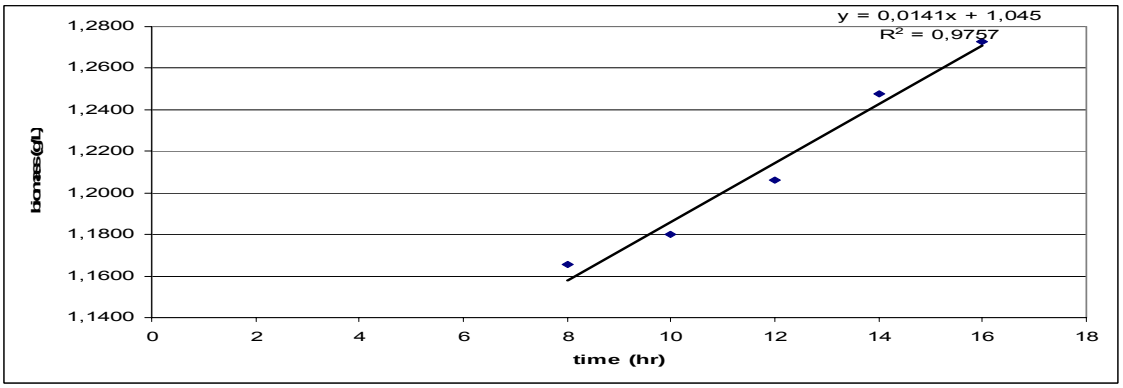

Figure A.17. Exponential phase of ΔCYT1 in continuous cultivation

Table A.16. Growth and metabolite profiles of BY4743 in nutritional limitation cultivations –no limitation-1

time (hr)	x_v kgcell/m^3	glucose (g/L)	acetaldehyde (g/L)	acetic acid (g/L)
0.0	0.2183	19.0694	0.0005	0.0025
2.0	0.2053	18.6462	0.0012	0.0116
4.0	0.2695	17.7912	0.0018	0.0327
8.0	0.3662	18.6203	0.0017	0.0176
12.0	0.4685	18.4044	0.0029	0.0100
14.5	0.7507	13.7925	0.0029	0.0355
16.5	1.0733	12.6093	0.0033	0.1188
19.5	1.7528	9.8370	0.0051	0.1088
23.5	2.5300	3.8432	0.0075	0.1499
28.5	2.7337	1.0105	0.0136	0.1909
32.5	2.2464	0.0518	0.0082	0.3366
36.5	2.4958	0.7773	0.0073	0.3587
40.5	2.4043	0.2073	0.0050	0.4675
44.5	2.3806	0.8464	0.0044	0.3771

Table A.17. Growth and metabolite profiles of BY4743 in nutritional limitation cultivations –no limitation-2

time (hr)	pyruvate (g/L)	succinic acid (g/L)	ethanol (g/L)	glycerol (g/L)
0.0	0.0009	0.0979	0.0115	0.0678
2.0	0.0014	0.0986	0.1152	0.1708
4.0	0.0004	0.0964	0.3801	0.1168
8.0	0.0011	0.0879	0.6680	0.1595
12.0	0.0007	0.0860	5.1713	0.1752
14.5	0.0005	0.0894	7.5785	0.2000
16.5	0.0002	0.0411	7.1984	0.3525
19.5	0.0001	0.0086	7.4979	0.4126
23.5	0.0008	0.0035	9.9972	0.3586
28.5	0.0011	0.1090	9.2946	0.4501
32.5	0.0040	0.1277	10.6997	0.5811
36.5	0.0037	0.1941	10.2621	0.5306
40.5	0.0058	0.1401	10.8149	0.5544
44.5	0.0095	0.1310	11.9436	0.4523

Table A.18. Determination of μ for constant growth region of BY4743 in nutritional limitation cultivations –no limitation

time (hr)	x_v (kgcell/m^3)	ln (x_v)	r_x (kgcells/m^3/hr)	μ (1/hr)	1/ μ (hr)
14.5	0.7507	-0.2868	0.1129	0.1504	6.6510
16.5	1.0733	0.0707	0.1613	0.1503	6.6546
19.5	1.7528	0.5612	0.2265	0.1292	7.7378

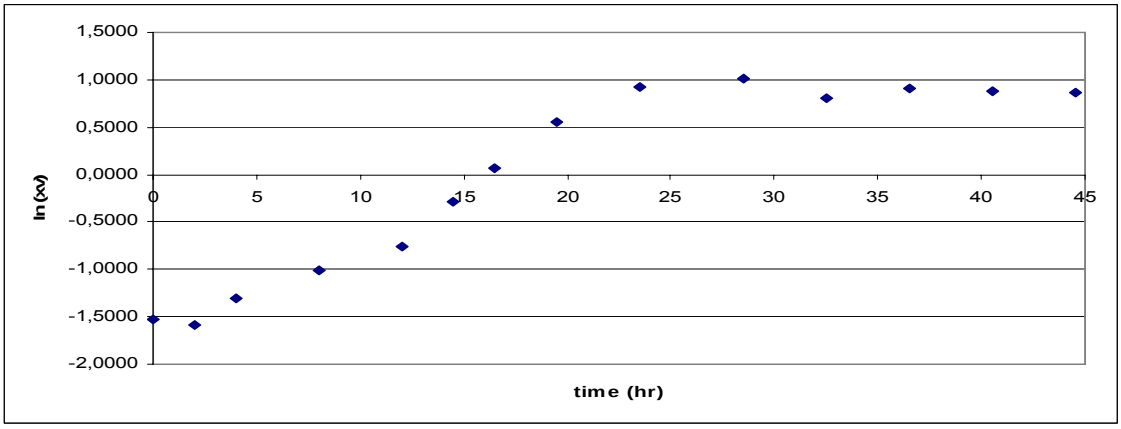

Figure A.18. ln (x_v) vs. time graph to determine the steady state of BY4743 in nutritional limitation cultivations –no limitation

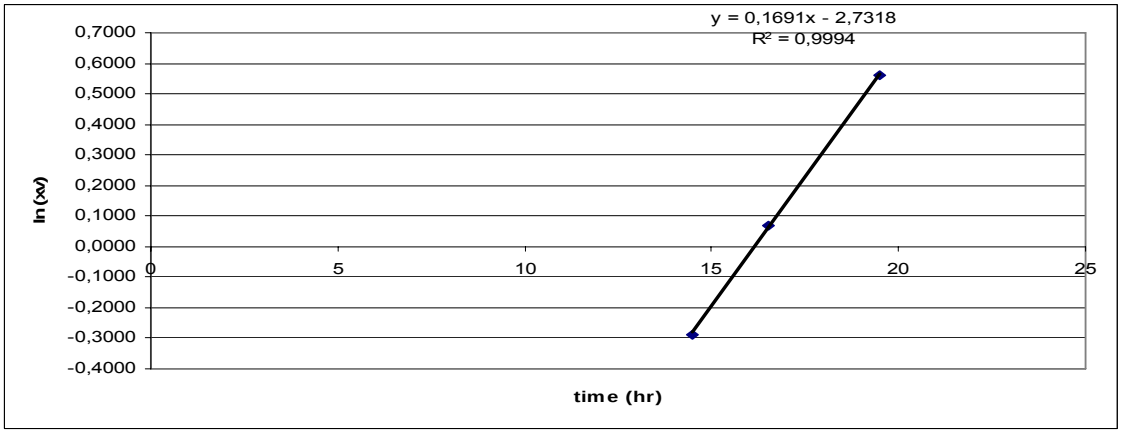

Figure A.19. Determination of μ_{max} of BY4743 in nutritional limitation cultivations –no limitation

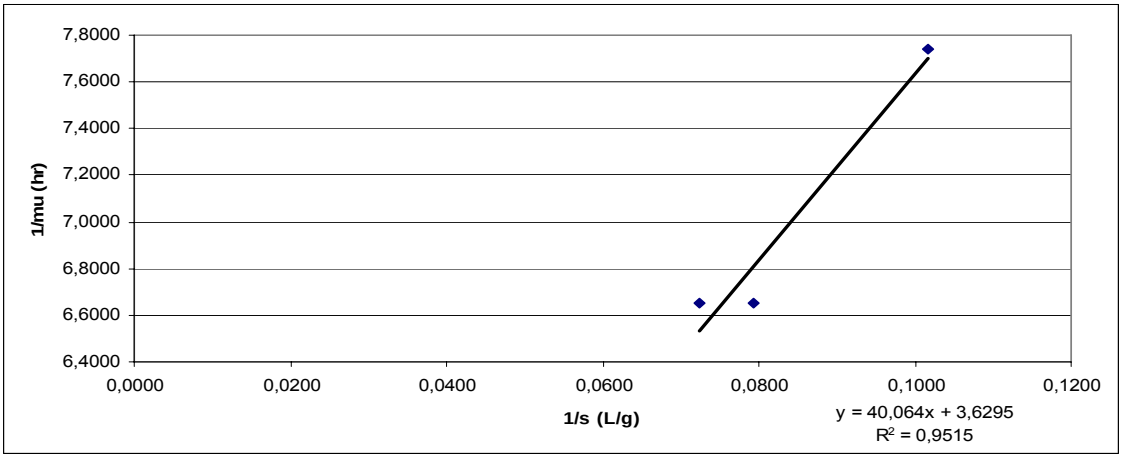

Figure A.20. Determination of K_s of BY4743 in nutritional limitation cultivations –no limitation

Table A.19. Growth and metabolite profiles of BY4743 in nutritional limitation cultivations –C limitation-1

time (hr)	x_v kgcell/m^3	glucose (g/L)	acetaldehyde (g/L)	acetic acid (g/L)
0.00	0.2006	2.5391	0.0033	0.0208
2.00	0.1925	1.7705	0.0023	0.0038
6.00	0.2287	1.8741	0.0025	0.0231
12.00	0.2853	1.3300	0.0017	0.0010
14.50	0.5364	0.2505	0.0003	0.0217
16.50	0.6683	0.5355	0.0007	0.0026
16.92	0.8990	20.5031	0.0270	0.0149
18.00	0.9264	17.9812	0.0237	0.0246
19.00	0.9817	16.8066	0.0221	0.0766
19.25	0.9817	13.5507	0.0178	0.0511
19.50	1.1127	13.0239	0.0171	0.0731
20.50	1.3006	13.2398	0.0174	0.1127
21.50	1.7531	13.6716	0.0180	0.0856
22.50	1.9310	12.8511	0.0169	0.1101
23.50	1.8370	13.4989	0.0178	0.1114
24.50	1.9102	13.6457	0.0180	0.1733
26.50	2.6937	9.7074	0.0128	0.2030
28.50	2.7179	7.2288	0.0095	0.2256
30.50	2.7179	6.1060	0.0080	0.2472
32.50	2.5821	4.9919	0.0066	0.2821
32.67	2.5821	17.8085	0.0234	0.3549
33.92	3.0952	17.1694	0.0226	0.3923
34.67	3.0952	17.7567	0.0234	0.4381
35.42	3.4535	16.5821	0.0218	0.4419
36.50	2.9568	15.7184	0.0207	0.4816
37.50	3.3141	17.3507	0.0228	0.5059
38.50	3.2346	13.1534	0.0173	0.4888
39.50	2.8873	12.3761	0.0163	0.5154
40.50	2.9263	12.3416	0.0162	0.5169
42.50	2.7926	12.9202	0.0170	0.5042
44.50	2.9168	7.1683	0.0094	0.5567

Table A.20. Growth and metabolite profiles of BY4743 in nutritional limitation cultivations –C limitation-2

time (hr)	pyruvate (g/L)	succinic acid (g/L)	ethanol (g/L)	glycerol (g/L)
0.00	0.0102	0.0590	0.5183	0.1211
2.00	0.0007	0.1046	0.8523	0.1811
6.00	0.0001	0.0882	1.0020	0.1216
12.00	0.0006	0.0619	1.3015	0.1758
14.50	0.0057	0.0795	1.0596	0.1869
16.50	0.0009	0.2228	1.1863	0.1316

Table A.20. Growth and metabolite profiles of BY4743 in nutritional limitation cultivations –C limitation-2-continued

16.92	0.0030	0.2105	1.9349	0.1628
18.00	0.0012	0.2128	2.9024	0.1218
19.00	0.0235	0.2493	3.8238	0.2822
19.25	0.0117	0.1991	4.4573	0.1847
19.50	0.0035	0.2530	4.5264	0.2195
20.50	0.0082	0.1860	6.1503	0.2601
21.50	0.0003	0.1703	6.2425	0.2597
22.50	0.0050	0.1693	5.4017	0.2728
23.50	0.0026	0.1257	5.6320	0.2905
24.50	0.0055	0.1325	5.4938	0.2302
26.50	0.0003	0.0871	7.2330	0.2050
28.50	0.0158	0.0948	8.3617	0.2167
30.50	0.0003	0.1248	8.8224	0.2260
32.50	0.0000	0.3003	8.6381	0.4764
32.67	0.0314	0.2667	10.5615	0.2510
33.92	0.0005	0.2538	9.6747	0.3757
34.67	0.0059	0.1865	10.7112	0.3065
35.42	0.0005	0.1711	10.8379	0.3802
36.50	0.0236	0.1823	12.1164	0.2866
37.50	0.0009	0.1710	10.3081	0.3273
38.50	0.0192	0.1914	15.2606	0.3261
39.50	0.0328	0.1604	15.9978	0.3314
40.50	0.0046	0.0957	13.4754	0.3134
42.50	0.0294	0.0231	12.1049	0.3683
44.50	0.0005	0.0055	16.2166	0.3505

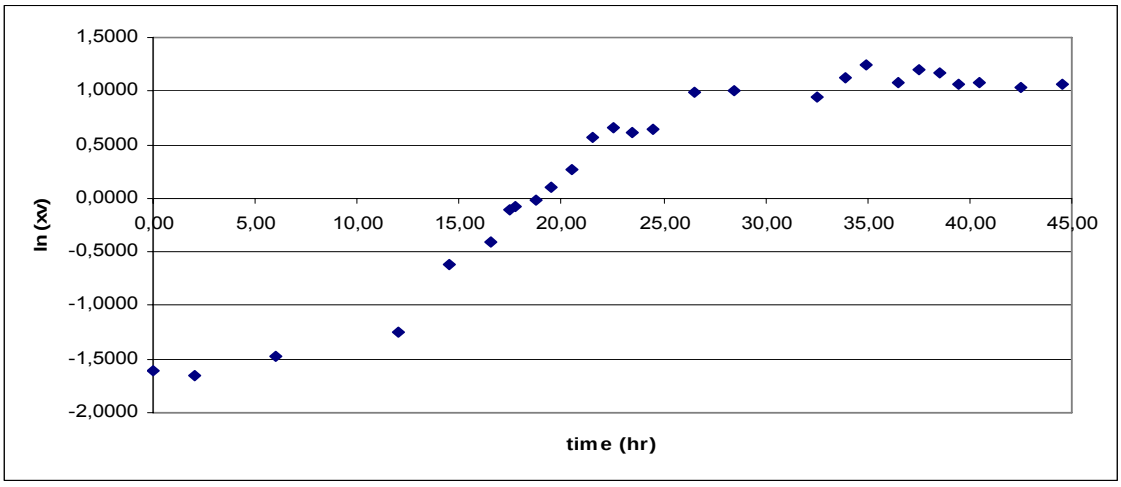

Figure A.21. ln (x_v) vs. time graph to determine the steady state of BY4743 in nutritional limitation cultivations –C limitation

Table A.21. Determination μ for constant growth region of BY4743 in nutritional limitation cultivations –C limitation

time (hr)	x_v (kgcell/m^3)	ln (x_v)	r_x (kgcells/m^3/hr)	μ (1/hr)	1/ μ (hr)
6.00	0.2287	-1.4753	0.0275	0.1203	8.3136
12.00	0.2853	-1.2543	0.0362	0.1269	7.8805
14.50	0.5364	-0.6229	0.0232	0.0432	23.1588

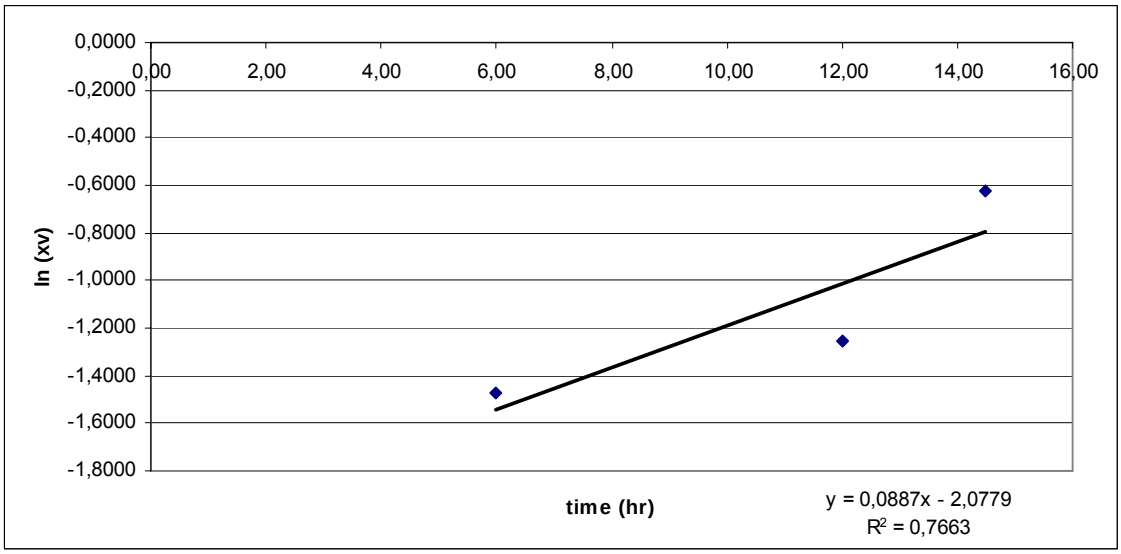

Figure A.22. Determination of μ_{max} of BY4743 in nutritional limitation cultivations – C limitation

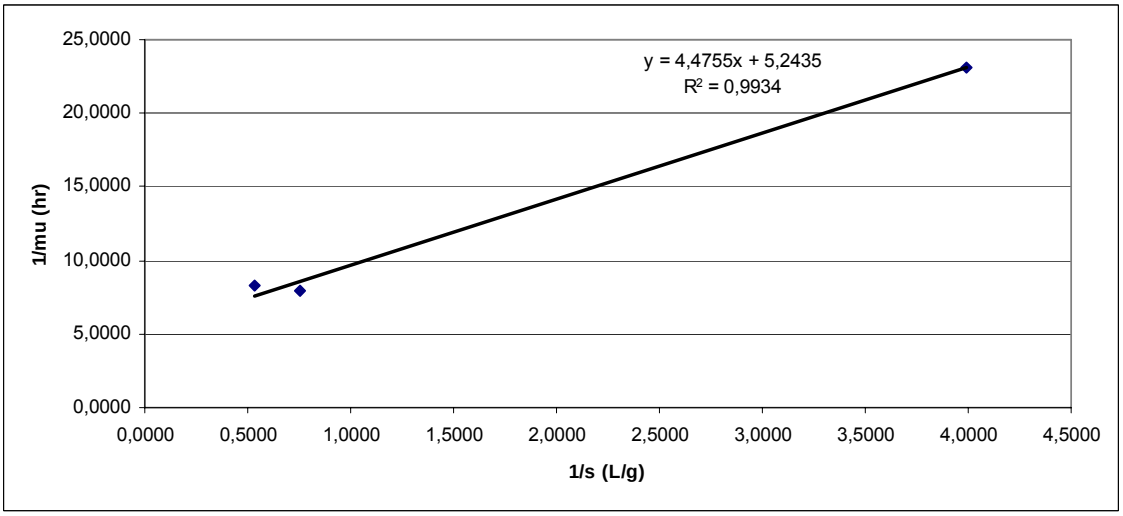

Figure A.23. Determination of K_s of BY4743 in nutritional limitation cultivations – C limitation

Table A.22. Growth and metabolite profiles of BY4743 in nutritional limitation cultivations – N limitation-1

time (hr)	x_v kgcell/m^3	glucose (g/L)	acetaldehyde (g/L)	acetic acid (g/L)
0.0	0.2102	18.5599	0.0000	0.0236
4.0	0.2384	19.4149	0.0001	0.0160
8.0	0.2966	16.3057	0.0000	0.0341
10.0	0.3280	15.3730	0.0002	0.0319
12.5	0.4835	11.5902	0.0011	0.0208
14.5	0.6739	13.5852	0.0097	0.0349
14.9	0.6739	11.4779	0.0071	0.0350
16.0	0.6739	11.7802	0.0074	0.0035
17.0	0.9884	10.9943	0.0075	0.0129
17.3	0.9884	9.9924	0.0066	0.0187
17.5	0.9884	7.6951	0.0068	0.0180
18.5	1.0544	8.0320	0.0082	0.0456
19.5	1.1423	7.1251	0.0066	0.0715
20.5	1.4918	8.1270	0.0079	0.0758
21.5	1.5629	7.9024	0.0054	0.0854
22.5	1.5689	7.9542	0.0047	0.1383
24.5	1.7713	8.9129	0.0030	0.1360
26.5	1.6660	6.8315	0.0020	0.2469
28.5	1.7247	5.8728	0.0020	0.1979
30.5	1.9446	3.5842	0.0007	0.1402
30.7	1.8149	0.1814	0.0054	0.1962
31.9	1.9265	0.3023	0.0086	0.2676
32.7	2.1396	0.0950	0.0081	0.3783
33.4	2.3880	1.4250	0.0096	0.4365
34.5	2.3375	0.2332	0.0092	0.4333
35.5	1.9012	0.3541	0.0089	0.4810
36.5	2.1959	0.5009	0.0078	0.4220
37.5	2.3985	0.2936	0.0076	0.1931
38.5	2.4285	0.0432	0.0067	0.2603
40.5	2.2617	0.0432	0.0058	0.3372
42.5	2.0617	0.3541	0.0040	0.4097
44.5	2.2054	0.1555	0.0055	0.4425

Table A.23. Growth and metabolite profiles of BY4743 in nutritional limitation cultivations – N limitation-2

time	pyruvate (g/L)	succinic acid (g/L)	ethanol (g/L)	glycerol (g/L)
0.0	0.0004	0.0726	0.2649	0.1463
4.0	0.0002	0.0650	0.1037	0.1118
8.0	0.0160	0.0563	0.3916	0.1215
10.0	0.0128	0.0564	1.1517	0.1227
12.5	0.0006	0.0751	0.6910	0.2050
14.5	0.0009	0.1766	0.5989	0.2408

Table A.23. Growth and metabolite profiles of BY4743 in nutritional limitation cultivations – N limitation-2-continued

14.9	0.0004	0.1436	1.0826	0.2609
16.0	0.0019	0.2294	3.0061	0.2393
17.0	0.0007	0.1362	6.0236	0.3839
17.3	0.0068	0.1731	6.5765	0.2237
17.5	0.0003	0.0954	6.8644	0.4016
18.5	0.0203	0.0921	9.3061	0.6521
19.5	0.0004	0.0788	9.4789	0.5194
20.5	0.0010	0.0814	8.7763	0.4700
21.5	0.0131	0.0773	9.0873	0.4884
22.5	0.0004	0.0912	9.0988	0.4573
24.5	0.0026	0.1237	9.2255	0.3879
26.5	0.0005	0.1422	8.8800	0.3841
28.5	0.0012	0.1165	9.8129	0.4705
30.5	0.0177	0.1182	9.3637	0.6183
30.7	0.0037	0.1424	6.2079	0.4971
31.9	0.0009	0.1624	7.9816	0.4665
32.7	0.0004	0.1874	5.6320	0.4773
33.4	0.0094	0.1856	6.3346	0.4549
34.5	0.0015	0.0780	4.3997	0.4616
35.5	0.0015	0.1069	3.5128	0.4673
36.5	0.0036	0.0807	3.6856	0.5055
37.5	0.0003	0.0792	3.7086	0.4596
38.5	0.0020	0.0943	2.0962	0.5008
40.5	0.0005	0.0046	2.7181	0.5376
42.5	0.0003	0.0850	2.0156	0.5537
44.5	0.0031	0.0867	1.1517	0.5759

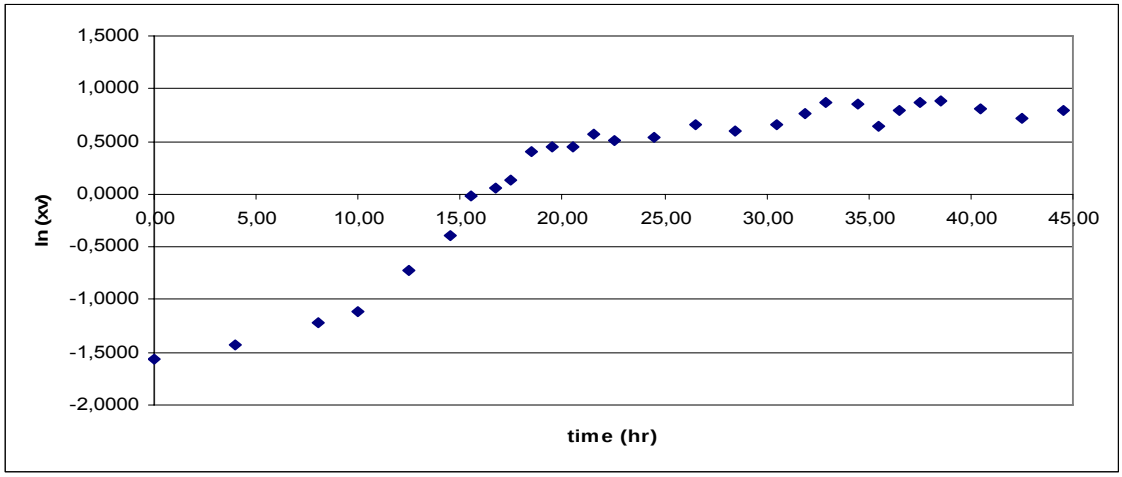

Figure A.24. ln (x_v) vs. time graph to determine the steady state of BY4743 in nutritional limitation cultivations – N limitation

Table A.24. Determination of μ for constant growth region of BY4743 in nutritional limitation cultivations – N limitation

time	x_v (kgcell/m^3)	ln (x_v)	r_x (kgcells/m^3/hr)	μ (1/hr)	1/ μ (hr)
8.00	0.2966	-1.2154	0.0504	0.1700	5.8840
10.00	0.3280	-1.1147	0.0502	0.1531	6.5331
12.50	0.4835	-0.7267	0.0580	0.1200	8.3302
14.50	0.6739	-0.3947	0.0866	0.1285	7.7803

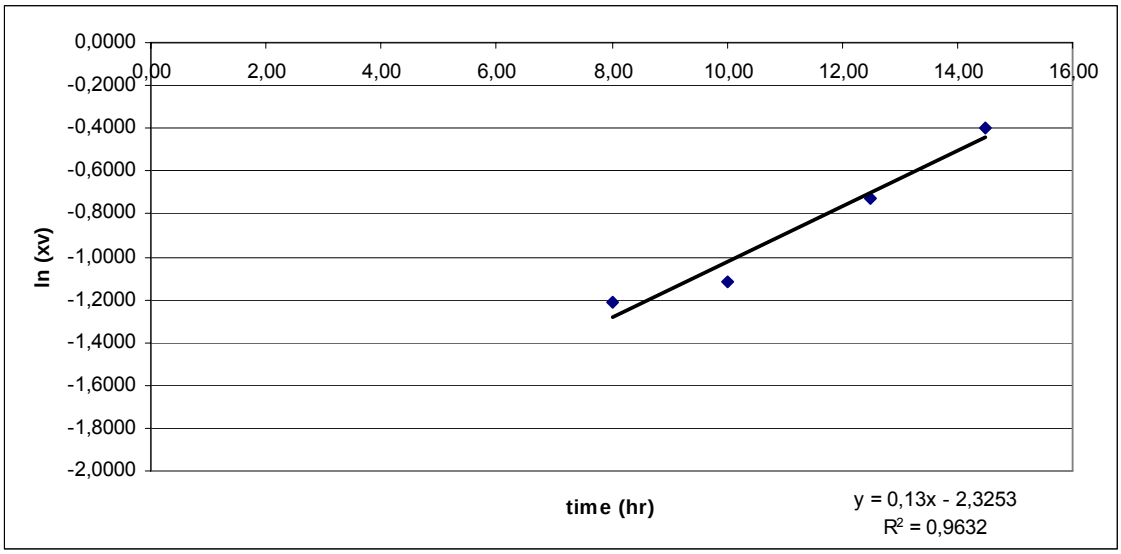

Figure A.25. Determination of μ_{max} of BY4743 in nutritional limitation cultivations – N limitation

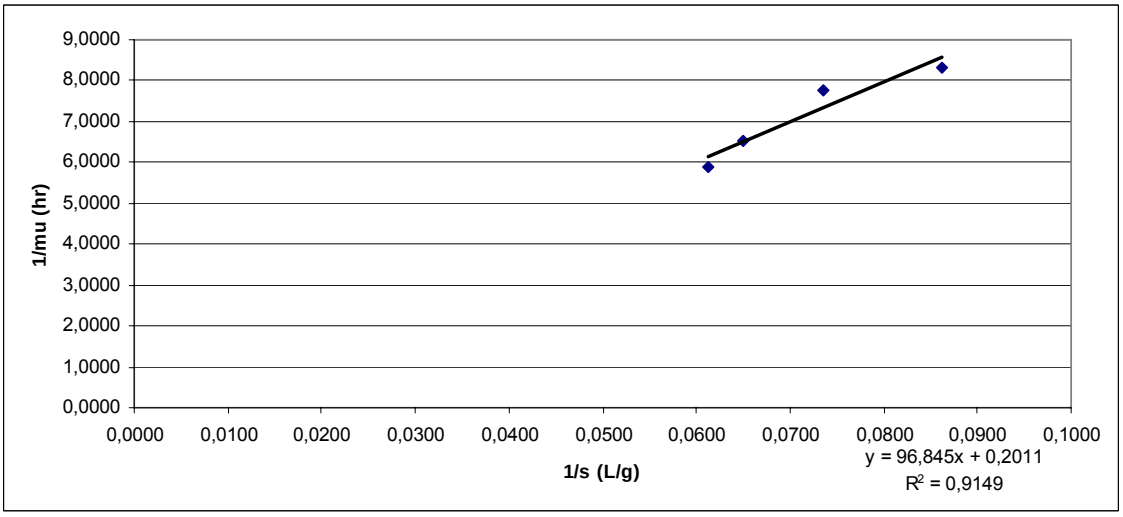

Figure A.26. Determination of K_s of BY4743 in nutritional limitation cultivations – N limitation

Table A.25. Gene expression data of BY4743 in C limitation and N limitation with pulse injections

Carbon Limitation			Nitrogen Limitation		
sample	time (hr)	expression	sample	time (hr)	expression
1	0.00	1.242	1	0.00	5.232
2	2.00	1.009	2	4.00	17.148
3	6.00	1.000	3	8.00	1.000
4	12.00	1.542	4	10.00	2.000
5	14.50	8.070	5	12.50	8.140
6	16.50	9.524	6	14.50	13.454
7	16.50	7.931	7	14.50	4.798
8	16.50	42.592	8	14.50	1.000
9	16.50	8.282	9	14.50	12.231
10	16.92	5.560	10	14.92	6.669
11	17.17	1.756	11	15.25	1.000
12	17.50	1.966	12	15.50	6.904
13	17.75	1.000	13	15.75	45.649
14	18.00	8.574	14	16.00	69.792
15	18.25	16.854	15	16.25	114.365
16	18.50	1.439	16	16.50	55.715
17	18.75	3.732	17	16.75	7.273
18	19.00	1.711	18	17.00	9.270
19	19.25	3.830	19	17.25	1.275
20	19.50	2.358	20	17.50	9.032
21	20.50	1.477	21	18.50	4.000
22	21.50	1.000	22	19.50	9.270
23	22.50	4.362	23	20.50	39.739
24	23.50	11.023	24	21.50	10.021
25	24.50	1.000	25	22.50	1.000
26	26.50	2.624	26	24.50	36.758
27	28.50	3.808	27	26.50	43.336
28	30.50	16.994	28	28.50	202.601
29	32.50	35.302	29	30.50	157.586
30	32.50	8.599	30	30.50	206.143
31	32.50	20.452	31	30.50	374.806
32	32.50	49.493	32	30.50	374.806
33	32.67	41.260	33	30.67	1.000
34	33.17	3.277	34	31.25	1.000
35	33.42	3.920	35	31.50	30.204
36	33.67	2.709	36	31.75	41.981
37	33.92	1.787	37	32.00	44.221
38	34.17	2.571	38	32.25	53.973
39	34.42	1.000	39	32.50	243.735
40	34.67	3.005	40	32.75	417.076
41	34.92	5.706	41	33.00	7.817
42	35.17	6.248	42	33.25	1.000
43	35.42	2.149	43	33.50	1.000

Table A.25. Gene expression data of BY4743 in C limitation and N limitation with pulse injections-continued

44	36.50	4.625	44	34.50	12.481
45	37.50	5.538	45	35.50	5.924
46	38.50	10.530	46	36.50	8.023
47	39.50	4.775	47	37.50	29.943
48	40.50	1.000	48	38.50	7.486
49	42.50	1.651	49	40.50	51.239
50	44.50	1.000	50	42.50	297.484
Not Applicable			51	44.50	297.484

A.3. DNA / RNA Concentration and Contamination Determinations

After the DNAs of the deletion mutants are extracted, they are checked for their concentration and contamination scores according to the principles stated in the Materials and Methods section. The following table shows the properties of the extracted samples (Table A.26).

Contamination and concentration results were also important in the optimization of RNA extraction via mechanical disruption. First, the procedure is applied via enzymatic lysis procedures to obtain a 5.81 μg RNA sample with an absorbance ratio of 1.73. Then optimization via mechanical disruption method is performed and the results are as follows for the following cases with 5 minutes at 500 rpm stored in RNA Stabilizing Reagent giving the optimum results (Table A.27).

Table A.26. DNA concentration and contamination results

Strain	A_{260}	A_{280}	Concentration (μg/ml)	$\frac{A_{260}}{A_{280}}$
ΔHO	0.0670	0.0356	134.0	1.88
ΔQDR3	0.0567	0.0307	113.4	1.85
ΔMIG1	0.0086	0.0041	17.2	2.10
ΔHAP4	0.0264	0.0139	52.8	1.90
ΔQCR7	0.0217	0.0122	43.4	1.78
ΔRIP1	0.0117	0.0067	23.4	1.75
ΔCYT1	0.0162	0.0075	32.4	2.15

Table A.27. RNA concentration and contamination results

Condition	A_{260}	A_{280}	Concentration (μg)	$\frac{A_{260}}{A_{280}}$
Stabilizing Reagent 3' 1500 rpm	0.0125	0.0014	6.75	8.93
Stabilizing Reagent 3' 1200 rpm	0.0125	0.0098	6.75	1.28
Stabilizing Reagent 5' 500 rpm	0.0216	0.0104	11.66	2.08
Stabilizing Reagent 5' 1000 rpm	0.0256	0.0014	13.82	18.3
Shock Freeze 3' 1500 rpm	0.0261	0.0009	14.09	29.00
Shock Freeze 3' 1200 rpm	0.163	0.0327	8.80	0.50
Shock Freeze 5' 500 rpm	0.0322	0.0287	17.39	1.12
Shock Freeze 5' 1000 rpm	0.0175	0.0137	9.45	1.30

A.4. Flux Balance Analysis – Small Scale Model

The list of the metabolites and their abbreviations that are taken into consideration in the model are given as follows:

AC	Acetic acid
ACAL	Acetalehyde
$ACCOA_{cyt}$	Acetyl Co-Enzyme A in cyt.
$ACCOA_{mit}$	Acetyl Co-Enzyme A in mit.
ADP	Adenosine di-phoshate
AKG	2-Oxoglutarate
ATP	Adenosine tri-phoshate
BIOM	Biomass
CIT	Citrate
CO_2	Carbon dioxide
DHAP	Dehydroxy-acetone-phosphate
E4P	D-Erythrose 4-phosphate
ETOH	Ethanol
FAD	FAD
$FADH_2$	$FADH_2$
FRUC6P	D-Fructose 1-phosphate
FRUCDP	D-Fructose 2,6-bisphosphate
FUM	Fumerate
G15L	D-6-phospho-glucono-δ-lactone
GA3P	D-Glucosamine 3-phosphate
GAL	Galacatose
GLUC	Glucose
GLUC6P	D-Glucose-6-phosphate
GLYO	Glycine
GOH	Glycerol
GOH3P	sn-Glycerol 3-phosphate
ISOCIT	Isocytrate
MAL	Malate

NAD_{cyt}	NAD_{cyt}
$NADH_{cyt}$	$NADH_{cyt}$
$NADH_{mit}$	$NADH_{mit}$
NAD_{mit}	NAD_{mit}
$NADP_{cyt}$	$NADP_{cyt}$
$NADPH_{cyt}$	$NADPH_{cyt}$
$NADPH_{mit}$	$NADPH_{mit}$
$NADP_{mit}$	$NADP_{mit}$
OAC	Oxaloacetate
O_2	Oxygen
P13G	3-phospho-D-glyceroyl-phosphate
P2G	2-phosphoglycerate
P3G	3-phosphoglycerate
P6G	6-phospho-gluconate
PEP	phosphoenolpyruvate
PYR	pyruvate
RIB5P	ribose-5-phosphate
RIBL5P	ribulose-5-phosphate
SED7P	sedoheptulose-7-phosphate
SUC	succinate
SUCCOA	Succinyl-Conezyme-A
XYL5P	xylulose-5-phosphate

The list of reactions is given as:

SUBSTRATE UPTAKE

(1) 1GLUC + 1ATP → 1GLUC6P + ADP

(2) 1GAL + 1ATP → 1GLUC6P + ADP

(3) 1ETOH + 1NAD_{cyt} → 1ACAL + 1$NADH_{cyt}$

GLYCOLYSIS AND GLUCONEOGENESIS

(4) 1GLU6P ↔ 1 FRUC6P

(5) 1FRUC6P + 1ATP → 1FRUCDP + 1ADP

(6) 1FRUCDP → 1FRUC6P

(7) 1FRUCDP ↔ 1GA3P + 1DHAP

(8) 1DHAP ↔ 1GA3P

(9) 1GA3P + 1NAD_{cyt} ↔ 1P13G +1$NADH_{cyt}$

(10) 1P13G + 1ADP ↔ 1P3G + 1ATP

(11) 1P3G ↔ 1P2G

(12) 1P2G ↔ 1PEP

(13) 1PEP + 1ADP → 1PYR + 1ATP

(14) 1DHAP +1$NADH_{cyt}$ → 1GOH3P + 1NAD_{cyt}

(15) 1GOH3P → 1GOH

(16) 1PYR → 1ACAL 1CO_2

(17) 1ACAL + 1$NADH_{cyt}$ → 1ETOH + 1NAD_{cyt}

(18) 1ACAL + 1$NADP_{cyt}$ → 1AC + 1$NADPH_{cyt}$

(19) 1ACAL + 1NAD_{mit} → 1AC + 1$NADH_{mit}$

(20) 1 AC + 2ATP → 1$ACCOA_{cyt}$ + 2ADP

(21) 1PYR + 1NAD_{mit} → 1$ACCOA_{mit}$ + 1$NADH_{mit}$ +1CO_2

(22) 1PYR + 1ATP + 1 CO_2 → 1OAC + 1ADP

(23) 1OAC + 1ATP → 1PEP + 1ADP + CO_2

PENTOSE PHOSPHATE PATHWAY

(24) 1GLUC6P + 1$NADP_{cyt}$ → 1G15L + 1$NADPH_{cyt}$

(25) 1G15L → 1P6G

(26) 1P6G + 1$NADP_{cyt}$ → 1RIBL5P + 1$NADPH_{cyt}$ + CO_2

(27) 1RIBL5P ↔ 1RIB5P

(28) 1RIBL5P ↔ 1XYL5P

(29) 1RIB5P + 1XYL5P ↔ 1SED7P + 1GA3P

(30) 1SED7P + 1GA3P ↔ 1FRUC6P + 1E4P

(31) 1XYL5P + 1E4P ↔ 1FRUC6P + 1GA3P

CITRIC ACID CYCLE

(32) 1OAC + 1$ACCOA_{mit}$ → 1CIT

(33) 1CIT ↔ 1ISOCIT

(34) 1ISOCIT + 1NAD_{mit} → 1AKG + 1$NADH_{mit}$ +1CO_2

(35) 1ISOCIT + 1$NADP_{mit}$ → 1AKG + 1$NADPH_{mit}$ + 1CO_2

(36) 1ISOCIT + 1$NADP_{cyt}$ → 1AKG + 1$NADPH_{cyt}$+ 1CO_2

(37) 1AKG + 1NAD_{mit} → 1SUCCOA + 1$NADH_{mit}$ + 1CO_2

(38) 1SUCCOA + 1ADP ↔ 1SUC + 1ATP

(39) 1SUC + 1FAD → 1FUM + 1$FADH_2$

(40) 1FUM + 1$FADH_2$ → 1SUC + 1FAD

(41) 1FUM ↔ 1MAL

(42) 1MAL + 1NAD_{mit} ↔ 1OAC + 1$NADH_{mit}$

(43) 1MAL + 1NAP_{mit} → 1PYR + 1CO_2 + 1$NADPH_{mit}$

(44) 1$ACCOA_{cyt}$ → 1$ACCOA_{mit}$

(45) 1$NADH_{cyt}$ + 1NAD_{mit} → 1NAD_{cyt} + 1$NADH_{mit}$

GLYOXYLATE SHUNT

(46) 1OAC + 1$ACCOA_{cyt}$ → 1CIT

(47) 1ISOCIT → 1GLYO + 1SUC

(48) 1GLYO + 1$ACCOA_{cyt}$ →1MAL

(49) 1MAL + 1NAD_{mit} ↔ 1OAC + $NADH_{mit}$

OXIDATIVE PHOSPHORYLATION

(50) 24ADP + 20$NADH_{mit}$ + 10O_2 → 24ATP + 20NAD_{mit}

(51) 24ADP + 20$FADH_2$ + 10O_2 → 24ATP + 20 FAD

(52) 1ATP → 1ADP

BIOMASS FORMATION

(53) 3ACCOAmit + 24ACCOAcyt + 11AKG + 3E4P + 6P3G + 1GOH3P + 6PEP + 18PYR + 3RIB5P + 5GLUC6P + 10OAC + 16NADcyt + 6NADmit + 90NADPHcyt + 22NADPHmit + 254 ATP → 16NADHcyt + 6NADHmit + 90NADPcyt + 22NADPmit + 254 ADP + 100BIOM

The code for this model is given as follows:

```
clear all;

Ameas=[0   0        0        0        ;
0 0        0        0        ;
0 0        0        0        ;
0 0        0        0        ;
```

```
0 0         0         0         ;
0 0         0         0         ;
0 0         0         0         ;
0 -1        0         0         ;
0 0         0         0         ;
0 0         0         0         ;
0 0         0         0         ;
0 0         0         0         ;
0 0         0         0         ;
0 0         0         0         ;
0 0         0         0         ;
0 0         0         0         ;
0 0         0         0         ;
0 0         0         0         ;
0 0         0         0         ;
0 0         0         0         ;
-10         0         0         ;
0 0         0         0         ;
0 0         0         0         ;
0 0         0         0         ;
0 0         0         0         ;
0 0         0         0         ;
0 0         0         0         ;
0 0         0         0         ;
0 0         0         0         ;
0 0         0         0         ;
0 0         0         0         ;
0 0         0         0         ;
0 0         0         0         ;
0 0         0         0         ;
0 0         0         0         ;
0 0         0         0         ;
0 0         0         0         ;
0 0         0         0         ;
0 0         0         0         ;
0 0         0         0         ;
0 0         0         0         ;
0 0         -1        0         ;
0 0         0         0         ;
0 0         0         0         ;
0 0         0         0         ;
0 0         0         -1        ;
0 0         0         0         ;
0 0         0         0         ;
];

%glucose, biomass, pyruvate, succinate ( in moles / mole of glucose)
```

```
Rmeas=[-1.0;1.0045;0.0042;0.0122];
b=-Ameas*Rmeas;


%the last 6 columns belong to the excreted and uptaken metabolites;
%ethanol,galactose,glycerol,acetaldeyde,acetic acid,oxygen,carbondioxide

Acalc=[0 0 0 0 0 0 0 0 0 0 0 0
0 0 0 0 0 0 0 0 0 0 0 1
1 -1 0 0 0 0 0 0 0 0 0 0
0 0 0 0 0 0 0 0 0 0 0 0
0 0 0 0 0 0 0 0 0 0 0 0
0 0 0 0 0 0 0 0 0 0 -1 0
;
0 0 1 0 0 0 0 0 0 0 0 0
0 0 0 0 0 0 0 0 0 1 -1 -1
0 0 0 0 0 0 0 0 0 0 0 0
0 0 0 0 0 0 0 0 0 0 0 0
0 0 0 0 0 0 0 0 0 0 0 0
0 0 0 0 0 0 0 0 -1 0 0 0 ;
0 0 0 0 0 0 0 0 0 0 0 0
0 0 0 0 0 0 0 0 0 0 0 0
1 0 0 0 0 0 0 0 0 0 0 0
0 0 0 0 0 0 0 0 0 0 0 0
0 0 0 0 0 0 0 -1 0 -1 0 -1 0
0 0 0 0 -24 0 0 0 0 0 0 0 ;
0 0 0 0 0 0 0 0 0 0 0 0
0 0 0 0 0 0 0 0 0 0 0 0
0 1 0 0 0 0 0 0 0 0 0 0
0 0 0 0 -1 0 0 0 0 0 0 0
0 0 0 0 0 0 0 1 0 0 0 0
0 0 0 0 -3 0 0 0 0 0 0 0 ;
1 1 0 0 0 1 0 0 0 0 0 0
-1 1 0 0 0 0 -1 0 0 0 0 0
2 0 1 1 0 0 0 0 0 0 0 0
0 0 0 0 0 0 0 0 0 0 -1 1
0 0 0 0 0 0 0 0 0 0 0 0
0 -24 -24 1 254 0 0 0 0 0 0 0 ;
0 0 0 0 0 0 0 0 0 0 0 0
0 0 0 0 0 0 0 0 0 0 0 0
0 0 0 0 0 0 0 0 0 0 0 0
0 0 0 0 0 0 0 1 1 1 -1 0 0
0 0 0 0 0 0 0 0 0 0 0 0
0 0 0 0 -11 0 0 0 0 0 0 0 ;
-1 -1 0 0 0 -1 0 0 0 0 0 0
1 -1 0 0 0 0 1 0 0 0 0 0 0
-2 0 -1 -1 0 0 0 0 0 0 0 0 0
0 0 0 0 0 0 0 0 0 0 0 1 -1
0 0 0 0 0 0 0 0 0 0 0 0 0
0 24 24 -1 -254 0 0 0 0 0 0 0 ;
```

```
    0 0    0    0    0    0    0    0    0    0    0    0    0
0    0    0    0    0    0    0    0    0    0    0    0    0
0    0    0    0    0    0    0    0    0    0    0    0    0
0    0    0    0    0    0    0    0    0    0    0    0    0
0    0    0    0    0    0    0    0    0    0    0    0    0
0    0    0    0  100    0    0    0    0    0    0    0    ;
    0 0    0    0    0    0    0    0    0    0    0    0    0
0    0    0    0    0    0    0    0    0    0    0    0    0
0    0    0    0    0    0    0    0    0    0    0    0    0
0    0    0    0    1   -1    1    0    0    0    0    0    0
0    0    0    0    0    0    0    0    0    1    0    0    0
0    0    0    0    0    0    0    0    0    0    0    0    ;
    0 0    0    0    0    0    0    0    0    0    0    0    0
0    0    0    0    0    0    0    0    0    1    0    0    0
0    1   -1    1    0    0    1    0    0    0    0    0    0
0    0    0    0    0    0    0    1    1    1    1    0    0
0    0    0    0    0    0    1    0    0    0    0    0    0
0    0    0    0    0    0    0    0    0    0    0   -1    ;
    0 0    0    0    0    0    0    1   -1   -1    1    0    0
0    0    0    0    0    0    0   -1    0    0    0    0    0
0    0    0    0    0    0    0    0    0    0    0    0    0
0    0    0    0    0    0    0    0    0    0    0    0    0
0    0    0    0    0    0    0    0    0    0    0    0    0
0    0    0    0    0    0    0    0    0    0    0    0    ;
    0 0    0    0    0    0    0    0    0    0    0    0    0
0    0    0    0    0    0    0    0    0    0    0    0    0
0    0    0    0    0    0    0    0    0    0    0    0    0
1   -1   -1    1    0    0    0    0    0    0    0    0    0
0    0    0    0    0    0    0    0    0    0    0    0    0
0    0    0    0   -3    0    0    0    0    0    0    0    ;
    0 0   -1    0    0    0    0    0    0    0    0    0    0
0    0    0    0    0    0    0    0    0    0    1    0    0
0    0    0    0    0    0    0    0    0    0    0    0    0
0    0    0    0    0    0    0    0    0    0    0    0    0
0    0    0    0    0    0    0    0    0    0    0    0    0
0    0    0    0    0   -1    0    0    0    0    0    0    ;
    0 0    0    0    0    0    0    0    0    0    0    0    0
0    0    0    0    0    0    0    0    0    0    0    0    0
0    0    0    0    0    0    0    0    0    0    0    0    0
0    0    0    0    0    0    0    0    0    0    0    0    0
-1   1    0    0    0    0    0    0    0    0    0    0    0
0    0   20    0    0    0    0    0    0    0    0    0    ;
    0 0    0    0    0    0    0    0    0    0    0    0    0
0    0    0    0    0    0    0    0    0    0    0    0    0
0    0    0    0    0    0    0    0    0    0    0    0    0
0    0    0    0    0    0    0    0    0    0    0    0    0
1   -1    0    0    0    0    0    0    0    0    0    0    0
0    0  -20    0    0    0    0    0    0    0    0    0    ;
    0 0    0    1   -1   -1    1    0    0    0    0    0    0
0    0    0    0    0    0    0    0    0    0    0    0    0
```

```
0   0   0   0   0   0   0   0   0   0   0   0   0
1   -1  1   -1  0   0   0   0   0   0   0   0   0
0   0   0   0   0   0   0   0   0   0   0   0   0
0   0   0   0   0   0   0   0   0   0   0   0   ;
    0 0 0   0   0   1   -1  -1  1   0   0   0   0
0   0   0   0   0   0   0   0   0   0   0   0   0
0   0   0   0   0   0   0   0   0   0   0   0   0
0   0   0   0   0   0   0   0   0   0   0   0   0
0   0   0   0   0   0   0   0   0   0   0   0   0
0   0   0   0   0   0   0   0   0   0   0   0   ;
    0 0 0   0   0   0   0   0   0   0   0   0   0
0   0   0   0   0   0   0   0   0   0   0   0   0
0   0   0   0   0   0   0   0   0   0   0   0   0
0   0   0   0   0   0   0   0   0   0   0   0   0
1   -1  -1  1   0   0   0   0   0   0   0   0   0
0   0   0   0   0   0   0   0   0   0   0   0   ;
    0 0 0   0   0   0   0   0   0   0   0   0   0
0   0   0   0   0   0   0   0   0   0   0   0   0
0   0   0   0   1   -1  0   0   0   0   0   0   0
0   0   0   0   0   0   0   0   0   0   0   0   0
0   0   0   0   0   0   0   0   0   0   0   0   0
0   0   0   0   0   0   0   0   0   0   0   0   ;
    0 0 0   0   0   0   0   1   -1  1   -1  -1  1
0   0   0   0   0   0   0   0   0   0   0   0   0
0   0   0   0   0   0   0   0   0   0   0   1   -1
-1  1   1   -1  0   0   0   0   0   0   0   0   0
0   0   0   0   0   0   0   0   0   0   0   0   0
0   0   0   0   0   0   0   0   0   0   0   0   ;
    0 -1  0   0   0   0   0   0   0   0   0   0   0
0   0   0   0   0   0   0   0   0   0   0   0   0
0   0   0   0   0   0   0   0   0   0   0   0   0
0   0   0   0   0   0   0   0   0   0   0   0   0
0   0   0   0   0   0   0   0   0   0   0   0   0
0   0   0   0   0   0   -1  0   0   0   0   0   ;
    -10 0   0   0   0   0   0   0   0   0   0   0
0   0   0   0   0   0   0   0   0   0   0   0   0
0   0   0   0   0   0   0   0   0   0   0   0   0
0   0   0   0   0   0   0   0   0   0   0   0   0
0   0   0   0   0   0   0   0   0   0   0   0   0
0   0   0   0   0   0   0   0   0   0   0   0   ;
    1 1 0   -1  1   0   0   0   0   0   0   0   0
0   0   0   0   0   0   0   0   0   0   0   0   0
0   0   0   0   -1  0   0   0   0   0   0   0   0
0   0   0   0   0   0   0   0   0   0   0   0   0
0   0   0   0   0   0   0   0   0   0   0   0   0
0   0   0   0   -25 0   0   0   0   0   0   0   ;
    0 0 0   0   0   0   0   0   0   0   0   0   0
0   0   0   0   0   0   0   0   0   0   0   0   0
0   0   0   0   0   0   0   0   0   0   0   0   0
0   0   0   0   0   0   0   0   0   0   0   0   0
```

```
0   0   0   0   0   0   0   0   0   0   1   -1  0
0   0   0   0   0   0   0   0   0   0   0   0   ;
    0 0 0   0   0   0   0   0   0   0   0   0   0
0   0   0   0   0   0   0   0   1   0   0   0   0
0   0   0   0   0   0   0   0   0   0   0   0   0
0   0   0   0   0   0   0   0   0   0   0   0   0
0   0   0   0   0   0   0   0   0   0   0   0   0
0   0   0   0   0   0   0   -1  0   0   0   0   ;
    0 0 0   0   0   0   0   0   0   0   0   0   0
0   0   0   0   0   0   0   1   -1  0   0   0   0
0   0   0   0   0   0   0   0   0   0   0   0   0
0   0   0   0   0   0   0   0   0   0   0   0   0
0   0   0   0   0   0   0   0   0   0   0   0   0
0   0   0   0   -1  0   0   0   0   0   0   0   ;
    0 0 0   0   0   0   0   0   0   0   0   0   0
0   0   0   0   0   0   0   0   0   0   0   0   0
0   0   0   0   0   0   0   0   0   0   0   0   0
0   0   0   0   0   1   -1  -1  -1  -1  0   0   0
0   0   0   0   0   0   0   0   0   0   -1  0   0
0   0   0   0   0   0   0   0   0   0   0   0   ;
    0 0 0   0   0   0   0   0   0   0   0   0   0
0   0   0   0   0   0   0   0   0   0   0   0   0
0   0   0   0   0   0   0   0   0   0   0   0   0
0   0   0   0   0   0   0   0   0   0   0   0   0
0   0   1   -1  -1  1   -1  0   0   0   0   1   -1
1   0   0   0   0   0   0   0   0   0   0   0   ;
    0 0 -1  0   0   0   0   0   0   0   0   -1  1
0   0   0   0   0   0   0   1   0   0   1   0   0
0   0   0   0   0   0   0   0   0   0   0   0   0
0   0   0   0   0   0   0   0   0   0   0   0   0
0   0   0   0   0   0   0   0   1   0   0   0   0
0   0   0   0   -16 0   0   0   0   0   0   0   ;
    0 0 1   0   0   0   0   0   0   0   0   1   -1
0   0   0   0   0   0   0   -1  0   0   -1  0   0
0   0   0   0   0   0   0   0   0   0   0   0   0
0   0   0   0   0   0   0   0   0   0   0   0   0
0   0   0   0   0   0   0   0   -1  0   0   0   0
0   0   0   0   16  0   0   0   0   0   0   0   ;
    0 0 0   0   0   0   0   0   0   0   0   0   0
0   0   0   0   0   0   0   0   0   0   0   0   1
0   1   0   0   0   0   0   0   0   0   0   0   0
0   0   0   0   0   0   0   1   0   0   1   0   0
0   0   0   0   1   -1  0   0   1   0   0   0   1
-1  -20 0   0   6   0   0   0   0   0   0   0   ;
    0 0 0   0   0   0   0   0   0   0   0   0   0
0   0   0   0   0   0   0   0   0   0   0   0   -1
0   -1  0   0   0   0   0   0   0   0   0   0   0
0   0   0   0   0   0   0   -1  0   0   -1  0   0
0   0   0   0   -1  1   0   0   -1  0   0   0   -1
1   20  0   0   -6  0   0   0   0   0   0   0   ;
```

```
    0 0     0     0     0     0     0     0     0     0     0     0     0
0     0     0     0     0     0     0     0     0     0     0    -1     0
0     0     0     0    -1     0    -1     0     0     0     0     0     0
0     0     0     0     0     0     0     0     0    -1     0     0     0
0     0     0     0     0     0     0     0     0     0     0     0     0
0     0     0     0    90     0     0     0     0     0     0     0     ;
    0 0     0     0     0     0     0     0     0     0     0     0     0
0     0     0     0     0     0     0     0     0     0     0     1     0
0     0     0     0     1     0     1     0     0     0     0     0     0
0     0     0     0     0     0     0     0     0     1     0     0     0
0     0     0     0     0     0     0     0     0     0     0     0     0
0     0     0     0   -90     0     0     0     0     0     0     0     ;
    0 0     0     0     0     0     0     0     0     0     0     0     0
0     0     0     0     0     0     0     0     0     0     0     0     0
0     0     0     0     0     0     0     0     0     0     0     0     0
0     0     0     0     0     0     0     0     1     0     0     0     0
0     0     0     0     0     0     1     0     0     0     0     0     0
0     0     0     0   -22     0     0     0     0     0     0     0     ;
    0 0     0     0     0     0     0     0     0     0     0     0     0
0     0     0     0     0     0     0     0     0     0     0     0     0
0     0     0     0     0     0     0     0     0     0     0     0     0
0     0     0     0     0     0     0     0    -1     0     0     0     0
0     0     0     0     0     0    -1     0     0     0     0     0     0
0     0     0     0    22     0     0     0     0     0     0     0     ;
    0 0     0     0     0     0     0     0     0     0     0     0     0
0     0     0     0     0     0     0     0     0     0     0     0     0
0     0     1    -1     0     0     0     0     0     0     0     0     0
0     0     0     0    -1     0     0     0     0     0     0     0     0
0     0     0     0     1    -1     0     0     0    -1     0     0     1
-1    0     0     0   -10     0     0     0     0     0     0     0     ;
    0 0     0     0     0     0     0     0     0     0     0     0     0
0     0     0     0     0     0     0     0     0     0     0     0     0
0     0     0     0     0     0     0     0     0     0     0     0     0
0     0     0     0     0     0     0     0     0     0     0     0     0
0     0     0     0     0     0     0     0     0     0     0     0     0
0   -10   -10     0     0     0     0     0     0     0    -1     0     ;
    0 0     0     0     0     0     0     0     0     0     0     1    -1
-1    1     0     0     0     0     0     0     0     0     0     0     0
0     0     0     0     0     0     0     0     0     0     0     0     0
0     0     0     0     0     0     0     0     0     0     0     0     0
0     0     0     0     0     0     0     0     0     0     0     0     0
0     0     0     0     0     0     0     0     0     0     0     0     ;
    0 0     0     0     0     0     0     0     0     0     0     0     0
0     0     1    -1    -1     1     0     0     0     0     0     0     0
0     0     0     0     0     0     0     0     0     0     0     0     0
0     0     0     0     0     0     0     0     0     0     0     0     0
0     0     0     0     0     0     0     0     0     0     0     0     0
0     0     0     0     0     0     0     0     0     0     0     0     ;
    0 0     0     0     0     0     0     0     0     0     0     0     0
1    -1    -1     1     0     0     0     0     0     0     0     0     0
```

0 0 0 0 0 0 0 0 0 0 0 0 0
0 0 0 0 0 0 0 0 0 0 0 0 0
0 0 0 0 0 0 0 0 0 0 0 0 0
0 0 0 0 -6 0 0 0 0 0 0 0 ;
0 0 0 0 0 0 0 0 0 0 0 0 0
0 0 0 0 0 0 0 0 0 0 0 0 0
0 0 0 0 0 1 -1 0 0 0 0 0 0
0 0 0 0 0 0 0 0 0 0 0 0 0
0 0 0 0 0 0 0 0 0 0 0 0 0
0 0 0 0 0 0 0 0 0 0 0 0 ;
0 0 0 0 0 0 0 0 0 0 0 0 0
0 0 0 0 1 -1 -1 0 0 0 0 0 0
0 0 0 1 0 0 0 0 0 0 0 0 0
0 0 0 0 0 0 0 0 0 0 0 0 0
0 0 0 0 0 0 0 0 0 0 0 0 0
0 0 0 0 -6 0 0 0 0 0 0 0 ;
0 0 0 0 0 0 0 0 0 0 0 0 0
0 0 0 0 0 0 1 0 0 -1 0 0 0
0 -1 -1 0 0 0 0 0 0 0 0 0 0
0 0 0 0 0 0 0 0 0 0 0 0 0
0 0 0 0 0 0 1 0 0 0 0 0 0
0 0 0 0 -18 0 0 0 0 0 0 0 ;
0 0 0 0 0 0 0 0 0 0 0 0 0
0 0 0 0 0 0 0 0 0 0 0 0 0
0 0 0 0 0 0 0 1 -1 0 0 -1 1
0 0 0 0 0 0 0 0 0 0 0 0 0
0 0 0 0 0 0 0 0 0 0 0 0 0
0 0 0 0 -3 0 0 0 0 0 0 0 ;
0 0 0 0 0 0 0 0 0 0 0 0 0
0 0 0 0 0 0 0 0 0 0 0 0 0
0 0 0 0 0 0 1 -1 1 -1 1 0 0
0 0 0 0 0 0 0 0 0 0 0 0 0
0 0 0 0 0 0 0 0 0 0 0 0 0
0 0 0 0 0 0 0 0 0 0 0 0 ;
0 0 0 0 0 0 0 0 0 0 0 0 0
0 0 0 0 0 0 0 0 0 0 0 0 0
0 0 0 0 0 0 0 0 0 0 0 1 -1
-1 1 0 0 0 0 0 0 0 0 0 0 0
0 0 0 0 0 0 0 0 0 0 0 0 0
0 0 0 0 0 0 0 0 0 0 0 0 ;
0 0 0 0 0 0 0 0 0 0 0 0 0
0 0 0 0 0 0 0 0 0 0 0 0 0
0 0 0 0 0 0 0 0 0 0 0 0 0
0 0 0 0 0 0 0 0 0 0 0 1 -1
-1 1 0 0 0 0 0 0 0 0 1 0 0
0 0 0 0 0 0 0 0 0 0 0 0 ;
0 0 0 0 0 0 0 0 0 0 0 0 0
0 0 0 0 0 0 0 0 0 0 0 0 0
0 0 0 0 0 0 0 0 0 0 0 0 0
0 0 0 0 0 0 0 0 0 0 1 -1 1

```
0     0     0     0     0     0     0     0     0     0     0     0     0
0     0     0     0     0     0     0     0     0     0     0     0     ;
      0 0     0     0     0     0     0     0     0     0     0     0     0
0     0     0     0     0     0     0     0     0     0     0     0     0
0     0     0     0     0     0     0     0     0     1     -1    -1    1
0     0     -1    1     0     0     0     0     0     0     0     0     0
0     0     0     0     0     0     0     0     0     0     0     0     0
0     0     0     0     0     0     0     0     0     0     0     0     ;
      ];

      lb=0*ones(77,1);
      ub=inf*ones(77,1);

      ub(72,1)=0;
      lb(72,1)=-inf;

      ub(2,1)=0;
      lb(2,1)=0;

      ub(3,1)=0;
      lb(3,1)=0;

      ub(76,1)=0;
      lb(76,1)=-inf;

      f=zeros(1,77);

      % max ETOH
       f(1,71)=-1;



      X=linprog(f,[],[],Acalc,b,lb,ub)
```

A.5. Flux Balance Analysis – Genome Scale Model and MOMA

Genome scale flux balance and minimization of metabolic adjustment procedures are carried out simultaneously and they are considered within the same code. The list of metabolites used in the code and the list of reactions are given in the following tables:

Table A.28. Complete list of metabolites

Abbreviation	Metabolite
13GLUCAN	1,3-beta-D-Glucan
13PDG	3-Phospho-D-glyceroyl phosphate
23DAACP	2,3-Dehydroacyl-[acyl-carrier-protein]

Table A.28. Complete list of metabolites -continued

23PDG	2,3-Bisphospho-D-glycerate
2HDACP	Hexadecenoyl-[acp]
2MANPD	("alpha"-D-mannosyl)(,2)-"beta"-D-mannosyl-diacetylchitobiosyldiphosphod olichol
2N6H	2-Nonaprenyl-6-hydroxyphenol
2NMHMBm	3-Demethylubiquinone-9M
2NPMBm	2-Nonaprenyl-6-methoxy-1,4-benzoquinoneM
2NPMMBm	2-Nonaprenyl-3-methyl-6-methoxy-1,4-benzoquinoneM
2NPMP	2-Nonaprenyl-6-methoxyphenol
2NPMPm	2-Nonaprenyl-6-methoxyphenolM
2NPPP	2-Nonaprenylphenol
2PG	2-Phospho-D-glycerate
3DDAH7P	2-Dehydro-3-deoxy-D-arabino-heptonate 7-phosphate
3HPACP	(3R)-3-Hydroxypalmitoyl-[acyl-carrier protein]
3PG	3-Phospho-D-glycerate
3PSER	3-Phosphoserine
3PSME	5-O-(1-Carboxyvinyl)-3-phosphoshikimate
4HBZ	4-Hydroxybenzoate
4HLT	4-Hydroxy-L-threonine
4HPP	3-(4-Hydroxyphenyl)pyruvate
4PPNCYS	(R)-4'-Phosphopantothenoyl-L-cysteine
4PPNTE	Pantetheine 4'-phosphate
4PPNTEm	Pantetheine 4'-phosphateM
4PPNTO	D-4'-Phosphopantothenate
5MTA	5'-Methylthioadenosine
6DGLC	D-Gal alpha 1->6D-Glucose
A6RP	5-Amino-6-ribitylamino-2,4 (1H, 3H)-pyrimidinedione
A6RP5P	5-Amino-6-(5'-phosphoribosylamino)uracil
A6RP5P2	5-Amino-6-(5'-phosphoribitylamino)uracil
AACCOA	Acetoacetyl-CoA
AACP	Acyl-[acyl-carrier-protein]
ABUTm	2-Aceto-2-hydroxy butyrateM
AC	Acetate
ACACP	Acyl-[acyl-carrier protein]
ACACPm	Acyl-[acyl-carrier protein]M
ACAL	Acetaldehyde
ACALm	AcetaldehydeM
ACAR	O-Acetylcarnitine
ACARm	O-AcetylcarnitineM
ACCOA	Acetyl-CoA
ACCOAm	Acetyl-CoAM
ACLAC	2-Acetolactate
ACLACm	2-AcetolactateM
ACm	AcetateM
ACNL	3-Indoleacetonitrile
ACOA	Acyl-CoA
ACP	Acyl-carrier protein

Table A.28. Complete list of metabolites -continued

ACPm	Acyl-carrier proteinM
ACTAC	Acetoacetate
ACTACm	AcetoacetateM
ACYBUT	gamma-Amino-gamma-cyanobutanoate
AD	Adenine
ADCHOR	4-amino-4-deoxychorismate
ADm	AdenineM
ADN	Adenosine
ADNm	AdenonsineM
ADP	ADP
ADPm	ADPM
ADPRIB	ADPribose
ADPRIBm	ADPriboseM
AGL3P	Acyl-sn-glycerol 3-phosphate
AHHMD	2-Amino-7,8-dihydro-4-hydroxy-6-(diphosphooxymethyl)pteridine
AHHMP	2-Amino-4-hydroxy-6-hydroxymethyl-7,8-dihydropteridine
AHM	4-Amino-5-hydroxymethyl-2-methylpyrimidine
AHMP	4-Amino-2-methyl-5-phosphomethylpyrimidine
AHMPP	2-Methyl-4-amino-5-hydroxymethylpyrimidine diphosphate
AHTD	2-Amino-4-hydroxy-6-(erythro-1,2,3-trihydroxypropyl)-dihydropteridine triphosphate
AICAR	1-(5'-Phosphoribosyl)-5-amino-4-imidazolecarboxamide
AIR	Aminoimidazole ribotide
AKA	2-Oxoadipate
AKAm	2-OxoadipateM
AKG	2-Oxoglutarate
AKGm	2-OxoglutarateM
AKP	2-Dehydropantoate
AKPm	2-DehydropantoateM
ALA	L-Alanine
ALAGLY	R-S-Alanylglycine
ALAm	L-AlanineM
ALAV	5-Aminolevulinate
ALAVm	5-AminolevulinateM
ALTRNA	L-Arginyl-tRNA(Arg)
AM6SA	2-Aminomuconate 6-semialdehyde
AMA	L-2-Aminoadipate
AMASA	L-2-Aminoadipate 6-semialdehyde
AMG	Methyl-D-glucoside
AMP	AMP
AMPm	AMPM
AMUCO	2-Aminomuconate
AN	Anthranilate
AONA	8-Amino-7-oxononanoate
APEP	Nalpha-Acetylpeptide
APROA	3-Aminopropanal
APROP	alpha-Aminopropiononitrile

Table A.28. Complete list of metabolites -continued

APRUT	N-Acetylputrescine
APS	Adenylylsulfate
ARAB	D-Arabinose
ARABLAC	D-Arabinono-1,4-lactone
ARG	L-Arginine
ARGSUCC	N-(L-Arginino)succinate
ASER	O-Acetyl-L-serine
ASN	L-Asparagine
ASP	L-Aspartate
ASPERMD	N1-Acetylspermidine
ASPm	L-AspartateM
ASPRM	N1-Acetylspermine
ASPSA	L-Aspartate 4-semialdehyde
ASPTRNA	L-Asparaginyl-tRNA(Asn)
ASPTRNAm	L-Asparaginyl-tRNA(Asn)M
ASUC	N6-(1,2-Dicarboxyethyl)-AMP
AT3P2	Acyldihydroxyacetone phosphate
ATN	Allantoin
ATP	ATP
ATPm	ATPM
ATRNA	tRNA(Arg)
ATRP	P1,P4-Bis(5'-adenosyl) tetraphosphate
ATT	Allantoate
bALA	beta-Alanine
BASP	4-Phospho-L-aspartate
bDG6P	beta-D-Glucose 6-phosphate
bDGLC	beta-D-Glucose
BIO	Biotin
BT	Biotin
C100ACP	Decanoyl-[acp]
C120ACP	Dodecanoyl-[acyl-carrier protein]
C120ACPm	Dodecanoyl-[acyl-carrier protein]M
C140	Myristic acid
C140ACP	Myristoyl-[acyl-carrier protein]
C140ACPm	Myristoyl-[acyl-carrier protein]M
C141ACP	Tetradecenoyl-[acyl-carrier protein]
C141ACPm	Tetradecenoyl-[acyl-carrier protein]M
C160	Palmitate
C160ACP	Hexadecanoyl-[acp]
C160ACPm	Hexadecanoyl-[acp]M
C161	1-Hexadecene
C161ACP	Palmitoyl-[acyl-carrier protein]
C161ACPm	Palmitoyl-[acyl-carrier protein]M
C16A	C16_aldehydes
C180	Stearate
C180ACP	Stearoyl-[acyl-carrier protein]

Table A.28. Complete list of metabolites -continued

C180ACPm	Stearoyl-[acyl-carrier protein]M
C181	1-Octadecene
C181ACP	Oleoyl-[acyl-carrier protein]
C181ACPm	Oleoyl-[acyl-carrier protein]M
C182ACP	Linolenoyl-[acyl-carrier protein]
C182ACPm	Linolenoyl-[acyl-carrier protein]M
CAASP	N-Carbamoyl-L-aspartate
CAIR	1-(5-Phospho-D-ribosyl)-5-amino-4-imidazolecarboxylate
CALH	2-(3-Carboxy-3-aminopropyl)-L-histidine
cAMP	3',5'-Cyclic AMP
CAP	Carbamoyl phosphate
CAR	Carnitine
CARm	CarnitineM
CBHCAP	3-Isopropylmalate
CBHCAPm	3-IsopropylmalateM
cCMP	3',5'-Cyclic CMP
cdAMP	3',5'-Cyclic dAMP
CDP	CDP
CDPCHO	CDPcholine
CDPDG	CDPdiacylglycerol
CDPDGm	CDPdiacylglycerolM
CDPETN	CDPethanolamine
CER2	Ceramide-2
CER3	Ceramide-3
CGLY	Cys-Gly
cGMP	3',5'-Cyclic GMP
CHCOA	6-Carboxyhexanoyl-CoA
CHIT	Chitin
CHITO	Chitosan
CHO	Choline
CHOR	Chorismate
cIMP	3',5'-Cyclic IMP
CIT	Citrate
CITm	CitrateM
CITR	L-Citrulline
CLm	CardiolipinM
CMP	CMP
CMPm	CMPM
CMUSA	2-Amino-3-carboxymuconate semialdehyde
CO2	CO2
CO2m	CO2M
COA	CoA
COAm	CoAM
CPAD5P	1-(2-Carboxyphenylamino)-1-deoxy-D-ribulose 5-phosphate
CPP	Coproporphyrinogen
CTP	CTP

Table A.28. Complete list of metabolites -continued

CTPm	CTPM
CYS	L-Cysteine
CYTD	Cytidine
CYTS	Cytosine
D45PI	1-Phosphatidyl-D-myo-inositol 4,5-bisphosphate
D6PGC	6-Phospho-D-gluconate
D6PGL	D-Glucono-1,5-lactone 6-phosphate
D6RP5P	2,5-Diamino-6-hydroxy-4-(5'-phosphoribosylamino)-pyrimidine
D8RL	6,7-Dimethyl-8-(1-D-ribityl)lumazine
DA	Deoxyadenosine
DADP	dADP
DAGLY	Diacylglycerol
DAMP	dAMP
DANNA	7,8-Diaminononanoate
DAPRP	1,3-Diaminopropane
DATP	dATP
DB4P	L-3,4-Dihydroxy-2-butanone 4-phosphate
DC	Deoxycytidine
DCDP	dCDP
DCMP	dCMP
DCTP	dCTP
DFUC	alpha-D-Fucoside
DG	Deoxyguanosine
DGDP	dGDP
DGMP	dGMP
DGPP	Diacylglycerol pyrophosphate
DGTP	dGTP
DHF	Dihydrofolate
DHFm	DihydrofolateM
DHMVAm	(R)-2,3-dihydroxy-3-methylbutanoateM
DHP	2-Amino-4-hydroxy-6-(D-erythro-1,2,3-trihydroxypropyl)-7,8-dihydropteridine
DHPP	Dihydroneopterin phosphate
DHPT	Dihydropteroate
DHSK	3-Dehydroshikimate
DHSP	Sphinganine 1-phosphate
DHSPH	3-Dehydrosphinganine
DHVALm	(R)-3-Hydroxy-3-methyl-2-oxobutanoateM
DIMGP	D-erythro-1-(Imidazol-4-yl)glycerol 3-phosphate
DIN	Deoxyinosine
DIPEP	Dipeptide
DMPP	Dimethylallyl diphosphate
DMZYMST	4,4-Dimethylzymosterol
DOL	Dolichol
DOLMANP	Dolichyl beta-D-mannosyl phosphate
DOLP	Dolichyl phosphate
DOROA	(S)-Dihydroorotate

Table A.28. Complete list of metabolites -continued

DPCOA	Dephospho-CoA
DPCOAm	Dephospho-CoAM
DPTH	2-[3-Carboxy-3-(methylammonio)propyl]-L-histidine
DQT	3-Dehydroquinate
DR1P	Deoxy-ribose 1-phosphate
DR5P	2-Deoxy-D-ribose 5-phosphate
DRIB	Deoxyribose
DSAM	S-Adenosylmethioninamine
DT	Thymidine
DTB	Dethiobiotin
DTBm	DethiobiotinM
DTDP	dTDP
DTMP	dTMP
DTP	1-Deoxy-d-threo-2-pentulose
DTTP	dTTP
DU	Deoxyuridine
DUDP	dUDP
DUMP	dUMP
DUTP	dUTP
E4P	D-Erythrose 4-phosphate
EPM	Epimelibiose
EPST	Episterol
ERGOST	Ergosterol
ERTEOL	Ergosta-5,7,22,24(28)-tetraenol
ERTROL	Ergosta-5,7,24(28)-trienol
ETH	Ethanol
ETHm	EthanolM
ETHM	Ethanolamine
F1P	D-Fructose 1-phosphate
F26P	D-Fructose 2,6-bisphosphate
F6P	beta-D-Fructose 6-phosphate
FAD	FAD
FADH2m	FADH2M
FADm	FADM
FALD	Formaldehyde
FDP	beta-D-Fructose 1,6-bisphosphate
FERIm	Ferricytochrome cM
FEROm	Ferrocytochrome cM
FEST	Fecosterol
FGAM	2-(Formamido)-N1-(5'-phosphoribosyl)acetamidine
FGAR	5'-Phosphoribosyl-N-formylglycinamide
FGT	S-Formylglutathione
FKYN	L-Formylkynurenine
FMN	FMN
FMNm	FMNM
FMRNAm	N-Formylmethionyl-tRNAM

Table A.28. Complete list of metabolites -continued

FOR	Formate
FORm	FormateM
FPP	trans,trans-Farnesyl diphosphate
FRU	D-Fructose
FTHF	10-Formyltetrahydrofolate
FTHFm	10-FormyltetrahydrofolateM
FUACAC	4-Fumarylacetoacetate
FUC	beta-D-Fucose
FUM	Fumarate
FUMm	FumarateM
G1P	D-Glucose 1-phosphate
G6P	alpha-D-Glucose 6-phosphate
GA1P	D-Glucosamine 1-phosphate
GA6P	D-Glucosamine 6-phosphate
GABA	4-Aminobutanoate
GABAL	4-Aminobutyraldehyde
GABALm	4-AminobutyraldehydeM
GABAm	4-AminobutanoateM
GAL1P	D-Galactose 1-phosphate
GAR	5'-Phosphoribosylglycinamide
GBAD	4-Guanidino-butanamide
GBAT	4-Guanidino-butanoate
GC	gamma-L-Glutamyl-L-cysteine
GDP	GDP
GDPm	GDPM
GDPMAN	GDPmannose
GGL	Galactosylglycerol
GL	Glycerol
GL3P	sn-Glycerol 3-phosphate
GL3Pm	sn-Glycerol 3-phosphateM
GLAC	D-Galactose
GLACL	1-alpha-D-Galactosyl-myo-inositol
GLAL	Glycolaldehyde
GLAM	Glucosamine
GLC	alpha-D-Glucose
GLN	L-Glutamine
GLP	Glycylpeptide
GLT	L-Glucitol
GLU	L-Glutamate
GLUGSAL	L-Glutamate 5-semialdehyde
GLUGSALm	L-Glutamate 5-semialdehydeM
GLUm	GlutamateM
GLUP	alpha-D-Glutamyl phosphate
GLX	Glyoxylate
GLY	Glycine
GLYCOGEN	Glycogen

Table A.28. Complete list of metabolites -continued

GLYm	GlycineM
GLYN	Glycerone
GMP	GMP
GN	Guanine
GNm	GuanineM
GPP	Geranyl diphosphate
GSN	Guanosine
GSNm	GuanosineM
GTP	GTP
GTPm	GTPM
GTRNA	L-Glutamyl-tRNA(Glu)
GTRNAm	L-Glutamyl-tRNA(Glu)M
GTRP	P1,P4-Bis(5'-guanosyl) tetraphosphate
H2O2	H2O2
H2S	Hydrogen sulfide
H2SO3	Sulfite
H3MCOA	(S)-3-Hydroxy-3-methylglutaryl-CoA
H3MCOAm	(S)-3-Hydroxy-3-methylglutaryl-CoAM
HACNm	But-1-ene-1,2,4-tricarboxylateM
HACOA	(3S)-3-Hydroxyacyl-CoA
HAN	3-Hydroxyanthranilate
HBA	4-Hydroxy-benzyl alcohol
HCIT	2-Hydroxybutane-1,2,4-tricarboxylate
HCITm	2-Hydroxybutane-1,2,4-tricarboxylateM
HCYS	Homocysteine
HEXT	H+EXT
HHTRNA	L-Histidyl-tRNA(His)
HICITm	HomoisocitrateM
HIS	L-Histidine
HISOL	L-Histidinol
HISOLP	L-Histidinol phosphate
HKYN	3-Hydroxykynurenine
Hm	H+M
HMB	Hydroxymethylbilane
HOMOGEN	Homogentisate
HPRO	trans-4-Hydroxy-L-proline
HSER	L-Homoserine
HTRNA	tRNA(His)
HYXN	Hypoxanthine
IAC	Indole-3-acetate
IAD	Indole-3-acetamide
ICIT	Isocitrate
ICITm	IsocitrateM
IDP	IDP
IDPm	IDPM
IGP	Indoleglycerol phosphate

Table A.28. Complete list of metabolites -continued

IGST	4,4-Dimethylcholesta-8,14,24-trienol
IIMZYMST	Intermediate_Methylzymosterol_II
IIZYMST	Intermediate_Zymosterol_II
ILE	L-Isoleucine
ILEm	L-IsoleucineM
IMACP	3-(Imidazol-4-yl)-2-oxopropyl phosphate
IMP	IMP
IMZYMST	Intermediate_Methylzymosterol_I
INAC	Indoleacetate
INS	Inosine
IPC	Inositol phosphorylceramide
IPPMAL	2-Isopropylmalate
IPPMALm	2-IsopropylmalateM
IPPP	Isopentenyl diphosphate
ISUCC	a-Iminosuccinate
ITCCOAm	Itaconyl-CoAM
ITCm	ItaconateM
ITP	ITP
ITPm	ITPM
IZYMST	Intermediate_Zymosterol_I
K	Potassium
KYN	L-Kynurenine
LAC	(R)-Lactate
LACALm	(S)-LactaldehydeM
LACm	(R)-LactateM
LCCA	a Long-chain carboxylic acid
LEU	L-Leucine
LEUm	L-LeucineM
LGT	(R)-S-Lactoylglutathione
LGTm	(R)-S-LactoylglutathioneM
LIPOm	LipoamideM
LLACm	(S)-LactateM
LLCT	L-Cystathionine
LLTRNA	L-lysyl-tRNA(Lys)
LLTRNAm	L-lysyl-tRNA(Lys)M
LNST	Lanosterol
LTRNA	tRNA(Lys)
LTRNAm	tRNA(Lys)M
LYS	L-Lysine
LYSm	L-LysineM
MACOA	2-Methylprop-2-enoyl-CoA
MAL	Malate
MALACP	Malonyl-[acyl-carrier protein]
MALACPm	Malonyl-[acyl-carrier protein]M
MALCOA	Malonyl-CoA
MALm	MalateM

Table A.28. Complete list of metabolites -continued

MALT	Malonate
MALTm	MalonateM
MAN	alpha-D-Mannose
MAN1P	alpha-D-Mannose 1-phosphate
MAN2PD	beta-D-Mannosyldiacetylchitobiosyldiphosphodolichol
MAN6P	D-Mannose 6-phosphate
MANNAN	Mannan
MELI	Melibiose
MELT	Melibiitol
MET	L-Methionine
METH	Methanethiol
METHF	5,10-Methenyltetrahydrofolate
METHFm	5,10-MethenyltetrahydrofolateM
METTHF	5,10-Methylenetetrahydrofolate
METTHFm	5,10-MethylenetetrahydrofolateM
MHIS	N(pai)-Methyl-L-histidine
MI	myo-Inositol
MI1P	1L-myo-Inositol 1-phosphate
MIP2C	Inositol-mannose-P-inositol-P-ceramide
MIPC	Mannose-inositol-P-ceramide
MLT	Maltose
MMET	S-Methylmethionine
MNT	D-Mannitol
MNT6P	D-Mannitol 1-phosphate
MTHF	5-Methyltetrahydrofolate
MTHFm	5-MethyltetrahydrofolateM
MTHGXL	Methylglyoxal
MTHN	Methane
MTHNm	MethaneM
MTHPTGLU	5-Methyltetrahydropteroyltri-L-glutamate
MTRNAm	L-Methionyl-tRNAM
MVL	(R)-Mevalonate
MVLm	(R)-MevalonateM
MYOI	myo-Inositol
MZYMST	4-Methylzymsterol
N4HBZ	3-Nonaprenyl-4-hydroxybenzoate
NA	Sodium
NAAD	Deamino-NAD+
NAADm	Deamino-NAD+M
NAC	Nicotinate
NACm	NicotinateM
NAD	NAD+
NADH	NADH
NADHm	NADHM
NADm	NAD+M
NADP	NADP+

Table A.28. Complete list of metabolites -continued

NADPH	NADPH
NADPHm	NADPHM
NADPm	NADP+M
NAG	N-Acetylglucosamine
NAGA1P	N-Acetyl-D-glucosamine 1-phosphate
NAGA6P	N-Acetyl-D-glucosamine 6-phosphate
NAGLUm	N-Acetyl-L-glutamateM
NAGLUPm	N-Acetyl-L-glutamate 5-phosphateM
NAGLUSm	N-Acetyl-L-glutamate 5-semialdehydeM
NAM	Nicotinamide
NAMm	NicotinamideM
NAMN	Nicotinate D-ribonucleotide
NAMNm	Nicotinate D-ribonucleotideM
NAORNm	N2-Acetyl-L-ornithineM
NH3	NH3
NH3m	NH3M
NPP	all-trans-Nonaprenyl diphosphate
NPRAN	N-(5-Phospho-D-ribosyl)anthranilate
O2	Oxygen
O2m	OxygenM
OA	Oxaloacetate
OACOA	3-Oxoacyl-CoA
OAHSER	O-Acetyl-L-homoserine
OAm	OxaloacetateM
OBUT	2-Oxobutanoate
OBUTm	2-OxobutanoateM
OFP	Oxidized flavoprotein
OGT	Oxidized glutathione
OHB	2-Oxo-3-hydroxy-4-phosphobutanoate
OHm	HO-M
OICAP	3-Carboxy-4-methyl-2-oxopentanoate
OICAPm	3-Carboxy-4-methyl-2-oxopentanoateM
OIVAL	(R)-2-Oxoisovalerate
OIVALm	(R)-2-OxoisovalerateM
OMP	Orotidine 5'-phosphate
OMVAL	3-Methyl-2-oxobutanoate
OMVALm	3-Methyl-2-oxobutanoateM
OPEP	Oligopeptide
ORN	L-Ornithine
ORNm	L-OrnithineM
OROA	Orotate
OSLHSER	O-Succinyl-L-homoserine
OSUC	Oxalosuccinate
OSUCm	OxalosuccinateM
OTHIO	Oxidized thioredoxin
OTHIOm	Oxidized thioredoxinM

Table A.28. Complete list of metabolites -continued

OXA	Oxaloglutarate
OXAm	OxaloglutarateM
P5C	(S)-1-Pyrroline-5-carboxylate
P5Cm	(S)-1-Pyrroline-5-carboxylateM
P5P	Pyridoxine phosphate
PA	Phosphatidate
PABA	4-Aminobenzoate
PAC	Phenylacetic acid
PAD	2-Phenylacetamide
PALCOA	Palmitoyl-CoA
PAm	PhosphatidateM
PANT	(R)-Pantoate
PANTm	(R)-PantoateM
PAP	Adenosine 3',5'-bisphosphate
PAPS	3'-Phosphoadenylylsulfate
PBG	Porphobilinogen
PC	Phosphatidylcholine
PC2	Sirohydrochlorin
PCHO	Choline phosphate
PDLA	Pyridoxamine
PDLA5P	Pyridoxamine phosphate
PDME	Phosphatidyl-N-dimethylethanolamine
PE	Phosphatidylethanolamine
PEm	PhosphatidylethanolamineM
PEP	Phosphoenolpyruvate
PEPD	Peptide
PEPm	PhosphoenolpyruvateM
PEPT	Peptide
PETHM	Ethanolamine phosphate
PGm	PhosphatidylglycerolM
PGPm	PhosphatidylglycerophosphateM
PHC	L-1-Pyrroline-3-hydroxy-5-carboxylate
PHE	L-Phenylalanine
PHEN	Prephenate
PHP	3-Phosphonooxypyruvate
PHPYR	Phenylpyruvate
PHSER	O-Phospho-L-homoserine
PHSP	Phytosphingosine 1-phosphate
PHT	O-Phospho-4-hydroxy-L-threonine
PI	Orthophosphate
PIm	OrthophosphateM
PIME	Pimelic Acid
PINS	1-Phosphatidyl-D-myo-inositol
PINS4P	1-Phosphatidyl-1D-myo-inositol 4-phosphate
PINSP	1-Phosphatidyl-1D-myo-inositol 3-phosphate
PL	Pyridoxal

Table A.28. Complete list of metabolites -continued

PL5P	Pyridoxal phosphate
PMME	Phosphatidyl-N-methylethanolamine
PMVL	(R)-5-Phosphomevalonate
PNTO	(R)-Pantothenate
PPHG	Protoporphyrinogen IX
PPHGm	Protoporphyrinogen IXM
PPI	Pyrophosphate
PPIm	PyrophosphateM
PPIXm	ProtoporphyrinM
PPMAL	2-Isopropylmaleate
PPMVL	(R)-5-Diphosphomevalonate
PRAM	5-Phosphoribosylamine
PRBAMP	N1-(5-Phospho-D-ribosyl)-AMP
PRBATP	N1-(5-Phospho-D-ribosyl)-ATP
PRFICA	1-(5'-Phosphoribosyl)-5-formamido-4-imidazolecarboxamide
PRFP	5-(5-Phospho-D-ribosylaminoformimino)-1-(5-phosphoribosyl)-imidazole-4-carboxamide
PRLP	N-(5'-Phospho-D-1'-ribulosylformimino)-5-amino-1-(5"-phospho-D-ribosyl)-4-imidazolecarboxamide
PRO	L-Proline
PROm	L-ProlineM
PRPP	5-Phospho-alpha-D-ribose 1-diphosphate
PRPPm	5-Phospho-alpha-D-ribose 1-diphosphateM
PS	Phosphatidylserine
PSm	PhosphatidylserineM
PSPH	Phytosphingosine
PTHm	HemeM
PTRSC	Putrescine
PURI5P	Pseudouridine 5'-phosphate
PYR	Pyruvate
PYRDX	Pyridoxine
PYRm	PyruvateM
QA	Pyridine-2,3-dicarboxylate
QAm	Pyridine-2,3-dicarboxylateM
QH2m	UbiquinolM
Qm	Ubiquinone-9M
R1P	D-Ribose 1-phosphate
R5P	D-Ribose 5-phosphate
RAF	Raffinose
RFP	Reduced flavoprotein
RGT	Glutathione
RGTm	GlutathioneM
RIB	D-Ribose
RIBFLAV	Riboflavin
RIBFLAVm	RiboflavinM
RIPm	alpha-D-Ribose 1-phosphateM
RL5P	D-Ribulose 5-phosphate
RMN	D-Rhamnose

Table A.28. Complete list of metabolites -continued

RTHIO	Reduced thioredoxin
RTHIOm	Reduced thioredoxinM
S17P	Sedoheptulose 1,7-bisphosphate
S23E	(S)-2,3-Epoxysqualene
S7P	Sedoheptulose 7-phosphate
SACP	N6-(L-1,3-Dicarboxypropyl)-L-lysine
SAH	S-Adenosyl-L-homocysteine
SAHm	S-Adenosyl-L-homocysteineM
SAICAR	1-(5'-Phosphoribosyl)-5-amino-4-(N-succinocarboxamide)-imidazole
SAM	S-Adenosyl-L-methionine
SAMm	S-Adenosyl-L-methionineM
SAMOB	S-Adenosyl-4-methylthio-2-oxobutanoate
SAPm	S-AminomethyldihydrolipoylproteinM
SER	L-Serine
SERm	L-SerineM
SLF	Sulfate
SLFm	SulfateM
SME	Shikimate
SME5P	Shikimate 3-phosphate
SOR	Sorbose
SOT	D-Sorbitol
SPH	Sphinganine
SPRM	Spermine
SPRMD	Spermidine
SQL	Squalene
SUC	Sucrose
SUCC	Succinate
SUCCm	SuccinateM
SUCCOAm	Succinyl-CoAM
SUCCSAL	Succinate semialdehyde
T3P1	D-Glyceraldehyde 3-phosphate
T3P2	Glycerone phosphate
T3P2m	Glycerone phosphateM
TAG16P	D-Tagatose 1,6-bisphosphate
TAG6P	D-Tagatose 6-phosphate
TAGLY	Triacylglycerol
TCOA	Tetradecanoyl-CoA
TGLP	N-Tetradecanoylglycylpeptide
THF	Tetrahydrofolate
THFG	Tetrahydrofolyl-[Glu](n)
THFm	TetrahydrofolateM
THIAMIN	Thiamin
THMP	Thiamin monophosphate
THPTGLU	Tetrahydropteroyltri-L-glutamate
THR	L-Threonine
THRm	L-ThreonineM

Table A.28. Complete list of metabolites -continued

THY	Thymine
THZ	5-(2-Hydroxyethyl)-4-methylthiazole
THZP	4-Methyl-5-(2-phosphoethyl)-thiazole
TPI	D-myo-inositol 1,4,5-trisphosphate
TPP	Thiamin diphosphate
TPPP	Thiamin triphosphate
TRE	alpha,alpha-Trehalose
TRE6P	alpha,alpha'-Trehalose 6-phosphate
TRNA	tRNA
TRNAm	tRNAM
TRP	L-Tryptophan
TRPm	L-TryptophanM
TRPTRNAm	L-Tryptophanyl-tRNA(Trp)M
TYR	L-Tyrosine
UDP	UDP
UDPG	UDPglucose
UDPGAL	UDP-D-galactose
UDPNAG	UDP-N-acetyl-D-galactosamine
UDPP	Undecaprenyl diphosphate
UGC	(-)-Ureidoglycolate
UMP	UMP
UPRG	Uroporphyrinogen III
URA	Uracil
UREA	Urea
UREAC	Urea-1-carboxylate
URI	Uridine
UTP	UTP
VAL	L-Valine
X5P	D-Xylose-5-phosphate
XAN	Xanthine
XMP	Xanthosine 5'-phosphate
XTSINE	Xanthosine
XUL	D-Xylulose
XYL	D-Xylose
ZYMST	Zymosterol

A.29. Complete list of reactions

RF	**GENE**	**REACTION**
# CARBOHYDRATE METABOLISM		
# GLYCOLYSIS/GLUCONEOGENESIS		
YCL040W	*GLK1*	GLC + ATP -> G6P + ADP
YCL040W	*GLK1*	MAN + ATP -> MAN6P + ADP
YCL040W	*GLK1*	bDGLC + ATP -> bDG6P + ADP
YFR053C	*HXK1*	bDGLC + ATP -> G6P + ADP
YFR053C	*HXK1*	GLC + ATP -> G6P + ADP

Table A.29. Complete list of reactions -continued

YFR053C	*HXK1*	MAN + ATP -> MAN6P + ADP
YFR053C	*HXK1*	ATP + FRU -> ADP + F6P
YGL253W	*HXK2*	bDGLC + ATP -> G6P + ADP
YGL253W	*HXK2*	GLC + ATP -> G6P + ADP
YGL253W	*HXK2*	MAN + ATP -> MAN6P + ADP
YGL253W	*HXK2*	ATP + FRU -> ADP + F6P
YBR196C	*PGI1*	G6P <-> F6P
YBR196C	*PGI1*	G6P <-> bDG6P
YBR196C	*PGI1*	bDG6P <-> F6P
YMR205C	*PFK2*	F6P + ATP -> FDP + ADP
YGR240C	*PFK1*	F6P + ATP -> FDP + ADP
YGR240C	*PFK1*	ATP + TAG6P -> ADP + TAG16P
YGR240C	*PFK1*	ATP + S7P -> ADP + S17P
YKL060C	*FBA1*	FDP <-> T3P2 + T3P1
YDR050C	*TPI1*	T3P2 <-> T3P1
YJL052W	*TDH1*	T3P1 + PI + NAD <-> NADH + 13PDG
YJR009C	*TDH2*	T3P1 + PI + NAD <-> NADH + 13PDG
YGR192C	*TDH3*	T3P1 + PI + NAD <-> NADH + 13PDG
YCR012W	*PGK1*	13PDG + ADP <-> 3PG + ATP
YKL152C	*GPM1*	13PDG <-> 23PDG
YKL152C	*GPM1*	3PG <-> 2PG
YDL021W	*GPM2*	3PG <-> 2PG
YOL056W	*GPM3*	3PG <-> 2PG
YGR254W	*ENO1*	2PG <-> PEP
YHR174W	*ENO2*	2PG <-> PEP
YMR323W	*ERR1*	2PG <-> PEP
YPL281C	*ERR2*	2PG <-> PEP
YOR393W	*ERR1*	2PG <-> PEP
YAL038W	*CDC19*	PEP + ADP -> PYR + ATP
YOR347C	*PYK2*	PEP + ADP -> PYR + ATP
YER178W	*PDA1*	PYRm + COAm + NADm -> NADHm + CO2m + ACCOAm
YBR221C	*PDB1*	
YNL071W	*LAT1*	
# CITRATE CYCLE (TCA CYCLE)		
YNR001C	*CIT1*	ACCOAm + OAm -> COAm + CITm
YCR005C	*CIT2*	ACCOA + OA -> COA + CIT
YPR001W	*CIT3*	ACCOAm + OAm -> COAm + CITm
YLR304C	*ACO1*	CITm <-> ICITm
YJL200C	*YJL200C*	CITm <-> ICITm
YNL037C	*IDH1*	ICITm + NADm -> CO2m + NADHm + AKGm
YOR136W	*IDH2*	
YDL066W	*IDP1*	ICITm + NADPm -> NADPHm + OSUCm
YLR174W	*IDP2*	ICIT + NADP -> NADPH + OSUC
YNL009W	*IDP3*	ICIT + NADP -> NADPH + OSUC

Table A.29. Complete list of reactions -continued

YDL066W	*IDP1*	OSUCm -> CO2m + AKGm
YLR174W	*IDP2*	OSUC -> CO2 + AKG
YNL009W	*IDP3*	OSUC -> CO2 + AKG
YIL125W	*KGD1*	AKGm + NADm + COAm -> CO2m + NADHm + SUCCOAm
YDR148C	*KGD2*	
YGR244C	*LSC2*	ATPm + SUCCm + COAm <-> ADPm + PIm + SUCCOAm
YOR142W	*LSC1*	ATPm + ITCm + COAm <-> ADPm + PIm + ITCCOAm
# ELECTRON TRANSPORT SYSTEM, COMPLEX II		
YKL141W	*SDH3*	SUCCm + FADm <-> FUMm + FADH2m
YKL148C	*SDH1*	
YLL041C	*SDH2*	
YDR178W	*SDH4*	
YLR164W	*YLR164W*	
YMR118C	*YMR118C*	
YJL045W	*YJL045W*	
YEL047C	*YEL047C*	FADH2m + FUM -> SUCC + FADm
YJR051W	*OSM1*	FADH2m + FUMm -> SUCCm + FADm
YPL262W	*FUM1*	FUMm <-> MALm
YPL262W	*FUM1*	FUM <-> MAL
YKL085W	*MDH1*	MALm + NADm <-> NADHm + OAm
YDL078C	*MDH3*	MAL + NAD <-> NADH + OA
YOL126C	*MDH2*	MAL + NAD <-> NADH + OA
# ANAPLEROTIC REACTIONS		
YER065C	*ICL1*	ICIT -> GLX + SUCC
YPR006C	*ICL2*	ICIT -> GLX + SUCC
YIR031C	*DAL7*	ACCOA + GLX -> COA + MAL
YNL117W	*MLS1*	ACCOA + GLX -> COA + MAL
YKR097W	*PCK1*	OA + ATP -> PEP + CO2 + ADP
YLR377C	*FBP1*	FDP -> F6P + PI
YGL062W	*PYC1*	PYR + ATP + CO2 -> ADP + OA + PI
YBR218C	*PYC2*	PYR + ATP + CO2 -> ADP + OA + PI
YKL029C	*MAE1*	MALm + NADPm -> CO2m + NADPHm + PYRm
# PENTOSE PHOSPHATE CYCLE		
YNL241C	*ZWF1*	G6P + NADP <-> D6PGL + NADPH
YNR034W	*SOL1*	D6PGL -> D6PGC
YCR073W-A	*SOL2*	D6PGL -> D6PGC
YHR163W	*SOL3*	D6PGL -> D6PGC
YGR248W	*SOL4*	D6PGL -> D6PGC
YGR256W	*GND2*	D6PGC + NADP -> NADPH + CO2 + RL5P
YHR183W	*GND1*	D6PGC + NADP -> NADPH + CO2 + RL5P
YJL121C	*RPE1*	RL5P <-> X5P
YOR095C	*RKI1*	RL5P <-> R5P

Table A.29. Complete list of reactions -continued

YBR117C	*TKL2*	R5P + X5P <-> T3P1 + S7P
YBR117C	*TKL2*	X5P + E4P <-> F6P + T3P1
YPR074C	*TKL1*	R5P + X5P <-> T3P1 + S7P
YPR074C	*TKL1*	X5P + E4P <-> F6P + T3P1
YLR354C	*TAL1*	T3P1 + S7P <-> E4P + F6P
YGR043C	*YGR043C*	T3P1 + S7P <-> E4P + F6P
YCR036W	*RBK1*	RIB + ATP -> R5P + ADP
YCR036W	*RBK1*	DRIB + ATP -> DR5P + ADP
YKL127W	*PGM1*	R1P <-> R5P
YKL127W	*PGM1*	G1P <-> G6P
YMR105C	*PGM2*	R1P <-> R5P
YMR105C	*PGM2*	G1P <-> G6P
# MANNOSE		
YER003C	*PMI40*	MAN6P <-> F6P
YFL045C	*SEC53*	MAN6P <-> MAN1P
YDL055C	*PSA1*	GTP + MAN1P -> PPI + GDPMAN
# FRUCTOSE		
YIL107C	*PFK26*	ATP + F6P -> ADP + F26P
YOL136C	*PFK27*	ATP + F6P -> ADP + F26P
YJL155C	*FBP26*	F26P -> F6P + PI
*U1_*	*U1_*	F1P + ATP -> FDP + ADP
# SORBOSE		
YJR159W	*SOR1*	SOT + NAD -> FRU + NADH
# GALACTOSE METABOLISM		
YBR020W	*GAL1*	GLAC + ATP -> GAL1P + ADP
YBR018C	*GAL7*	UTP + GAL1P <-> PPI + UDPGAL
YBR019C	*GAL10*	UDPGAL <-> UDPG
YHL012W	*YHL012W*	G1P + UTP <-> UDPG + PPI
YKL035W	*UGP1*	G1P + UTP <-> UDPG + PPI
YBR184W	*YBR184W*	MELI -> GLC + GLAC
YBR184W	*YBR184W*	DFUC -> GLC + GLAC
YBR184W	*YBR184W*	RAF -> GLAC + SUC
YBR184W	*YBR184W*	GLACL <-> MYOI + GLAC
YBR184W	*YBR184W*	EPM <-> MAN + GLAC
YBR184W	*YBR184W*	GGL <-> GL + GLAC
YBR184W	*YBR184W*	MELT <-> SOT + GLAC
YBR299W	*MAL32*	MLT -> 2 GLC
YGR287C	*YGR287C*	MLT -> 2 GLC
YGR292W	*MAL12*	MLT -> 2 GLC
YIL172C	*YIL172C*	MLT -> 2 GLC
YJL216C	*YJL216C*	MLT -> 2 GLC
YJL221C	*FSP2*	MLT -> 2 GLC
YJL221C	*FSP2*	6DGLC -> GLAC + GLC
YBR018C	*GAL7*	UDPG + GAL1P <-> G1P + UDPGAL
# TREHALOSE		
YBR126C	*TPS1*	UDPG + G6P -> UDP + TRE6P

Table A.29. Complete list of reactions -continued

YML100W	*TSL1*	UDPG + G6P -> UDP + TRE6P
YMR261C	*TPS3*	UDPG + G6P -> UDP + TRE6P
YDR074W	*TPS2*	TRE6P -> TRE + PI
YPR026W	*ATH1*	TRE -> 2 GLC
YBR001C	*NTH2*	TRE -> 2 GLC
YDR001C	*NTH1*	TRE -> 2 GLC
# GLYCOGEN METABOLISM (SUCOROSE AND SUGAR METABOLISM)		
YEL011W	*GLC3*	GLYCOGEN + PI -> G1P
YPR160W	*GPH1*	GLYCOGEN + PI -> G1P
YFR015C	*GSY1*	UDPG -> UDP + GLYCOGEN
YLR258W	*GSY2*	UDPG -> UDP + GLYCOGEN
# PYRUVATE METABOLISM		
YAL054C	*ACS1*	ATP + AC + COA -> AMP + PPI + ACCOA
YLR153C	*ACS2*	ATP + AC + COA -> AMP + PPI + ACCOA
YDL168W	*SFA1*	FALD + RGT + NAD <-> FGT + NADH
YJL068C	*YJL068C*	FGT <-> RGT + FOR
YGR087C	*PDC6*	PYR -> CO2 + ACAL
YLR134W	*PDC5*	PYR -> CO2 + ACAL
YLR044C	*PDC1*	PYR -> CO2 + ACAL
YBL015W	*ACH1*	ACCOA -> COA + AC
YDL131W	*LYS21*	ACCOA + AKG -> HCIT + COA
YDL182W	*LYS20*	ACCOA + AKG -> HCIT + COA
YDL182W	*LYS20*	ACCOAm + AKGm -> HCITm + COAm
YGL256W	*ADH4*	ETH + NAD <-> ACAL + NADH
YMR083W	*ADH3*	ETHm + NADm <-> ACALm + NADHm
YMR303C	*ADH2*	ETH + NAD <-> ACAL + NADH
YBR145W	*ADH5*	ETH + NAD <-> ACAL + NADH
YOL086C	*ADH1*	ETH + NAD <-> ACAL + NADH
YDL168W	*SFA1*	ETH + NAD <-> ACAL + NADH
# GLYOXYLATE AND DICARBOXYLATE METABOLISM		
# GLYOXAL PATHWAY		
YML004C	*GLO1*	RGT + MTHGXL <-> LGT
YDR272W	*GLO2*	LGT -> RGT + LAC
YOR040W	*GLO4*	LGTm -> RGTm + LACm
# ENERGY METABOLISM		
# OXIDATIVE PHOSPHORYLATION		
YBR011C	*IPP1*	PPI -> 2 PI
YMR267W	*PPA2*	PPIm -> 2 PIm
*U2_*	*U2_*	FOR + Qm -> QH2m + CO2 +2 HEXT
YML120C	*NDI1*	NADHm + Qm -> QH2m + NADm
YDL085W	*NDH2*	NADH + Qm -> QH2m + NAD
YMR145C	*NDH1*	NADH + Qm -> QH2m + NAD
YHR042W	*NCP1*	NADPH + 2 FERIm -> NADP + 2 FEROm

Table A.29. Complete list of reactions -continued

YKL141W	*SDH3*	FADH2m + Qm <-> FADm + QH2m
YKL148C	*SDH1*	
YLL041C	*SDH2*	
YDR178W	*SDH4*	
# ELECTRON TRANSPORT SYSTEM, COMPLEX III		
YEL024W	*RIP1*	QH2m + 2 FERIm + 1.5 Hm -> Qm + 2 FEROm
Q0105	*CYTB*	
YOR065W	*CYT1*	
YBL045C	*COR1*	
YPR191W	*QCR1*	
YPR191W	*QCR2*	
YFR033C	*QCR6*	
YDR529C	*QCR7*	
YJL166W	*QCR8*	
YGR183C	*QCR9*	
YHR001W-A	*QCR10*	
# ELECTRON TRANSPORT SYSTEM, COMPLEX IV		
Q0045	*COX1*	4 FEROm + O2m + 6 Hm -> 4 FERIm
Q0250	*COX2*	
Q0275	*COX3*	
YDL067C	*COX9*	
YGL187C	*COX4*	
YGL191W	*COX13*	
YHR051W	*COX6*	
YIL111W	*COX5B*	
YLR038C	*COX12*	
YLR395C	*COX8*	
YMR256C	*COX7*	
YNL052W	*COX5A*	
# ATP SYNTHASE		
YBL099W	*ATP1*	ADPm + PIm -> ATPm + 3 Hm
YPL271W	*ATP15*	
YDL004W	*ATP16*	
Q0085	*ATP6*	
YBR039W	*ATP3*	
YBR127C	*VMA2*	
YPL078C	*ATP4*	
YDR298C	*ATP5*	
YDR377W	*ATP17*	
YJR121W	*ATP2*	
YKL016C	*ATP7*	
YLR295C	*ATP14*	
Q0080	*ATP8*	
Q0130	*ATP9*	

Table A.29. Complete list of reactions -continued

YOL077W-A	*ATP19*	
YPR020W	*ATP20*	
YML054C	*CYB2*	2 FERIm + LLACm -> PYRm + 2 FEROm
YDL174C	*DLD1*	2 FERIm + LACm -> PYRm + 2 FEROm
# METHANE METABOLISM		
YPL275W	*YPL275W*	FOR + NAD -> CO2 + NADH
YPL276W	*YPL276W*	FOR + NAD -> CO2 + NADH
YOR388C	*FDH1*	FOR + NAD -> CO2 + NADH
# NITROGEN METABOLISM		
YBR208C	*DUR1*	ATP + UREA + CO2 <-> ADP + PI + UREAC
YBR208C	*DUR1*	UREAC -> 2 NH3 + 2 CO2
YJL126W	*NIT2*	ACNL -> INAC + NH3
# SULFUR METABOLISM		
YJR137C	*ECM17*	H2SO3 + 3 NADPH <-> H2S + 3 NADP
# LIPID METABOLISM		
# FATTY ACID BIOSYNTHESIS		
YER015W	*FAA2*	ATP + LCCA + COA <-> AMP + PPI + ACOA
YIL009W	*FAA3*	ATP + LCCA + COA <-> AMP + PPI + ACOA
YOR317W	*FAA1*	ATP + LCCA + COA <-> AMP + PPI + ACOA
YMR246W	*FAA4*	ATP + LCCA + COA <-> AMP + PPI + ACOA
YKR009C	*FOX2*	HACOA + NAD <-> OACOA + NADH
YIL160C	*POT1*	OACOA + COA -> ACOA + ACCOA
YPL028W	*ERG10*	2 ACCOA <-> COA + AACCOA
YPL028W	*ERG10*	2 ACCOAm <-> COAm + AACCOAm
# FATTY ACIDS METABOLISM		
# MITOCHONDRIAL TYPE II FATTY ACID SYNTHASE		
YKL192C	*ACP1*	NADHm + Qm -> NADm + QH2m
YER061C	*CEM1*	
YOR221C	*MCT1*	
YKL055C	*OAR1*	
YKL192C/YER061C/YOR221C/YKL055C	*ACP1/CEM1/ MCT1/OAR1*	ACACPm + 4 MALACPm + 8 NADPHm -> 8 NADPm + C100ACPm + 4 CO2m + 4 ACPm
YKL192C/YER061C/YOR221C/YKL055C	*ACP1/CEM1/ MCT1/OAR1*	ACACPm + 5 MALACPm + 10 NADPHm -> 10 NADPm + C120ACPm + 5 CO2m + 5 ACPm
YKL192C/YER061C/YOR221C/YKL055C	*ACP1/CEM1/ MCT1/OAR1*	ACACPm + 6 MALACPm + 12 NADPHm -> 12 NADPm + C140ACPm + 6 CO2m + 6 ACPm
YKL192C/YER061C/YOR221C/YKL055C	*ACP1/CEM1/ MCT1/OAR1*	ACACPm + 6 MALACPm + 11 NADPHm -> 11 NADPm + C141ACPm+ 6 CO2m + 6 ACPm
YKL192C/YER061C/YOR221C/YKL055C	*ACP1/CEM1/ MCT1/OAR1*	ACACPm + 7 MALACPm + 14 NADPHm -> 14 NADPm + C160ACPm + 7 CO2m + 7 ACPm
YKL192C/YER061C/YOR221C/YKL055C	*ACP1/CEM1/ MCT1/OAR1*	ACACPm + 7 MALACPm + 13 NADPHm -> 13 NADPm + C161ACPm + 7 CO2m + 7 ACPm
YKL192C/YER061C/YOR221C/YKL055C	*ACP1/CEM1/ MCT1/OAR1*	ACACPm + 8 MALACPm + 16 NADPHm -> 16 NADPm + C180ACPm + 8 CO2m + 8 ACPm

Table A.29. Complete list of reactions -continued

YKL192C/YER061C/YOR221C/YKL055C	*ACP1/CEM1/ MCT1/OAR1*	ACACPm + 8 MALACPm + 15 NADPHm -> 15 NADPm + C181ACPm + 8 CO2m + 8 ACPm
YKL192C/YER061C/YOR221C/YKL055C	*ACP1/CEM1/ MCT1/OAR1*	ACACPm + 8 MALACPm + 14 NADPHm -> 14 NADPm + C182ACPm + 8 CO2m + 8 ACPm
# CYTOSOLIC FATTY ACID SYNTHESIS		
YNR016C	*ACC1*	ACCOA + ATP + CO2 <-> MALCOA + ADP + PI
YKL182W	*FAS1*	MALCOA + ACP <-> MALACP + COA
YPL231W	*FAS2*	
YKL182W	*FAS1*	ACCOA + ACP <-> ACACP + COA
YER061C	*CEM1*	MALACPm + ACACPm -> ACPm + CO2m + 3OACPm
YGR037C/YNR016C/YKL182W/YPL231W	*ACB1/ACC1/ FAS1/FAS2/*	ACACP + 4 MALACP + 8 NADPH -> 8 NADP + C100ACP + 4 CO2 + 4 ACP
YGR037C/YNR016C/YKL182W/YPL231W	*ACB1/ACC1/ FAS1/FAS2/*	ACACP + 5 MALACP + 10 NADPH -> 10 NADP + C120ACP + 5 CO2 + 5 ACP
YGR037C/YNR016C/YKL182W/YPL231W	*ACB1/ACC1/ FAS1/FAS2/*	ACACP + 6 MALACP + 12 NADPH -> 12 NADP + C140ACP + 6 CO2 + 6 ACP
YGR037C/YNR016C/YKL182W/YPL231W	*ACB1/ACC1/ FAS1/FAS2/*	ACACP + 6 MALACP + 11 NADPH -> 11 NADP + C141ACP + 6 CO2 + 6 ACP
YGR037C/YNR016C/YKL182W/YPL231W	*ACB1/ACC1/ FAS1/FAS2/*	ACACP + 7 MALACP + 14 NADPH -> 14 NADP + C160ACP + 7 CO2 + 7 ACP
YGR037C/YNR016C/YKL182W/YPL231W	*ACB1/ACC1/ FAS1/FAS2/*	ACACP + 7 MALACP + 13 NADPH -> 13 NADP + C161ACP + 7 CO2 + 7 ACP
YGR037C/YNR016C/YKL182W/YPL231W	*ACB1/ACC1/ FAS1/FAS2/*	ACACP + 8 MALACP + 16 NADPH -> 16 NADP + C180ACP + 8 CO2 + 8 ACP
YGR037C/YNR016C/YKL182W/YPL231W	*ACB1/ACC1/ FAS1/FAS2/*	ACACP + 8 MALACP + 15 NADPH -> 15 NADP + C181ACP + 8 CO2 + 8 ACP
YGR037C/YNR016C/YKL182W/YPL231W	*ACB1/ACC1/ FAS1/FAS2/*	ACACP + 8 MALACP + 14 NADPH -> 14 NADP + C182ACP + 8 CO2 + 8 ACP
YKL182W	*FAS1*	3HPACP <-> 2HDACP
YKL182W	*FAS1*	AACP + NAD <-> 23DAACP + NADH
# FATTY ACID DEGRADATION		
YGL205W/YKR009C/YIL160C	*POX1/FOX2/ POT3*	C140 + ATP + 7 COA + 7 FADm + 7 NAD -> AMP + PPI + 7 FADH2m + 7 NADH + 7 ACCOA
YGL205W/YKR009C/YIL160C	*POX1/FOX2/ POT3*	C160 + ATP + 8 COA + 8 FADm + 8 NAD -> AMP + PPI + 8 FADH2m + 8 NADH + 8 ACCOA
YGL205W/YKR009C/YIL160C	*POX1/FOX2/ POT3*	C180 + ATP + 9 COA + 9 FADm + 9 NAD -> AMP + PPI + 9 FADH2m + 9 NADH + 9 ACCOA
# PHOSPHOLIPID BIOSYNTHESIS		
*U3_*	*U3_*	GL3P + 0.017 C100ACP + 0.062 C120ACP + 0.1 C140ACP + 0.27 C160ACP + 0.169 C161ACP + 0.055 C180ACP + 0.235 C181ACP + 0.093 C182ACP -> AGL3P + ACP
*U4_*	*U4_*	GL3P + 0.017 C100ACP + 0.062 C120ACP + 0.1 C140ACP + 0.27 C160ACP + 0.169 C161ACP + 0.055 C180ACP + 0.235 C181ACP + 0.093 C182ACP -> AGL3P + ACP

Table A.29. Complete list of reactions -continued

*U5_*	*U5_*	T3P2 + 0.017 C100ACP + 0.062 C120ACP + 0.1 C140ACP + 0.27 C160ACP + 0.169 C161ACP + 0.055 C180ACP + 0.235 C181ACP + 0.093 C182ACP -> AT3P2 + ACP
*U6_*	*U6_*	T3P2 + 0.017 C100ACP + 0.062 C120ACP + 0.1 C140ACP + 0.27 C160ACP + 0.169 C161ACP + 0.055 C180ACP + 0.235 C181ACP + 0.093 C182ACP -> AT3P2 + ACP
*U7_*	*U7_*	AT3P2 + NADPH -> AGL3P + NADP
YDL052C	*SLC1*	AGL3P + 0.017 C100ACP + 0.062 C120ACP + 0.100 C140ACP + 0.270 C160ACP + 0.169 C161ACP + 0.055 C180ACP + 0.235 C181ACP + 0.093 C182ACP -> PA + ACP
*U8_*	*U8_*	AGL3P + 0.017 C100ACP + 0.062 C120ACP + 0.100 C140ACP + 0.270 C160ACP + 0.169 C161ACP + 0.055 C180ACP + 0.235 C181ACP + 0.093 C182ACP -> PA + ACP
YBR029C	*CDS1*	PAm + CTPm <-> CDPDGm + PPIm
YBR029C	*CDS1*	PA + CTP <-> CDPDG + PPI
YER026C	*CHO1*	CDPDG + SER <-> CMP + PS
YER026C	*CHO1*	CDPDGm + SERm <-> CMPm + PSm
YGR170W	*PSD2*	PS -> PE + CO2
YNL169C	*PSD1*	PSm -> PEm + CO2m
YGR157W	*CHO2*	SAM + PE -> SAH + PMME
YJR073C	*OPI3*	SAM + PMME -> SAH + PDME
YJR073C	*OPI3*	PDME + SAM -> PC + SAH
YLR133W	*CKI1*	ATP + CHO -> ADP + PCHO
YGR202C	*PCT1*	PCHO + CTP -> CDPCHO + PPI
YNL130C	*CPT1*	CDPCHO + DAGLY -> PC + CMP
YDR147W	*EKI1*	ATP + ETHM -> ADP + PETHM
YGR007W	*MUQ1*	PETHM + CTP -> CDPETN + PPI
YHR123W	*EPT1*	CDPETN + DAGLY <-> CMP + PE
YJL153C	*INO1*	G6P -> MI1P
YHR046C	*INM1*	MI1P -> MYOI + PI
YPR113W	*PIS1*	CDPDG + MYOI -> CMP + PINS
YJR066W	*TOR1*	ATP + PINS -> ADP + PINSP
YKL203C	*TOR2*	ATP + PINS -> ADP + PINSP
YLR240W	*VPS34*	ATP + PINS -> ADP + PINSP
YNL267W	*PIK1*	ATP + PINS -> ADP + PINS4P
YLR305C	*STT4*	ATP + PINS -> ADP + PINS4P
YFR019W	*FAB1*	PINS4P + ATP -> D45PI + ADP
YDR208W	*MSS4*	PINS4P + ATP -> D45PI + ADP
YPL268W	*PLC1*	D45PI -> TPI + DAGLY
YCL004W	*PGS1*	CDPDGm + GL3Pm <-> CMPm + PGPm
*U9_*	*U9_*	PGPm -> PIm + PGm
YDL142C	*CRD1*	CDPDGm + PGm -> CMPm + CLm

Table A.29. Complete list of reactions -continued

YDR284C	*DPP1*	PA -> DAGLY + PI
YDR503C	*LPP1*	DGPP -> PA + PI
# SPHINGOGLYCOLIPID METABOLISM		
YDR062W	*LCB2*	PALCOA + SER -> COA + DHSPH + CO2
YMR296C	*LCB1*	PALCOA + SER -> COA + DHSPH + CO2
YBR265W	*TSC10*	DHSPH + NADPH -> SPH + NADP
YDR297W	*SUR2*	SPH + O2 + NADPH -> PSPH + NADP
*U10_*	*U10_*	PSPH + C260COA -> CER2 + COA
*U11_*	*U11_*	PSPH + C240COA -> CER2 + COA
YMR272C	*SCS7*	CER2 + NADPH + O2 -> CER3 + NADP
YKL004W	*AUR1*	CER3 + PINS -> IPC
YBR036C	*CSG2*	IPC + GDPMAN -> MIPC
YPL057C	*SUR1*	IPC + GDPMAN -> MIPC
YDR072C	*IPT1*	MIPC + PINS -> MIP2C
YOR171C	*LCB4*	SPH + ATP -> DHSP + ADP
YLR260W	*LCB5*	SPH + ATP -> DHSP + ADP
YOR171C	*LCB4*	PSPH + ATP -> PHSP + ADP
YLR260W	*LCB5*	PSPH + ATP -> PHSP + ADP
YJL134W	*LCB3*	DHSP -> SPH + PI
YKR053C	*YSR3*	DHSP -> SPH + PI
YDR294C	*DPL1*	DHSP -> PETHM + C16A
# STEROL BIOSYNTHESIS		
YML126C	*HMGS*	H3MCOA + COA <-> ACCOA + AACCOA
YLR450W	*HMG2*	MVL + COA + 2 NADP <-> H3MCOA + 2 NADPH
YML075C	*HMG1*	MVL + COA + 2 NADP <-> H3MCOA + 2 NADPH
YMR208W	*ERG12*	ATP + MVL -> ADP + PMVL
YMR208W	*ERG12*	CTP + MVL -> CDP + PMVL
YMR208W	*ERG12*	GTP + MVL -> GDP + PMVL
YMR208W	*ERG12*	UTP + MVL -> UDP + PMVL
YMR220W	*ERG8*	ATP + PMVL -> ADP + PPMVL
YNR043W	*MVD1*	ATP + PPMVL -> ADP + PI + IPPP + CO2
YPL117C	*IDI1*	IPPP <-> DMPP
YJL167W	*ERG20*	DMPP + IPPP -> GPP + PPI
YJL167W	*ERG20*	GPP + IPPP -> FPP + PPI
YHR190W	*ERG9*	2 FPP + NADPH -> NADP + SQL
YGR175C	*ERG1*	SQL + O2 + NADP -> S23E + NADPH
YHR072W	*ERG7*	S23E -> LNST
YHR007C	*ERG11*	LNST + RFP + O2 -> IGST + OFP
YNL280C	*ERG24*	IGST + NADPH -> DMZYMST + NADP
YGR060W	*ERG25*	3 O2 + DMZYMST -> IMZYMST
YGL001C	*ERG26*	IMZYMST -> IIMZYMST + CO2
YLR100C	*YLR100C*	IIMZYMST + NADPH -> MZYMST + NADP
YGR060W	*ERG25*	3 O2 + MZYMST -> IZYMST
YGL001C	*ERG26*	IZYMST -> IIZYMST + CO2
YLR100C	*YLR100C*	IIZYMST + NADPH -> ZYMST + NADP
YML008C	*ERG6*	ZYMST + SAM -> FEST + SAH

Table A.29. Complete list of reactions -continued

YMR202W	*ERG2*	FEST -> EPST
YLR056W	*ERG3*	EPST + O2 + NADPH -> NADP + ERTROL
YMR015C	*ERG5*	ERTROL + O2 + NADPH -> NADP + ERTEOL
YGL012W	*ERG4*	ERTEOL + NADPH -> ERGOST + NADP
*U12_*	*U12_*	LNST + 3 O2 + 4 NADPH + NAD -> MZYMST + CO2 + 4 NADP + NADH
*U13_*	*U13_*	MZYMST + 3 O2 + 4 NADPH + NAD -> ZYMST + CO2 + 4 NADP + NADH
*U14_*	*U14_*	ZYMST + SAM -> ERGOST + SAH
# NUCLEOTIDE METABOLISM		
# HISTIDINE BIOSYNTHESIS		
YOL061W	*PRS5*	R5P + ATP <-> PRPP + AMP
YBL068W	*PRS4*	R5P + ATP <-> PRPP + AMP
YER099C	*PRS2*	R5P + ATP <-> PRPP + AMP
YHL011C	*PRS3*	R5P + ATP <-> PRPP + AMP
YKL181W	*PRS1*	R5P + ATP <-> PRPP + AMP
YIR027C	*DAL1*	ATN <-> ATT
YIR029W	*DAL2*	ATT <-> UGC + UREA
YIR032C	*DAL3*	UGC <-> GLX + 2 NH3 + CO2
# PURINE METABOLISM		
YJL005W	*CYR1*	ATP -> cAMP + PPI
YDR454C	*GUK1*	GMP + ATP <-> GDP + ADP
YDR454C	*GUK1*	DGMP + ATP <-> DGDP + ADP
YDR454C	*GUK1*	GMP + DATP <-> GDP + DADP
YMR300C	*ADE4*	PRPP + GLN -> PPI + GLU + PRAM
YGL234W	*ADE5,7*	PRAM + ATP + GLY <-> ADP + PI + GAR
YDR408C	*ADE8*	GAR + FTHF -> THF + FGAR
YGR061C	*ADE6*	FGAR + ATP + GLN -> GLU + ADP + PI + FGAM
YGL234W	*ADE5,7*	FGAM + ATP -> ADP + PI + AIR
YOR128C	*ADE2*	CAIR <-> AIR + CO2
YAR015W	*ADE1*	CAIR + ATP + ASP <-> ADP + PI + SAICAR
YLR359W	*ADE13*	SAICAR <-> FUM + AICAR
YLR028C	*ADE16*	AICAR + FTHF <-> THF + PRFICA
YMR120C	*ADE17*	AICAR + FTHF <-> THF + PRFICA
YLR028C	*ADE16*	PRFICA <-> IMP
YMR120C	*ADE17*	PRFICA <-> IMP
YNL220W	*ADE12*	IMP + GTP + ASP -> GDP + PI + ASUC
YLR359W	*ADE13*	ASUC <-> FUM + AMP
YAR073W	*FUN63*	IMP + NAD -> NADH + XMP
YHR216W	*PUR5*	IMP + NAD -> NADH + XMP
YML056C	*IMD4*	IMP + NAD -> NADH + XMP
YLR432W	*IMD3*	IMP + NAD -> NADH + XMP
YAR075W	*YAR075W*	IMP + NAD -> NADH + XMP
YMR217W	*GUA1*	XMP + ATP + GLN -> GLU + AMP + PPI + GMP
YML035C	*AMD1*	AMP -> IMP + NH3
YGL248W	*PDE1*	cAMP -> AMP

Table A.29. Complete list of reactions -continued

YOR360C	*PDE2*	cAMP -> AMP
YOR360C	*PDE2*	cdAMP -> DAMP
YOR360C	*PDE2*	cIMP -> IMP
YOR360C	*PDE2*	cGMP -> GMP
YOR360C	*PDE2*	cCMP -> CMP
YDR530C	*APA2*	ADP + ATP -> PI + ATRP
YCL050C	*APA1*	ADP + GTP -> PI + ATRP
YCL050C	*APA1*	GDP + GTP -> PI + GTRP
# PYRIMIDINE METABOLISM		
YJL130C	*URA2*	CAP + ASP -> CAASP + PI
YLR420W	*URA4*	CAASP <-> DOROA
YKL216W	*URA1*	DOROA + O2 <-> H2O2 + OROA
YKL216W	*PYRD*	DOROA + Qm <-> QH2m + OROA
YML106W	*URA5*	OROA + PRPP <-> PPI + OMP
YMR271C	*URA10*	OROA + PRPP <-> PPI + OMP
YEL021W	*URA3*	OMP -> CO2 + UMP
YKL024C	*URA6*	ATP + UMP <-> ADP + UDP
YHR128W	*FUR1*	URA + PRPP -> UMP + PPI
YPR062W	*FCY1*	CYTS -> URA + NH3
*U15_*	*U15_*	DU + ATP -> DUMP + ADP
*U16_*	*U16_*	DT + ATP -> ADP + DTMP
YNR012W	*URK1*	URI + GTP -> UMP + GDP
YNR012W	*URK1*	CYTD + GTP -> GDP + CMP
YNR012W	*URK1*	URI + ATP -> ADP + UMP
YLR209C	*PNP1*	DU + PI <-> URA + DR1P
YLR209C	*PNP1*	DT + PI <-> THY + DR1P
YLR245C	*CDD1*	CYTD -> URI + NH3
YLR245C	*CDD1*	DC -> NH3 + DU
YJR057W	*CDC8*	DTMP + ATP <-> ADP + DTDP
YDR353W	*TRR1*	OTHIO + NADPH -> NADP + RTHIO
YHR106W	*TRR2*	OTHIOm + NADPHm -> NADPm + RTHIOm
YBR252W	*DUT1*	DUTP -> PPI + DUMP
YOR074C	*CDC21*	DUMP + METTHF -> DHF + DTMP
*U17_*	*U17_*	DCMP + ATP <-> ADP + DCDP
*U18_*	*U18_*	CMP + ATP <-> ADP + CDP
YHR144C	*DCD1*	DCMP <-> DUMP + NH3
YBL039C	*URA7*	UTP + GLN + ATP -> GLU + CTP + ADP + PI
YJR103W	*URA8*	UTP + GLN + ATP -> GLU + CTP + ADP + PI
YBL039C	*URA7*	ATP + UTP + NH3 -> ADP + PI + CTP
YJR103W	*URA8*	ATP + UTP + NH3 -> ADP + PI + CTP
YNL292W	*PUS4*	URA + R5P <-> PURI5P
YPL212C	*PUS1*	URA + R5P <-> PURI5P
YGL063W	*PUS2*	URA + R5P <-> PURI5P
YFL001W	*DEG1*	URA + R5P <-> PURI5P
# SALVAGE PATHWAYS		
YML022W	*APT1*	AD + PRPP -> PPI + AMP

Table A.29. Complete list of reactions -continued

YDR441C	*APT2*	AD + PRPP -> PPI + AMP
YNL141W	*AAH1*	ADN -> INS + NH3
YNL141W	*AAH1*	DA -> DIN + NH3
YLR209C	*PNP1*	DIN + PI <-> HYXN + DR1P
YLR209C	*PNP1*	DA + PI <-> AD + DR1P
YLR209C	*PNP1*	DG + PI <-> GN + DR1P
YLR209C	*PNP1*	HYXN + R1P <-> INS + PI
YLR209C	*PNP1*	AD + R1P <-> PI + ADN
YLR209C	*PNP1*	GN + R1P <-> PI + GSN
YLR209C	*PNP1*	XAN + R1P <-> PI + XTSINE
YJR133W	*XPT1*	XAN + PRPP -> XMP + PPI
YDR400W	*URH1*	GSN -> GN + RIB
YDR400W	*URH1*	ADN -> AD + RIB
YJR105W	*YJR105W*	ADN + ATP -> AMP + ADP
YDR226W	*ADK1*	ATP + AMP <-> 2 ADP
YDR226W	*ADK1*	GTP + AMP <-> ADP + GDP
YDR226W	*ADK1*	ITP + AMP <-> ADP + IDP
YER170W	*ADK2*	ATPm + AMPm <-> 2 ADPm
YER170W	*ADK2*	GTPm + AMPm <-> ADPm + GDPm
YER170W	*ADK2*	ITPm + AMPm <-> ADPm + IDPm
YGR180C	*RNR4*	
YIL066C	*RNR3*	ADP + RTHIO -> DADP + OTHIO
YJL026W	*RNR2*	
YKL067W	*YNK1*	UDP + ATP <-> UTP + ADP
YKL067W	*YNK1*	CDP + ATP <-> CTP + ADP
YKL067W	*YNK1*	DGDP + ATP <-> DGTP + ADP
YKL067W	*YNK1*	DUDP + ATP <-> DUTP + ADP
YKL067W	*YNK1*	DCDP + ATP <-> DCTP + ADP
YKL067W	*YNK1*	DTDP + ATP <-> DTTP + ADP
YKL067W	*YNK1*	DADP + ATP <-> DATP + ADP
YKL067W	*YNK1*	GDP + ATP <-> GTP + ADP
YKL067W	*YNK1*	IDP + ATP <-> ITP + IDP
*U19_*	*U19_*	DAMP + ATP <-> DADP + ADP
YNL141W	*AAH1*	AD -> NH3 + HYXN
*U20_*	*U20_*	INS + ATP -> IMP + ADP
*U21_*	*U21_*	GSN + ATP -> GMP + ADP
YDR399W	*HPT1*	HYXN + PRPP -> PPI + IMP
YDR399W	*HPT1*	GN + PRPP -> PPI + GMP
*U22_*	*U22_*	URI + PI <-> URA + R1P
YKL024C	*URA6*	UMP + ATP <-> UDP + ADP
YKL024C	*URA6*	DUMP + ATP <-> DUDP + ADP
*U23_*	*U23_*	CMP -> CYTS + R5P
YHR144C	*DCD1*	DCTP -> DUTP + NH3
*U24_*	*U24_*	DUMP -> DU + PI

Table A.29. Complete list of reactions -continued

*U25_*	*U25_*	DTMP -> DT + PI
*U26_*	*U26_*	DAMP -> DA + PI
*U27_*	*U27_*	DGMP -> DG + PI
*U28_*	*U28_*	DCMP -> DC + PI
*U29_*	*U29_*	CMP -> CYTD + PI
*U30_*	*U30_*	AMP -> PI + ADN
*U31_*	*U31_*	GMP -> PI + GSN
*U32_*	*U32_*	IMP -> PI + INS
*U33_*	*U33_*	XMP -> PI + XTSINE
*U34_*	*U34_*	UMP -> PI + URI
YER070W	*RNR1*	ADP + RTHIO -> DADP + OTHIO
YER070W	*RNR1*	GDP + RTHIO -> DGDP + OTHIO
YER070W	*RNR1*	CDP + RTHIO -> DCDP + OTHIO
YER070W	*RNR1*	UDP + RTHIO -> OTHIO + DUDP
*U35_*	*U35_*	ATP + RTHIO -> DATP + OTHIO
*U36_*	*U36_*	GTP + RTHIO -> DGTP + OTHIO
*U37_*	*U37_*	CTP + RTHIO -> DCTP + OTHIO
*U38_*	*U38_*	UTP + RTHIO -> OTHIO + DUTP
*U39_*	*U39_*	GTP -> GSN + 3 PI
*U40_*	*U40_*	DGTP -> DG + 3 PI
YML035C	*AMD1*	AMP -> AD + R5P
YBR284W	*YBR284W*	AMP -> AD + R5P
YJL070C	*YJL070C*	AMP -> AD + R5P
# AMINO ACID METABOLISM		
# GLUTAMATE METABOLISM (AMINOSUGARS METABOLISM)		
YMR250W	*GAD1*	GLU -> GABA + CO2
YGR019W	*UGA1*	GABA + AKG -> SUCCSAL + GLU
YBR006W	*YBR006W*	SUCCSAL + NADP -> SUCC + NADPH
YKL104C	*GFA1*	F6P + GLN -> GLU + GA6P
YFL017C	*GNA1*	ACCOA + GA6P <-> COA + NAGA6P
YEL058W	*PCM1*	NAGA1P <-> NAGA6P
YDL103C	*QRI1*	UTP + NAGA1P <-> UDPNAG + PPI
YBR023C	*CHS3*	UDPNAG -> CHIT + UDP
YBR038W	*CHS2*	UDPNAG -> CHIT + UDP
YNL192W	*CHS1*	UDPNAG -> CHIT + UDP
YHR037W	*PUT2*	GLUGSALm + NADPm -> NADPHm + GLUm
*U41_*	*U41_*	P5Cm + NADm -> NADHm + GLUm
YDL171C	*GLT1*	AKG + GLN + NADH -> NAD + 2 GLU
YDL215C	*GDH2*	GLU + NAD -> AKG + NH3 + NADH
YAL062W	*GDH3*	AKG + NH3 + NADPH -> GLU + NADP
YOR375C	*GDH1*	AKG + NH3 + NADPH -> GLU + NADP
YPR035W	*GLN1*	GLU + NH3 + ATP -> GLN + ADP + PI
YEL058W	*PCM1*	GA6P <-> GA1P
*U42_*	*U42_*	GLN -> GLU + NH3
*U43_*	*U43_*	GLN -> GLU + NH3

Table A.29. Complete list of reactions -continued

# GLUCOSAMINE		
U44_	*U44_*	GA6P -> F6P + NH3
# ARABINOSE		
YBR149W	*ARA1*	ARAB + NAD -> ARABLAC + NADH
YBR149W	*ARA1*	ARAB + NADP -> ARABLAC + NADPH
# XYLOSE		
YGR194C	*XKS1*	XUL + ATP -> X5P + ADP
# MANNITOL		
*U45_*	*U45_*	MNT6P + NAD <-> F6P + NADH
# ALANINE AND ASPARTATE METABOLISM		
YKL106W	*AAT1*	OAm + GLUm <-> ASPm + AKGm
YLR027C	*AAT2*	OA + GLU <-> ASP + AKG
YAR035W	*YAT1*	COAm + ACARm -> ACCOAm + CARm
YML042W	*CAT2*	ACCOA + CAR -> COA + ACAR
YDR111C	*YDR111C*	PYR + GLU <-> AKG + ALA
YLR089C	*YLR089C*	PYRm + GLUm <-> AKGm + ALAm
YPR145W	*ASN1*	ASP + ATP + GLN -> GLU + ASN + AMP + PPI
YGR124W	*ASN2*	ASP + ATP + GLN -> GLU + ASN + AMP + PPI
YLL062C	*MHT1*	SAM + HCYS -> SAH + MET
YPL273W	*SAM4*	SAM + HCYS -> SAH + MET
# ASPARAGINE		
YCR024C	*YCR024C*	ATPm + ASPm + TRNAm -> AMPm + PPIm + ASPTRNAm
YHR019C	*DED81*	ATP + ASP + TRNA -> AMP + PPI + ASPTRNA
YLR155C	*ASP3-1*	ASN -> ASP + NH3
YLR157C	*ASP3-2*	ASN -> ASP + NH3
YLR158C	*ASP3-3*	ASN -> ASP + NH3
YLR160C	*ASP3-4*	ASN -> ASP + NH3
YDR321W	*ASP1*	ASN -> ASP + NH3
# GLYCINE, SERINE AND THREONINE METABOLISM		
YER081W	*SER3*	3PG + NAD -> NADH + PHP
YIL074C	*SER33*	3PG + NAD -> NADH + PHP
YOR184W	*SER1*	PHP + GLU -> AKG + 3PSER
YGR208W	*SER2*	3PSER -> PI + SER
YBR263W	*SHM1*	THFm + SERm <-> GLYm + METTHFm
YLR058C	*SHM2*	THF + SER <-> GLY + METTHF
YFL030W	*YFL030W*	ALA + GLX <-> PYR + GLY
YDR019C	*GCV1*	GLYm + THFm + NADm -> METTHFm + NADHm + CO2 + NH3
YDR019C	*GCV1*	GLY + THF + NAD -> METTHF + NADH + CO2 + NH3
YER052C	*HOM3*	ASP + ATP -> ADP + BASP
YDR158W	*HOM2*	BASP + NADPH -> NADP + PI + ASPSA

Table A.29. Complete list of reactions -continued

YJR139C	*HOM6*	ASPSA + NADH -> NAD + HSER
YJR139C	*HOM6*	ASPSA + NADPH -> NADP + HSER
YHR025W	*THR1*	HSER + ATP -> ADP + PHSER
YCR053W	*THR4*	PHSER -> PI + THR
YGR155W	*CYS4*	SER + HCYS -> LLCT
YEL046C	*GLY1*	GLY + ACAL -> THR
YMR189W	*GCV2*	GLYm + LIPOm <-> SAPm + CO2m
YCL064C	*CHA1*	THR -> NH3 + OBUT
YER086W	*ILV1*	THRm -> NH3m + OBUTm
YCL064C	*CHA1*	SER -> PYR + NH3
YIL167W	*YIL167W*	SER -> PYR + NH3
*U46_*	*U46_*	THR + NAD -> GLY + AC + NADH
# METHIONINE METABOLISM		
YFR055W	*YFR055W*	LLCT -> HCYS + PYR + NH3
YER043C	*SAH1*	SAH -> HCYS + ADN
YER091C	*MET6*	HCYS + MTHPTGLU -> THPTGLU + MET
*U47_*	*U47_*	HCYS + MTHF -> THF + MET
YAL012W	*CYS3*	LLCT -> CYS + NH3 + OBUT
YNL277W	*MET2*	ACCOA + HSER <-> COA + OAHSER
YLR303W	*MET17*	OAHSER + METH -> MET + AC
YLR303W	*MET17*	OAHSER + H2S -> AC + HCYS
YLR303W	*MET17*	OAHSER + H2S -> AC + HCYS
YML082W	*YML082W*	OSLHSER <-> SUCC + OBUT + NH3
YDR502C	*SAM2*	MET + ATP -> PPI + PI + SAM
YLR180W	*SAM1*	MET + ATP -> PPI + PI + SAM
YLR172C	*DPH5*	SAM + CALH -> SAH + DPTH
# CYSTEINE BIOSYNTHESIS		
YJR010W	*MET3*	SLF + ATP -> PPI + APS
YKL001C	*MET14*	APS + ATP -> ADP + PAPS
YFR030W	*MET10*	H2SO3 + 3 NADPH <-> H2S + 3 NADP
*U48_*	*U48_*	SER + ACCOA -> COA + ASER
YGR012W	*YGR012W*	ASER + H2S -> AC + CYS
YOL064C	*MET22*	PAP -> AMP + PI
YPR167C	*MET16*	PAPS + RTHIO -> OTHIO + H2SO3 + PAP
YCL050C	*APA1*	ADP + SLF <-> PI + APS
# BRANCHED CHAIN AMINO ACID METABOLISM (VALINE, LEUCINE AND ISOLEUCINE)		
YHR208W	*BAT1*	OICAPm + GLUm <-> AKGm + LEUm
YHR208W	*BAT1*	OMVALm + GLUm <-> AKGm + ILEm
YJR148W	*BAT2*	OMVAL + GLU <-> AKG + ILE
YJR148W	*BAT2*	OIVAL + GLU <-> AKG + VAL
YJR148W	*BAT2*	OICAP + GLU <-> AKG + LEU
YMR108W	*ILV2*	OBUTm + PYRm -> ABUTm + CO2m
YCL009C	*ILV6*	
YMR108W	*ILV2*	2 PYRm -> CO2m + ACLACm

Table A.29. Complete list of reactions -continued

YCL009C	*ILV6*	
YLR355C	*ILV5*	ACLACm + NADPHm -> NADPm + DHVALm
YLR355C	*ILV5*	ABUTm + NADPHm -> NADPm + DHMVAm
YJR016C	*ILV3*	DHVALm -> OIVALm
YJR016C	*ILV3*	DHMVAm -> OMVALm
YNL104C	*LEU4*	ACCOAm + OIVALm -> COAm + IPPMALm
YGL009C	*LEU1*	CBHCAP <-> IPPMAL
YGL009C	*LEU1*	PPMAL <-> IPPMAL
YCL018W	*LEU2*	IPPMAL + NAD -> NADH + OICAP + CO2
# LYSINE BIOSYNTHESIS/DEGRADATION		
*U49_*	*U49_*	HCITm <-> HACNm
YDR234W	*LYS4*	HICITm <-> HACNm
YIL094C	*LYS12*	HICITm + NADm <-> OXAm + CO2m + NADHm
*U50_*	*U50_*	OXAm <-> CO2m + AKAm
*U51_*	*U51_*	AKA + GLU <-> AMA + AKG
YBR115C	*LYS2*	AMA + NADPH + ATP -> AMASA + NADP + AMP + PPI
YGL154C	*LYS5*	
YBR115C	*LYS2*	AMA + NADH + ATP -> AMASA + NAD + AMP + PPI
YGL154C	*LYS5*	
YNR050C	*LYS9*	GLU + AMASA + NADPH <-> SACP + NADP
YIR034C	*LYS1*	SACP + NAD <-> LYS + AKG + NADH
YDR037W	*KRS1*	ATP + LYS + LTRNA -> AMP + PPI + LLTRNA
YNL073W	*MSK1*	ATPm + LYSm + LTRNAm -> AMPm + PPIm + LLTRNAm
YDR368W	*YPR1*	
# ARGININE METABOLISM		
YMR062C	*ECM40*	GLUm + ACCOAm -> COAm + NAGLUm
YER069W	*ARG5*	NAGLUm + ATPm -> ADPm + NAGLUPm
YER069W	*ARG5*	NAGLUPm + NADPHm -> NADPm + PIm + NAGLUSm
YOL140W	*ARG8*	NAGLUSm + GLUm -> AKGm + NAORNm
YMR062C	*ECM40*	NAORNm + GLUm -> ORNm + NAGLUm
YJL130C	*URA2*	GLN + 2 ATP + CO2 -> GLU + CAP + 2 ADP + PI
YJR109C	*CPA2*	GLN + 2 ATP + CO2 -> GLU + CAP + 2 ADP + PI
YOR303W	*CPA1*	
YJL088W	*ARG3*	ORN + CAP -> CITR + PI
YLR438W	*CAR2*	ORN + AKG -> GLUGSAL + GLU
YOL058W	*ARG1*	CITR + ASP + ATP <-> AMP + PPI + ARGSUCC
YHR018C	*ARG4*	ARGSUCC <-> FUM + ARG
YKL184W	*SPE1*	ORN -> PTRSC + CO2
YOL052C	*SPE2*	SAM <-> DSAM + CO2
YPR069C	*SPE3*	PTRSC + SAM -> SPRMD + 5MTA

Table A.29. Complete list of reactions -continued

YLR146C	*SPE4*	DSAM + SPRMD -> 5MTA + SPRM
YDR242W	*AMD2*	GBAD -> GBAT + NH3
YMR293C	*YMR293C*	GBAD -> GBAT + NH3
YPL111W	*CAR1*	ARG -> ORN + UREA
YDR341C	*YDR341C*	ATP + ARG + ATRNA -> AMP + PPI + ALTRNA
YHR091C	*MSR1*	ATP + ARG + ATRNA -> AMP + PPI + ALTRNA
YHR068W	*DYS1*	SPRMD + Qm -> DAPRP + QH2m
# HISTIDINE METABOLISM		
YER055C	*HIS1*	PRPP + ATP -> PPI + PRBATP
YCL030C	*HIS4*	PRBATP -> PPI + PRBAMP
YCL030C	*HIS4*	PRBAMP -> PRFP
YIL020C	*HIS6*	PRFP -> PRLP
YOR202W	*HIS3*	DIMGP -> IMACP
YIL116W	*HIS5*	IMACP + GLU -> AKG + HISOLP
YFR025C	*HIS2*	HISOLP -> PI + HISOL
YCL030C	*HIS4*	HISOL + 2 NAD -> HIS + 2 NADH
YBR248C	*HIS7*	PRLP + GLN -> GLU + AICAR + DIMGP
YPR033C	*HTS1*	ATP + HIS + HTRNA -> AMP + PPI + HHTRNA
YBR034C	*HMT1*	SAM + HIS -> SAH + MHIS
YCL054W	*SPB1*	
YML110C	*COQ5*	
YOR201C	*PET56*	
YPL266W	*DIM1*	
# PHENYLALANINE, TYROSINE AND TRYPTOPHAN BIOSYNTHESIS (AROMATIC AMINO ACIDS)		
YBR249C	*ARO4*	E4P + PEP -> PI + 3DDAH7P
YDR035W	*ARO3*	E4P + PEP -> PI + 3DDAH7P
YDR127W	*ARO1*	3DDAH7P -> DQT + PI
YDR127W	*ARO1*	DQT -> DHSK
YDR127W	*ARO1*	DHSK + NADPH -> SME + NADP
YDR127W	*ARO1*	SME + ATP -> ADP + SME5P
YDR127W	*ARO1*	SME5P + PEP -> 3PSME + PI
YGL148W	*ARO2*	3PSME -> PI + CHOR
YPR060C	*ARO7*	CHOR -> PHEN
YNL316C	*PHA2*	PHEN -> CO2 + PHPYR
YHR137W	*ARO9*	PHPYR + GLU <-> AKG + PHE
YBR166C	*TYR1*	PHEN + NADP -> 4HPP + CO2 + NADPH
YGL202W	*ARO8*	4HPP + GLU -> AKG + TYR
YHR137W	*ARO9*	4HPP + GLU -> AKG + TYR
*U52_*	*U52_*	PHEN + NAD -> 4HPP + CO2 + NADH
YER090W	*TRP2*	CHOR + GLN -> GLU + PYR + AN
YKL211C	*TRP3*	CHOR + GLN -> GLU + PYR + AN
YDR354W	*TRP4*	AN + PRPP -> PPI + NPRAN
YDR007W	*TRP1*	NPRAN -> CPAD5P
YKL211C	*TRP3*	CPAD5P -> CO2 + IGP

Table A.29. Complete list of reactions -continued

YGL026C	*TRP5*	IGP + SER -> T3P1 + TRP
YDR256C	*CTA1*	2 H2O2 -> O2
YGR088W	*CTT1*	2 H2O2 -> O2
YKL106W	*AAT1*	4HPP + GLU <-> AKG + TYR
YLR027C	*AAT2*	4HPP + GLU <-> AKG + TYR
YMR170C	*ALD2*	ACAL + NAD -> NADH + AC
YMR169C	*ALD3*	ACAL + NAD -> NADH + AC
YOR374W	*ALD4*	ACALm + NADm -> NADHm + ACm
YOR374W	*ALD4*	ACALm + NADPm -> NADPHm + ACm
YER073W	*ALD5*	ACALm + NADPm -> NADPHm + ACm
YPL061W	*ALD6*	ACAL + NADP -> NADPH + AC
YJR078W	*YJR078W*	TRP + O2 -> FKYN
*U53_*	*U53_*	FKYN -> FOR + KYN
YLR231C	*YLR231C*	KYN -> ALA + AN
YBL098W	*YBL098W*	KYN + NADPH + O2 -> HKYN + NADP
YLR231C	*YLR231C*	HKYN -> HAN + ALA
YJR025C	*BNA1*	HAN + O2 -> CMUSA
*U54_*	*U54_*	CMUSA -> CO2 + AM6SA
*U55_*	*U55_*	AM6SA + NAD -> AMUCO + NADH
*U56_*	*U56_*	AMUCO + NADPH -> AKA + NADP + NH3
*U57_*	*U57_*	4HPP + O2 -> HOMOGEN + CO2
*U58_*	*U58_*	HOMOGEN + O2 -> MACAC
*U59_*	*U59_*	MACAC -> FUACAC
*U60_*	*U60_*	FUACAC -> FUM + ACTAC
YDR268W	*MSW1*	ATPm + TRPm + TRNAm -> AMPm + PPIm + TRPTRNAm
YDR242W	*AMD2*	PAD -> PAC + NH3
YDR242W	*AMD2*	IAD -> IAC + NH3
*U61_*	*U61_*	SPRMD + ACCOA -> ASPERMD + COA
*U62_*	*U62_*	ASPERMD + O2 -> APRUT + APROA + H2O2
*U63_*	*U63_*	APRUT + O2 -> GABAL + APROA + H2O2
*U64_*	*U64_*	SPRM + ACCOA -> ASPRM + COA
*U65_*	*U65_*	ASPRM + O2 -> ASPERMD + APROA + H2O2
# PROLINE BIOSYNTHESIS		
YDR300C	*PRO1*	GLU + ATP -> ADP + GLUP
YOR323C	*PRO2*	GLUP + NADH -> NAD + PI + GLUGSAL
YOR323C	*PRO2*	GLUP + NADPH -> NADP + PI + GLUGSAL
*U66_*	*U66_*	GLUGSAL <-> P5C
*U67_*	*U67_*	GLUGSALm <-> P5Cm
YER023W	*PRO3*	P5C + NADPH -> PRO + NADP
YER023W	*PRO3*	PHC + NADPH -> HPRO + NADP
YER023W	*PRO3*	PHC + NADH -> HPRO + NAD
YLR142W	*PUT1*	PROm + NADm -> P5Cm + NADHm
# METABOLISM OF OTHER AMINO ACID		
# BETA-ALANINE METABOLISM		

Table A.29. Complete list of reactions -continued

*U68_*	*U68_*	GABALm + NADm -> GABAm + NADHm
YER073W	*ALD5*	LACALm + NADm <-> LLACm + NADHm
# CYANOAMINO ACID METABOLISM		
YJL126W	*NIT2*	APROP -> ALA + NH3
YJL126W	*NIT2*	ACYBUT -> GLU + NH3
# PROTEINS, PEPTIDES AND AMINO ACIDS METABOLISM		
YLR195C	*NMT1*	TCOA + GLP -> COA + TGLP
YDL040C	*NAT1*	ACCOA + PEPD -> COA + APEP
YGR147C	*NAT2*	ACCOA + PEPD -> COA + APEP
# GLUTATHIONE BIOSYNTHESIS		
YJL101C	*GSH1*	CYS + GLU + ATP -> GC + PI + ADP
YOL049W	*GSH2*	GLY + GC + ATP -> RGT + PI + ADP
YBR244W	*GPX2*	2 RGT + H2O2 <-> OGT
YIR037W	*HYR1*	2 RGT + H2O2 <-> OGT
YKL026C	*GPX1*	2 RGT + H2O2 <-> OGT
YPL091W	*GLR1*	NADPH + OGT -> NADP + RGT
YLR299W	*ECM38*	RGT + ALA -> CGLY + ALAGLY
# METABOLISM OF COMPLEX CARBOHYDRATES		
# STARCH AND SUCROSE METABOLISM		
YGR032W	*GSC2*	UDPG -> 13GLUCAN + UDP
YLR342W	*FKS1*	UDPG -> 13GLUCAN + UDP
YMR306W	*FKS3*	UDPG -> 13GLUCAN + UDP
YDR261C	*EXG2*	13GLUCAN -> GLC
YGR282C	*BGL2*	13GLUCAN -> GLC
YLR300W	*EXG1*	13GLUCAN -> GLC
YOR190W	*SPR1*	13GLUCAN -> GLC
# GLYCOPROTEIN BIOSYNTHESIS / DEGRADATION		
YMR013C	*SEC59*	CTP + DOL -> CDP + DOLP
YPR183W	*DPM1*	GDPMAN + DOLP -> GDP + DOLMANP
YAL023C	*PMT2*	DOLMANP -> DOLP + MANNAN
YDL093W	*PMT5*	DOLMANP -> DOLP + MANNAN
YDL095W	*PMT1*	DOLMANP -> DOLP + MANNAN
YGR199W	*PMT6*	DOLMANP -> DOLP + MANNAN
YJR143C	*PMT4*	DOLMANP -> DOLP + MANNAN
YOR321W	*PMT3*	DOLMANP -> DOLP + MANNAN
YBR199W	*KTR4*	MAN2PD + 2 GDPMAN -> 2 GDP + 2MANPD
YBR205W	*KTR3*	MAN2PD + 2 GDPMAN -> 2 GDP + 2MANPD
YDR483W	*KRE2*	MAN2PD + 2 GDPMAN -> 2 GDP + 2MANPD
YJL139C	*YUR1*	MAN2PD + 2 GDPMAN -> 2 GDP + 2MANPD
YKR061W	*KTR2*	MAN2PD + 2 GDPMAN -> 2 GDP + 2MANPD
YOR099W	*KTR1*	MAN2PD + 2 GDPMAN -> 2 GDP + 2MANPD
YPL053C	*KTR6*	MAN2PD + 2 GDPMAN -> 2 GDP + 2MANPD

Table A.29. Complete list of reactions -continued

# AMINOSUGARS METABOLISM		
YER062C	*HOR2*	GL3P -> GL + PI
YIL053W	*RHR2*	GL3P -> GL + PI
YLR307W	*CDA1*	CHIT -> CHITO + AC
YLR308W	*CDA2*	CHIT -> CHITO + AC
# METABOLSIM OF COMPLEX LIPIDS		
# GLYCEROL (GLYCEROLIPID METABOLISM)		
YFL053W	*DAK2*	GLYN + ATP -> T3P2 + ADP
YML070W	*DAK1*	GLYN + ATP -> T3P2 + ADP
YDL022W	*GPD1*	T3P2 + NADH -> GL3P + NAD
YOL059W	*GPD2*	T3P2 + NADH -> GL3P + NAD
YHL032C	*GUT1*	GL + ATP -> GL3P + ADP
YIL155C	*GUT2*	GL3P + FADm -> T3P2 + FADH2m
*U69_*	*U69_*	DAGLY + 0.017 C100ACP + 0.062 C120ACP + 0.100 C140ACP + 0.270 C160ACP + 0.169 C161ACP + 0.055 C180ACP + 0.235 C181ACP + 0.093 C182ACP -> TAGLY + ACP
# METABOLISM OF COFACTORS, VITAMINS, AND OTHER SUBSTANCES		
# THIAMINE (VITAMIN B1) METABOLISM		
YOR143C	*THI80*	ATP + THIAMIN -> AMP + TPP
YOR143C	*THI80*	ATP + TPP -> AMP + TPPP
*U70_*	*U70_*	AIR -> AHM
YOL055C	*THI20*	AHM + ATP -> AHMP + ADP
YPL258C	*THI21*	AHM + ATP -> AHMP + ADP
YPR121W	*THI22*	AHM + ATP -> AHMP + ADP
YOL055C	*THI20*	AHMP + ATP -> AHMPP + ADP
*U71_*	*U71_*	T3P1 + PYR -> DTP
*U72_*	*U72_*	DTP + TYR + CYS -> THZ + HBA + CO2
*U73_*	*U73_*	DTP + TYR + CYS -> THZ + HBA + CO2
*U74_*	*U74_*	DTP + TYR + CYS -> THZ + HBA + CO2
*U75_*	*U75_*	DTP + TYR + CYS -> THZ + HBA + CO2
YPL214C	*THI6*	THZ + ATP -> THZP + ADP
YPL214C	*THI6*	THZP + AHMPP -> THMP + PPI
*U76_*	*U76_*	THMP + ATP <-> TPP + ADP
*U77_*	*U77_*	THMP -> THIAMIN + PI
# RIBOFLAVIN METABOLISM		
YBL033C	*RIB1*	GTP -> D6RP5P + FOR + PPI
YBR153W	*RIB7*	D6RP5P -> A6RP5P + NH3
YBR153W	*RIB7*	A6RP5P + NADPH -> A6RP5P2 + NADP
*U78_*	*U78_*	A6RP5P2 -> A6RP + PI
*U79_*	*U79_*	RL5P -> DB4P + FOR
YBR256C	*RIB5*	DB4P + A6RP -> D8RL + PI
YOL143C	*RIB4*	

Table A.29. Complete list of reactions -continued

YAR071W	*PHO11*	FMN -> RIBFLAV + PI
YDR236C	*FMN1*	RIBFLAV + ATP -> FMN + ADP
YDR236C	*FMN1*	RIBFLAVm + ATPm -> FMNm + ADPm
YDL045C	*FAD1*	FMN + ATP -> FAD + PPI
*U80_*	*U80_*	FMNm + ATPm -> FADm + PPIm
# VITAMIN B6 (PYRIDOXINE) BIOSYNTHESIS METABOLISM		
*U81_*	*U81_*	PYRDX + ATP -> P5P + ADP
*U82_*	*U82_*	PDLA + ATP -> PDLA5P + ADP
*U83_*	*U83_*	PL + ATP -> PL5P + ADP
YBR035C	*PDX3*	PDLA5P + O2 -> PL5P + H2O2 + NH3
YBR035C	*PDX3*	P5P + O2 <-> PL5P + H2O2
YBR035C	*PDX3*	PYRDX + O2 <-> PL + H2O2
YBR035C	*PDX3*	PL + O2 + NH3 <-> PDLA + H2O2
YBR035C	*PDX3*	PDLA5P + O2 -> PL5P + H2O2 + NH3
YOR184W	*SER1*	OHB + GLU <-> PHT + AKG
YCR053W	*THR4*	PHT -> 4HLT + PI
*U84_*	*U84_*	PDLA5P -> PDLA + PI
# PANTOTHENATE AND COA BIOSYNTHESIS		
*U85_*	*U85_*	3 MALCOA -> CHCOA + 2 COA + 2 CO2
*U86_*	*U86_*	ALA + CHCOA <-> CO2 + COA + AONA
YNR058W	*BIO3*	SAM + AONA <-> SAMOB + DANNA
YNR057C	*BIO4*	CO2 + DANNA + ATP <-> DTB + PI + ADP
YGR286C	*BIO2*	DTB + CYS <-> BT
# FOLATE BIOSYNTHESIS		
YGR267C	*FOL2*	GTP -> FOR + AHTD
*U87_*	*U87_*	AHTD -> PPI + DHPP
YDR481C	*PHO8*	AHTD -> DHP + 3 PI
YDL100C	*YDL100C*	DHPP -> DHP + PI
YNL256W	*FOL1*	DHP -> AHHMP + GLAL
YNL256W	*FOL1*	AHHMP + ATP -> AMP + AHHMD
YNR033W	*ABZ1*	CHOR + GLN -> ADCHOR + GLU
*U88_*	*U88_*	ADCHOR -> PYR + PABA
YNL256W	*FOL1*	PABA + AHHMD -> PPI + DHPT
YNL256W	*FOL1*	PABA + AHHMP -> DHPT
*U89_*	*U89_*	DHPT + ATP + GLU -> ADP + PI + DHF
YOR236W	*DFR1*	DHFm + NADPHm -> NADPm + THFm
YOR236W	*DFR1*	DHF + NADPH -> NADP + THF
*U90_*	*U90_*	ATPm + FTHFm -> ADPm + PIm + MTHFm
*U91_*	*U91_*	ATP + FTHF -> ADP + PI + MTHF
YKL132C	*RMA1*	THF + ATP + GLU <-> ADP + PI + THFG
YMR113W	*FOL3*	THF + ATP + GLU <-> ADP + PI + THFG
YOR241W	*MET7*	THF + ATP + GLU <-> ADP + PI + THFG
# ONE CARBON POOL BY FOLATE		

Table A.29. Complete list of reactions -continued

YPL023C	*MET12*	METTHFm + NADPHm -> NADPm + MTHFm
YGL125W	*MET13*	METTHFm + NADPHm -> NADPm + MTHFm
YBR084W	*MIS1*	METTHFm + NADPm <-> METHFm + NADPHm
YGR204W	*ADE3*	METTHF + NADP <-> METHF + NADPH
YBR084W	*MIS1*	THFm + FORm + ATPm -> ADPm + PIm + FTHFm
YGR204W	*ADE3*	THF + FOR + ATP -> ADP + PI + FTHF
YBR084W	*MIS1*	METHFm <-> FTHFm
YGR204W	*ADE3*	METHF <-> FTHF
YKR080W	*MTD1*	METTHF + NAD -> METHF + NADH
YBL013W	*FMT1*	FTHFm + MTRNAm -> THFm + FMRNAm
# COENZYME A BIOSYNTHESIS		
YBR176W	*ECM31*	OIVAL + METTHF -> AKP + THF
YHR063C	*PAN5*	AKP + NADPH -> NADP + PANT
YLR355C	*ILV5*	AKPm + NADPHm -> NADPm + PANTm
YIL145C	*YIL145C*	PANT + bALA + ATP -> AMP + PPI + PNTO
YDR531W	*YDR531W*	PNTO + ATP -> ADP + 4PPNTO
*U92_*	*U92_*	4PPNTO + CTP + CYS -> CMP + PPI + 4PPNCYS
*U93_*	*U93_*	4PPNCYS -> CO2 + 4PPNTE
*U94_*	*U94_*	4PPNTE + ATP -> PPI + DPCOA
*U95_*	*U95_*	4PPNTEm + ATPm -> PPIm + DPCOAm
*U96_*	*U96_*	DPCOA + ATP -> ADP + COA
*U97_*	*U97_*	DPCOAm + ATPm -> ADPm + COAm
*U98_*	*U98_*	ASP -> CO2 + bALA
YPL148C	*PPT2*	COA -> PAP + ACP
# NAD BIOSYNTHESIS		
YGL037C	*PNC1*	NAM <-> NAC + NH3
YOR209C	*NPT1*	NAC + PRPP -> NAMN + PPI
*U99_*	*U99_*	ASP + FADm -> FADH2m + ISUCC
*U100_*	*U100_*	ISUCC + T3P2 -> PI + QA
YFR047C	*QPT1*	QA + PRPP -> NAMN + CO2 + PPI
YLR328W	*YLR328W*	NAMN + ATP -> PPI + NAAD
YHR074W	*QNS1*	NAAD + ATP + NH3 -> NAD + AMP + PPI
YJR049C	*UTR1*	NAD + ATP -> NADP + ADP
YEL041W	*YEL041W*	NAD + ATP -> NADP + ADP
YPL188W	*POS5*	NAD + ATP -> NADP + ADP
*U101_*	*U101_*	NADP -> NAD + PI
*U102_*	*U102_*	NAD -> NAM + ADPRIB
*U103_*	*U103_*	ADN + PI <-> AD + RIP
*U104_*	*U104_*	GSN + PI <-> GN + RIP
# NICOTINIC ACID SYNTHESIS FROM TRP		
YFR047C	*QPT1*	QAm + PRPPm -> NAMNm + CO2m + PPIm
YLR328W	*YLR328W*	NAMNm + ATPm -> PPIm + NAADm
YLR328W	*YLR328W*	NMNm + ATPm -> NADm + PPIm

Table A.29. Complete list of reactions -continued

YHR074W	*QNS1*	NAADm + ATPm + NH3m -> NADm + AMPm + PPIm
YJR049C	*UTR1*	NADm + ATPm -> NADPm + ADPm
YPL188W	*POS5*	NADm + ATPm -> NADPm + ADPm
YEL041W	*YEL041W*	NADm + ATPm -> NADPm + ADPm
*U105_*	*U105_*	NADPm -> NADm + PIm
YLR209C	*PNP1*	ADNm + PIm <-> ADm + RIPm
YLR209C	*PNP1*	GSNm + PIm <-> GNm + RIPm
YGL037C	*PNC1*	NAMm <-> NACm + NH3m
YOR209C	*NPT1*	NACm + PRPPm -> NAMNm + PPIm
*U106_*	*U106_*	NADm -> NAMm + ADPRIBm
# UPTAKE PATHWAYS		
# PORPHYRIN METABOLISM		
YDR232W	*HEM1*	SUCCOAm + GLYm -> ALAVm + COAm + CO2m
YGL040C	*HEM2*	2 ALAV -> PBG
YDL205C	*HEM3*	4 PBG -> HMB + 4 NH3
YOR278W	*HEM4*	HMB -> UPRG
YDR047W	*HEM12*	UPRG -> 4 CO2 + CPP
YDR044W	*HEM13*	O2 + CPP -> 2 CO2 + PPHG
YER014W	*HEM14*	O2 + PPHGm -> PPIXm
YOR176W	*HEM15*	PPIXm -> PTHm
YGL245W	*YGL245W*	GLU + ATP -> GTRNA + AMP + PPI
YOL033W	*MSE1*	GLUm + ATPm -> GTRNAm + AMPm + PPIm
YKR069W	*MET1*	SAM + UPRG -> SAH + PC2
# QUINONE BIOSYNTHESIS		
YKL211C	*TRP3*	CHOR -> 4HBZ + PYR
YER090W	*TRP2*	CHOR -> 4HBZ + PYR
YPR176C	*BET2*	4HBZ + NPP -> N4HBZ + PPI
YJL031C	*BET4*	
YGL155W	*CDC43*	
YBR003W	*COQ1*	4HBZ + NPP -> N4HBZ + PPI
YNR041C	*COQ2*	4HBZ + NPP -> N4HBZ + PPI
YPL172C	*COX10*	4HBZ + NPP -> N4HBZ + PPI
YDL090C	*RAM1*	4HBZ + NPP -> N4HBZ + PPI
YKL019W	*RAM2*	
YBR002C	*RER2*	4HBZ + NPP -> N4HBZ + PPI
YMR101C	*SRT1*	4HBZ + NPP -> N4HBZ + PPI
YDR538W	*PAD1*	N4HBZ -> CO2 + 2NPPP
*U107_*	*U107_*	2NPPP + O2 -> 2N6H
YPL266W	*DIM1*	2N6H + SAM -> 2NPMP + SAH
*U108_*	*U108_*	2NPMPm + O2m -> 2NPMBm
YML110C	*COQ5*	2NPMBm + SAMm -> 2NPMMBm + SAHm
YGR255C	*COQ6*	2NPMMBm + O2m -> 2NMHMBm
YOL096C	*COQ3*	2NMHMBm + SAMm -> QH2m + SAHm
# MEMBRANE TRANSPORT		

Table A.29. Complete list of reactions -continued

# MITOCHONDRIAL MEMBRANE TRANSPORT		
# THE FOLLOWINGS DIFFUSE THROUGH THE INNER MITOCHONDRIAL MEMBRANE IN A NON-CARRIER-MEDIATED MANNER:		
*U109_*	*U109_*	O2 <-> O2m
*U110_*	*U110_*	CO2 <-> CO2m
*U111_*	*U111_*	ETH <-> ETHm
*U112_*	*U112_*	NH3 <-> NH3m
*U113_*	*U113_*	MTHN <-> MTHNm
*U114_*	*U114_*	THFm <-> THF
*U115_*	*U115_*	METTHFm <-> METTHF
*U116_*	*U116_*	SERm <-> SER
*U117_*	*U117_*	GLYm <-> GLY
*U118_*	*U118_*	CBHCAPm <-> CBHCAP
*U119_*	*U119_*	OICAPm <-> OICAP
*U120_*	*U120_*	PROm <-> PRO
*U121_*	*U121_*	CMPm <-> CMP
*U122_*	*U122_*	ACm <-> AC
*U123_*	*U123_*	ACAR -> ACARm
*U124_*	*U124_*	CARm -> CAR
*U125_*	*U125_*	ACLAC <-> ACLACm
*U126_*	*U126_*	ACTAC <-> ACTACm
*U127_*	*U127_*	SLF -> SLFm + Hm
*U128_*	*U128_*	THRm <-> THR
*U129_*	*U129_*	AKAm -> AKA
YMR056C	*AAC1*	ADP + ATPm + PI -> Hm + ADPm + ATP + PIm
YBL030C	*PET9*	ADP + ATPm + PI -> Hm + ADPm + ATP + PIm
YBR085W	*AAC3*	ADP + ATPm + PI -> Hm + ADPm + ATP + PIm
YJR077C	*MIR1*	PI <-> Hm + PIm
YER053C	*YER053C*	PI + OHm <-> PIm
YLR348C	*DIC1*	MAL + SUCCm <-> MALm + SUCC
YLR348C	*DIC1*	MAL + PIm <-> MALm + PI
YLR348C	*DIC1*	SUCC + PIm -> SUCCm + PI
*U130_*	*U130_*	MALT + PIm <-> MALTm + PI
YKL120W	*OAC1*	OA <-> OAm + Hm
YBR291C	*CTP1*	CIT + MALm <-> CITm + MAL
YBR291C	*CTP1*	CIT + PEPm <-> CITm + PEP
YBR291C	*CTP1*	CIT + ICITm <-> CITm + ICIT
*U131_*	*U131_*	IPPMAL <-> IPPMALm
*U132_*	*U132_*	LAC <-> LACm + Hm
*U133_*	*U133_*	PYR <-> PYRm + Hm
*U134_*	*U134_*	GLU <-> GLUm + Hm
*U135_*	*U135_*	GLU + OHm -> GLUm
YOR130C	*ORT1*	ORN + Hm <-> ORNm

Table A.29. Complete list of reactions -continued

YOR100C	*CRC1*	CARm + ACAR -> CAR + ACARm
*U136_*	*U136_*	OIVAL <-> OIVALm
*U137_*	*U137_*	OMVAL <-> OMVALm
YIL134W	*FLX1*	FAD + FMNm -> FADm + FMN
*U138_*	*U138_*	RIBFLAV <-> RIBFLAVm
*U139_*	*U139_*	DTB <-> DTBm
*U140_*	*U140_*	H3MCOA <-> H3MCOAm
*U141_*	*U141_*	MVL <-> MVLm
*U142_*	*U142_*	PA <-> PAm
*U143_*	*U143_*	4PPNTE <-> 4PPNTEm
*U144_*	*U144_*	AD <-> ADm
*U145_*	*U145_*	PRPP <-> PRPPm
*U146_*	*U146_*	DHF <-> DHFm
*U147_*	*U147_*	QA <-> QAm
*U148_*	*U148_*	OPP <-> OPPm
*U149_*	*U149_*	SAM <-> SAMm
*U150_*	*U150_*	SAH <-> SAHm
YJR095W	*SFC1*	SUCC + FUMm -> SUCCm + FUM
YPL134C	*ODC1*	AKGm + OXA <-> AKG + OXAm
YOR222W	*ODC2*	AKGm + OXA <-> AKG + OXAm
# MALATE ASPARTATE SHUTTLE		
# INCLUDED ELSEWHERE		
# GLYCEROL PHOSPHATE SHUTTLE		
*U151_*	*U151_*	T3P2m -> T3P2
*U152_*	*U152_*	GL3P -> GL3Pm
# PLASMA MEMBRANE TRANSPORT		
# CARBOHYDRATES		
YHR092C	*HXT4*	GLCxt -> GLC
YLR081W	*GAL2*	GLCxt -> GLC
YOL156W	*HXT11*	GLCxt -> GLC
YDR536W	*STL1*	GLCxt -> GLC
YHR094C	*HXT1*	GLCxt -> GLC
YOL156W	*HXT11*	GLCxt -> GLC
YEL069C	*HXT13*	GLCxt -> GLC
YDL245C	*HXT15*	GLCxt -> GLC
YJR158W	*HXT16*	GLCxt -> GLC
YFL011W	*HXT10*	GLCxt -> GLC
YNR072W	*HXT17*	GLCxt -> GLC
YMR011W	*HXT2*	GLCxt -> GLC
YHR092C	*HXT4*	GLCxt -> GLC
YDR345C	*HXT3*	GLCxt -> GLC
YHR096C	*HXT5*	GLCxt -> GLC
YDR343C	*HXT6*	GLCxt -> GLC
YDR342C	*HXT7*	GLCxt -> GLC
YJL214W	*HXT8*	GLCxt -> GLC
YJL219W	*HXT9*	GLCxt -> GLC

Table A.29. Complete list of reactions -continued

YLR081W	*GAL2*	GLACxt -> GLAC
YFL011W	*HXT10*	GLACxt -> GLAC
YOL156W	*HXT11*	GLACxt -> GLAC
YNL318C	*HXT14*	GLACxt -> GLAC
YJL219W	*HXT9*	GLACxt -> GLAC
YDR536W	*STL1*	GLACxt -> GLAC
YFL055W	*AGP3*	GLUxt <-> GLU
YDR536W	*STL1*	GLUxt <-> GLU
YKR039W	*GAP1*	GLUxt <-> GLU
YCL025C	*AGP1*	GLUxt <-> GLU
YPL265W	*DIP5*	GLUxt <-> GLU
YDR536W	*STL1*	GLUxt <-> GLU
YHR094C	*HXT1*	FRUxt -> FRU
YFL011W	*HXT10*	FRUxt -> FRU
YOL156W	*HXT11*	FRUxt -> FRU
YEL069C	*HXT13*	FRUxt -> FRU
YDL245C	*HXT15*	FRUxt -> FRU
YJR158W	*HXT16*	FRUxt -> FRU
YNR072W	*HXT17*	FRUxt -> FRU
YMR011W	*HXT2*	FRUxt -> FRU
YDR345C	*HXT3*	FRUxt -> FRU
YHR092C	*HXT4*	FRUxt -> FRU
YHR096C	*HXT5*	FRUxt -> FRU
YDR343C	*HXT6*	FRUxt -> FRU
YDR342C	*HXT7*	FRUxt -> FRU
YJL214W	*HXT8*	FRUxt -> FRU
YJL219W	*HXT9*	FRUxt -> FRU
YHR094C	*HXT1*	MANxt -> MAN
YFL011W	*HXT10*	MANxt -> MAN
YOL156W	*HXT11*	MANxt -> MAN
YEL069C	*HXT13*	MANxt -> MAN
YDL245C	*HXT15*	MANxt -> MAN
YJR158W	*HXT16*	MANxt -> MAN
YNR072W	*HXT17*	MANxt -> MAN
YMR011W	*HXT2*	MANxt -> MAN
YDR345C	*HXT3*	MANxt -> MAN
YHR092C	*HXT4*	MANxt -> MAN
YHR096C	*HXT5*	MANxt -> MAN
YDR343C	*HXT6*	MANxt -> MAN
YDR342C	*HXT7*	MANxt -> MAN
YJL214W	*HXT8*	MANxt -> MAN
YJL219W	*HXT9*	MANxt -> MAN
YDR497C	*ITR1*	MIxt + HEXT -> MI
YOL103W	*ITR2*	MIxt + HEXT -> MI
*U153_*	*U153_*	MLTxt + HEXT -> MLT
YIL162W	*SUC2*	SUCxt -> GLCxt + FRUxt

Table A.29. Complete list of reactions -continued

*U154_*	*U154_*	SUCxt + HEXT -> SUC
YBR298C	*MAL31*	MALxt + HEXT <-> MAL
*U155_*	*U155_*	MALxt + AKG <-> MAL + AKGxt
*U156_*	*U156_*	AMGxt <-> AMG
*U157_*	*U157_*	SORxt <-> SOR
*U158_*	*U158_*	ARABxt <-> ARAB
*U159_*	*U159_*	FUCxt + HEXT <-> FUC
*U160_*	*U160_*	GLTLxt + HEXT -> GLTL
*U161_*	*U161_*	GLTxt + HEXT -> GLT
*U162_*	*U162_*	GLAMxt + HEXT <-> GLAM
YLL043W	*FPS1*	GLxt <-> GL
YKL217W	*JEN1*	LACxt + HEXT <-> LAC
*U163_*	*U163_*	MNTxt + HEXT -> MNT
*U164_*	*U164_*	MELIxt + HEXT -> MELI
*U165_*	*U165_*	NAGxt + HEXT -> NAG
*U166_*	*U166_*	RMNxt + HEXT -> RMN
*U167_*	*U167_*	RIBxt + HEXT -> RIB
*U168_*	*U168_*	TRExt + HEXT -> TRE
*U170_*	*U170_*	XYLxt <-> XYL
# AMINO ACIDS		
YKR039W	*GAP1*	ALAxt + HEXT <-> ALA
YPL265W	*DIP5*	ALAxt + HEXT <-> ALA
YCL025C	*AGP1*	ALAxt + HEXT <-> ALA
YOL020W	*TAT2*	ALAxt + HEXT <-> ALA
YOR348C	*PUT4*	ALAxt + HEXT <-> ALA
YKR039W	*GAP1*	ARGxt + HEXT <-> ARG
YEL063C	*CAN1*	ARGxt + HEXT <-> ARG
YNL270C	*ALP1*	ARGxt + HEXT <-> ARG
YKR039W	*GAP1*	ASNxt + HEXT <-> ASN
YCL025C	*AGP1*	ASNxt + HEXT <-> ASN
YDR508C	*GNP1*	ASNxt + HEXT <-> ASN
YPL265W	*DIP5*	ASNxt + HEXT <-> ASN
YFL055W	*AGP3*	ASPxt + HEXT <-> ASP
YKR039W	*GAP1*	ASPxt + HEXT <-> ASP
YPL265W	*DIP5*	ASPxt + HEXT <-> ASP
YKR039W	*GAP1*	CYSxt + HEXT <-> CYS
YDR508C	*GNP1*	CYSxt + HEXT <-> CYS
YBR068C	*BAP2*	CYSxt + HEXT <-> CYS
YDR046C	*BAP3*	CYSxt + HEXT <-> CYS
YBR069C	*VAP1*	CYSxt + HEXT <-> CYS
YOL020W	*TAT2*	CYSxt + HEXT <-> CYS
YKR039W	*GAP1*	GLYxt + HEXT <-> GLY
YOL020W	*TAT2*	GLYxt + HEXT <-> GLY
YPL265W	*DIP5*	GLYxt + HEXT <-> GLY
YOR348C	*PUT4*	GLYxt + HEXT <-> GLY
YKR039W	*GAP1*	GLNxt + HEXT <-> GLN

Table A.29. Complete list of reactions -continued

YCL025C	*AGP1*	GLNxt + HEXT <-> GLN
YDR508C	*GNP1*	GLNxt + HEXT <-> GLN
YPL265W	*DIP5*	GLNxt + HEXT <-> GLN
YGR191W	*HIP1*	HISxt + HEXT <-> HIS
YKR039W	*GAP1*	HISxt + HEXT <-> HIS
YCL025C	*AGP1*	HISxt + HEXT <-> HIS
YBR069C	*VAP1*	HISxt + HEXT <-> HIS
YBR069C	*TAT1*	ILExt + HEXT <-> ILE
YKR039W	*GAP1*	ILExt + HEXT <-> ILE
YCL025C	*AGP1*	ILExt + HEXT <-> ILE
YBR068C	*BAP2*	ILExt + HEXT <-> ILE
YDR046C	*BAP3*	ILExt + HEXT <-> ILE
YBR069C	*VAP1*	ILExt + HEXT <-> ILE
YBR069C	*TAT1*	LEUxt + HEXT <-> LEU
YKR039W	*GAP1*	LEUxt + HEXT <-> LEU
YCL025C	*AGP1*	LEUxt + HEXT <-> LEU
YBR068C	*BAP2*	LEUxt + HEXT <-> LEU
YDR046C	*BAP3*	LEUxt + HEXT <-> LEU
YBR069C	*VAP1*	LEUxt + HEXT <-> LEU
YDR508C	*GNP1*	LEUxt + HEXT <-> LEU
YKR039W	*GAP1*	METxt + HEXT <-> MET
YCL025C	*AGP1*	METxt + HEXT <-> MET
YDR508C	*GNP1*	METxt + HEXT <-> MET
YBR068C	*BAP2*	METxt + HEXT <-> MET
YDR046C	*BAP3*	METxt + HEXT <-> MET
YGR055W	*MUP1*	METxt + HEXT <-> MET
YHL036W	*MUP3*	METxt + HEXT <-> MET
YKR039W	*GAP1*	PHExt + HEXT <-> PHE
YCL025C	*AGP1*	PHExt + HEXT <-> PHE
YOL020W	*TAT2*	PHExt + HEXT <-> PHE
YBR068C	*BAP2*	PHExt + HEXT <-> PHE
YDR046C	*BAP3*	PHExt + HEXT <-> PHE
YKR039W	*GAP1*	PROxt + HEXT <-> PRO
YOR348C	*PUT4*	PROxt + HEXT <-> PRO
YBR069C	*TAT1*	TRPxt + HEXT <-> TRP
YKR039W	*GAP1*	TRPxt + HEXT <-> TRP
YBR069C	*VAP1*	TRPxt + HEXT <-> TRP
YOL020W	*TAT2*	TRPxt + HEXT <-> TRP
YBR068C	*BAP2*	TRPxt + HEXT <-> TRP
YDR046C	*BAP3*	TRPxt + HEXT <-> TRP
YBR069C	*TAT1*	TYRxt + HEXT <-> TYR
YKR039W	*GAP1*	TYRxt + HEXT <-> TYR
YCL025C	*AGP1*	TYRxt + HEXT <-> TYR
YBR068C	*BAP2*	TYRxt + HEXT <-> TYR
YBR069C	*VAP1*	TYRxt + HEXT <-> TYR
YOL020W	*TAT2*	TYRxt + HEXT <-> TYR

Table A.29. Complete list of reactions -continued

YDR046C	*BAP3*	TYRxt + HEXT <-> TYR
YKR039W	*GAP1*	VALxt + HEXT <-> VAL
YCL025C	*AGP1*	VALxt + HEXT <-> VAL
YDR046C	*BAP3*	VALxt + HEXT <-> VAL
YBR069C	*VAP1*	VALxt + HEXT <-> VAL
YBR068C	*BAP2*	VALxt + HEXT <-> VAL
YFL055W	*AGP3*	SERxt + HEXT <-> SER
YCL025C	*AGP1*	SERxt + HEXT <-> SER
YDR508C	*GNP1*	SERxt + HEXT <-> SER
YKR039W	*GAP1*	SERxt + HEXT <-> SER
YPL265W	*DIP5*	SERxt + HEXT <-> SER
YBR069C	*TAT1*	THRxt + HEXT <-> THR
YCL025C	*AGP1*	THRxt + HEXT <-> THR
YKR039W	*GAP1*	THRxt + HEXT <-> THR
YDR508C	*GNP1*	THRxt + HEXT <-> THR
YNL268W	*LYP1*	LYSxt + HEXT <-> LYS
YKR039W	*GAP1*	LYSxt + HEXT <-> LYS
YLL061W	*MMP1*	MMETxt + HEXT -> MMET
YPL274W	*SAM3*	SAMxt + HEXT -> SAM
YOR348C	*PUT4*	GABAxt + HEXT -> GABA
YDL210W	*UGA4*	GABAxt + HEXT -> GABA
YBR132C	*AGP2*	CARxt <-> CAR
YGL077C	*HNM1*	CHOxt + HEXT -> CHO
YNR056C	*BIO5*	BIOxt + HEXT -> BIO
YDL210W	*UGA4*	ALAVxt + HEXT -> ALAV
YKR039W	*GAP1*	ORNxt + HEXT <-> ORN
YEL063C	*CAN1*	ORNxt + HEXT <-> ORN
*U171_*	*U171_*	PTRSCxt + HEXT -> PTRSC
*U172_*	*U172_*	SPRMDxt + HEXT -> SPRMD
YKR093W	*PTR2*	DIPEPxt + HEXT -> DIPEP
YKR093W	*PTR2*	OPEPxt + HEXT -> OPEP
YKR093W	*PTR2*	PEPTxt + HEXT -> PEPT
YBR021W	*FUR4*	URAxt + HEXT -> URA
*U173_*	*U173_*	NMNxt + HEXT -> NMN
YER056C	*FCY2*	CYTSxt + HEXT -> CYTS
YER056C	*FCY2*	ADxt + HEXT -> AD
YER056C	*FCY2*	GNxt + HEXT <-> GN
YER060W	*FCY21*	CYTSxt + HEXT -> CYTS
YER060W	*FCY21*	ADxt + HEXT -> AD
YER060W	*FCY21*	GNxt + HEXT <-> GN
YER060W-A	*FCY22*	CYTSxt + HEXT -> CYTS
YER060W-A	*FCY22*	ADxt + HEXT -> AD
YER060W-A	*FCY22*	GNxt + HEXT <-> GN
YGL186C	*YGL186C*	CYTSxt + HEXT -> CYTS
YGL186C	*YGL186C*	ADxt + HEXT -> AD

Table A.29. Complete list of reactions -continued

YGL186C	*YGL186C*	GNxt + HEXT <-> GN
*U174_*	*U174_*	ADNxt + HEXT -> ADN
*U175_*	*U175_*	GSNxt + HEXT -> GSN
YBL042C	*FUI1*	URIxt + HEXT -> URI
*U176_*	*U176_*	CYTDxt + HEXT -> CYTD
*U177_*	*U177_*	INSxt + HEXT -> INS
*U178_*	*U178_*	XTSINExt + HEXT -> XTSINE
*U179_*	*U179_*	DTxt + HEXT -> DT
*U180_*	*U180_*	DINxt + HEXT -> DIN
*U181_*	*U181_*	DGxt + HEXT -> DG
*U182_*	*U182_*	DAxt + HEXT -> DA
*U183_*	*U183_*	DCxt + HEXT -> DC
*U184_*	*U184_*	DUxt + HEXT -> DU
*U185_*	*U185_*	ADNxt + HEXT -> ADN
YBL042C	*FUI1*	URIxt + HEXT -> URI
*U186_*	*U186_*	CYTDxt + HEXT -> CYTD
*U187_*	*U187_*	DTxt + HEXT -> DT
*U188_*	*U188_*	DAxt + HEXT -> DA
*U189_*	*U189_*	DCxt + HEXT -> DC
*U190_*	*U190_*	DUxt + HEXT -> DU
*U191_*	*U191_*	ADNxt + HEXT -> ADN
*U192_*	*U192_*	GSNxt + HEXT -> GSN
YBL042C	*FUI1*	URIxt + HEXT -> URI
*U193_*	*U193_*	CYTDxt + HEXT -> CYTD
*U194_*	*U194_*	INSxt + HEXT -> INS
*U195_*	*U195_*	DTxt + HEXT -> DT
*U196_*	*U196_*	DINxt + HEXT -> DIN
*U197_*	*U197_*	DGxt + HEXT -> DG
*U198_*	*U198_*	DAxt + HEXT -> DA
*U199_*	*U199_*	DCxt + HEXT -> DC
*U200_*	*U200_*	DUxt + HEXT -> DU
*U201_*	*U201_*	HYXNxt + HEXT <-> HYXN
*U202_*	*U202_*	XANxt <-> XAN
# METABOLIC BY-PRODUCTS		
YCR032W	*BPH1*	ACxt + HEXT <-> AC
*U203_*	*U203_*	FORxt <-> FOR
*U204_*	*U204_*	ETHxt <-> ETH
*U205_*	*U205_*	SUCCxt + HEXT <-> SUCC
YKL217W	*JEN1*	PYRxt + HEXT -> PYR
# OTHER COMPOUNDS		
YHL016C	*DUR3*	UREAxt + 2 HEXT <-> UREA
YGR121C	*MEP1*	NH3xt <-> NH3
YNL142W	*MEP2*	NH3xt <-> NH3
YPR138C	*MEP3*	NH3xt <-> NH3

Table A.29. Complete list of reactions -continued

YJL129C	*TRK1*	Kxt + HEXT <-> K
YBR294W	*SUL1*	SLFxt -> SLF
YLR092W	*SUL2*	SLFxt -> SLF
YGR125W	*YGR125W*	SLFxt -> SLF
YML123C	*PHO84*	PIxt + HEXT <-> PI
*U206_*	*U206_*	CITxt + HEXT <-> CIT
*U207_*	*U207_*	FUMxt + HEXT <-> FUM
*U208_*	*U208_*	C140xt -> C140
*U209_*	*U209_*	C160xt -> C160
*U210_*	*U210_*	C161xt -> C161
*U211_*	*U211_*	C180xt -> C180
*U212_*	*U212_*	C181xt -> C181
*U213_*	*U213_*	AKGxt + HEXT <-> AKG
YLR138W	*NHA1*	NAxt <-> NA + HEXT
YCR028C	*FEN2*	PNTOxt + HEXT <-> PNTO
*U214_*	*U214_*	ATP -> ADP + PI
YCR024C-A	*PMP1*	ATP -> ADP + PI + HEXT
YEL017C-A	*PMP2*	ATP -> ADP + PI + HEXT
YGL008C	*PMA1*	ATP -> ADP + PI + HEXT
YPL036W	*PMA2*	ATP -> ADP + PI + HEXT
*U215_*	*U215_*	GLALxt <-> GLAL
*U216_*	*U216_*	ACALxt <-> ACAL
YLR237W	*THI7*	THMxt + HEXT -> THIAMIN
YOR071C	*YOR071C*	THMxt + HEXT -> THIAMIN
YOR192C	*YOR192C*	THMxt + HEXT -> THIAMIN
YIR028W	*DAL4*	ATNxt -> ATN
YJR152W	*DAL5*	ATTxt -> ATT
*U217_*	*U217_*	MTHNxt <-> MTHN
*U218_*	*U218_*	PAPxt <-> PAP
*U219_*	*U219_*	DTTPxt <-> DTTP
*U220_*	*U220_*	THYxt <-> THY + HEXT
*U221_*	*U221_*	GA6Pxt <-> GA6P
YGR065C	*VHT1*	BTxt + HEXT <-> BT
*U222_*	*U222_*	AONAxt + HEXT <-> AONA
*U223_*	*U223_*	DANNAxt + HEXT <-> DANNA
*U224_*	*U224_*	OGTxt -> OGT
*U225_*	*U225_*	SPRMxt -> SPRM
*U226_*	*U226_*	PIMExt -> PIME
*U227_*	*U227_*	O2xt <-> O2
*U228_*	*U228_*	CO2xt <-> CO2
YOR011W	*AUS1*	ERGOSTxt <-> ERGOST
YOR011W	*AUS1*	ZYMSTxt <-> ZYMST
*U229_*	*U229_*	RFLAVxt + HEXT -> RIBFLAV

The abbreviations for extracellular metabolites are the following: AC, ACAL, AD, ADN, AKG, ALA, AONA, ARAB, ARG, ASN, ASP, ATN, BT, C140, C160, C161, C180, C181, CHO, CIT, CO2, CYS, CYTD, CYTS, DA, DANNA, DC, DG, DIN, DIPEP, DT, DTTP, DU, ETH, FOR, FRU, FUC, FUM, GA6P, GABA, GL, GL3P, GLAC, GLAL, GLAM, GLCN, GLN, GLT, GLU, GLY, GN, GSN, HIS, ILE, INS, INS, LAC, LEU, LYS, MAL, MAN, MAN, MDAP, MELI, MET, MI, MK, MMET, MNT, MTHN, MVL, NA, OGT, OPEP, ORN, PAP, PEPT, PHE, PIME, PNTO, PRO, PTRC, PYR, PYRDX, RIB, RMN, SAM, SER, SOR, SPMD, SPRM, SUC, SUCC, THR, THY, TRE, TRP, TYR, URA, UREA, URI, VAL, XAN, XTSN.

The main code for genome scale flux balance analysis and MOMA is given as:

```
clear all

load stoich_sparse822_1172
load gene
load metname
load revirrev

extmet = textread('extmet.txt','%s','delimiter',',');
  for i = 1:length(extmet)
     extmet2{i} = [extmet{i} 'xt'];
  end

[metnum rxnnum] = size(stoich_sparse);

for i = 1:length(extmet2) % secreted
   a= strmatch(extmet2{i},metname,'exact');
   rxnnum = rxnnum + 1;
   stoich_sparse(a,rxnnum) = -1;
   lb(rxnnum) = 0; ub(rxnnum) = 1000;

   % aa= strmatch(extmet{i},metname,'exact');
   % stoich_sparse(aa,rxnnum) = 1;
end

 upmet = {'SLF' 'ZYMST' 'ERGOST' 'O2' 'NH3' 'PI' 'GLC'};
upmet2 = {'SLFxt' 'ZYMSTxt' 'ERGOSTxt' 'O2xt' 'NH3xt' 'PIxt' 'GLCxt'};
for i = 1:length(upmet2) % uptaken
   a= strmatch(upmet2{i},metname,'exact');
   rxnnum = rxnnum + 1;
   stoich_sparse(a,rxnnum) = -1;
   lb(rxnnum) = -1000; ub(rxnnum) = 0;
```

```
 %   aa= strmatch(upmet{i},metname,'exact');
 %   stoich_sparse(aa,rxnnum) = 1;
end

revirrev = cellstr(revirrev');
for i = 1:length(revirrev) % reflect direcn of reactions as lb ub.
   if length(strfind(revirrev{i},'I') ) ~= 0
      lb(i) = 0; ub(i) = 1000;
   else
      lb(i) = -1000; ub(i) = 1000;
   end
end

allrxnname = [gene; {'Growth'}; extmet2'; upmet2'];

 lb(1125) = -1000; % JEN1- to allow PYR secretion
 ub(1125) = 0;

 % FBA
 % ====

f = zeros(1,length(allrxnname));
% f(strmatch('O2xt',allrxnname,'exact')) = -1;
% f(strmatch('GLCxt',allrxnname,'exact')) = -1; % COMPLEX IV
% f(strmatch('BIOMxt',allrxnname,'exact')) = 1;
 f(strmatch('ETHxt',allrxnname,'exact')) =-1;
b = zeros(metnum,1);

% MEAS RATES
% ============
% meas = [GLC  BIOM  AC     ACAL    SUCC   GOH   PYR]
  Rm = [-3.7709          0.1          0.00         0.00         0.0459      0.0  0.0158]; % BY4743
%  Rm = [-3.5923         0.1          0.00         0.00         0.0355      0.0  0.0091]; % HO
%  Rm = [-4.6573         0.1          0.00         0.00         0.0585      0.0  0.0174]; % QDR3
%  Rm = [-5.3862         0.1          0.00         0.00         0.0898      0.0  0.0097]; % MIG1
%  Rm = [-3.6086         0.1          0.00         0.00         0.0902      0.0  0.0036]; % HAP4
%  Rm = [-3.9853         0.1          0.00         0.00         0.0308  0.0  0.0184]; % QCR7
%  Rm = [-15.6168       0.1          0.00         0.00         0.0020      0.0  0.0501]; % RIP1
%  Rm = [-8.2437         0.1          0.00         0.00         0.0197      0.0  0.0030]; % CYT1


% metaboite units:mmole/gDW/hr - biomass unit:g/gDW/hr%

lb(strmatch('GLCxt',allrxnname,'exact')) = Rm(1);
ub(strmatch('GLCxt',allrxnname,'exact')) = Rm(1);

lb(strmatch('Growth',allrxnname,'exact')) = Rm(2);
ub(strmatch('Growth',allrxnname,'exact')) = Rm(2);

%lb(strmatch('ACxt',allrxnname,'exact')) = Rm(3);
```

```
%ub(strmatch('ACxt',allrxnname,'exact')) = Rm(3);

%lb(strmatch('ACALxt',allrxnname,'exact')) = Rm(4);
%ub(strmatch('ACALxt',allrxnname,'exact')) = Rm(4);

lb(strmatch('SUCCxt',allrxnname,'exact')) = Rm(5);
ub(strmatch('SUCCxt',allrxnname,'exact')) = Rm(5);

%lb(strmatch('GLxt',allrxnname,'exact')) = Rm(6);
%ub(strmatch('GLxt',allrxnname,'exact')) = Rm(6);

lb(strmatch('PYRxt',allrxnname,'exact')) = Rm(7);
ub(strmatch('PYRxt',allrxnname,'exact')) = Rm(7);

%---------------------------------------------------------------

lb(strmatch('ZYMSTxt',allrxnname,'exact')) = 0;
ub(strmatch('ZYMSTxt',allrxnname,'exact')) = 0;

lb(strmatch('ERGOSTxt',allrxnname,'exact')) = 0;
ub(strmatch('ERGOSTxt',allrxnname,'exact')) = 0;

% lb(strmatch('Growth',allrxnname,'exact')) = 0.281;
% ub(strmatch('Growth',allrxnname,'exact')) = 0.281;
%
% lb(strmatch('NH3xt',allrxnname,'exact')) = -2.5;
% ub(strmatch('NH3xt',allrxnname,'exact')) = -0.5;
% %
% lb(strmatch('SLFxt',allrxnname,'exact')) = -0.03;
% ub(strmatch('SLFxt',allrxnname,'exact')) = -0.007;
% %

lb(strmatch('PIxt',allrxnname,'exact')) = -1000;
ub(strmatch('PIxt',allrxnname,'exact')) = 1000;

lb(strmatch('U214_',allrxnname,'exact')) = 1; % ATP maintenance
ub(strmatch('U214_',allrxnname,'exact')) = 1;

%   e = zeros(length(allrxnname),1);
%   [objfs,X] = lp_solve(-f,stoich_sparse,b,e,lb',ub',[],[]); % LP SOLVE 5.1
%
%   display('------------'); display('FBA Solution'); display('------------');
% sim_out(X,allrxnname);

 % return

  [X, objfun] = linprog(f,[],[],stoich_sparse,b,lb',ub'); %MOSEK- TOMLAB OR MATLAB
  %objfun

 %1: Primal simplex. 2: Dual simplex. 3: Network simplex. 4: Barrier. 5: Sifting.
```

```
 cpxControl.LPMETHOD = 2; % 6: Concurrent..

[Xcp,slack,vv,rc,f_k,ninf, sinf, Inform] = ...
    cplex(f,stoich_sparse,lb,ub,b,[],cpxControl); % TOMLAB/CPLEX
Inform
display('------------'); display('FBA Solution'); display('------------');
sim_out(Xcp,allrxnname);


%return


% MOMA FOR DEFICIENT STRAINS %
%========================== %

%  Rmm = [-3.5923      0.1         0.00        0.00        0.0355      0.0  0.0091]; % HO
%  Rmm = [-4.6573      0.1         0.00        0.00        0.0585      0.0  0.0174]; % QDR3
%  Rmm = [-5.3862      0.1         0.00        0.00        0.0898      0.0  0.0097]; % MIG1
%  Rmm = [-3.6086      0.1         0.00        0.00        0.0902      0.0  0.0036]; % HAP4
%  Rmm = [-3.9853      0.1         0.00        0.00        0.0308  0.0  0.0184]; % QCR7
%  Rmm = [-15.6168     0.1         0.00        0.00        0.0020      0.0  0.0501]; % RIP1
  Rmm = [-8.2437      0.1         0.00        0.00        0.0197      0.0  0.0030]; % CYT1


lb(strmatch('GLCxt',allrxnname,'exact')) = Rmm(1);  %5.667;%4.706;%   2.994;
ub(strmatch('GLCxt',allrxnname,'exact')) = Rmm(1);  %5.667;%4.706;%    2.994;

lb(strmatch('Growth',allrxnname,'exact')) = Rmm(2);
ub(strmatch('Growth',allrxnname,'exact')) = Rmm(2);

%lb(strmatch('ACxt',allrxnname,'exact')) = Rmm(3);   %0.0333;%0.0243;%    0.009;
%ub(strmatch('ACxt',allrxnname,'exact')) = Rmm(3);   %0.0333;%0.0243;%    0.009;

%lb(strmatch('ACALxt',allrxnname,'exact')) = Rmm(4);   %0.01587;%0.01324;%    0.0049;
%ub(strmatch('ACALxt',allrxnname,'exact')) = Rmm(4);   %0.01587;%0.01324;%    0.0049;

lb(strmatch('SUCCxt',allrxnname,'exact')) = Rmm(5);   %0.0169;%0.0124;%  0.0137;
ub(strmatch('SUCCxt',allrxnname,'exact')) = Rmm(5); %0.0169;%0.0124;%  0.0137;

%lb(strmatch('GLxt',allrxnname,'exact')) = Rmm(6);  %0.456;%0.434;% 0.206;
%ub(strmatch('GLxt',allrxnname,'exact')) = Rmm(6);  %0.456;%0.434;% 0.206;

lb(strmatch('PYRxt',allrxnname,'exact')) = Rm(7);
ub(strmatch('PYRxt',allrxnname,'exact')) = Rm(7);

 H3 = eye(length(allrxnname),length(allrxnname));
 f3 = -Xcp;
 f3 = zeros(1,length(allrxnname)); f3(1:length(gene)) = -X(1:length(gene));
  [X3, objfun3] = quadprog(H3,f3,[],[],stoich_sparse,b,lb',ub');
 cpxControl.LPMETHOD = 2; % 6: Concurrent..
```

```
 [Xcp3,slack3,vv3,rc3,f_k3,ninf3, sinf3, Inform3] = ...
    cplex(f3,stoich_sparse,lb,ub,b,[],cpxControl,[],[],[],[],[],[],[],[],H3); % TOMLAB/CPLEX
Inform3 %plot(stoich_sparse*Xcp3-b)
%  return
%  load XcpM_all;
%  for i = 1:length(allrxnname);%size(XcpM_all,2)
%   f3 = -full(XcpM_all(:,i));
%  f3 = zeros(1,length(allrxnname)); f3(1:length(gene)) = -X(1:length(gene));
%   [X3, objfun3] = quadprog(H3,f3,[],[],stoich_sparse,b,lb',ub');
%  cpxControl.LPMETHOD = 2; % 6: Concurrent..
%
%  [Xcp3M(:,i),slack3,vv3,rc3,f_k3(i),ninf3, sinf3, Inform3] = ...
%      cplex(f3,stoich_sparse,lb,ub,b,[],cpxControl,[],[],[],[],[],[],[],[],H3); % TOMLAB/CPLEX
% Inform3 % plot(stoich_sparse*Xcp3-b)
%  end
%
%  x_eth3 = [Xcp3M(strmatch('ETHxt',allrxnname,'exact'),1:length(allrxnname))  ];
% %subplot(211); plot(x_eth3);
%
% b03=[Xcp3M(strmatch('CO2xt',allrxnname,'exact'),1:length(allrxnname)) ];
% b13=[Xcp3M(strmatch('O2xt',allrxnname,'exact'),1:length(allrxnname)) ];
%
% RQ3 = -b03./b13;
% %subplot(212); plot(RQ3);
% XcpM_all =  [XcpM_max XcpM_min];
% save XcpM_all XcpM_all;

display('MOMA Solution')
display('-------------')
sim_out(Xcp3,allrxnname);

return
```

The subprograms are given as the followings:

adkoy

```
%FUNCTION DEFINITION

function stoich = adkoy(out, metname, index) % out is the reactant with its coefficient in string form

global stoich    % if not; the main program (or command window) will forget
            % the entries generated in the previous executions of the
            % function.
global depo_metnum_match % stores the counted/processed met. names
                  % to test if any metabolite remains untouched.
out = strtrim(out); % a metabolite either with or without coefficients

if length(strmatch(out, metname, 'exact')) ~= 0    % if  the stoich. coeff is 1 and not explicitly written in the input file.
  metnum_match = strmatch(out,metname,'exact');   % identify the place of metabolite 'out' in 'metname' vector.
```

```
  stoich(metnum_match,index) = -1;              % assign stoichiometric coefficient as -1;
  depo_metnum_match(metnum_match)= 1;
else
  space_count = findstr(' ',char(out)); % determine the number of spaces in 'out'.

  if length(space_count) == 1 % if the number of spaces is ONE.
    [outa, outb] = strread(char(out),'%s %s','delimiter',' '); % separate the reactant from
                                                % its stoich. coeff. if available.

    if length(str2num(char(outa)))~= 0 %if there exists a stoich. coeff (different than 1) for the metabolite.
      metnum_match = strmatch(outb,metname,'exact'); % identify the place of metabolite 'outb' in 'metname' vector.
      depo_metnum_match(metnum_match)= 1;
      stoich(metnum_match,index) = -str2num(char(outa)); %assign stoichiometric coefficient as -outa
    elseif length(str2num(char(outa))) == 0; figure; xlabel(out);
    end


  elseif length(space_count) == 2 % if the number of spaces is TWO.
    [outa, outb, outc] = strread(char(out),'%s %s %s','delimiter',' ')

    if length(str2num(char(outa)))~= 0 % if there exists a stoich. coeff for the metabolite.

      outb = char(strtrim(outb)) % convert to character arrays and remove blanks.
      outc = char(strtrim(outc))
      comb = cellstr(strcat([outb blanks(1) outc])) % put the other pieces back after the stoichiometry is identified.
      metnum_match = strmatch(comb,metname,'exact') % identify the place of metabolite 'outb outc' in 'metname' vector.
      depo_metnum_match(metnum_match)= 1;
      stoich(metnum_match,index) = -str2num(char(outa)); % assign stoichiometric coefficient as -outa
    elseif length(str2num(char(outa))) == 0; figure; xlabel(out);
    end


  else
   figure; xlabel(strcat(out,num2str(index))); % else if the number of space is higher than TWO.
  end      %   if length(space_count) == 1 : 4 % if the number of spaces is ONE. (to FOUR)

end        %   if length(strmatch(out, metname, 'exact')) ~= 0 : else


return
```

adkoy_prdct

```
%FUNCTION DEFINITION

function stoich = adkoy(out, metname, index) % out is the reactant with its coefficient in string form

global stoich    % if not; the main program (or command window) will forget
```

```
            % the entries generated in the previous executions of the
            % function.
global depo_metnum_match
out = strtrim(out);

if length(strmatch(out, metname, 'exact')) ~= 0    % if  the stoich. coeff is 1 and not explicitly written in the input file.
  metnum_match = strmatch(out,metname,'exact');   % identify the place of metabolite 'out' in 'metname' vector.
  depo_metnum_match(metnum_match)= 1;
  stoich(metnum_match,index) = 1;                % assign stoichiometric coefficient as -1;
else
  space_count = findstr(' ',char(out)); % determine the number of spaces in 'out'.

  if length(space_count) == 1 % if the number of spaces is ONE.
     [outa, outb] = strread(char(out),'%s %s','delimiter',' '); % separate the reactant from its stoich. coeff. if available.

      if length(str2num(char(outa)))~= 0 %if there exist a stoich. coeff for the first metabolite
         metnum_match = strmatch(outb,metname,'exact'); % identify the place of metabolite 'out1b' in 'metname' vector.
         depo_metnum_match(metnum_match)= 1;
         stoich(metnum_match,index) = str2num(char(outa)); %assign stoichiometric coefficient as -outa
      elseif length(str2num(char(outa))) == 0; figure; xlabel(out);
       end


  elseif length(space_count) == 2
         [outa, outb, outc] = strread(char(out),'%s %s %s','delimiter',' ')

      if length(str2num(char(outa)))~= 0 %if there exist a stoich. coeff for the first metabolite
         outb = char(strtrim(outb)) %convert to character arrays
         outc = char(strtrim(outc))
         comb = cellstr(strcat([outb blanks(1) outc])) % put the other pieces back after the stoichiometry is identified.
         metnum_match = strmatch(comb,metname,'exact') % identify the place of metabolite 'out1b' in 'metname' vector.
         depo_metnum_match(metnum_match)= 1;
         stoich(metnum_match,index) = str2num(char(outa)); %assign stoichiometric coefficient as -outa
      elseif length(str2num(char(outa))) == 0; figure; xlabel(out);
       end


  else
  figure; xlabel(strcat(out,num2str(index)));  % else if the number of space is higher than four.

  end

end

return
```

text2mat

```
clear all
% Do not forget to change the arrow in one metabolite in rxn FSP2_2 to '--'
% both in met and rxn list.

tic
global stoich
global depo_metnum_match % stores the counted/processed met. names
                         % to test if any metabolite remains untouched.

%metname = textread('mets_712.txt', '%s','delimiter', '\t'); % a string of met. names.
[metname, fullmetname] = textread('Metabolite_List_Webpage.txt','%s %s','delimiter','\t');
metname = strtrim(metname); % remove unnecessary whitespaces

extmet = textread('extmet.txt','%s','delimiter',',');

for i = 1:length(extmet)
   extmet{i} = [extmet{i} 'xt'];
end

metname = [metname; extmet];

metname_ek = {'OPP' 'OPPm' 'RFLAVxt' 'SLFxt' 'ZYMSTxt' 'ERGOSTxt' 'O2xt' 'ATTxt' 'NH3xt' 'Kxt' 'AMGxt' 'XTSINExt' ...
   'SPRMDxt' 'PTRSCxt' 'XYLxt' 'ALAVxt' 'THMxt' 'HYXNxt' 'PIxt' 'NMNxt' 'NAGxt' 'BIOxt' 'CARxt' 'GLTLxt' 'MLTxt' 'GLCxt'...
   'NMN' 'GLTL' 'RIP' 'C100ACPm' 'NMNm' 'C260COA' 'MACAC' 'C240COA' 'AACCOAm'};

metname = [metname; metname_ek'];
metname = strtrim(metname);

mm=1;
for i = 1: length(metname)    % check the number of whitespace a met. name has.
  if_space = findstr(' ',char(metname(i)));
  no_of_space(i) = length(if_space);
end
% plot(no_of_space);  % metabolites 128, 140, 253, 317 have more than one
% space.


[orf, ec, gene, gene_desc, rxn] = textread('Reaction_List_Webpage.txt','%s %s %s %s %s','delimiter','\t','commentstyle','shell','headerlines',1);
rxn = strtrim(rxn);

% for some ORFs, there is no corresponding rxn. (or that ORF catalzyes  not a different rxn.)
% for these cases, corresponding rxn field is empty. Below is a loop to
% find and remove these lines.
m = 1;
for i = 1:length(rxn)
   if isempty(rxn{i}) == 1
     K(m) = i;
     m = m+1;
```

```
    end
  end

  rxn(K) = [];
  gene(K) = [];
  for i = 1: length(rxn)
  [rctant(i), prduct(i)] = strread(rxn{i},'%s %s', 'delimiter', '>');
  end
  rctant = rctant';       prduct = prduct';

  j=1; % remove remaining '-' and '->' from rctant elements.
  for i = 1:length(rctant)
    if isempty( strfind(rctant{i}, ' -') ) == 0 % if rctant includes ' -'
      rctant{i} = strrep(rctant{i},' -',''); % replace (remove) ' -' and '<-'.
      revirrev(i) = 'I'; % irreversible rxn.
    elseif isempty( strfind(rctant{i}, ' <-') ) == 0 % if rctant includes ' -'
      revirrev(i) = 'R'; % irreversible rxn.
    else
       hata(j) = i;    j = j +1;
    end
  end
  rctant = strtrim(rctant);

  reactant = rctant;  prdct = prduct;

  % now, a very good separation of reactants and products was achieved.

  %=========================================================
  %************   STOICH. COEFFS OF REACTANTS   ************
  %=========================================================

  for i = 1:length(reactant) %i.e: = 13. % for REACTANTS
    if length(strfind(reactant{i}, ' + ')) == 0 %there is ONE reactant
      %out1 = strread(reactant{i},'%s','delimiter','+'); % identify the reactant individually
       out1 = reactant{i}; %the line above is unnecessary for 1 reactant case, and leads to wrong results for rxns U101, U102,
FNADH, FNADPH.
      stoich =  adkoy(out1, metname, i);
      % sparse_stoich = sparse(stoich)
  % ------------------------------------------------------------------------
    elseif length(strfind(reactant{i}, ' + '))== 1 % there are TWO reactants
                                % note that, I use ' + ', not '+' to determine the
                                % number of reactants. Otherwise, I can get some
                                % misleading results since some met. names include '+'.

      reactant(i) = strrep(reactant(i),' + ',' @ ');% since there are some met. names including '+',
                                  % such as NAD+, NADP+, I replace all ' + ' with ' @ '.
                                  % Hence, there will be no confusion.

      [out1, out2] = strread(reactant{i},'%s %s','delimiter','@'); % identify the reactants individually
```

```
    stoich =  adkoy(out1, metname, i);
    stoich =  adkoy(out2, metname, i);
%-------------------------------------------------------------------------

 elseif length(strfind(reactant{i}, ' + '))== 2 % there are THREE reactants
    reactant(i) = strrep(reactant(i),' + ',' @ ');
    [out1, out2, out3] = strread(reactant{i},'%s %s %s','delimiter','@');

    stoich =  adkoy(out1, metname, i);
    stoich =  adkoy(out2, metname, i);
    stoich =  adkoy(out3, metname, i);
% ---------------------------------------------------------------

  elseif length(strfind(reactant{i}, ' + '))== 3 % there are FOUR reactants
    reactant(i) = strrep(reactant(i),' + ',' @ ');
    [out1, out2, out3, out4] = strread(reactant{i},'%s %s %s %s','delimiter','@');

    stoich =  adkoy(out1, metname, i);
    stoich =  adkoy(out2, metname, i);
    stoich =  adkoy(out3, metname, i);
    stoich =  adkoy(out4, metname, i);
% ---------------------------------------------------------------
  elseif length(strfind(reactant{i}, ' + '))== 4 % there are FIVE reactants (valid for only a few reactants)
    reactant(i) = strrep(reactant(i),' + ',' @ ');
    [out1, out2, out3, out4, out5] = strread(reactant{i},'%s %s %s %s %s','delimiter','@');

    stoich =  adkoy(out1, metname, i);
    stoich =  adkoy(out2, metname, i);
    stoich =  adkoy(out3, metname, i);
    stoich =  adkoy(out4, metname, i);
    stoich =  adkoy(out5, metname, i);
% ---------------------------------------------------------------
   elseif length(strfind(reactant{i}, ' + '))== 5 % there are SIX reactants (valid for only a few reactants)
    reactant(i) = strrep(reactant(i),' + ',' @ ');
    [out(1), out(2), out(3), out(4), out(5), out(6)] = strread(reactant{i},'%s %s %s %s %s %s','delimiter','@');

    for k = 1:6
    stoich =  adkoy(out(k), metname, i);
    end
% ---------------------------------------------------------------
   elseif length(strfind(reactant{i}, ' + '))== 6 % there are SEVEN reactants (valid for only a few reactants)
    reactant(i) = strrep(reactant(i),' + ',' @ ');
    [out(1), out(2), out(3), out(4), out(5), out(6), out(7)] = strread(reactant{i},'%s %s %s %s %s %s %s','delimiter','@');
   i
    for k = 1:7
    stoich =  adkoy(out(k), metname, i);
    end
% ---------------------------------------------------------------
   elseif length(strfind(reactant{i}, ' + '))== 7 % there are EIGHT reactants (valid for only a few reactants)
    reactant(i) = strrep(reactant(i),' + ',' @ ');
```

```
            [out(1), out(2), out(3), out(4), out(5), out(6), out(7) out(8)] = strread(reactant{i},'%s %s %s %s %s %s %s %s','delimiter','@');

            for k = 1:8
             stoich =  adkoy(out(k), metname, i);
            end
          % ------------------------------------------------------------------

           elseif length(strfind(reactant{i}, ' + '))== 8 % there are EIGHT reactants (valid for only a few reactants)
             reactant(i) = strrep(reactant(i),' + ',' @ ');
             [out(1), out(2), out(3), out(4), out(5), out(6), out(7) out(8) out(9)] = strread(reactant{i},'%s %s %s %s %s %s %s %s %s','delimiter','@');

            for k = 1:9
             stoich =  adkoy(out(k), metname, i);
            end
          % ------------------------------------------------------------------

           elseif length(strfind(reactant{i}, ' + '))== 9 % there are NINE reactants (valid for only a few reactants)
             reactant(i) = strrep(reactant(i),' + ',' @ ');
             [out(1), out(2), out(3), out(4), out(5), out(6), out(7) out(8) out(9) out(10)] = strread(reactant{i},'%s %s %s %s %s %s %s %s %s %s','delimiter','@');

            for k = 1:10
             stoich =  adkoy(out(k), metname, i);
            end
          % ------------------------------------------------------------------

           else % if there are rxns with more than 8 products, count them (mm), and give the rxn no (i).
             vvv(mm) = i;
             mm= mm+1;
           end
          %    if length(strfind(reactant{i}, ' + '))== 6 % there are SEVEN reactants
          %       figure
          %       xlabel(reactant(i));
          %    end

          end
          stoich_sparse = sparse(stoich);

          %=========================================================
          %************   STOICH. COEFFS OF PRODUCTS   ************%
          %=========================================================

          for i = 1:length(prdct) %i.e: = 13. % for PRODUCTS

            if length(strfind(prdct{i}, ' + '))== 0 %there is ONE prdct
             out1 = strread(prdct{i},'%s','delimiter','@'); % identify the prdct individually

             stoich =  adkoy_prdct(out1, metname, i);
```

```
% ------------------------------------------------------------------

  elseif length(strfind(prdct{i}, ' + '))== 1 %there are TWO prdcts
    prdct(i) = strrep(prdct(i),' + ',' @ ');
    [out1, out2] = strread(prdct{i},'%s %s','delimiter','@');

    stoich =  adkoy_prdct(out1, metname, i);
    stoich =  adkoy_prdct(out2, metname, i);
%---------------------------------------------------------------------------

  elseif length(strfind(prdct{i}, ' + '))== 2 %there are THREE prdcts
    prdct(i) = strrep(prdct(i),' + ',' @ ');
    [out1, out2, out3] = strread(prdct{i},'%s %s %s','delimiter','@');

    stoich =  adkoy_prdct(out1, metname, i);
    stoich =  adkoy_prdct(out2, metname, i);
    stoich =  adkoy_prdct(out3, metname, i);
% ------------------------------------------------------------------

  elseif length(strfind(prdct{i}, ' + '))== 3 %there are FOUR prdcts
    prdct(i) = strrep(prdct(i),' + ',' @ ');
    [out1, out2, out3, out4] = strread(prdct{i},'%s %s %s %s','delimiter','@'); % identify the prdcts individually

    stoich =  adkoy_prdct(out1, metname, i);
    stoich =  adkoy_prdct(out2, metname, i);
    stoich =  adkoy_prdct(out3, metname, i);
    stoich =  adkoy_prdct(out4, metname, i);
% ------------------------------------------------------------------
  elseif length(strfind(prdct{i}, ' + '))== 4 % there are FIVE prdcts (valid for only a few cases in GSM_751).
    prdct(i) = strrep(prdct(i),' + ',' @ ');
    [out1, out2, out3, out4, out5] = strread(prdct{i},'%s %s %s %s %s','delimiter','@'); % identify the prdcts individually

    stoich =  adkoy_prdct(out1, metname, i);
    stoich =  adkoy_prdct(out2, metname, i);
    stoich =  adkoy_prdct(out3, metname, i);
    stoich =  adkoy_prdct(out4, metname, i);
    stoich =  adkoy_prdct(out5, metname, i);
% ------------------------------------------------------------------
  elseif length(strfind(prdct{i}, ' + '))== 5 % there are SIX prdcts (valid for only a few cases in GSM_751).
    prdct(i) = strrep(prdct(i),' + ',' @ ');
     [out(1), out(2), out(3), out(4), out(5), out(6)] = strread(prdct{i},'%s %s %s %s %s %s','delimiter','@');

    for k = 1:6
     stoich =  adkoy_prdct(out(k), metname, i);
    end
% ------------------------------------------------------------------

  elseif length(strfind(prdct{i}, ' + '))== 6 % there are SEVEN prdcts (valid for only a few cases in GSM_751).
    prdct(i) = strrep(prdct(i),' + ',' @ ');
     [out(1), out(2), out(3), out(4), out(5), out(6) out(7)] = strread(prdct{i},'%s %s %s %s %s %s %s','delimiter','@');
```

```
    for k = 1:7
     stoich =  adkoy_prdct(out(k), metname, i);
    end
% ---------------------------------------------------------------

  elseif length(strfind(prdct{i}, ' + '))== 7 % there are EIGHT prdcts (valid for only a few cases in GSM_751).
    prdct(i) = strrep(prdct(i),' + ',' @ ');
     [out(1), out(2), out(3), out(4), out(5), out(6) out(7) out(8)] = strread(prdct{i},'%s %s %s %s %s %s %s %s','delimiter','@');

    for k = 1:8
     stoich =  adkoy_prdct(out(k), metname, i);
    end
% ---------------------------------------------------------------

  else
   vvv(mm) = i;
   mm= mm+1;
 end
% ---------------------------------------------------------------
%    if length(strfind(prdct{i}, ' + '))== 6 %there are SEVEN prdcts
%        figure
%        xlabel(prdct(i));
%    end

end

stoich_sparse = sparse(stoich)
toc
vvv
return
gronum = 1173;
stoich_sparse(strmatch('ALA',metname,'exact'),gronum) = -0.4588;
stoich_sparse(strmatch('ARG',metname,'exact'),gronum) = -0.1607;
stoich_sparse(strmatch('ASN',metname,'exact'),gronum) = -0.1017;
stoich_sparse(strmatch('ASP',metname,'exact'),gronum) = -0.2975;
stoich_sparse(strmatch('CYS',metname,'exact'),gronum) = -0.0066;
stoich_sparse(strmatch('GLN',metname,'exact'),gronum) = -0.1054;
stoich_sparse(strmatch('GLU',metname,'exact'),gronum) = -0.3018;
stoich_sparse(strmatch('GLY',metname,'exact'),gronum) = -0.2904;
stoich_sparse(strmatch('HIS',metname,'exact'),gronum) = -0.0663;
stoich_sparse(strmatch('ILE',metname,'exact'),gronum) = -0.1927;
stoich_sparse(strmatch('LEU',metname,'exact'),gronum) = -0.2964;
stoich_sparse(strmatch('LYS',metname,'exact'),gronum) = -0.2862;
stoich_sparse(strmatch('MET',metname,'exact'),gronum) = -0.0507;
stoich_sparse(strmatch('PHE',metname,'exact'),gronum) = -0.1339;
stoich_sparse(strmatch('PRO',metname,'exact'),gronum) = -0.1647;
stoich_sparse(strmatch('SER',metname,'exact'),gronum) = -0.1854;
stoich_sparse(strmatch('THR',metname,'exact'),gronum) = -0.1914;
stoich_sparse(strmatch('TRP',metname,'exact'),gronum) = -0.0284;
```

```
stoich_sparse(strmatch('TYR',metname,'exact'),gronum) = -0.102;
stoich_sparse(strmatch('VAL',metname,'exact'),gronum) = -0.2646;

stoich_sparse(strmatch('AMP',metname,'exact'),gronum) = -0.046;
stoich_sparse(strmatch('GMP',metname,'exact'),gronum) = -0.046;
stoich_sparse(strmatch('CMP',metname,'exact'),gronum) = -0.0447;
stoich_sparse(strmatch('UMP',metname,'exact'),gronum) = -0.0599;
stoich_sparse(strmatch('DAMP',metname,'exact'),gronum) = -0.0036;
stoich_sparse(strmatch('DCMP',metname,'exact'),gronum) = -0.0024;
stoich_sparse(strmatch('DTMP',metname,'exact'),gronum) = -0.0036;
stoich_sparse(strmatch('DGMP',metname,'exact'),gronum) = -0.0024;

stoich_sparse(strmatch('GLYCOGEN',metname,'exact'),gronum) = -0.5185;
stoich_sparse(strmatch('TRE',metname,'exact'),gronum) = -0.0234;
stoich_sparse(strmatch('MANNAN',metname,'exact'),gronum) = -0.8079;
stoich_sparse(strmatch('13GLUCAN',metname,'exact'),gronum) = -1.1348;
stoich_sparse(strmatch('TAGLY',metname,'exact'),gronum) = -0.0066;
stoich_sparse(strmatch('ERGOST',metname,'exact'),gronum) = -0.0007;
stoich_sparse(strmatch('ZYMST',metname,'exact'),gronum) = -0.0015;

stoich_sparse(strmatch('PA',metname,'exact'),gronum) = -0.0006;
stoich_sparse(strmatch('PC',metname,'exact'),gronum) = -0.006;
stoich_sparse(strmatch('PE',metname,'exact'),gronum) = -0.0045;
stoich_sparse(strmatch('PINS',metname,'exact'),gronum) = -0.0053;
stoich_sparse(strmatch('PS',metname,'exact'),gronum) = -0.0017;

stoich_sparse(strmatch('ATP',metname,'exact'),gronum) = -59.276001;
stoich_sparse(strmatch('SLF',metname,'exact'),gronum) = -0.02;

stoich_sparse(strmatch('ADP',metname,'exact'),gronum) = 59.276001;
stoich_sparse(strmatch('PI',metname,'exact'),gronum) =  59.305000;
```

sim_out

```
function a = f(X,rxnname)


a0=X(strmatch('Growth',rxnname,'exact'));
a1=X(strmatch('ETHxt',rxnname,'exact'));
a2=X(strmatch('GLxt',rxnname,'exact'))  ;
a3=X(strmatch('SUCCxt',rxnname,'exact'));
a4=X(strmatch('ACxt',rxnname,'exact') );
a5=X(strmatch('ACALxt',rxnname,'exact') );
a6=X(strmatch('LACxt',rxnname,'exact') );
a7=X(strmatch('PYRxt',rxnname,'exact'));

b0=X(strmatch('CO2xt',rxnname,'exact'));
b1=X(strmatch('O2xt',rxnname,'exact'));
```

```
b2=X(strmatch('NH3xt',rxnname,'exact'));
b3=X(strmatch('SLFxt',rxnname,'exact')) ;
b4=X(strmatch('PIxt',rxnname,'exact')) ;
b5=X(strmatch('GLCxt',rxnname,'exact')) ;

['BIOM: ' num2str(a0,'%3.2f') ', ETH: ' num2str(a1,'%3.2f') ', GOH: ' num2str(a2,'%3.2f')...
    ', SUCC: ' num2str(a3,'%3.2f') ', AC: ' num2str(a4,'%3.2f') ', PYR: ' num2str(a7,'%3.2f\n\n')...
'CO2: ' num2str(b0,'%3.3f') ', O2: ' num2str(b1,'%3.3f') ', NH3: ' num2str(b2,'%3.3f') ...
', SULF: ' num2str(b3,'%3.3f') ', PI: ' num2str(b4,'%3.3f') ', GLC: ' num2str(b5,'%3.2f')]

Ysx = (a0/-b5)/0.18; % g/g Yx/s
RQ = -b0/b1;
Yse = (a1/-b5)/3; % Cmol/Cmol Eth yield
Yseg = (a1/-b5)*(23/30)/3; % g/g Eth yield

c1=X(strmatch('ERGOSTxt',rxnname,'exact')) ;
c2=X(strmatch('ZYMSTxt',rxnname,'exact')) ;
['ETH yield : ' num2str(Yse,'%3.3f') ' Cmol/Cmol  or ' num2str(Yseg,'%3.3f') ' g/g,' ...
'  BIOM yield : ' num2str(Ysx,'%3.3f') ' g/g' '   RQ : ' num2str(RQ,'%3.2f\n\n') ...
'ZYMST: ' num2str(c1,'%3.5f') ', ERGOST: ' num2str(c2,'%3.5f') ]
```

A.6. Principle Component Analysis

The mean centered and scaled input matrix becomes:

$$\begin{bmatrix} 0.0505 & -0.7114 & 0.9272 & -0.2033 & 0.4682 \\ -0.6969 & -1.7966 & -0.0740 & -0.5827 & 0.4435 \\ -0.1836 & 0.0216 & 1.1602 & 0.2588 & 0.2045 \\ -1.1722 & -0.0756 & 0.0079 & 1.4085 & 0.0748 \\ -1.1057 & 1.3735 & -1.0626 & 1.4223 & 1.4913 \\ 0.4483 & -0.1391 & 1.1728 & -1.0920 & 0.1578 \\ 1.5981 & 0.1775 & -1.1445 & -0.0493 & -1.7771 \\ 1.0614 & 1.1500 & -0.9870 & -1.1621 & -1.0629 \end{bmatrix}$$

The principle components (PCs) are found to be:

$$\begin{bmatrix} -0.6295 & -0.0395 & 0.1692 & 0.1520 & -0.7419 \\ -0.1067 & 0.6371 & 0.7287 & 0.0183 & 0.2266 \\ 0.2015 & -0.6242 & 0.5336 & 0.5260 & 0.0917 \\ 0.4480 & 0.4473 & -0.2414 & 0.6605 & -0.3237 \\ 0.5925 & -0.0531 & 0.3121 & -0.5135 & -0.5339 \end{bmatrix}$$

The score matrix is given as:

$$\begin{bmatrix} 0.4173 & -1.1498 & 0.1801 & 0.1077 & -0.2977 \\ 0.6172 & -1.3552 & -1.1875 & -0.7903 & 0.0550 \\ 0.5842 & -0.5982 & 0.6051 & 0.6487 & 0.0546 \\ 1.4228 & 0.6192 & -0.5660 & 0.7165 & 0.3575 \\ 1.8561 & 2.1390 & 0.3688 & -0.5283 & -0.2224 \\ -0.4267 & -1.3352 & 0.9132 & -0.1198 & 0.0126 \\ -2.3306 & 0.8367 & -0.7535 & 0.5241 & -0.2857 \\ -2.1401 & 0.8436 & 0.4399 & -0.5586 & 0.3261 \end{bmatrix}$$

The eigenvalues are given in the latent vector:

$$\begin{bmatrix} 2.3657 \\ 1.6671 \\ 0.5515 \\ 0.3501 \\ 0.0657 \end{bmatrix}$$

From these eigenvalues, the first one belonging to the first principle component covers 47 per cent and the second eigenvalue covers 33 per cent of the overall data. The sum up to cover 80 per cent and hence above the 67 per cent limit. Therefore the first two PCs are considered to be sufficient for further analyses.

The code for the process is:

```
clear all;

X=[1.6647  9.022    0.0376  0.1464  2.9158  ;
0.7756     7.233    0.0217  0.1134  2.8904  ;
1.3862     10.2304  0.0413  0.1866  2.6439  ;
0.2102     10.0701  0.023   0.2866  2.5102  ;
0.2893     12.459   0.006   0.2878  3.9706  ;
2.138      9.9655   0.0415  0.0691  2.5958  ;
3.5058     10.4873  0.0047  0.1598  0.6009  ;
2.8673     12.0905  0.0072  0.063   1.3373  ;
];
```

```
ax=auto(X);

[PC, SCORE, LATENT, TSQUARE] = PRINCOMP(ax)
```

REFERENCES

Alberts, B. , D. Bray, J. Lewis, M. Raff, K. Roberts, and J.D. Watson, 1994, *Molecular Biology of The Cell*, Third Edition, Garland Publishing, New York.

Bach, H. J. , Tomanova, M. Schloter and J. C. Munch, 2002, "Enumeration of Total Bacteria and Bacteria with Genes for Proteolytic Activity in Pure Cultures and in Environmental Samples by Quantitative PCR Mediated Amplification", *Journal of Microbiological Methods*, Vol. 49, pp. 235-245.

Baganz, F. , A. Hayes, D. Marren, D. C. Gardner and S. G. Oliver, 1997, "Suitability of Replacement Markers for Functional Analysis Studies in *Saccharomyces cerevisiae*", *Yeast*, Vol. 13, pp. 1563-1573.

Baganz, F. , A. Hayes, R. Farquhar, P. R. Butler, D. C. Gardner and S. G. Oliver, 1998, "Quantitative Analysis of Yeast Gene Function Using Competition Experiments in Continuous Culture", *Yeast*, Vol. 14, pp. 1417-1427.

Berden J. A. , H. Boumans and L. Grivell, 1998, "The Respiratory Chain in Yeast Behaves as a Single Functional Unit", *The Journal of Biological Chemistry*, Vol. 273, No. 9, pp. 4872-4877.

Boeckman, F. , M. Brisson and L. Tan, 2002, "Real-Time PCR: General Considerations", *BIO-RAD Technical Note 2593*, Bulletin 2697.

Bro, C. and J. Nielsen, 2004, "Impact of 'ome' Analyses on Inverse Metabolic Engineering", *Metabolic Engineering*, Vol. 6, pp. 204-211.

Brons, J. F. , M. de Jong, M. Valens, L. A. Grivell, M. Bolotin-Fukuhara and J. Blom, 2002, "Dissection of the Promoter of the HAP4 Gene in *S. cerevisiae* Unveils a Complex Regulatory Framework of Transcriptional Regulation", *Yeast*, Vol. 19, pp. 923-932.

Buchholtz, A. , J.Hurlebaus, C. Wandrey and R. Takors, 2002, "Metabolomics: Quantification of Intracellular Metabolite Dynamics", *Biomolecular Engineering*, Vol. 19, pp. 5-15.

Buschlen, S. , J-M Amillet, B. Guiard, A. Fournier, C. Marcireau and M. Bolotin-Fukuhara, 2003, "The S. cerevisiae HAP Complex, a Key Regulator of Mitochondrial Function, Coordinates Nuclear and Mitochondrial Gene Expression", *Comparative and Functional Genomics*, Vol.4, pp. 37-46.

Cortassa S. and M. A. Aon, 1997, "Distributed Control of the Glycolytic Flux in Wild-Type Cell and Catabolite Repression Mutants of *Saccharomyces cerevisiae* Growing in Carbon-Limited Chemostat Cultures", *Enzyme and Microbial Technology*, Vol. 21, pp. 596-602.

Covert, M. W. , C. H. Schilling and B. Palsson, 2001, "Regulation of Gene Expression in Flux Balance Models of Metabolism", *Journal of Theoretical Biology*, Vol. 213, pp. 73-88.

Çakır, T. , B. Kırdar and K. Ö. Ülgen, 2003, "Metabolic Pathway Analysis of Yeast Strengthens the Bridge Between Transcriptomics and Metabolic Networks", *Biotechnology and Bioengineering*, Vol. 86, No. 3, pp. 251-260.

Dheda, K. , J. F. Huggett, S. A. Bustin, M. A. Johnson, G. Rook and A. Zumla, 2004, "Validation of Housekeeping Genes for Normalizing RNA Expression in Real-Time PCR", *BioTechniques*, Vol. 37, No. 1, pp. 112-119.

Edwards, J. S. and B. O. Palsson, 2000, "Metabolic Flux Balance Analysis and the in Silico Analysis of *Escherichia coli* K-12 Gene Deletion", *BMC Bioiformatics*, Vol. 1/1/ 1471-2105.

Feldmann, H. , 2001, "Yeast Molecular Biology", http://biochemie.web.med.uni-muenchen.de /Yeast_Biology/.

Förster, J. , I. Famili, P. Fu, B. O. Palsson and J. Nielsen, 2003, "Genome-Scale Reconstruction of the *Saccharomyces cerevsiae* Metabolic Network", *Genome Research*, Vol. 13, pp. 244-253.

Gill, R. T. , 2003, "Enabling Inverse Metabolic Engineering Through Genomics", *Current Opinion in Biotechnology*, Vol. 14, pp.484-490.

Ginziger, D. G. , 2002, "Gene Quantification Using Real-Time Quantitative PCR: An Emerging Technology Hits Mainstream", *Experimental Hematology*, Vol. 30, pp. 503-512.

Gombert, A. K. and J. Nielsen, 2000, "Mathematical Modeling of Metabolism", *Current Opinion in Biotechnology*, Vol. 11, pp.180-186.

Gombert, A. K. , M. Moreira dos Santos, B. Christensen and J. Nielsen, 2001, "Network Identification and Flux Quantification in the Central Metabolism of *Saccharomyces cerevisiae* under Different Conditions of Glucose Repression", Journal of Bacteriology, Vol. 183, No. 4, pp. 1441-1451.

Güldener U. , M. Münsterkötter, G. Kastenmüller, N. Strack, J. van Helden, C. Lemer, J. Richelles, S. J. Wodak, J. Garcia-Martinez, J. E. Perez-Ortin, H. Michael, A. Kaps, E. Talla, B. Dujon, B. Andre, J. L. Souciet, J. de Montigny, E. Bon, C. Gaillardin, H. W. Mewes, 2005, "CYGD: the Comprehensive Yeast Genome Database", *Nucleic Acids Research*, Jan 1;33 Database issue:D364-8.

Hutter, A. and S. G. Oliver, 1998, "Ethanol Production Using Nuclear Petite Yeast Mutants", *Appl. Microbiol. Biotechnol*., Vol. 49, pp. 511-516.

Jiang, T. and A. E. Keating, 2005, "AVID: An Integrative Framework for Discovering Functional Relationships Among Proteins", manuscript in preparation.

Jothikumar N. and M. W. Griffiths, 2002, "Rapid Detection of *Escherichia coli O157*:H7 with Multiplex Real-Time PCR Assays", *Applied and Environmental Microbiology*, Vol. 68, No. 6, pp. 3169-3171.

Klein, C. J. L. , L. Olsson and J. Nielsen, 1998, "Glucose Control in *Saccharomyces cerevisiae*: the Role of MIG1 in Metabolic Functions", *Microbiology*, Vol. 144, pp. 13-24.

Klein, C. J. L. , J. J. Rasmussen, B. Ronnow, L. Olsson and J. Nielsen, 1999, "Investigation of the Impact of MIG1 and MIG2 on the Physiology of in *Saccharomyces cerevisiae*", *Journal of Biotechnology*, Vol. 68, pp. 197-212.

Lange, C. , J. H. Nett, B. L. Trumpower and C. Hunte, 2001, "Specific Roles of Protein-Phospholipid Interactions in the Yeast Cytochrome bc1 Complex Structure", *The European Molecular Biology Organization Journal*, Vol. 20, No. 23, pp. 6591-6600.

Lange, C. , H. Palsdottir and C. Hunt, 2002, "Structure/Function Analysis in the Yeast Cytochrome bc1 Complex", unpublished study.

Lascaris, R. , H. J. Bussemaker, A. Boorsma, M. Piper, H. van der Spek, L. Grivell and J. Blom, 2002, "Hap4p Overexpression in Glucose-Grown *Saccharomyces cerevisiae* Induces Cells to Enter a Novel Metabolic State", *Genome Biology*, Vol. 4, Issue 1, Article R3.

Lascaris, R. , J. Piwowarski, H. van der Spek, J. Teixeira de Mattos, L. Grivell and J. Blom, 2004, "Overexpresion of HAP4 in Glucose-Derepressed Yeast Cells Reveals Respiratory Control of Glucose-Regulated Genes", *Microbiology*, Vol. 150, pp. 929-934.

Malaney, S. , B. L. Trumpower, C. M. Deber and B. H. Robinson, 1997, "The N Terminus of the Qcr7 Protein of the Cytochrome bc1 Complex Is Not Essential for Import into Mitochondria in *Saccharomyces cerevisiae* but Is Essential for Assembly of the Complex", *The Journal of Biological Chemistry*, Vol. 272, No. 28, pp. 17495-17501.

Neuvians, T. P. , M. W. Pfaffl, B. Berisha and D. Schams, “The mRNA Expression of the Members of the IGF-system in Bovine Corpus Luteum During Induced Luteolysis”, *Domestic Animal Endocrinology*, Vol. 25, pp. 359-372.

Overbergh, L. , A. Giulietti, D. Valckx, B. Decallonne, R. Bouillon and C. Mathieu, 2003, “The Use of Real-Time Reverse Transcriptase PCR for the Quantification of Cytokine Gene Expression”, *Journal of Biomolecular Techniques*, Vol. 14, pp. 33-43.

Panoutsopolou, K. , A. Hutter, P. Jones, D. C. J. Gardner and S. G. Oliver, 2001, “Improvement of Ethanol Production by an Industrial Yeast Strain via Multiple Gene Deletion”, *Journal of the Institute of Brewing*, Vol. 107, pp. 49-53.

Pfaffl, M. W. , I. G. Lange, A. Daxenberger and H. H. D. Meyer, 2001, “Tissue Specific Expression Pattern of Estrogen Receptors (ER): Quantification of ERα and ERβ mRNA with Real-Time PCR”, *AP MIS*, Vol. 109, pp. 345-355.

Pfaffl, M. W. , I. G. Lange and H. H. D. Meyer, 2003, “The Gastrointestinal Tract as Target of Steroid Hormone Action: Quantification of Steroid Receptor mRNA Expression (AR, ERα, ERβ and PR) in 10 Bovine Gastrointestinal Tract Compartments by Kinetic RT-PCR”, *Journal of Steroid Biochemistry and Molecular Biology*, Vol. 84, pp. 159-166.

Price, N. D. , J. L. Reed and B. O. Palsson, 2004, “Genome-Scale Models of Microbial Cells: Evaluating the Consequences of Constraints”, *Nature Reviews Microbiology*, Vol. 2, pp. 886-897.

Reist, M. , M. W. Pfaffl, C. Morel, M. Meylan, G. Hirsbrunner, J. W. Blum and A. Steiner, 2003, “Quantitative mRNA Analysis of Eight Bovine 5-HT Receptor Subtypes in Brain, Abomasum and Intestine by Real Time RT-PCR”, *Journal of Receptors and Signal Transduction*, Vol. 23, No. 4, pp. 271-287.

Sheikh K. , J. Förster and L. K. Nielsen, 2005, "Modeling Hybridoma Cell Metabolism Using a Generic Genome-Scale Metabolic Model of *Mus musculus*", *Biotechnological Progress*, Vol. 21, pp. 112-121.

Stuart R. A. , C. M. Cruciat, K. Hell, H. Fölsch and W. Neupert, 1999, "BCS1p, an AAA-family Member, is a Chaperone for the Assembly of the Cytochrome bc_1 Complex", *The EMBO Journal*, Vol. 18, No. 19, pp. 5226-5233.

Stuart R. A. , C. M. Cruciat, S. Brunner, F. Baumann and W. Neupert, 2000, "The Cytochrome bc_1 and Cytochrome c Oxidase Complexes in Yeast Mitochondria", *The Journal of Biological Chemistry*, Vol. 275, No. 24, pp. 18093-18098.

Tenreiro, S. , R. C. Vargas, M. C. Teixeira, C. Magnani and I. Sa-Correia, 2005, "The Yeast Multidrug Transporter Qdr3 (Ybr043c): Localization and Role as a Determinant of Resistance to Quinidine, Barban, Cisplatin, and Bleomycin", *Biochemical and Biophysical Research Communications*, Vol. 327, pp. 952-959.

ter Schure, E. G. , N. A. W. van Riel and C. T. Verrips, 2000, "The Role of Ammonia Metabolism in Nitrogen Catabolite Repression in in *Saccharomyces cerevisiae*", *FEMS Microbiology Reviews*, Vol. 24, pp. 67-83.

Vandesompele, J. , K. De Preter, F. Pattyn, B. Poppe, N. Van Roy, A. De Paepe and F. Speleman, 2002, "Accurate Normalization of Real-Time Quantitative RT-PCR Data by Geometric Averaging of Multiple Internal Control Genes", *Genome Biology*, Vol. 3, No. 7, pp. 1-12.

van Maris, A. J. A. , B. M. Bakker, M. Brandt, A. Boorsma, M. J. T. de Mattos, L. A. Grivell, J. T. Pronk and J. Blom, 2001, "Modulating the Distribution of Fluxes Among Respiration and Fermentation by Overepression of HAP4 in *Saccharomyces cerevisiae*", *FEMS Yeast Research*, Vol. 1, pp. 139-149.

Walker, G. M. , 1998, *Yeast Physiology and Biotechnology*, John Wiley and Sons, New York.

Westergaard, S. L. , A. P. Oliveira, C. Bro, L. Olsson and J. Nielsen, 2005, "Comparative Functional Genomics of *Saccharomyces cerevisiae* Mutants with Altered Glucose Repression Patterns", manuscript in preparation.

Wold S. , K. Esbensen and P. Geladi, 1987, "Principle Component Analysis", *Chemometrics and Intelligent Laboratory Systems*, Vol. 2, pp. 37-52.

Zara, V. , I. Palmisano, L. Conte and B. L. Trumpower, 2004, "Futher Insights into the Assembly of the Yeast Cytochrome bc1 Complex Based on Analysis of Single and Double Deletion Mutants Lacking Supernumerary Subunits and Cytochrome b", *European Journal of Biochemisty*, Vol. 271, pp. 1209-1218.